
Methodological aspects and algorithms for estimating soil strength and their applications with the model *REPRO*

Habilitationsschrift

eingereicht an der

Naturwissenschaftlichen Fakultät III - Agrar- und Ernährungswissenschaften,
Geowissenschaften und Informatik

(Dekan Herr Prof. Dr. Matthias Müller-Hannemann)

der

Martin-Luther-Universität Halle-Wittenberg

von

Herr Dr. agr. Jan Rücknagel

geb. am 15.02.1977 in Weimar

Gutachter

Prof. Dr. Robert Mikutta

Prof. Dr. Hans-Peter Kaul

Prof. Dr. Stephan Peth

Datum der Verteidigung: Halle (Saale), den 18.01.2021

Table of contents

Summary.....	6
1. Introduction	9
1.1. General introduction	9
1.2. Behaviour of soil under vertical stress	10
1.3. Assessment and solutions to avoid the risk of soil compaction	13
1.4. Scope and aim of the work	15
2. Methodological aspects, module conception and validation	18
2.1. Variance of mechanical precompression stress in graphic estimations using the Casagrande method and derived mathematical models.....	18
2.1.1. Introduction	19
2.1.2. Materials and methods.....	20
2.1.3. Results and discussion	23
2.1.4. Conclusions	29
2.2. Indicator based assessment of the soil compaction risk at arable sites using the model <i>REPRO</i>	31
2.2.1. Introduction	31
2.2.2. Materials and methods.....	33
2.2.2.1. Module structure and algorithms.....	33
2.2.2.2. Validation of the module	33
2.2.2.3. Examples of module application	37
2.2.3. Results and discussion	40
2.2.3.1. Module structure and algorithms.....	40
2.2.3.1.1. Soil water content data	41
2.2.3.1.2. Estimation of soil strength.....	41
2.2.3.1.3. Calculation of soil stress.....	43
2.2.3.1.4. Comprehensive assessment	43
2.2.3.2. Validation of the module	46
2.2.3.3. Examples of module application	51
2.2.4. Conclusions	53
3. Detailed algorithms for determination of soil strength.....	57
3.1. A simple model to estimate change in precompression stress as a function of water content on the basis of precompression stress at field capacity	57

3.1.1. Introduction	58
3.1.2. Materials and methods.....	59
3.1.2.1. Analysis of data from previous studies	59
3.1.2.2. Relationships between matric potential and water content	59
3.1.2.3. Soil compression tests	60
3.1.2.4. Statistical analysis	61
3.1.3. Results and discussion.....	61
3.1.3.1. Principal changes in stress/strain behaviour.....	61
3.1.3.2. Derivation of the model.....	67
3.1.3.2.1. Change in precompression stress with matric potential	67
3.1.3.2.2. Change in water content	69
3.1.3.2.3. Principal approach in deriving the model.....	69
3.1.3.2.4. Differentiating according to soil texture class.....	71
3.1.3.3. Validation of the model.....	72
3.1.4. Conclusions	74
3.2. The influence of soil gravel content on compaction behaviour and precompression stress	75
3.2.1. Introduction	76
3.2.2. Materials and methods.....	77
3.2.2.1. Preparation of artificial samples.....	77
3.2.2.2. Extraction of naturally occurring samples.....	79
3.2.2.3. Soil compression tests	79
3.2.2.4. Statistical analysis	80
3.2.3. Results	81
3.2.3.1. Gravel content in disturbed soil samples.....	81
3.2.3.1.1. Stress/density curves	81
3.2.3.1.2. Mechanical precompression stress	84
3.2.3.2. Gravel content in naturally structured soil samples.....	85
3.2.4. Discussion.....	87
3.2.4.1. Bulk density of the fine earth and of the whole soil.....	87
3.2.4.2. Precompression stress.....	88
3.2.5. Conclusions	90
3.3. Uniaxial compression behaviour and soil physical quality of topsoils under conventional and conservation tillage	91

3.3.1. Introduction	91
3.3.2. Materials and methods.....	93
3.3.2.1. Test sites and variants.....	93
3.3.2.2. Soil compression tests	93
3.3.2.3. Determination of soil physical parameters	96
3.3.2.4. Statistical analysis	97
3.3.3. Results and discussion.....	97
3.3.3.1. Soil physical parameters.....	97
3.3.3.2. Stress/strain and stress/bulk density behaviour	99
3.3.3.3. Stress/bulk density behaviour of whole soil and aggregates	102
3.3.4. Conclusions	106
3.4. Visual structure assessment and mechanical soil properties of re-cultivated soils made up of loess.....	107
3.4.1. Introduction	107
3.4.2. Materials and methods.....	109
3.4.2.1. Data acquisition	109
3.4.2.2. Soil compression tests	110
3.4.2.3. Determination of aggregate density.....	110
3.4.2.4. Determination of packing density.....	111
3.4.2.5. Statistical analysis	113
3.4.3. Results and discussion.....	114
3.4.3.1. Morphological characterisation of soil structure and soil mechanical properties	114
3.4.3.2. Stress/bulk density behaviour of whole soil and aggregates	117
3.4.4. Conclusions	118
4. Applications of the module concept	119
4.1. Impact on soil physical properties of using large-grain legumes for catch crop cultivation under different tillage conditions.....	119
4.1.1. Introduction	120
4.1.2. Materials and methods.....	121
4.1.2.1. Site description and precipitation data.....	121
4.1.2.2. Treatments and experimental conditions.....	122
4.1.2.3. Crop and soil sampling	128
4.1.2.4. Calculation of Soil Compaction Index	129
4.1.2.5. Statistical analysis	129

4.1.3. Results	130
4.1.3.1. Catch crop yield.....	130
4.1.3.2. Air capacity and saturated hydraulic conductivity	130
4.1.3.3. Precompression stress.....	133
4.1.3.4. Soil Compaction Index	134
4.1.4. Discussion.....	135
4.1.4.1. Catch crop yield.....	135
4.1.4.2. Air capacity, saturated hydraulic conductivity and Soil Compaction Index .	135
4.1.4.3. Precompression stress.....	137
4.1.5. Conclusions	138
4.2. Impact on soil compaction of driving agricultural machinery over ground frozen near the surface.....	139
4.2.1. Introduction	139
4.2.2. Materials and methods.....	140
4.2.3. Results and discussion	143
4.3. Environmental impacts of different crop rotations in terms of soil compaction	146
4.3.1. Introduction	147
4.3.2. Materials and methods.....	148
4.3.2.1. Field site and experimental design	148
4.3.2.2. Investigations into soil structure at the field trial Aiterhofen.....	148
4.3.2.3. Modelling the soil compaction risk	149
4.3.2.3.1. Model structure.....	149
4.3.2.3.2. Input parameters	150
4.3.2.3.3. Model validation.....	151
4.3.2.4. Statistical analysis	153
4.3.3. Results	154
4.3.3.1. Measured soil structure for the field trial Aiterhofen.....	154
4.3.3.2. Soil compaction risk modelled for the model farm Aiterhofen.....	155
4.3.3.2.1. Model validation.....	155
4.3.3.2.2. Soil Compaction Index for crop - specific operations.....	156
4.3.3.2.3. Soil compaction risk of entire crop rotations	158
4.3.4. Discussion.....	160
4.3.4.1. Soil structure measured at the field trial Aiterhofen.....	160
4.3.4.2. Soil compaction risk modelled for the model farm Aiterhofen.....	161

4.3.5. Conclusions	163
5. Synthesis and general discussion.....	166
5.1. Suitability of precompression stress as a parameter for soil strength.....	166
5.2. Categorisation of precompression stress values	168
5.3. Integration of algorithms in the <i>REPRO</i> software package.....	170
5.4. Application of algorithms in other model concepts and sustainability assessments ...	174
5.5. Discussion of module accuracy in general	175
5.6. Discussion of applications of the module concept	178
5.7. Options for further validations and development	180
6. General conclusions.....	182
7. References	184

Summary

Economic pressure on farms is resulting in ever-larger agricultural structures, with higher demands on the tractive forces and hopper capacities of agricultural machinery necessitating increasingly heavy equipment. As a result of this trend, the risk of soil compaction when machinery passes over agricultural land is increasing. However, soil compaction impairs all essential soil functions – which form the basis of life for humans, animals, plants and soil organisms. This is associated with considerable costs for agriculture and society. Alleviating existing compaction is an energy-intensive and costly process and not always effective in the long term, which is why prevention of soil compaction is the preferred method. Mathematical-empirical models, which can facilitate quantitative situational analyses and precise practical recommendations under specific conditions, are an efficient tool that can help to avoid soil compaction. Due to their comparatively simple structures with only a small number of input parameters, so-called pseudo-analytical models are particularly suitable for applications in PC-based scientific and practical consulting models. These models reduce the stresses applied by the wheel to the vertical stress in the load axis as the only and usually highest component of stress. At the same time, logarithmic models – or regression equations derived from them – serve to describe the stress/strain behaviour of the soil under static conditions, delivering a ratio between vertical stress at a certain soil depth and soil strength.

However, existing pseudo-analytical models have a number of shortcomings and potential for improvement, in terms not only of various details and algorithms, but also of fundamental questions of evaluation and their potential for application in complex crop production issues. The present research therefore contributes to developing these models further. Specifically, it is intended first and foremost to help clarify the question of whether precompression stress, and the methodological procedure used to determine it, are actually suitable for identifying soil strength in agricultural soils, and how precompression stress relates to changes in other important soil properties and functions. Several chapters are also dedicated to developing and validating innovative partial algorithms for modelling precompression stress and the risk of soil compaction in agricultural soils. They deal with soil water content as a key factor in the formation of soil compaction, the effect of the gravel content on soil strength, the compaction behaviour of soils under conventional and conservation tillage, and thus the verification of standard values as well as the relationship between visual soil structure evaluation and soil mechanical properties. All of the algorithms developed are incorporated into the module for calculating the risk of soil compaction in the software *REPRO*, and possible applications and examples of this module are presented which can be used to address important questions in plant cultivation or for sustainability assessments of farming systems. These include the cultivation of catch crops as compared to fallow land in order to explain the influence of different passes on soil structure, and modelling the risk of soil compaction in entire crop rotations with winter wheat, sugar beet and silage maize.

As a methodological basis for answering the questions, numerous soil compression tests were carried out in the laboratory at a matric potential of -6 kPa (= field capacity). In parallel, tests were conducted with higher matric potentials (-10 to -1500 kPa), selected fine soils were mixed with staggered proportions of quartz gravel, and samples from a natural site with staggered gravel contents were investigated. In all of the soil compression tests carried out under drained conditions, loading steps of 5–550 kPa (in some cases up to 2500 kPa) were successively applied to the soil core samples. The resulting stress/dry bulk density functions were used to determine precompression stress using the graphical method according to Casagrande (1936). In order to validate the model, numerous test passes were carried out with agricultural machinery in the field, with the Soil Compaction Index (SCI) calculated in parallel using *REPRO*. Tests were carried out with passes by individual machines as well as on the level of operations involving driving along permanent traffic lanes and with random traffic on field. In addition, investigations were carried out on several long-term soil tillage trials and in field trials with catch crops and crop rotation trials with winter wheat, sugar beet and silage maize. In all of the field trials, soil physical parameters such as dry bulk density, air capacity, saturated hydraulic conductivity, and in some cases packing density as a visually derived parameter, were determined at different depths. Sites with a broad range of textures were selected for all parts of the research, albeit with a focus on soils of the Silt Loam textural class.

Overall, there is considerable variation in the precompression stresses determined in the course of this research on different soils at comparable matric potential, depending on the intensity of soil tillage, sampling depth, and general soil structure properties, such as for example aggregate shape or aggregate arrangement. These factors are more important than texture, which is why soil texture should be viewed critically as a sole criterion for classifying precompression stress. All arable sites show more or less typical compression behaviour, and the methodological investigations to determine precompression stress as a parameter for soil strength demonstrate that, above all, the graphical method for deriving precompression stress is generally suitable for determining reproducible values. The results of the work also make clear that precompression stress is related to other important soil properties and functions, such as packing density as a quality parameter for the soil structure, and that precompression stress is therefore suitable in principle as a guideline for soil strength.

The individual newly developed model algorithms were successfully validated in numerous tests. Above all, however, the overall validation provides further indirect indications as to the accuracy of the algorithms, including those that were not tested individually, and how they interact in the overall context. The SCI calculated with *REPRO* describes in logarithmic terms how the calculated soil stress exceeds the soil strength, and is thus closely related to the average slope of the virgin compression line in the stress/bulk density diagram. This relationship between the SCI and changes in dry bulk density can be mapped very well across all module validations. In addition, the change in saturated hydraulic conductivity also shows a close relationship to the calculated SCI. Overall, the SCI thus allows a comparison of the compaction

risk across different trials, sites and depths. In addition, the model validation trials make it clear that the precompression stress values determined in the uniaxial laboratory test can be used to derive the soil compaction risk in the field. However, there are indications that multiple passes by machinery on the same day, despite no changes to the calculated SCI, actually have a higher compaction effect than single passes, although the soil compression tests on which the algorithms are based were performed with a relatively long load duration until consolidation. There are further indications that the frequency of passes may mask the effect of increasing wheel loads and tyre inflation pressures. The observations suggest that additional systematic tests should be carried out.

From the modelling examples involving crop cultivation, it can generally be deduced that general wheel load limits alone cannot satisfy the complex requirements of different cropping systems. The use of complex model concepts, such as those used in *REPRO*, could promote greater awareness of the problem of soil compaction and contribute to the development of individual response strategies. More globally, the model concept can help decision-makers in agricultural and environmental policy to plan and review specific agro-environmental measures. Continuing this scientific work, it would be conceivable to consider less common arable sites as well as grassland and forest sites when further developing and validating the individual algorithms, so as to enable their universal application without site restrictions – but also because there is a considerable need to prevent soil compaction at these sites as well.

1. Introduction

1.1. General introduction

International trade networks with interconnected global agricultural markets, coupled with increasing changes in how people work, are continuing to put increased economic pressure on farms in industrialised nations. As a result, the total number of farms in Germany and the number of people employed in this sector continue to decline, while the quantity of large-scale farms exceeding 100 ha – and the importance of agricultural contractors using their machinery on more than one farm – is on the rise (DBV, 2018). These larger agricultural structures are placing increased demands in crop production on the tractive forces of agricultural machinery, the hopper capacities of harvesting machines, and the organisation and efficiency of work processes. Consequently, machinery is also getting heavier, while tyre size as well as chassis and machine dimensions are restricted for mechanical reasons or due to road traffic regulations. One example of particularly heavy vehicles are six-row self-propelled sugar beet harvesters. Already weighing up to 30 t when empty, their hoppers can carry up to a further 30 t of sugar beet (Ziegler, 2010).

As a result of this trend, the risk of soil compaction when passing over agricultural land is continuing to rise, which is why soil compaction is a particularly serious problem in parts of the world where agriculture is highly mechanised (Schjonning et al., 2015). In Europe alone, 33 million ha of land are affected by soil compaction (van den Akker and Canarache, 2001). In Germany, experts from soil protection and agricultural authorities estimate the proportion of compacted arable land to be about 10–20 % (UBA, 2013). This is equivalent to around 1.2 to 2.3 million ha. Regionally, Eckert et al. (2006) for example report upper subsoil compaction in 16–17 % of all arable land in Thuringia. In a study of 24 sites across Saxony-Anhalt, Thuringia, Saxony and Brandenburg, all of which had been cultivated without a plough and at a reduced tillage depth for many years, Götze et al. (2013) found that the functional requirements on the soil structure in the lower topsoil were not fully reached in the majority of the sites investigated. In investigations by Brunotte et al. (2008) in South Lower Saxony, 10 out of 47 areas of arable land sampled were classified as compacted when considering the criteria “air capacity” and “saturated conductivity”. In addition, Gieska et al. (2003) reported increasing physical degradation of soils in the Hildesheim Börde region over the last decades.

Soil compaction is defined as an increase in soil density, or a decrease in pore volume and a change in soil structure, for example due to shearing (Horn, 2001; Ad-Hoc Arbeitsgruppe Boden, 2005). When soil is compacted, changes in the properties of the pore system are associated with a variety of impairments of all essential soil functions that form the basis of life for humans, animals, plants and soil organisms. Among other things, soil compaction leads to reduced infiltration and an increase in surface run-off and erosion (Fleige and Horn, 2000). Earthworm burrow systems are destroyed by compaction (Jegou et al., 2002). Restrictions in living conditions for soil biota and a decrease in microbial activity as well as an increase in N₂O emissions through denitrification are possible (Beylich et al., 2010; Weisskopf et al., 2010). Root growth

is reduced in compacted soil layers (Lipiec et al., 2012). The decrease in macro pore volume and root quantity leads to a reduction in the uptake of water and nutrients by plants due to longer flow distances (Bohne and Hartge, 1990). Against the backdrop of climate change, one extremely important factor in the future will be that the risk of drought on compacted soils may increase in spring (Hartmann et al., 2012). At individual sites, increasing penetration resistance can also be associated with an increase in infestations with the pathogen *Rhizoctonia solani* in sugar beet (Schulze, 2017). From both an agricultural and ecological perspective, it is also particularly relevant that a high level of soil compaction can lead to significant yield losses. Numerous trials with agricultural crops on arable land and grassland have reported yield decreases of up to approximately 30 % – and in individual cases even higher – depending on load intensity and associated changes in physical soil properties as well as weather conditions (e.g. Brunotte and Sommer, 2000; Voorhees, 2000; Herbst and Hofmann, 2005; Wild et al., 2012; Hargreaves et al., 2019; Pöhlitz, 2019). Moreover, soil compaction causes greater yield uncertainty. Yield depressions can be observed in particular in years with increased environmental stresses, such as prolonged dry or wet periods (Voorhees, 2000). As a result, the site's yield potential can only be insufficiently exploited, thus reducing the efficiency of all resources used, from fertilizers to pesticides (Herbst and Hofmann, 2005). These consequences are particularly problematic in view of the fact that soil compaction can persist over a long period of time, with a risk of long-term damage (Alakukku, 1996; Berisso et al., 2013; Etana et al., 2013).

All in all, soil compaction entails high costs for agriculture and society (Chamen et al., 2015). The targeted improvement of compacted soil is energy-intensive and costly. Depending on subsequent cultivation, it is also quite possible for the soil to return to its original compacted state after only a few years or passes by agricultural machinery (Werner and Reich, 1993; Canarache et al., 2000; Chamen et al., 2015). Economic analyses also show that strategies aimed at avoiding soil compaction in the first place are more cost-effective than improving compacted soils (Chamen et al., 2015), which is why the focus should be on preventive measures to avoid compaction in everyday practice. This is also provided for in *Bundesbodenschutzgesetz* (“Germany’s Federal Soil Protection Act”) (BBodSchG, 1998), which includes provisions on the obligation to take precautions.

1.2. Behaviour of soil under vertical stress

When a saturated or unsaturated soil is compressed by a load, the resulting stress is transmitted not only via the solid particles, but also via the liquid and gaseous phases. If the water cannot drain away quickly enough after the air-filled pore space has been compressed, the load is initially borne completely by the water, since it has no significant inherent strength, is incompressible and behaves hydrostatically. This results in excess pore water pressure (Fazekas and Horn, 2005). As a result, the water exits the pores and the applied pressure gradually shifts to the solid particles of the soil. The soil settles, which causes an increase in the number of grain contact points. Once settlement is complete, which is known as consolidation, the pore water pressure

is zero. If settlement behaviour is represented logarithmically over time, the process can be divided into three sections: immediate settlement, primary consolidation and secondary compression. Immediate settlement takes place at the moment when the load is applied by squeezing out existing pore air. Primary consolidation corresponds to the consolidation theory described above. The time it takes for a soil to become consolidated depends on the permeability of the soil and the drainage conditions (Schanz, 2007).

In agricultural soil mechanics, in addition to settlement behaviour over time, the behaviour of the soil under increasing stress is particularly relevant. This stress/strain behaviour is traditionally investigated under drained conditions using an oedometer by gradually increasing the loading steps on soil core samples (Bradford and Gupta, 1986). The volume change of the sample is measured as settlement. However, there are sometimes considerable differences internationally in the way in which soil compression tests are carried out. According to DIN 18135 (2012), these tests are carried out in soil mechanics with restricted lateral expansion, under drained conditions and with unknown consolidation behaviour, with a load time of up to 24 hours per loading step. In international agricultural soil mechanics, on the other hand, load times of between a few minutes (Salire et al., 1994) and several hours (Pöhlitz et al., 2019) are often seen, sometimes with (Rücknagel et al., 2007) and sometimes without (Keller et al., 2011) subsequent relaxation phases. Some experiments even use strain-controlled stress application procedures with a constant speed (Schjonning and Lamande, 2018). The size of the soil core samples used varies between 100 cm³ (e.g. $d = 6.1 \text{ cm} / h = 3.4 \text{ cm}$; Schjonning and Lamande, 2018) and 235 cm³ (e.g. $d = 10.0 \text{ cm} / h = 3.0 \text{ cm}$; Stahl et al., 2005). Sometimes investigations are carried out with unrestricted lateral expansion (Dawidowski et al., 2000; Mosaddeghi et al., 2007). In individual studies, the loading steps are not applied successively to one soil sample, but rather each loading step is applied to a separate soil sample (Lebert, 1989; Pöhlitz et al., 2018).

Semi-logarithmic diagrams are normally used to represent soil compression tests. The abscissa indicates the pressure in logarithmic form, while the ordinate reflects either the settlement or a parameter derived from it, such as void ratio, dry bulk density, relative settlement or the specific volume (Mosaddeghi et al., 2003). Such soil compression curves of pre-compacted soils can typically be divided into two sections. In the recompression section, the curve initially has a low slope. The deformation is elastic and reversible (Lebert and Horn, 1992). When the pre-compression stress is exceeded, the soil is then plastically deformed in the virgin compression section due to the increase in the number of grain contacts. The slope of the so-called virgin compression line is greater than that of the recompression line and is used to characterise the compressibility of soils. In the semi-logarithmic diagram, it is referred to as the compression index (C_c) and is calculated using the change in the void ratio ε and the change in stress p with a logarithmically divided load axis (DIN 18135, 2012).

According to Topp et al. (1997), precompression stress reflects the maximum pressure that has acted on the soil in the past, if it is determined under the same load conditions. In the topsoil, precompression stress results among other things from stress exerted when machinery is driven

over the ground, from tillage activity aimed at loosening the soil, and from the formation of soil structures caused by drying and shrinking processes, the effects of frost and biogenic aggregate formation. In the subsoil, precompression stress is also affected by the load from the overlying soil layers as well as previous coverings of ice. Precompression stress is very often used as a soil mechanical criterion for susceptibility to compaction, or as a criterion for the maximum carrying capacity of soils (e.g. DVWK, 1995; Arvidsson and Keller, 2004; Horn and Fleige, 2009; Lebert, 2010). If the soil compression tests are conducted with too short a loading time and consolidation is therefore not complete, this will result in higher precompression stress values (Fazekas and Horn, 2005).

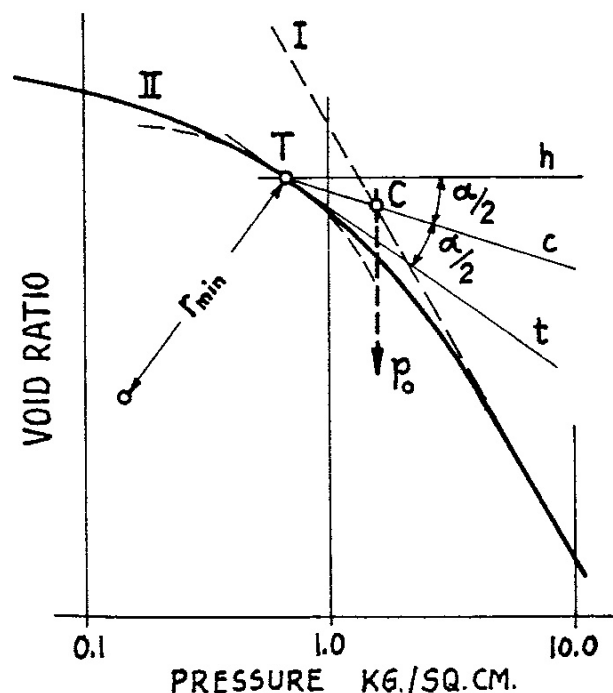


Figure 1.2.1. Estimation of precompression stress according to the original method of Casagrande (1936).

There are many different ways to determine precompression stress graphically or mathematically (e.g. Dias Junior and Pierce, 1995; Cavalieri et al., 2008). In agricultural soil mechanics, graphical derivation of precompression stress according to Casagrande (1936) is used as a standard method (Fig. 1.2.1), on which newer, more advanced methods are regularly based (e.g. Baumgartl and Köck, 2004; Lamande et al., 2017). According to the Casagrande method (1936), a tangent (t) and a parallel to the abscissa (h) are placed at the point with the greatest curvature (T) of the stress/strain function (II). The point of intersection (C) of the angle bisector of these two lines (c) with the virgin compression line (I) corresponds to precompression stress (P_0). However, where to place a tangent at the point of greatest curvature is a subjective decision made by the experimenter. The method should be made more objective by means of mathematical and computer-aided evaluations (Dawidowski and Koolen, 1994). The precompression

stress values vary depending on whether the tests are evaluated using the stress/strain curves, the stress/void ratio curves or the stress/dry bulk density curves (Mosaddeghi et al., 2003).

1.3. Assessment and solutions to avoid the risk of soil compaction

In order to estimate the extent and thus also the risk of soil compaction on agricultural land, it is possible to carry out direct measurements of soil physical parameters, e.g. air capacity and saturated hydraulic conductivity, or a visual examination of the soil in terms of the quality and performance of the soil structure, e.g. based on packing density (e.g. Brunotte et al., 2008; Götze et al., 2013). Such measurements are not only complex and expensive, but the results also only reflect the effects of farming in recent years or decades. Another option – albeit a very expensive one – for assessing the risk of soil compaction is to carry out driving trials with standard agricultural machinery and at typical sites. There are numerous examples of this in the literature (e.g. Schäfer-Landefeld et al., 2004; Koch et al., 2008; Zink et al., 2010).

Such investigations often yield a variety of basic recommendations as measures for *Gute fachliche Praxis* (“Good Professional Practice”) in order to prevent soil compaction. The concept of *Bodenschonendes Befahren* (“Soil-Conserving Field Traffic”) (Brunotte et al., 2013) includes, for example, strategies for “precautionary measures in crop production”, “working methods for soil use” and “technical possibilities for reducing soil stress”. Some of the recommendations these contain include enlarging the tyre contact area, the ability to adjust tyre inflation pressure, combining working steps, separating the traffic lanes from plant cultivation areas, and matching field lengths with the hopper capacity of harvesters.

It is, however, extremely difficult to deliver an exact quantitative estimation of which measures are necessary under the specific conditions and which contribute to reducing the risk of soil compaction, because a large number of factors are involved and interact in complex ways. For this reason, mathematical-empirical models are a good way to develop situational analyses and precise practical recommendations. These models can be used to limit the need for complex measurements, to simulate soil compaction behaviour, and to derive effective measures from the risks identified. Different procedures for calculating the stress propagation and deformation behaviour mean a distinction is made between two model types: numerical models and pseudo-analytical models (Defossez and Richard, 2002). The different models are applied depending on the goal of the modelling. Figure 1.3.1 provides an overview of the main models used in agricultural soil mechanics.

Numerical models include finite element models (FEMs). These attempt to model the process of stress propagation and soil deformation simultaneously and make it possible to represent stress and deformation behaviour during loading in three dimensions, including the associated shear processes (Defossez and Richard, 2002). It is also possible to map anisotropic conditions in the soil by breaking them down into individual elements with differentiated stress/strain behaviour. However, finite element models require a large number of at times highly specific

mechanical parameters, making them suitable only for specific problems. Applications of numerical models in the field of soil compaction on agricultural land include investigating how heavy machinery impacts upon the soil structure under specific boundary conditions (Berli et al., 2003; Poodt et al., 2003).

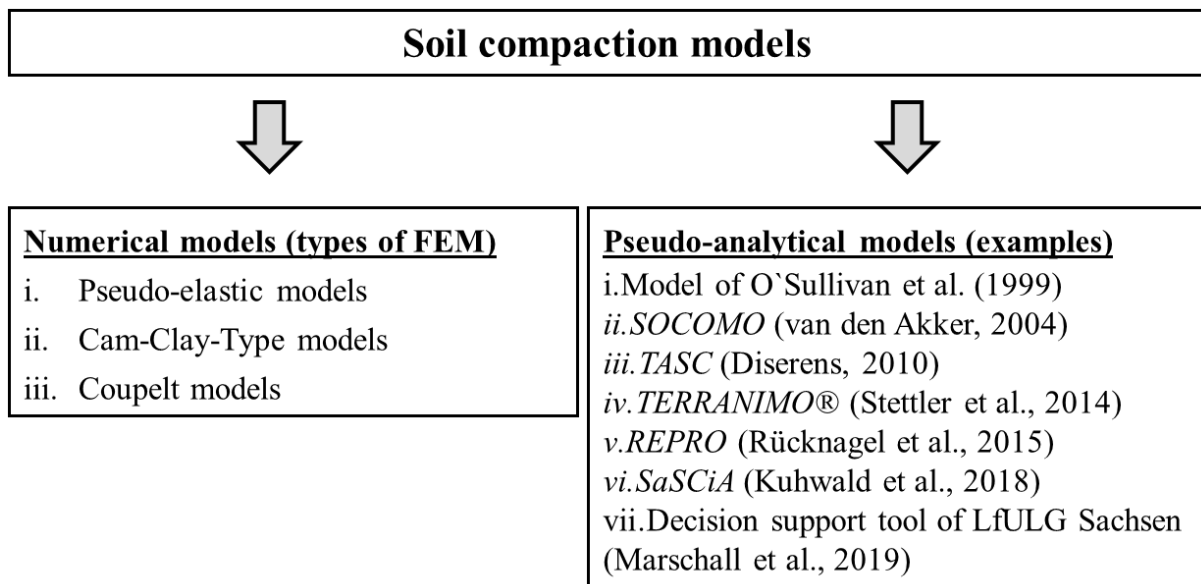


Figure 1.3.1. Classification of soil compaction models according to Defosse and Richard (2002) with examples of important models.

By contrast, pseudo-analytical models reduce the stresses applied by the wheel to the vertical stress in the load axis (σ_z) as the sole – and usually highest – component of stress. Calculation is based on the theories by Boussinesq and Fröhlich (cited in Söhne, 1953) or equations derived from this (e.g. Koolen et al., 1992). In order to account for the less than ideal behaviour of soils with regard to the assumptions of the Boussinesq theory, concentration factors are used for the different soil conditions. In parallel to this, the stress/strain behaviour of the soil is described in logarithmic models or by regression equations derived from them (e.g. Schjonning and Lamande, 2018). Pseudo-analytical models thus only define input-output relationships, e.g. the vertical stress in the load axis (σ_z) at a particular soil depth compared to precompression stress (σ_P), without mapping the process. As a result, the models indicate the risk of compaction as the ratio between vertical stress (σ_z) at a certain depth and precompression stress (σ_P) (e.g. *TERRANIMO*® model, Stettler et al., 2019) or a soil depth up to which a risk of compaction can be expected (e.g. *TASC* model, Diserens, 2010). Building on this, some model concepts are used to show the risk of compaction based on soil data, or their combination with soil water contents from map records. This results in small-scale maps which indicate risk categories or susceptibility to compaction (Lebert, 2010; van den Akker and Hoogland, 2011), which can in turn be used, for example, to calculate wheel load carrying capacity and present this information in maps (van den Akker and Hoogland, 2011; Schjonning et al., 2015). Data from individual

farms is also used to estimate the subsoil compaction risk on a large scale and with high-resolution soil maps (Horn and Fleige, 2009). Consequently, general recommendations are often made for a maximum wheel load (e.g. Horn and Fleige, 2009: <3.3 Mg at field capacity). Due to their comparatively simple structures, pseudo-analytical models require only a small number of input parameters, which is why they are often used in PC-based or online practical consulting and training models alongside the applications mentioned above.

1.4. Scope and aim of the work

Existing pseudo-analytical models have a number of shortcomings and potential for improvement, in terms not only of various details and algorithms, but also of fundamental questions of evaluation and their potential for application in complex crop production issues. The present work therefore contributes to developing these models further, concentrating on the following key points:

Methodological aspects, model conception and validation

As an important parameter for the stability of the soil structure, precompression stress plays a central role in many compaction models as well as in all of the chapters of this work. However, a number of major differences have been recorded between stress/strain behaviour in situ in wheeling experiments and stress/strain behaviour in oedometer laboratory tests and the precompression stress values identified in laboratory tests, and laboratory tests are not always helpful for evaluating compaction in the field (Keller and Lamande, 2010). A further point of criticism regarding the use of precompression stress as a parameter for maximum soil strength is its lack of relation to other important soil properties and functions (Stahl et al., 2005). For this reason, this work is intended to help clarify the question of whether precompression stress, and the methodological procedure used to determine it, are actually suitable for determining soil strength in agricultural soils. Deriving precompression stress in laboratory tests is complicated by the fact that, as already described, there are numerous methods for determining it graphically or mathematically. Chapter 2.1., therefore, first contains a methodological consideration on determining precompression stress based on the results of classical soil compression tests in the oedometer. Specifically, it investigates: differences in precompression stress values when calculated by different experimenters using the traditional graphical method according to Casagrande (1936); the reproducibility of the graphical results which can be expected from selected mathematical models; and the influence of the boundary conditions of the soil compression tests on the result.

All of the algorithms and databases developed during this study were integrated into the *REPRO* (*REPRO*duction of soil fertility) farm balance model as a module for calculating the risk of soil compaction (Hülsbergen, 2003; Küstermann et al., 2008, Küstermann et al., 2010). The computer model *REPRO* was conceived as a complex balancing model to describe nutrient and energy flows as well as the ecological and economic assessment of farm systems. In addition

to the individual model algorithms, the overall module for calculating the risk of soil compaction has also been validated here in a large number of tests (chapter 2.2.). The accuracy of the calculations of the risk of compaction was examined not only for individual passes by machinery, but also for aggregated levels, such as operations involving driving along permanent traffic lanes and along random traffic at field and at whole farm level. Overall, these validations also provide information about the extent to which precompression stress is suitable as a parameter for maximum soil strength and how it is related to changes in other important soil properties and functions.

Algorithms for determination of soil strength

The second main focus of this work is addressed by the subsequent chapters, which describe in greater detail the development and validation of the innovative partial algorithms for modelling precompression stress and the risk of soil compaction. Above all, water content is a key factor in the formation of soil compaction, and should therefore play a special role in further development of the model (Defossez and Richard, 2002). Chapter 3.1. deals with quantifying the influence of water content on the mechanical stability of the soil structure. It presents a regression model and its extensive validation, which can be used to deliver individual estimates of precompression stress as a function of soil water content as a percentage of field capacity – which is a convenient parameter to obtain.

Many arable sites have significant proportions of gravel or stones with a diameter of more than 2.0 mm (Batjes, 1997). Until now, however, compaction models have not taken into account a possible effect of the gravel content on the mechanical stability of the soil. For this reason, special investigations were carried out here on the influence of the gravel content on the precompression stress of the soil (chapter 3.2.) and these results were implemented in the module as regression data sets.

The master data of the *REPRO* model contain standard values for the soil physical parameters of aggregate density and dry bulk density, which can be used to calculate the stability of the soil structure (Rücknagel et al., 2007). In addition to the soil texture, the values differ in the topsoil depending on soil tillage (conventional tillage vs. conservation tillage). Studies on the initial condition of the soil structure and on the compaction behaviour of soils under conventional and conservation tillage are at the centre of the considerations in chapter 3.3. and thus verify the standard values and algorithms in *REPRO*.

While the use of such standard values as a basis for the calculation of mechanical stability allows for a broad and simplified application of the module, they cannot sufficiently reflect individual soil conditions at different sites and at different times. Directly measuring soil physical and mechanical properties is highly laborious and is therefore usually only feasible for scientific purposes. A visual assessment of the soil structure, also commonly referred to as a spade test, is one way of offering a more individual adaptation to local soil properties. Chapter 3.4. demonstrates relationships between the visual evaluation of a soil's structure and its

physical and mechanical properties, which in turn are incorporated into the module and also provide information about the relationship between precompression stress and other important soil properties and functions.

Applications of the module concept

Until now, compaction models have concentrated exclusively on analysing individual machines or machine combinations with specified, mostly staggered soil water contents. They lack any aggregation to higher levels, and there is no relation to specific agricultural systems or crop rotations, and nor is there any concrete link between the annual cycle of soil water content and the actual date when the machines are used. For this reason, they do not take into account the conditions of complex agricultural systems and cannot be applied to them, and nor can they provide answers to general plant cultivation questions. This considerable deficit is overcome with the implementation in *REPRO*, and this study presents some possible applications and examples of the module which can be used to address important questions in plant cultivation or for sustainability assessments of farming systems. Chapter 4.1. shows how the module can explain the influence of different passes by machinery on the soil structure during the cultivation of catch crops in comparison with fallow land. In addition, the module application supports the explanation of the compaction behaviour in the case of a single crossing with a tractor in an individual test (chapter 4.2.). Another example models the risk of soil compaction of entire crop rotations with winter wheat, sugar beet and silage maize (chapter 4.3.). In Germany, these crops account for a considerable overall area (Statistisches Bundesamt, 2018). By calculating scenarios, this makes it possible to assess the risk of soil compaction associated with cultivation, and derive measures to reduce the risk, at an early stage. One example of where the analysis and assessment of the risk of soil compaction at whole farm level are carried out, is in the context of the *Deutsche Landwirtschaftsgesellschaft* (“German Agricultural Society”) sustainability certification process (DLG, 2019). Findings in this regard and an analysis of possible relationships with the underlying system are already presented in chapter 2.2.

Synthesis and general discussion

This paper concludes with a general discussion (chapter 5). In addition to the questions already raised, it begins by categorising all precompression stresses and also questions the relationship between precompression stress and texture. It also describes how the individual algorithms are reflected in the PC software *REPRO*, what limits the modelling has, and what further potential for development still exists.

2. Methodological aspects, module conception and validation

2.1. Variance of mechanical precompression stress in graphic estimations using the Casagrande method and derived mathematical models

Published in: Soil & Tillage Research 106 (2010), 165-170

Jan Rücknagel¹, Robert Brandhuber², Bodo Hofmann¹, Matthias Lebert³, Karin Marschall⁴, Rainer Paul⁵, Oliver Stock⁶, Olaf Christen¹

¹Institute of Agricultural and Nutritional Sciences, Department Agronomy and Organic Farming, University of Halle-Wittenberg, Betty-Heimann-Str. 5, 06120 Halle/Saale (Germany)

²Bayerische Landesanstalt für Landwirtschaft, Vöttinger Str. 38, 85354 Freising (Germany)

³Ingenieurbüro für Bodenphysik, Gutenbergstr. 26, 24118 Kiel (Germany)

⁴Helmholtz-Zentrum für Umweltforschung GmbH – UFZ, Permoserstr. 15, 04318 Leipzig (Germany)

⁵Thüringer Landesanstalt für Landwirtschaft, Naumburger Str. 98, 07743 Jena (Germany)

⁶Institute of Geology and Mineralogy, University of Cologne, Zülpicher Str. 49a, 50674 Cologne (Germany)

Abstract

Mechanical precompression stress is a yardstick for the strength and compressibility of soils. The default method for the estimation of precompression stress is the graphic method according to Casagrande. It involves a subjective perception by the engineer who not only determines the point of the highest curvature visually, but decides also which points are to be used for generating the virgin compression line. In order to avoid such subjective approaches, mathematical models for the determination of precompression stress have been developed emanating from the Casagrande method. These models estimate the smallest radius of the curvature based on the minimum of the second numerical derivative. The paper has the aim to quantify the variance of subjectivity implied by the person executing the graphic method, the variance of different model approaches and the accuracy of the latter in handling the graphic values. Additionally we wanted to investigate the effect of different parameters on the ordinate of the diagram and the effect of the first load step on the precompression stress. To understand these relationships, stress/bulk density functions and stress/void ratio functions measured on 13 sites were analysed by five experienced but independent engineers and by use of three mathematical models.

The mean errors of precompression stress estimations by the different testers were 0.01 to 0.12 and by the models 0.10 to 0.87 on a logarithmic scale. Expressed in kPa, increasing mean errors were observed with rising precompression stress, due to delogarithmization. For the graphical determination, they reached approx. 10 – 20 kPa at precompression stress levels of 60 to 150 kPa in typical subsoils; this means 15% on average. The handling of graphically obtained values by help of mathematical models disclosed considerable deviations between them. In the logarithmic variant, the mean absolute errors varied from 0.09 (9 kPa) to 0.40 (30 kPa) and the determination coefficients from 0.71 to 0.96. Another influence on the level of precompression

stress has been observed when different variables were plotted on the ordinate of the graph. The graphically obtained values of precompression stress and those shown in the dry bulk density graph exceed the values calculated on the basis of the void ratio by the factor 1.2 to 1.5. Furthermore, it can be stated that in soil compression tests with an initial load of 25 kPa higher precompression stress values were obtained than with lower initial loads (5 kPa), if the precompression values were low.

2.1.1. Introduction

For the estimation of precompression stress in soil experiments, the graphic determination according to Casagrande (1936) continues to be the preferred method in soil science (e.g. Feng et al., 2001; Trautner and Arvidson, 2003; Arvidson and Keller, 2004; Berli et al., 2004; Rücknagel et al., 2007). The graphic estimation of the precompression stress is done using diagrams with abscissa in logarithmic scale. The steps of the applied pressure are freely adjustable. For analyses of cultivated soils, usually initial loads between 5 kPa (Rücknagel et al., 2007) and 25 kPa (Arvidson and Keller, 2004) have been used. The highest load varies in most experiments between 400 kPa (Peng et al., 2004) and 800 kPa (Lebert, 1989; Arvidson und Keller, 2004; Keller et al., 2004). Along the ordinate of the graphs, dry bulk density, void ratio or strain are plotted. A tangent against the highest point of the curvature and a parallel to the abscissa are drawn. The point of intersection of the bisector of the angle between these two straight lines and the virgin compression line describes the precompression stress. The fitting of the tangent at the point of smallest radius of curvature and which load step is used for the virgin compression line is subject to personal judgment and thus might differ between the different experimenters. As a consequence the figures for the precompression stress might show some variance due to this personal procedure.

This has led to the development of models which are much less based on personal and subjective judgement and estimate the precompression stress according to the Casagrande method. The smallest radius of curvature might be estimated by using the second derivative directly for the measured data (e.g. Dawidowski and Koolen, 1994) or by using the minimum of an optimal fitted function (e.g. Baumgartl and Köck, 2004). Various mathematical methods are available for fitting the function to the values obtained in the soil-compression test (Sigmoidal Fit, Polynomial Fit). In some cases the resulting levels of precompression stress differ markedly (Cavaliere et al., 2008), which makes it difficult to compare absolute values of precompression stress. Therefore, the paper is targeted at:

1. Quantifying the variances of precompression stress with the Casagrande method when different assistants are involved.
2. Quantifying the accuracy of different mathematical models in rendering the graphic results.

3. Determination of the influence of different variables on the ordinate on the precompression stress.
4. Analysis to which extent the chosen initial load influences the obtained values of precompression stress.

2.1.2. Materials and methods

From data collected by Rücknagel et al. (2007), 13 soil compression tests were selected with precompression stress levels between approx. 20 kPa and 160 kPa at a matric potential of -6 kPa (pF 1.8) (Table 2.1.1). In a first step, these tests were graphically analysed by five persons each, all of them experienced in the application of the Casagrande method. The stress/bulk density functions as well as the stress/void ratio functions are given in EXCEL diagrams with single dots connected by lines. A mathematical smoothing has not been applied. Using the axes of the diagram without any scale as well as no information on the different sites we had the intention, that the person doing the assessment is not biased e.g. by the dry bulk density. The curves in the figures are given in diagrams in a size of 210 x 297 mm (DIN EN ISO 216, format A4). On the abscissa, the pressure was plotted on a logarithmic scale. The load interval of the curves was 5 to 550 kPa (8 steps).

Table 2.1.1. Test sites and precompression stress values at a matric potential of -6 kPa measured by Rücknagel et al. (2007); $\log \sigma_P$, logarithm precompression stress; σ_P , precompression stress unit kPa; ¹ FAO (1998).

Site no.	Site and depth (cm)	Taxonomy ¹	Texture (g kg ⁻¹)		$\log \sigma_P$	σ_P (kPa)
			Clay	Sand		
2	Marienborn 33-36	Haplic Phaeozem	220	90	1.68	48
3	Hechtsheim I 19-22	Chernozem	150	110	1.73	54
8	Buttstädt I 19-22	Eutric Leptosol	460	170	1.87	74
9	Wöllstein 19-22	Eutric Cambisol	310	230	2.20	159
12	Sprendlingen I 33-36	Calcaric Regosol	450	70	2.06	115
16	Bad Kreuznach I 33-36	Haplic Luvisol	360	200	2.00	100
17	Bad Kreuznach II 19-22	Haplic Luvisol	240	230	1.34	22
18	Bad Kreuznach II 33-36	Haplic Luvisol	290	210	1.70	50
19	Bernburg I 19-22	Chernozem	210	120	1.85	71
20	Bernburg I 33-36	Chernozem	210	110	1.95	89
25	Bad Lauchstädt II 19-22	Chernozem	210	110	1.40	25
27	Bernburg IV 15-25	Chernozem	200	100	1.44	28
32	Halle 15-25	Luvic Phaeozem	80	660	2.16	145

In the stress/bulk density curves, an additional variant with a load interval of 25 to 550 kPa (6 steps) each was tested. The stress/bulk density curves are not from different oedometer tests. The graphic analyses is only based without the first two load steps. The dry bulk densities were estimated with soil compression tests using soil cores. The void ratios were calculated based on this relation [void ratio = (particle density/dry bulk density) – 1]. The particle densities for the different sites ranged between 2.60 and 2.66 g cm⁻³.

Parallel to the graphic determination, precompression stress was estimated using the following models and application conditions. The models were used exclusively for estimating the pre-compression stress of stress/void ratio functions. The load interval of the curves was, according to the graphical analysis 8 steps from 5 to 550 kPa and 6 steps from 25 to 550 kPa. In the second analysis we used the curves without the first two load steps. The detailed steps of determination have been described in the cited publications:

1. Dawidowski and Koolen (1994): In this approach we have the option to take already available data from the soil compression test and mathematically smooth the data with data reduction and data filtering. In this analysis, however, we did not use those functions because the experimental data showed a typical gradient without any outlier and only eight data pairs were available for stress/strain functions. In the next step we calculated the first finite divided differences (FD), (2.1.-1) and second differences (SD), (2.1.-2), (x_i corresponds to the applied stress interval, y_i to the corresponding void ratio or dry bulk density).

$$FD_j = (y_{i+1} - y_i) / (x_{i+1} - x_i) \quad (2.1.-1)$$

$$SD_j = FD_{j+1} - FD_j \quad (2.1.-2)$$

The point with the minimum of the second differences is the point with the smallest radius of curvature of the stress/strain function. Thru this point runs a tangent with half the slope calculated from the first difference.

The virgin compression line will be found where the absolute value of SD is minimum (data pair i.e. e_v and $\log \sigma_v$). So the virgin compression line is defined by the following equation:

$$\frac{e - e_v}{\log \sigma - \log \sigma_v} = \overline{FD}_v \quad (2.1.-3)$$

\overline{FD}_v is an average slope of the vicinity values. An average of five neighbouring points is usually used according to Dawidowski and Koolen (1994):

$$\overline{FD}_v = \frac{1}{5}(FD_{v-2} + FD_{v-1} + FD_v + FD_{v+1} + FD_{v+2}) \quad (2.1.-4)$$

If, like in this experiment, only a limited number of load steps is available it is possible, that not all five data points are linear on the virgin compression line. This is not in accordance

with the Casagrande method. In the PC model used in this work, which in general uses the algorithms of Dawidowski and Koolen (1994) not five data points are used necessarily. For the odd number (e.g. 3) of the pairs, it uses a similar formula:

$$\overline{FD}_v = \frac{1}{3}(FD_{v-1} + FD_v + FD_{v+1}) \quad (2.1.-5)$$

For the even number (e.g. 4), the average value of the pairs is calculated in such a way that one additional pair at greater stresses are also included. For example, if 4 data pairs are used:

$$\overline{FD}_v = \frac{1}{4}(FD_{v-1} + FD_v + FD_{v+1} + FD_{v+2}) \quad (2.1.-6)$$

The intersection of the virgin compression line with the bisector of the angle corresponds with the precompression stress.

2. Baumgartl and Köck (2004): This model is based on the modified version (2.1.-7) of the hydraulic model of van Genuchten (1980), where the soil mechanical parameters point of maximum curvature (1st zero-point of the 3rd derivative of this function) and virgin compression line as the tangent through the inflection point (zero-point of the 2nd derivative of this function) are determined purely mathematically.

$$e = e_{\min} + (e_{\max} - e_{\min}) [1 + (\alpha\sigma)^n]^{-m} \quad (2.1.-7)$$

In our curve fittings, the maximum void ratio (e_{\max}) was set to the measured value at the beginning of each test. The minimum void ratio (e_{\min}) was freely fitted for values greater than 0.27. For smaller void ratios, the fitting was repeated with e_{\min} fixed to 0.27. The assumption of this constraint was necessary, since the unlimited compaction of a soil close to or to its particle density is physically unrealistic. The parameters α and n were freely fitted, while m was fixed using $m = 1 - 1/n$.

3. Model of the University of Weimar: It represents a laboratory-internal model of the Chair of Soil Mechanics, which has not yet been published. It is supplemented by an EXCEL table. At first, data points from the soil-compression test (x_i corresponds to the applied stress interval, y_i to the corresponding void ratio) were entered for the numerical generation of the 1st (2.1.-1) and 2nd (2.1.-8) derivative:

$$y_i'' = (y_{i+1} - 2y_i + y_{i-1}) / (x_{i+1} - x_i)^2 \quad (2.1.-8)$$

The data point with the minimum of the 2nd derivative represents the point of maximum curvature of the stress/void ratio. Then, the procedure strictly follows the Casagrande method. The straight lines are described by linear functions. Against the point of maximum curvature a tangent is drawn with the slope computed from the 1st derivative; through the point runs the bisector of the angle with the half slope and a parallel to the abscissa with zero slope. The virgin compression line cuts the last data point. The slope is then calculated

based on formula (2.1.-1) based on the last two data points. The level of mechanical pre-compression stress is obtained by equating the functions of bisector and virgin compression line.

The analysis for the precompression stress in this project was done in logarithmic calculations directly based on the diagrams or derived from the models. The stress was also given in the unit kPa (σ_p). Both options for presentation are useful in our opinion, because delogarithmization might lead to a shift in variances. For describing the variance observed between the different assistants and the models, the mean absolute error (MAE) of the precompression stress values was used. Apart from this, the maximum differences have been indicated. The accuracy of each model in handling the graphically determined values has been determined, in addition to the mean absolute error (MAE), by use of the root mean square error (RMSE), the coefficient of determination (R^2), the index of agreement (IA) as well as the slope (m) and the point of intersection (x_0) of the linear function for the comparison between graphically and mathematically calculated precompression levels. The mean absolute error (MAE) is a simple parameter to describe average differences (O_i corresponds to the observed values; P_i corresponds to the predicted values; n corresponds to the number of values):

$$\text{MAE} = \sum |P_i - O_i| / n \quad (2.1.-9)$$

The index of agreement (IA) is intended to be a descriptive measure, and it is both a relative and bounded measure which can be widely used in order to make cross-comparisons between models. For more details see Willmott (1982), (\bar{O} corresponds to the mean of the observed values):

$$\text{IA} = 1 - \left[\frac{\sum (P_i - O_i)^2}{\sum (|P_i - \bar{O}| + |O_i - \bar{O}|)^2} \right] \quad (2.1.-10)$$

2.1.3. Results and discussion

The mean absolute errors of precompression stress for these curves between the engineers and between the models were compiled in Tables 2.1.2a and 2.1.2b in log and kPa units. The results refer to the estimation in the stress/void ratio diagram. The stress/dry bulk density diagram allows principally to draw analogous conclusions (data not shown).

In graphic determinations errors from log 0.01 to 0.12 and 1 to 25 kPa were obtained. The maximum errors rank between 0.02 and 0.23 on the log scale and between 1 and 57 kPa. However, the mean errors of precompression stress between the tested models amount to 0.10 – 0.87 and 7 – 52 kPa and the maximum errors to 0.15 – 1.31 and 10 – 77 kPa.

In the kPa variant, in contrast to logarithmic scale a continuous rise of the mean absolute error was observed between manual estimation with increasing precompression stress due to delogarithmization (Figs. 2.1.1a and 2.1.1b). A transfer of the results in Figures 2.1.1b to typical arable sites would imply that for soils with low precompression stress in the range of 30 – 60 kPa, as frequently encountered in ploughed topsoils, a mean variance of 5 – 10 kPa would have to be expected between two independent testers (graphic estimation).

Table 2.1.2a. Mean (MAE) and maximum errors of precompression stress estimation between the testing persons (graphic determination) and between the models; void ratio on the ordinate of the graph; logarithmic calculation.

Site no.	Graphic calculation		Model calculation	
	MAE	Maximum errors	MAE	Maximum errors
2	0.01	0.02	0.16	0.24
3	0.12	0.23	0.44	0.66
8	0.02	0.05	0.20	0.30
9	0.07	0.16	0.10	0.15
12	0.07	0.14	0.21	0.31
16	0.08	0.18	0.38	0.57
17	0.04	0.04	0.87	1.31
18	0.07	0.17	0.29	0.43
19	0.03	0.07	0.37	0.55
20	0.05	0.10	0.15	0.23
25	0.07	0.17	0.31	0.46
27	0.03	0.04	0.40	0.60
32	0.11	0.16	0.31	0.47

Table 2.1.2b. Mean (MAE) and maximum errors of precompression stress estimation between the testing persons (graphic determination) and between the models; void ratio on the ordinate of the graph; unit kPa.

Site no.	Graphic calculation		Model calculation	
	MAE	Maximum errors	MAE	Maximum errors
2	1	2	17	27
3	5	9	16	23
8	2	5	16	24
9	25	57	23	35
12	10	21	23	35
16	18	37	51	77
17	1	3	14	21
18	6	14	17	25
19	5	10	29	43
20	7	15	17	25
25	2	6	7	10
27	1	1	17	25
32	25	38	52	77

In case of higher precompression stress (60 to 150 kPa), as usual in subsoils, errors of 10 to 20 kPa in graphical determinations are possible. Thus, the mean errors for the tested range of precompression stress is about 15 % between the testers in the graphic procedure.

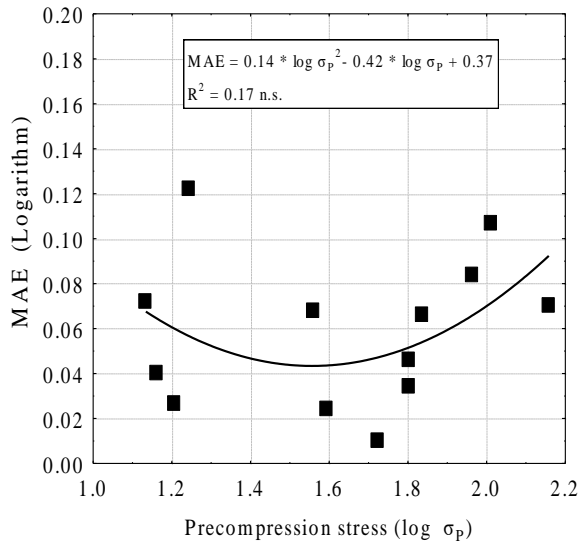


Figure 2.1.1a. Mean error of precompression stress estimation (MAE) between the testing persons (graphical determination) in dependence on the precompression stress level; logarithmic calculation.

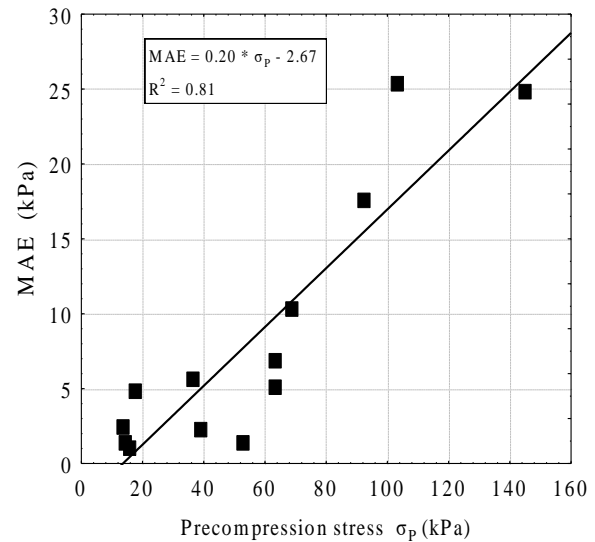


Figure 2.1.1b. Mean error of precompression stress estimation (MAE) between the testing persons (graphical determination) in dependence on the precompression stress level; unit kPa.

Apart from the variance between the models and between the different test persons, importance has to be attached to the accuracy of the different models in the handling of the graphic results. Here, the mean values of the five graphic estimations in the frame of these studies can be used as a basis for comparison of the models. Important statistic parameters for the accuracy rating are given in Tables 2.1.3a and 2.1.3b. There are essential deviations among the applied models. The best description of the graphically obtained precompression values has been provided by the Weimar model. It furnished mean absolute errors of 9 kPa (logarithmic estimation: 0.09) and RMSE of 11 kPa (logarithmic form: 0.11). Coefficient of determination and index of agreement are very high. The variate pairs of the comparison between graphically obtained and computed precompression stress agree well with the course of the 1:1 curve ($m=0.88$ or 0.91 ; $x_0=0.19$ or 2.6). According to the method developed at the university of Weimar, the second derivative was calculated using three data pairs (formula 2.1.-8). Such a small number of experimental data pairs might have substantial effects on the precompression stress. The use of the last two data points for the virgin compression line is also an intrinsic problem of the method, because the shape of the stress/void ratio function can be affected by the highest load steps chosen. In our work we did not vary the highest load steps. For that reason we are unable to quantify the effects on the accuracy of the model. In general we would recommend applying a

high number of load steps, in order to improve the quality of the stress/strain functions. On the other hand, this greatly increases the duration of the measurements with the risk of a partial drying of the soil samples. This is the reason why in most experiments only 6 (Arvidson and Keller, 2004) to 16 (Gysi, 2001) load steps were chosen.

Table 2.1.3a. Error parameters for the models compared with graphical determination; logarithmic calculation.

	Dawidowski and Koolen (1994)	Baumgartl and Köck (2004)	University of Weimar
Mean absolute error (MAE)	0.40	0.11	0.09
Root mean square error (RMSE)	0.47	0.16	0.11
Coefficient of determination (R^2)	0.79	0.78	0.89
Index of agreement (IA)	0.74	0.92	0.97
Slope (m)	1.28	0.71	0.88
Intercept (x_0)	-0.86	0.45	0.19

Table 2.1.3b. Error parameters for the models compared with graphical determination; unit kPa.

	Dawidowski and Koolen (1994)	Baumgartl and Köck (2004)	University of Weimar
Mean absolute error (MAE)	30	15	9
Root mean square error (RMSE)	36	24	11
Coefficient of determination (R^2)	0.91	0.71	0.96
Index of agreement (IA)	0.74	0.85	0.98
Slope (m)	0.52	0.52	0.91
Intercept (x_0)	-2.6	17.9	2.6

The largest differences (MAE and RMSE) were recorded in the approach by Dawidowski and Koolen (1994). In this model, the variate pairs in the logarithmic chart show a considerably steeper slope than the 1:1 line ($m=1.28$), however, after delogarithmization to kPa they become markedly flatter ($m=0.52$). Also the values determined according to Baumgartl and Köck (2004) show a flatter course than the 1:1 line ($m=0.71$ or $m=0.52$). The points of intersection

x_o with the ordinate were above zero. According to this, low precompression levels may be overestimated and high loads underestimated. The MAE with 15 kPa and the RMSE with 24 kPa rank in the midfield of the tested models and confirm the range compared by Baumgartl and Köck (2004) (p. 63, Table 4). Thus, no model fulfilled entirely the hopes for high accuracy in the representation of precompression stress values obtained with the graphic model. Moreover, they are not completely free from subjective decisions. For example, users of the methods by Dawidowski and Koolen (1994) may decide whether the function „Reduction“ or „Filtering“ should be applied for smoothing the experimental data. In the present paper, neither of them has been applied, because the authors considered the course of the test data as typical without marked outliers, and not more than eight pairs of variates were available for each stress-strain test.

Experiments by Mosaddeghi et al. (2003) revealed that precompression stress values in kPa units, obtained in the stress/bulk density graph, were 1.3 times higher than the values determined in the stress/void ratio graph. The same observation has been made with the graphic method in our study. According to this, stress values obtained on the basis of the dry bulk density in logarithmic form ranked constantly 0.08 – 0.10 above the values computed by means of the void ratio (Fig. 2.1.2a). An increasing differentiation with rising precompression stress in graphical determinations is shown by the kPa units (Fig. 2.1.2b).

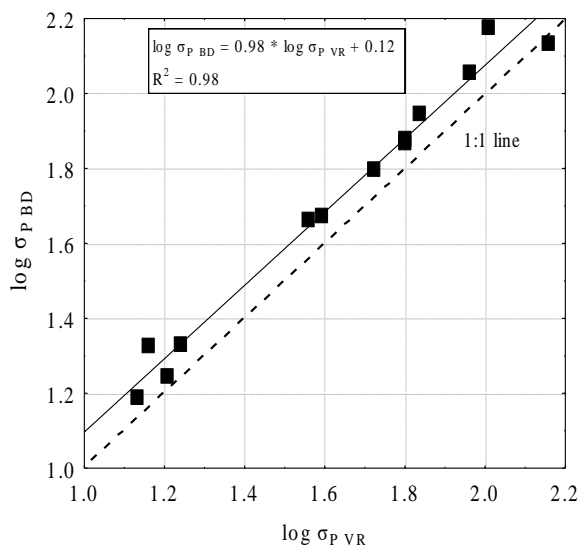


Figure 2.1.2a. Relationship between the precompression stress values graphical determined in a stress/void ratio graph ($\log \sigma_{P\ VR}$) and a stress/dry bulk density graph ($\log \sigma_{P\ BD}$); logarithmic calculation.

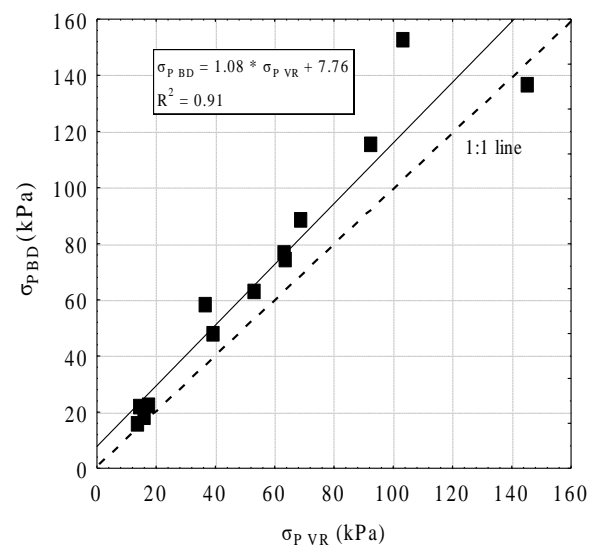


Figure 2.1.2b. Relationship between the precompression stress values graphical determined in a stress/void ratio graph ($\sigma_{P\ VR}$) and a stress/dry bulk density graph ($\sigma_{P\ BD}$); unit kPa.

Mosaddeghi et al. (2003) explained the differences in precompression stress by a non-linear relationship between dry bulk density and void ratio. These non-linear relationships lead to a

course of the stress/void ratio curve below the stress/dry bulk density curve when the starting and end points of the curves were coincident (Fig. 2.1.3). As result, the point of maximum curvature is shifted towards lower stress levels, and the slope of the virgin compression line becomes less steep. Generally, the investigations demonstrated that for comparisons of absolute precompression stress levels the same variable on the graph ordinate has to be used or it would be recommendable to convert the precompression stress values.

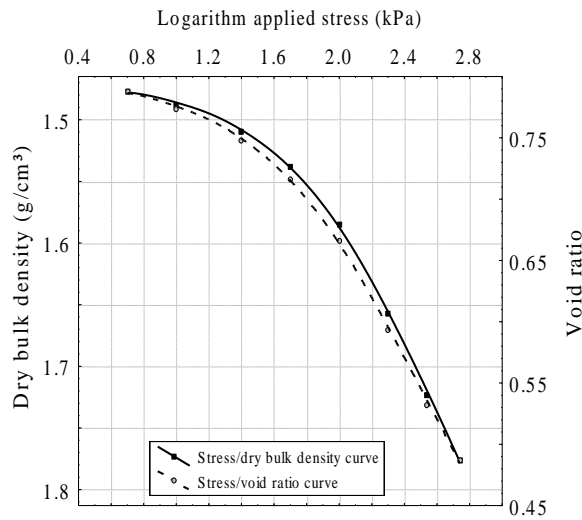


Figure 2.1.3. Course of stress/void ratio and stress/dry bulk density curves on the example “Bad Kreuznach I 33-36” (Table 1, site no. 16).

Beside the ordinate variables, also the first load step in diagrams influenced the precompression stress. In this paper, an increase of the first load step from 5 to 25 kPa caused an overestimation of low precompression stress levels (Fig. 2.1.4).

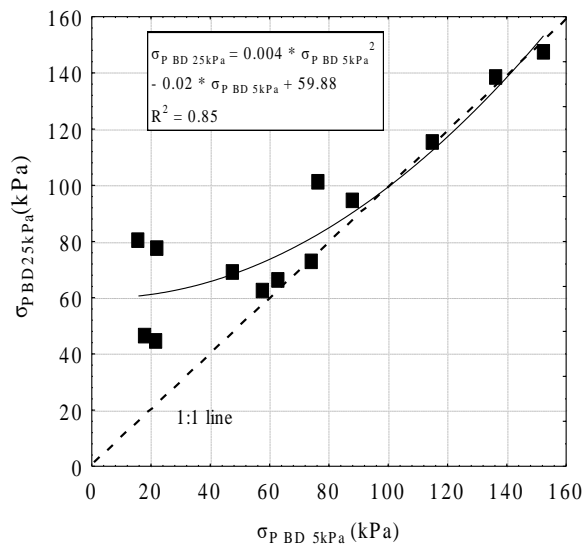


Figure 2.1.4. Relationship of precompression stress levels graphical determined in the stress/dry bulk density graph at an initial load of 5 ($\sigma_{P BD 5kPa}$) and 25 kPa ($\sigma_{P BD 25kPa}$); unit kPa.

This concerns mainly values < 60 kPa, where overestimation reached up to approx. 80 kPa. The same effect has been observed also with the models by Dawidowski and Koolen (1994) and the Weimar method (Fig. 2.1.5).

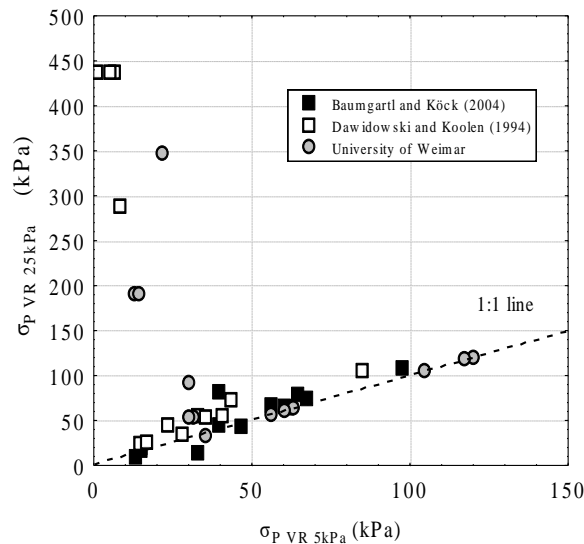


Figure 2.1.5. Relationship of precompression stress levels determined with the models in the stress/void ratio graph at an initial load of 5 ($\log \sigma_{P VR 5kPa}$) and 25 kPa ($\log \sigma_{P VR 25kPa}$); unit kPa.

Precompressions below 50 kPa were overestimated by up to 400 kPa. Only the values computed by Baumgartl and Köck (2004) followed largely the course of the 1:1 line. In this case it might be useful to determine the point of highest curvature on a generated function and not on single values, because this allows to get derivatives in the peripheral areas of the low, here not depicted load intervals. Therefore, loosened soils with low precompression stress, recommend to apply trials with low initial axial load (≤ 10 kPa) or to use the model of Baumgartl and Köck (2004). With increasing precompression stress, the values obtained by graphical determination and by use of the models by Dawidowski and Koolen (1994) as well as from Weimar University furnish approximate results, and therefore it is sufficient for soils with expected high precompression stress to start the stress-strain tests at an initial load of 25 kPa.

2.1.4. Conclusions

The study allows to draw the following conclusions on the use of the graphic method and the tested mathematical models for estimating mechanical precompression stress:

1. The mean error of precompression stress values obtained with the graphic method according to Casagrande reaches about 15%, which is low and a tolerable level for most practical purposes. A participation of several independent persons may further improve the variance values and thus also reproducibility and comparability of the obtained results.

2. No model fulfilled entirely the hopes for high accuracy in the representation of precompression stress values obtained with the graphic model. The method developed at the University of Weimar and the model by Baumgartl and Köck (2004) are mostly qualified for the reproduction of graphic values.
3. When absolute precompression stress situations are to be compared, attention should be paid to which parameter is placed on the ordinate of the chart; this refers to both the applied models and the graphic analysis. Regarding the original publication by Casagrande (1936), it seems to be purposeful to consider the void ratio.
4. The stress-strain tests and the plotting of the curves should start at a low load level (≤ 10 kPa), especially if the given site is characterized by low precompression stress.

Acknowledgements

The authors would like to thank Dr. M.R. Mosaddeghi, Department of Soil Science, Bu-Ali Sina University Hamadan, Iran, for his assistance in the computing of precompression stress according to the method by Dawidowski and Koolen (1994) and also Prof. Dr. T. Schanz, University of Weimar, for the permission to use the laboratory-internal method for the estimation of precompression stress. We would like to thank Prof. Dr. J. Spilke, Biometrics and Informatics in Agriculture, University of Halle-Wittenberg for his advice on the statistical analysis.

2.2. Indicator based assessment of the soil compaction risk at arable sites using the model *REPRO*

Published in: Ecological Indicators 52 (2015), 341-352

Jan Rücknagel¹, Bodo Hofmann¹, Peter Deumelandt², Frank Reinicke², Jana Bauhardt^{1,2}, Kurt-Jürgen Hülsbergen³, Olaf Christen¹

¹ Institute of Agricultural and Nutritional Sciences, Department Agronomy and Organic Farming, University of Halle-Wittenberg, Betty-Heimann-Str. 5, 06120 Halle/Saale (Germany)

² Privates Institut für Nachhaltige Landbewirtschaftung GmbH, Reilstr. 128, 06114 Halle/Saale (Germany)

³ Technische Universität München, Lehrstuhl für Ökologischen Landbau und Pflanzenbausysteme, Liesel-Beckmann-Straße 2, 85354 Freising (Germany)

Abstract

Soil compaction impairs all essential soil functions, which are crucial for the lives of humans, animals, plants and soil organisms. In order to secure the various soil functions, soil compaction must be avoided. One successful method of preventing soil compaction could be based on the precautionary principle, and mathematical modelling might be used to support farmers or consultants when making decisions about husbandry operations. This paper presents a model which calculates an indicator and assesses the risk of soil compaction on arable land based on site-specific data including information on soil, weather and specific husbandry. The first step is to estimate the soil strength in response to soil stress for a topsoil (20 cm) and a subsoil (35 cm) layer. The estimations of these parameters take into account changes in soil moisture throughout the year. Soil strength compared with soil stress is used to calculate the indicator Soil Compaction Index (SCI) for each time the machinery passes over the soil. The results from the separate passes are then integrated for a comprehensive assessment of the risk of soil compaction at farm level. The model was validated in numerous trials. It was found that the calculated SCI was a good reflection of the actual change in soil structure. The model is already being applied on arable farms in Germany. As an example presented in this paper, the calculations for the subsoil at these farms result in low to medium compaction risks.

2.2.1. Introduction

Arable land is required to ensure the production of food and renewable resources in the long term. It also serves as a habitat for many wild plants and soil fauna. This is why protecting the soil on such land is a key objective of sustainable land management. Apart from maintaining soil organic matter, this also includes avoiding wind and water erosion (Van Dijk and Bruijnzeel, 2003) as well as anthropogenic soil compaction (Bojorquez-Tapia et al., 2013).

The occurrence of soil compaction down to the subsoil has already been reported on particularly frequently in regions where agriculture is highly industrialised (e.g. Fulajtár, 2000; Houšková, 2002). In these regions the increasing size of arable crop farms as well as contract work on larger farms is increasing the need for farm machinery with greater traction. The reason for this tendency reflects the economies of scale in arable farming. The need for combine harvesters with greater traction and larger holding tank capacities inevitably causes higher axle loads. As a consequence, the risk of harmful compaction in agricultural soil, especially under wet conditions and where little soil strength is present, increases dramatically (Arvidsson et al., 2003; Trautner and Arvidsson, 2003; Rücknagel et al., 2012a).

Soil compaction severely restricts a number of important ecological soil functions (Nawaz et al., 2013). Air capacity decreases and gas exchange is restricted (Ball and Robertson, 1994; Horn and Rostek, 2000). Another likely consequence of soil compaction and the establishment of platy and coherent soil structures is reduced water infiltration, with water run-off and erosion (Horn et al., 1995). In some cases even yield decrease has been observed (Voorhees, 2000). Additionally, soil compaction in the subsoil may persist for considerably long periods of time (Alakukku, 1996; Berisso et al., 2012).

This means that in order to maintain the various soil functions it is absolutely imperative to avoid soil compaction. General recommendations for reducing the risk of soil compaction, especially in the subsoil, have already been described (Schjonning et al., 2012). While there have been approaches involving the creation of large-scale maps identifying regions with different levels of susceptibility to soil compaction (van den Akker and Hoogland, 2011), these do not sufficiently allow for individual and regional agricultural management conditions.

However, complicated interactions mean that it is extremely difficult to perform a sound quantitative risk assessment based upon site-specific details concerning soil, weather and husbandry. Therefore the only feasible approach is to use mathematical modelling, which incorporates the fundamental processes for analysis and recommendation and thus reduces the need for expensive and time-consuming measurements. Different procedures for calculating the stress propagation and deformation behaviour mean a distinction is made between two model types – numerical (finite element method) and pseudo-analytic models (Defosse and Richard, 2002). Numerical models allow the three-dimensional stress distribution and resulting deformations to be calculated simultaneously, and they also consider both volume changes and shearing processes. However, they do require a large number of mechanical parameters and are particularly well suited to specific issues and individual case studies (Poody et al., 2003). On the other hand, the pseudo-analytic models often reduce the stresses from the wheel to the vertical stress in the load axle as the only stress component, meaning they only require a small number of input parameters. Calculation is based on the theories by Boussinesq and Fröhlich (cited in Söhne, 1953). Pseudo-analytic models only define input-output relationships, such as vertical principal stress at a specific soil depth compared with soil strength, without mapping the process. Their

comparatively simple structures and the smaller amount of data they require mean they are highly suited to application-oriented consultation and training models.

Recent pseudo-analytic modelling approaches tend to focus on the effect of single machinery passes or working steps (e.g. O'Sullivan et al., 1999; Keller et al., 2007). Despite this, we understand the risk of soil compaction to be one single component in a complex farming system, a system which requires an understanding of the individual site's soil, weather and husbandry conditions. With this in mind, the approach to assessing the risk of soil compaction in arable land presented in this paper is an integrated module in the *REPRO* software programme (Küstermann et al., 2008; Küstermann et al., 2010). Its incorporation into *REPRO* is important because *REPRO* provides all the necessary information concerning the timing and types of husbandry activities as well as all available details about machinery. The need for additional input parameters in order to calculate the soil compaction risk is therefore low. Combined with the soil water content data from a specific site, this approach allows for the calculation of the soil compaction risk for that very farm. Compared with other models, the module is also equipped with a number of modified or specially developed algorithms and regression equations, especially for the estimation of soil strength. The *REPRO* module can be used by trained farmers and consultants. As well as describing the module, this article presents extensive validations as well as results from the module's previous application on arable farms in Germany.

2.2.2. Materials and methods

2.2.2.1. Module structure and algorithms

The *REPRO* computer model (*REPRO*duction of soil fertility) is a complex balance model used to describe material and energy flows as well as for the ecological and economic assessment of farms (Küstermann et al., 2008; Küstermann et al., 2010). *REPRO* is divided into individual and interconnected modules, which are used for instance to quantify carbon fluxes and greenhouse gas emissions, to calculate energy balances (Hülsbergen et al. 2001) or to estimate the risk of soil erosion. The module presented in this paper enables the calculation and assessment of the soil compaction risk in the topsoil (20 cm depth) and subsoil (35 cm depth) of arable land.

2.2.2.2. Validation of the module

This paper focuses primarily on validations of the algorithms used for comprehensive assessment; the validation of individual regression models, such as for the calculation of soil strength based on water content, has already been demonstrated in previous papers (e.g. Rücknagel et al., 2012a). For the purposes of validation, numerous field trials were carried out and the Soil Compaction Index calculated in parallel using *REPRO*. To begin with, trials were performed involving passes with individual machines so as to verify how accurate the calculation of the Soil Compaction Index was for single working steps (SCI_{SP}) (Table 2.2.1 Part A).

Table 2.2.1. Description of the test sites and machinery parameters for the module validation; SOM - soil organic matter, SWC - soil water content at wheeling time; ¹ FAO soil classification; ² axle with the highest load; ³ description according to Koch et al. (2008).

Site code	Site and depth (cm)	Taxonomy ¹	Texture (g kg ⁻¹)			SOM (g kg ⁻¹)	SWC (%FC)	Wheel load ² (kg)	Inflation pressure ² (kPa)	Wheel dimension ²
			Clay	Silt	Sand					
Part A: Passes with single machines										
1.1.	Lossa 20	Albic Luvisol	150	690	160	17	97	6700	300	1050/50 R 32
1.2.	Lossa 35	Albic Luvisol	250	670	80	6	95	6700	300	1050/50 R 32
2.1.	Zwenkau I 20	Haplic Albeluvisol	110	660	230	28	75	4000	70	20.8 R 38
2.2.	Zwenkau I 35	Haplic Albeluvisol	110	660	230	10	86	4000	70	20.8 R 38
2.3.	Zwenkau II 20	Haplic Albeluvisol	110	660	230	28	75	4000	90	20.8 R 38
2.4.	Zwenkau III 20	Haplic Albeluvisol	110	660	230	28	75	4000	130	20.8 R 38
2.5.	Zwenkau IV 20	Haplic Albeluvisol	110	660	230	28	75	4000	170	20.8 R 38
2.6.	Zwenkau IV 35	Haplic Albeluvisol	110	660	230	10	86	4000	170	20.8 R 38
3.1.	Rothenberga I 20	Albic Luvisol	190	600	210	17	93	7200	250	1050/50 R 32
3.2.	Rothenberga II 20	Albic Luvisol	140	810	50	22	83	2000	160	18.4 R 30
3.3.	Rothenberga III 20	Albic Luvisol	140	810	50	22	83	1150	160	18.4 R 30
3.4.	Rothenberga IV 20	Albic Luvisol	140	810	50	22	83	1150	60	18.4 R 30
3.5.	Rothenberga V 20	Albic Luvisol	140	810	50	22	90	4300	80	680/75 R 32
3.6.	Rothenberga VI 20	Albic Luvisol	130	780	90	21	95	4100	80	680/75 R 32
3.7.	Rothenberga VII 20	Albic Luvisol	160	750	90	18	88	1500	80	480/70 R 38
3.8.	Rothenberga VIII 20	Albic Luvisol	160	750	90	18	88	1900	300	12.5-20
3.9.	Rothenberga IX 20	Albic Luvisol	160	750	90	18	88	1900	550	9.00-20
4.1.	Friemar 20	Haplic Phaeozem	250	720	30	-	85	4100	250	650/75 R 32
4.2.	Friemar 35	Haplic Phaeozem	250	720	30	-	82	4100	250	650/75 R 32

Table 2.2.1 (continuation). Description of the test sites and machinery parameters for the module validation; SOM - soil organic matter, SWC - soil water content at wheeling time; ¹ FAO soil classification; ² axle with the highest load; ³ description according to Koch et al. (2008).

Site code	Site and depth (cm)	Taxonomy ¹	Texture (g kg ⁻¹)			SOM (g kg ⁻¹)	SWC (%FC)	Wheel load ² (kg)	Inflation pressure ² (kPa)	Wheel dimension ²
			Clay	Silt	Sand					
Part A: Passes with single machines										
5.1.	Fortuna I 20	Calcaric Regosol	150	800	50	24	75	5400	105	650/65 R 42
5.2.	Fortuna I 35	Calcaric Regosol	150	800	50	24	75	5400	105	650/65 R 42
Part B: Passes along permanent traffic lanes										
6.1.	Rothenberga X 20	Albic Luvisol	130	820	50	18	86-95	3000	130	16.9 R 38
7.1.	Fortuna II 20	Calcaric Regosol	150	800	50	24	75	5400	105	650/65 R 42
7.2.	Fortuna II 35	Calcaric Regosol	150	800	50	24	75	5400	105	650/65 R 42
Part C: Passes with random traffic on field level										
8.1. ³	Harste FBMW 20	Stagnic Luvisol	120	830	50	11	99-109	9330-10360	200-310	1050/50 R 32
8.2. ³	Harste FBMW 35	Stagnic Luvisol	120	830	50	8	87-102	9330-10360	200-310	1050/50 R 32
8.3. ³	Harste LBW 35	Stagnic Luvisol	120	830	50	8	98-104	9330-10360	200-310	1050/50 R 32
9.1.	Halle 20	Luvic Phaeozem	80	260	660	20	100	1700-1900	120-175	e. g. 16.9 R 34, 480/70 R 34
10.1.	Hechtsheim II 20	Chernozem	150	700	150	50	47-99	1100-10000	95-250	e.g. 270/80 R 32,
10.2.	Hechtsheim II 35	Chernozem	170	740	90	54	47-99	1100-10000	95-250	540/65 R 30
11.1.	Wöllstein 20	Eutric Cambisol	310	460	230	32	49-99	1100-11000	180-250	e.g. 16.9 R 34,
11.2.	Wöllstein 35	Eutric Cambisol	290	450	260	40	49-99	1100-11000	180-250	620/75 R 34
12.1.	Großstorkwitz 20	Chernozem	220	680	100	43	53-100	1800-8300	80-360	e.g. 18.4 R 38,
12.2.	Großstorkwitz 35	Chernozem	220	680	100	33	53-100	1800-8300	80-360	800/70 R 38

This was to help identify potential error ranges that would otherwise be included in the rest of the comprehensive assessment. This was followed by more complex trials aimed at testing how accurate the calculation of the Soil Compaction Index was for passes with permanent traffic lanes (SCI_{PTL}) and random traffic lanes (SCI_{RT}) (Table 2.2.1 Parts B and C). The trials with permanent traffic lanes involve single-year results with between six and ten passes each, while the validation of the Soil Compaction Index for passes with random traffic include up to six trial years. This also enables the verification of whether calculation is possible for longer periods.

Sites with a broad textural range were selected (80-310 g kg⁻¹ clay, 50-660 g kg⁻¹ sand). Be that as it may, one area of focus is soils from the “Silt Loam” textural class. On the days when the passes were performed, soil water content was between 47 and 109 per cent of the respective field capacity. This means that the range of soil water content levels for arable crops commonly found in Central Europe was largely covered. During the trials involving passes with single machines and passes along permanent traffic lanes, the respective soil water content was determined directly on site at the time of the pass, and the values added to *REPRO*. The calculation of the Soil Compaction Index for passes with random traffic on field level, however, was based on modelled soil water content data from the German Weather Service. Here it was not possible to measure the soil water content each time the ground was driven over.

Most of the machines used were fitted with radial tyres of different sizes. In individual cases some machines had cross-ply tyres. The inflation pressure varied between 60 and 550 kPa. This was measured on each machine. The wheel load, however, had to be estimated in some cases based on technical specifications provided by the machine manufacturer; overall it was between 1100 and 11000 kg.

In the calculations, the input parameter used for soil strength in the topsoil (20 cm) is also pre-compression stress. When validating the model this has the advantage that the change in soil structure can be considered directly in relation to the Soil Compaction Index. The intention was that the Soil Compaction Index would be able to reflect changes in structure caused by the soil being driven over. As a rule, precompression stress was calculated with *REPRO* according to equation (2.2.-1) using dry bulk density and aggregate density. Both of these parameters were determined for the trial areas. This does not include trials 3.7 – 5.2. and 7.1 – 7.2. (Table 2.2.1), where the precompression stress levels measured at field capacity were used directly.

During each of the validation trials, soil core samples (volume 250 cm³, n=8-12) were taken at soil depths 17-23 cm (approximately 20 cm) and 32-38 cm (approximately 35 cm) before the first pass over the soil as well as after the last pass or after the investigation period had ended. These were used to identify the dry bulk density and saturated hydraulic conductivity of the soil. The dry bulk density corresponds to the quotient of the dry mass of a naturally deposited soil sample and its total volume (unit g cm⁻³). It is a measure of the state of soil compaction. Saturated hydraulic conductivity is the parameter of Darcy’s law applied to saturated water movement within the soil as a measure of the hydraulic permeability of water-saturated soil (unit cm d⁻¹). Apart from size and shape, soil permeability for water is influenced heavily by

pore continuity. Determination takes place in a stationary facility according to the principle described by Klute and Dirksen (1986). In the following, the change in saturated hydraulic conductivity is shown as the difference between the logarithms before the soil was driven over and afterwards (or after the investigation period had ended), because, according to the Shapiro-Wilk test, the saturated hydraulic conductivities and their differences are not normally distributed.

2.2.2.3. Examples of module application

So far, the *REPRO* module has been applied on 15 conventional farms – for a period of two years each – in order to assess the risk of soil compaction on arable land as part of the German Agricultural Society's (*Deutsche Landwirtschafts-Gesellschaft – DLG*) "Sustainable Agriculture" certification process (Table 2.2.2; farms no. 1-13 years 2011-2012, farm no. 14 years 2010-2011, farm no. 15 years 2006-2007). The DLG's "Sustainable Agriculture" certificate involves examining sustainability based on different ecological (e.g. nitrogen balance, strength of crop protection agents, risk of soil erosion and compaction), economic (e.g. changes in equity and profit rate) and social (e.g. employee participation and social engagement) indicators. Taken together, these individual indicators give a general overview of how sustainable the respective farm is. This can shed light on strengths and weaknesses, allowing the farmer to take specific action to improve certain areas.

The farms where the module has been used to assess the risk of soil compaction are spread across almost the whole of Germany. The individual sites' average annual rainfall varies between around 550 and 850 mm, and the mean annual air temperature is between 8.5 and 10.5 °C. The most common soil texture classes in the topsoil are "Loamy Sand", "Sandy Loam", "Loam" and "Clay Loam". The size of the farms (arable land) is between 38 and 2224 ha. Winter wheat is the principle crop on each farm, accounting for up to 69 per cent of the respective arable land. Cultivation on some of the farms is dominated by other combine crops such as winter rape and winter barley (e.g. farms no. 7 and 12). Some of the other farms have very high levels of maize or sugar beet (e.g. farms no. 1, 3 and 4). Tillage is mostly performed conventionally using a plough. Just three farms (farms no. 2, 10 and 13) carry out conservation tillage without a plough on virtually all their arable land. Some of the farms' machinery is very small, with wheel loads of less than 2000 kg, although some larger machines with wheel loads of more than 10000 kg are also used. There is a correspondingly wide range of inflation pressures of between 50 and 500 kPa. In most cases involving single passes with machinery – above all passes along permanent traffic lanes – the wheeled area is equivalent to less than 5% of the total land area. Especially when harvesting sugar beet, it is possible that the entire area will be driven over (wheeled area of single passes 100%). All in all, the farms included in the module's application cover the major site and climatic conditions, farm sizes and conventional arable farming systems typically found in Germany.

Table 2.2.2. Characterisation of farms on module application.

Farm No.	Site characterisation		Farm characterisation			Machinery characterisation			
	Annual precipitation (mm)	Mean annual temperature (°C)	Frequent soil texture	Arable land (ha)	Important crops and their share of arable land (%)	Share of conservation tillage (%)	Wheel loads (kg)	Inflation pressures (kPa)	Wheeled area of single passes (%/100)
1	857	8.7	Sandy Loam	80	Winter wheat (42), Silage maize (29), Winter rape (23)	30	1700-4200	120-160	0.05-0.58
2	743	8.6	Clay Loam	94	Winter wheat (60), Sugar beet (24), Winter rape (15)	100	3000-5550	50-120	0.04-0.53
3	743	8.6	Sandy Loam, Clay Loam	102	Winter wheat (33), Potato (31), Sugar beet (30)	67	1650-7450	100-250	0.04-0.71
4	817	8.4	Sandy Loam	77	Winter wheat (37), Silage and grain maize (33), Winter barley (13)	46	2100-4800	120-200	0.07-0.84
5	743	8.6	Loam	38	Winter wheat (40), Potato (28), Sugar beet (16)	32	2200-7800	80-350	0.02-0.83
6	642	10.8	Loam	105	Winter wheat (47), Winter rape (17), Silage maize (12)	26	1800-4800	140-250	0.04-0.89
7	623	9.7	Loam	97	Winter wheat (38), Winter rape (23), Winter barley (12)	73	1950-8400	150-300	0.04-0.70
8	746	9.7	Loamy Sand, Loam	175	Winter wheat (37), Silage and grain maize (27), Winter barley (15)	54	2250-8050	100-150	0.04-0.59

Table 2.2.2 (continuation). Characterisation of farms on module application.

Farm No.	Site characterisation		Farm characterisation				Machinery characterisation		
	Annual precipitation (mm)	Mean annual temperature (°C)	Frequent soil texture	Arable land (ha)	Important crops and their share of arable land (%)	Share of conservation tillage (%)	Wheel loads (kg)	Inflation pressures (kPa)	Wheeled area of single passes (%/100)
9	552	8.5	Clay Loam, Clay	2224	Winter wheat (41), Winter rape (19), Winter barley (8)	77	1900-9250	100-200	0.03-1.00
10	544	8.5	Sandy Loam, Clay Loam	1635	Winter wheat (40), Winter rape (18), Spring barley (17)	94	2100-12450	100-240	0.04-1.00
11	567	8.5	Loam, Clay Loam	1844	Winter wheat (47), Winter rape (18), Silage maize (10)	84	2350-8300	100-500	0.02-0.89
12	516	8.9	Loamy Sand, Loam	902	Winter wheat (53), Winter rape (27), Winter barley (16)	38	3100-8400	70-120	0.03-0.47
13	636	9.7	Loam	153	Winter wheat (64), Sugar beet (30), Pasture (4)	100	1750-11000	100-240	0.04-1.00
14	732	9.5	Loamy Sand, Sandy Loam	709	Winter wheat (69), Sugar beet (17), Silage maize (9)	52	2200-6850	80-180	0.04-1.00
15	589	9.2	Sandy Loam	1341	Winter wheat (33), Winter rape (19), Silage maize (13), Sugar beet (6)	61	1900-6850	100-240	0.02-1.00

The calculation of the Soil Compaction Index using REPRO was based on farming data provided by the farms themselves, soil water content information calculated by the German Weather Service as well as standard values concerning each soil type's strength. All information about inflation pressure came directly from the farms, while the wheel loads were calculated based on machinery specifications.

2.2.3. Results and discussion

2.2.3.1. Module structure and algorithms

The module links soil water content, the soil strength in the face of mechanical stresses, and resulting soil stress in a number of calculation steps through to evaluating the compaction risk at farm level (Fig. 2.2.1). To this end, the module uses previously entered land management data with the appropriate agronomic dates. It contains numerous databases. Regression equations serve to calculate individual values step by step.

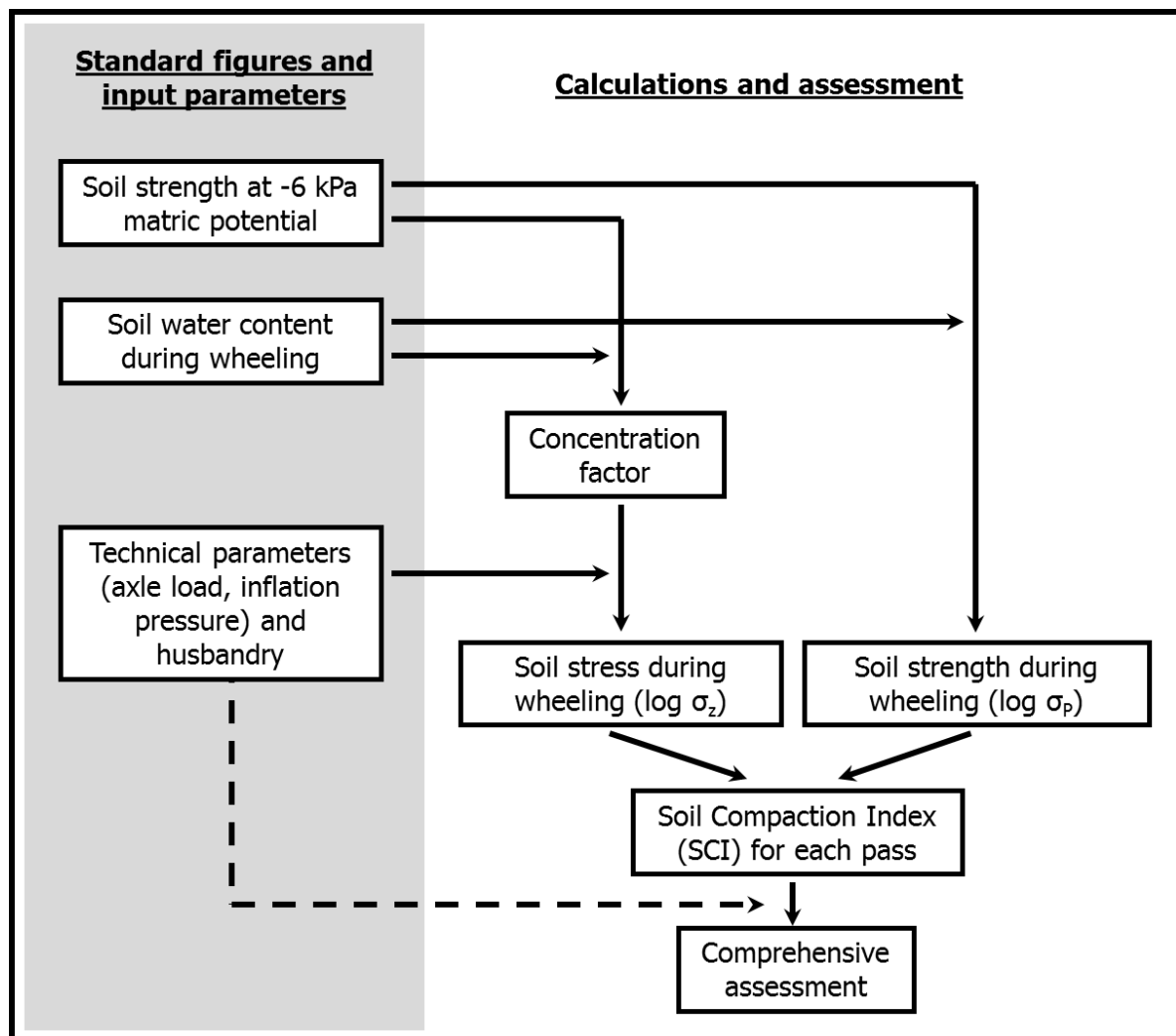


Figure 2.2.1. Conception and calculation steps for the soil compaction risk indicator (Soil Compaction Index) in the *REPRO* module.

2.2.3.1.1. Soil water content data

Soil strength and stress propagation in the soil are heavily influenced by a soil's water content at the moment when machinery is driven over it, which is why soil water content represents an important input parameter in the module. In Central Europe, soil water content is subject to a seasonal cycle characterised in principle by decreasing water content levels when vegetation begins in the spring, a minimum in the summer months and the recovery of water content levels in the autumn. Just how pronounced this seasonal cycle is depends on a site's geographic location, the actual weather conditions and growing season in any one year, soil properties and the crop grown. In order to account for these factors, a database was integrated into REPRO containing data on soil water content as a percentage of field capacity on a daily basis for different sites, two soil depths (20 and 35 cm) and three groups of crop type with similar growth patterns (1: cereals, grain legumes, 2: root and leaf crops, 3: perennial fodder plants).

When the module has been used so far, in most cases soil water content levels calculated by the German Weather Service (DWD) have been used. These are available across Germany for up to 180 climate stations. Furthermore, the existing data can be added to at any time – for example by including data from elsewhere, such as from series of experiments.

2.2.3.1.2. Estimation of soil strength

For soil strength, different target values are used at both depths. At a depth of 35 cm (subsoil), maintaining precompression stress guarantees that the existing soil structure remains largely unaffected in terms of its geometry and pore volume. It is difficult for soil in this layer to recover from compaction through tillage and agronomic measures alone. By contrast, in the lower topsoil (20 cm depth) soil strength depends on the minimum requirements for intact soil structure (air capacity ≥ 8 per cent by volume, saturated hydraulic conductivity $\geq 10 \text{ cm d}^{-1}$) (Werner and Paul, 1999). For the topsoil, taking these values as a basis is more beneficial than using precompression stress, because soil structure – and hence precompression stress as well – is subject to constant change, partly because of soil tillage. This also ensures the long-term preservation of important soil properties and the yield function when permanently switching to conservation tillage. In order to estimate soil strength as a logarithm of the stress value (unit kPa) at a matric potential of -6 kPa (which corresponds to field capacity in German-speaking countries) at depths of 20 and 35 cm, users of the model have several options depending on data availability:

1. Soil strength ($\log \sigma_{P-6\text{kPa}}$) is determined using a method by Rücknagel et al. (2007) based on dry bulk density (BD) and aggregate density (AD) at a matric potential of -6 kPa for each of a farm's fields (2.2.-1):

$$\log \sigma_{P-6\text{kPa}} = -3.15 * AD/BD + 0.60 * BD + 4.49 \quad (2.2.-1)$$

If no measurement data are available for the dry bulk density and aggregate density, standard values may be used for the respective soil depth. These are linked to the main soil texture

classes (“Loamy Sand”, “Sandy Loam”, “Silt Loam”, “Loam”, “Clay Loam”, “Clay”) and are subdivided according to conventional and conservation tillage.

2. If measured soil strength values are available, for example from series of field trials or mapping, these can be used directly in the module.
3. In addition, it is possible to assess the soil structure on site using the packing density (PD). Packing density (PD) is an integrated parameter which combines various soil structural properties affected by the degree of compaction and is assessed visually in the field (DIN 19682-10, 2007). It should give an indication of a number of important soil functions, such as water and air porosity as well as root resistance. The assessment of packing density is based on the macroscopic properties aggregate size, cohesion of the soil structure, aggregate arrangement as an indication of the properties of the aggregate space, proportion of biogenic macropores (root and earthworm channels) and root distribution. The PD was divided into five levels (1-5). Following Rücknagel et al. (2013a), in the module the soil strength of the subsoil ($\log \sigma_{P-6kPa}$) is estimated based on the PD levels:

$$\text{PD level 1: } \log \sigma_{P-6kPa} = 1.30$$

$$\text{PD level 2: } \log \sigma_{P-6kPa} = 1.70$$

$$\text{PD level 3: } \log \sigma_{P-6kPa} = 1.90$$

$$\text{PD levels 4 and 5: } \log \sigma_{P-6kPa} = 2.30$$

The specified methods of estimating soil strength assume gravel-free sites. At sites whose gravel content (GR) is above 10-15 per cent by volume, soil strength is sometimes considerably higher. The following formula (2.2.-2) can be used to calculate the change in soil strength at a matric potential of -6 kPa as gravel content increases ($\Delta \log \sigma_{P-GR}$) in relation to the texture of the fine earth (texture-dependent constants a and b; e is Euler’s number) (Rücknagel et al., 2013b):

$$\Delta \log \sigma_{P-GR} = a * e^{(b * GR)} \quad (2.2.-2)$$

All calculations described thus far are based on soil water content at a matric potential of -6 kPa (field capacity). In order to assess passes over the soil by machinery throughout the year, it is also necessary to know the soil strength for drier conditions. To this end, a correction value ($\Delta \log \sigma_{P-WC}$) is calculated using the soil strength at field capacity ($\log \sigma_{P-6kPa}$) and the water content – at the moment the soil is driven over – as a percentage of field capacity (%FC) (Rücknagel et al., 2012a) (2.2.-3):

$$\Delta \log \sigma_{P-WC} = a + b * \log \sigma_{P-6kPa} + c * \%FC + d * \%FC^2 + e * \log \sigma_{P-6kPa} * \%FC \quad (2.2.-3)$$

The constants (a, b, c, d, e) in formula (3) are dependent on different soil types.

The soil strength ($\log \sigma_P$) (logarithm of the value in kPa) for one of the farm's fields at the respective depths of 20 cm and 35 cm can be calculated overall using formula (2.2.-4) at any given time; this requires the soil strength at field capacity ($\log \sigma_{P-6kPa}$), plus the stabilisation through any gravel content present ($\Delta \log \sigma_{P-GR}$), followed by the calculated change in soil strength as a function of soil water content ($\Delta \log \sigma_{P-WC}$):

$$\log \sigma_P = (\log \sigma_{P-6kPa} + \Delta \log \sigma_{P-GR}) + \Delta \log \sigma_{P-WC} \quad (2.2.-4)$$

2.2.3.1.3. Calculation of soil stress

The calculation of the vertical soil stress σ_z (major principle stress) using wheel load (P) and double inflation pressure (p_i) at soil depth z is based on Koolen et al. (1992):

$$\sigma_z = 2 * p_i * (1 - \cos^v (\arctan ((1/z) * (P/(\pi * 2 * p_i/100))^{1/2}))) \quad (2.2.-5)$$

This formula (2.2.-5) was validated based on 117 measurements, including those of Hammel (1994), Gysi et al. (1999), Arvidsson et al. (2000), Weisskopf et al. (2000), Horn et al. (2003), Trautner and Arvidsson (2003) and Keller et al. (2004). The vertical soil stress was calculated in parallel to the soil strength for soil depths of 20 cm and 35 cm. The concentration factors (v) used are not the values suggested by Söhne (1953) of 4 (hard and dry soil), 5 (firm and normally moist soil) and 6 (soft and wet soil); instead the concentration factors are calculated directly for the respective conditions, based on soil strength and soil water content according to equation (2.2.-6). In this regression model the concentration factor decreases with increasing soil strength ($\log \sigma_{P-6kPa}$) and decreasing water content as a percentage of field capacity (%FC). The regression equation is based on the sources specified above, if the concentration factors are calculated using the measured soil stresses. When calculating the concentration factors, the respective soil water content and soil strength are taken into account at depths of 20 and 35 cm.

$$v = -2.0 * \log \sigma_{P-6kPa} + 0.03 * \%FC + 3.2 \quad (2.2.-6)$$

2.2.3.1.4. Comprehensive assessment

All evaluations are first performed on the basis of each of the farm's individual fields. In the first step, the difference is established – at depths of 20 and 35 cm – between the logarithm of the calculated soil stress ($\log \sigma_z$) and the soil strength ($\log \sigma_P$) for each time the field is crossed (always the heaviest axle of the tractor or other agricultural machine and the associated trailer or towed implement with its own undercarriage) (2.2.-7):

$$SCI_{SP} = \log \sigma_z - \log \sigma_P \quad (2.2.-7)$$

As a dimensionless index (Soil Compaction Index) (SCI_{SP}), this difference makes it possible to estimate how far the soil strength has been exceeded. Values greater than 0 indicate that soil stress is greater than the soil strength. Negative values, where soil stress does not exceed soil strength, are set to 0 for the subsequent stages of evaluation. These passes by machinery do not cause soil compaction, although they cannot offset the effects of those passes with values greater than 0.

Given the fact that the passes with machinery over a particular field occur either along permanent traffic lanes or at random, it is not possible to simply add all the SCI_{SP} of the various passes during a growing season. With this in mind, we distinguish between passes along traffic lanes – for example during fertilizer and pesticide application – and random passes during tillage, harvest, seeding etc.

In the permanent traffic lanes, every new time the machinery passes over the ground it drives along the same track, and hence over the same area. Numerous passes may occur throughout the year. A lower Soil Compaction Index cannot offset a higher one, meaning the highest individual values are what determine the soil compaction risk. For this reason, calculation is based on these passes over the soil. The Soil Compaction Index for the passes along permanent traffic lanes (SCI_{PTL}) is calculated according to equation (2.2.-8). In this formula SCI_{MEAN} is the average value of the passes along permanent traffic lanes and SCI_{MAX} the maximum value:

$$SCI_{PTL} = ((SCI_{MEAN} + SCI_{MAX}) / 2 + SCI_{MAX}) / 2 \quad (2.2.-8)$$

When calculating the Soil Compaction Index for passes with random traffic, it is important to bear in mind that, for the single passes, varying indices as well as varying wheeled areas (as a proportion of the total area) may apply. Some sort of reference to the area traversed is therefore necessary in order to estimate the risk of soil compaction. First, the Soil Compaction Indices of the passes with random traffic are summarised in groups with increments of 0.10 (0.00-0.10, 0.11-0.20, 0.21-0.30, 0.31-0.40 etc.), and for each group the total wheeled area (A_{GR}) is identified. In order to account for the potential overlap of lanes, the wheeled area is multiplied by an estimated value of 0.75 and thus reduced.

The Soil Compaction Index of all passes with random traffic (SCI_{RT}) is then calculated using formula (2.2.-9) as the sum of each group's mean Soil Compaction Index multiplied by the respective wheeled area (A_{GR}):

$$SCI_{RT} = \sum (SCI_{GRM} * A_{GR}) \quad (2.2.-9)$$

The group with the highest Soil Compaction Indices is considered first. The values are added up until a maximum proportional area of 1.0 is reached.

In order to calculate the field's overall index (SCI_{FIELD}), it is necessary to offset the indices of the passes along permanent traffic lanes against those of passes with random traffic. This is done by using the proportional areas of passes along permanent traffic lanes (A_{PTL}) and those of passes with random traffic (A_{RT}) (2.2.-10):

$$SCI_{FIELD} = SCI_{PTL} * A_{PTL} + SCI_{RT} * A_{RT} \quad (2.2.-10)$$

An example in the Appendix illustrates how the Soil Compaction Index is calculated for a field with winter wheat.

The Soil Compaction Indices of a farm's individual fields can be calculated and displayed for different observational levels (SCI_{LEVEL}), such as for crop types, crop rotation and ultimately the whole farm. This requires the Soil Compaction Indices, for each year, of those fields (SCI_{FIELD}) that belong to the respective observational level, and also their areas (A_{FIELD}) (2.2.-11):

$$SCI_{LEVEL} = \sum (SCI_{FIELD} * A_{FIELD}) / \sum A_{FIELD} \quad (2.2.-11)$$

A temporal calculation of the compaction risk is also possible. Here it is not possible to offset the indices against each other as simple arithmetic means, since individual compaction events occurring over the years can add up over of a long period. Soil Compaction Indices summarised for several years are calculated first of all on the basis of the individual field using the formulae (2.2.-8) for passes along permanent traffic lanes, (2.2.-9) for passes with random traffic and (2.2.-10) for the overall index, whereby all passes during the entire multi-year period are used as a basis for the calculations. Spanning more than one year and applying to different observational levels, the summary for the farm in question is then created using the Soil Compaction Indices of the field sections calculated previously and their areas – similarly to formula (2.2.-11).

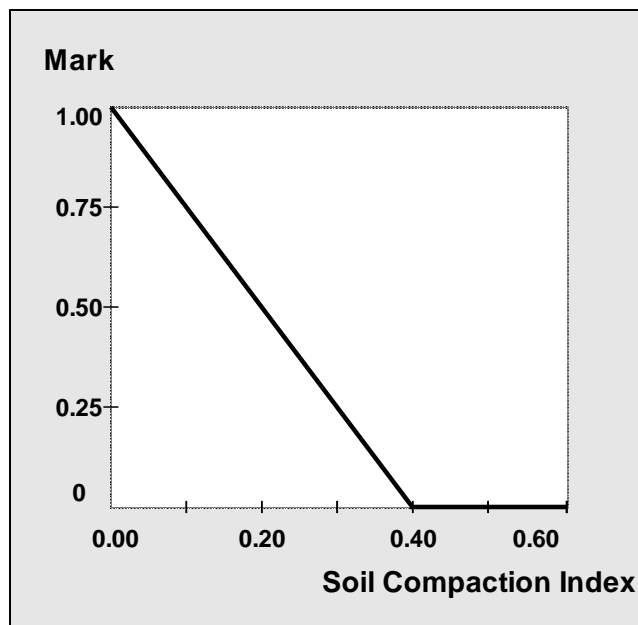


Figure 2.2.2. Sliding assessment of the Soil Compaction Index at farm level created with a mark scale between 0 (most unfavourable ecological situation) and 1 (most favourable ecological situation).

The final assessment of the Soil Compaction Index at farm level is based on the use of a mark function (Fig. 2.2.2). The figure's y-axis is set between zero and one, with one representing the most favourable ecological conditions and zero the most unfavourable. The normalisation technique incorporated into *REPRO* allows values specified in units of measure to be converted into dimensionless values. This method is of advantage when it comes to assessing non-linear or only partially linear correlations. Furthermore, it can be used to summarise different indicators as a whole-farm assessment.

The path of the normalisation function depends on the compaction behaviour of the soil. If the soil strength is exceeded, this results in a plastic deformation (increase in dry bulk density) of the soil. This can be characterised by the slope of the so-called virgin compression line on the stress/bulk density diagram. The slope is 0.20 on average (ranges of measured values 0.10-0.30), and is determined from numerous soil compression tests (Rücknagel et al., 2007; Rücknagel et al., 2012a). Accordingly, in theory it is to be expected that for every time the soil strength is exceeded by 0.10 there will be an average increase in dry bulk density of 0.02 g cm^{-3} . The reference values chosen for the normalisation function were the Soil Compaction Index 0.00 and the mark 1.00 as well as the Soil Compaction Index of 0.40 and a mark of 0.00. In the *REPRO* module all the calculated indices and the final assessment are represented in tables and graphs.

2.2.3.2. Validation of the module

Table 2.2.3 shows a summary of the aggregate density, dry bulk density and saturated hydraulic conductivity before the first pass and after the last pass or after the investigation period had ended for the module validation. Across all validations there is a strong positive correlation between the calculated Soil Compaction Index and the measured change in dry bulk density as well as a strong negative correlation with the measured logarithmic change in saturated hydraulic conductivity (Table 2.2.4). These relationships, in particular for the logarithmic change in saturated hydraulic conductivity, are more evident in the topsoil than in the subsoil.

If the correlation relationship is broken down into trials involving passes with single machines, passes along permanent traffic lanes, or those with random traffic on field level, there are no discernible differences. In all three cases strong positive correlations can be seen, in particular between the Soil Compaction Index and the change in dry bulk density. The correlations are however considerably weaker for the change in saturated hydraulic conductivity. It is thus more difficult to predict the change in pore continuity than the change in soil density. Generally speaking, various reasons are conceivable to explain the remaining variability of the individual values. First of all it should be considered that, once precompression stress is exceeded, the degree of change in a soil's structure is particularly dependent on the slope of the virgin compression lines in the compression test, and in turn this slope is largely dependent on the initial dry bulk density and void ratio (Keller et al., 2011), and often also the clay content (Larson et

al., 1980). The compaction effect can therefore be different for soils with different textures and initial densities yet the same Soil Compaction Index.

Table 2.2.3. Aggregate density (AD), dry bulk density (BD) and saturated hydraulic conductivity (k_s) before the first pass and after the last pass or after the investigation period had ended for the module validation.

Site code	Site and depth (cm)	AD (g cm ⁻³)	BD (g cm ⁻³)		k_s (cm d ⁻¹)	
			before the first pass	after the last pass	before the first pass	after the last pass
Part A: Passes with single machines						
1.1.	Lossa 20	1.66	1.45	1.48	37	4
1.2.	Lossa 35	1.67	1.49	1.53	33	12
2.1.	Zwenkau I 20	1.52	1.21	1.27	174	103
2.2.	Zwenkau I 35	1.68	1.55	1.56	23	14
2.3.	Zwenkau II 20	1.52	1.21	1.27	174	49
2.4.	Zwenkau III 20	1.52	1.21	1.29	174	19
2.5.	Zwenkau IV 20	1.52	1.21	1.33	174	35
2.6.	Zwenkau IV 35	1.68	1.55	1.52	23	17
3.1.	Rothenberga I 20	1.68	1.51	1.58	27	11
3.2.	Rothenberga II 20	1.55	1.21	1.34	97	17
3.3.	Rothenberga III 20	1.55	1.21	1.30	97	20
3.4.	Rothenberga IV 20	1.55	1.21	1.28	97	53
3.5.	Rothenberga V 20	1.54	1.25	1.37	86	7
3.6.	Rothenberga VI 20	1.57	1.26	1.39	143	11
3.7.	Rothenberga VII 20	-	1.35	1.42	51	21
3.8.	Rothenberga VIII 20	-	1.35	1.51	51	2
3.9.	Rothenberga IX 20	-	1.35	1.52	51	3
4.1.	Friemar 20	-	1.23	1.45	363	13
4.2.	Friemar 35	-	1.43	1.47	24	7
5.1.	Fortuna I 20	-	1.39	1.46	50	34
5.2.	Fortuna I 35	-	1.47	1.48	26	19
Part B: Passes along permanent traffic lanes						
6.1.	Rothenberga X 20	1.48	1.43	1.45	7	4
7.1.	Fortuna II 20	-	1.39	1.53	50	8
7.2.	Fortuna II 35	-	1.47	1.54	26	12

Table 2.2.3 (continuation). Aggregate density (AD), dry bulk density (BD) and saturated hydraulic conductivity (k_s) before the first pass and after the last pass or after the investigation period had ended for the module validation.

Site code	Site and depth (cm)	AD	BD		k_s	
		(g cm^{-3})	(g cm^{-3})		(cm d^{-1})	
		before the first pass	before the first pass	after the last pass	before the first pass	after the last pass
Part C: Passes with random traffic on field level						
8.1.	Harste FBMW 20	1.56	1.51	1.60	16	4
8.2.	Harste FBMW 35	1.56	1.49	1.53	97	55
8.3.	Harste LBW 35	1.54	1.50	1.54	104	28
9.1.	Halle 20	1.85	1.58	1.71	19	6
10.1.	Hechtsheim II 20	1.51	1.24	1.40	261	139
10.2.	Hechtsheim II 35	1.44	1.33	1.31	41	86
11.1.	Wöllstein 20	1.60	1.49	1.49	16	24
11.2.	Wöllstein 35	1.55	1.42	1.39	44	35
12.1.	Großstorkwitz 20	1.53	1.33	1.49	19	4
12.2.	Großstorkwitz 35	1.51	1.34	1.38	61	85

Table 2.2.4. Correlation coefficients (r) with their error probability (p-value) between calculated Soil Compaction Indices and the change in dry bulk density (Δ BD) and logarithm change in saturated hydraulic conductivity ($\Delta \log k_s$).

	Δ BD		$\Delta \log k_s$	
	r	p-value	r	p-value
All module validations (n=34)	0.83	<0.001	-0.77	<0.001
Module validations in topsoil (20 cm), (n=23)	0.69	<0.001	-0.75	<0.001
Module validations in subsoil (35 cm), (n=11)	0.73	0.01	-0.22	0.53
Passes with single machines (n=21)	0.81	<0.001	-0.78	<0.001
Passes along permanent traffic lanes (n=3)	1.00	0.03	-0.98	0.14
Passes with random traffic on field level (n=10)	0.94	<0.001	-0.56	0.09

Furthermore, a soil's compaction behaviour in the field can also deviate significantly from compaction behaviour recorded in a laboratory compression test; in the field it is possible for permanent settlement to already occur below the precompression stress value (Keller and Lamande, 2010). Furthermore, the method used to calculate the vertical soil stress, which we

adopted from Koolen et al. (1992), is based on the assumptions that the contact area is even, circular and horizontal and that the stress is distributed equally in the vicinity of the contact area. Although these assumptions, as well as the limitation of machine-specific parameters to wheel load and inflation pressure, simplify the calculations, the shape of the contact area – which is in fact elliptical (Febo et al., 2000) – and the often uneven distribution of stress across it (Hammel, 1994) are not taken into account. The theories of Boussinesq and Fröhlich, on the other hand, which form the basis of the calculation of stress distribution, also only apply to an ideally elastic, homogeneous, isotropic and infinite medium. However, the naturally deposited soil does not sufficiently meet these requirements, which is why the vertical stress, compared to measurements, cannot always be calculated satisfactorily (Lamande and Schjonning, 2011a; Lamande and Schjonning, 2011b). Koolen et al. (1992) already verified their equation in numerous measurements themselves; in doing so they also noted that variations may occur, especially in carcasses that are either very stiff or particularly flexible as well as in the case of excessive inflation pressure for the respective wheel load.

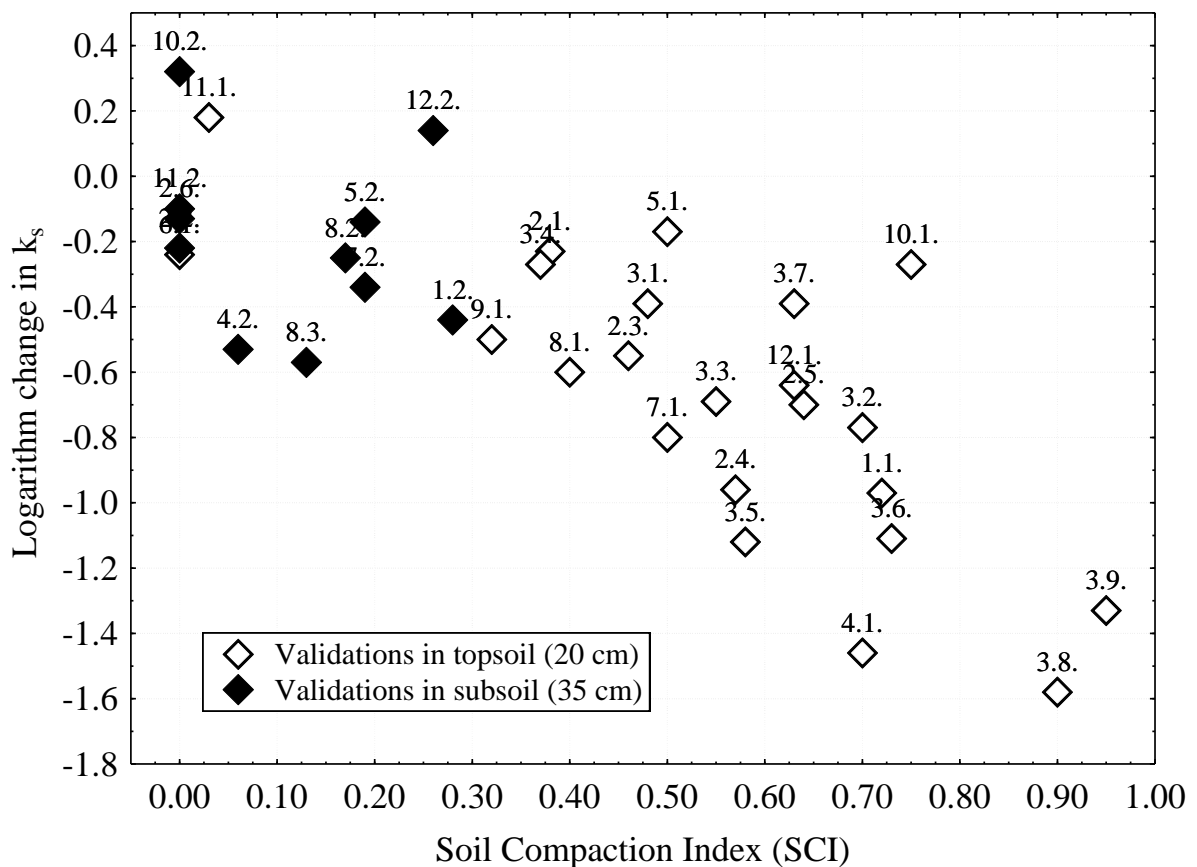


Figure 2.2.3. Relationship between calculated Soil Compaction Index and the logarithm change in saturated hydraulic conductivity (k_s) at module validations; numbers indicate site codes according to Table 2.2.1.

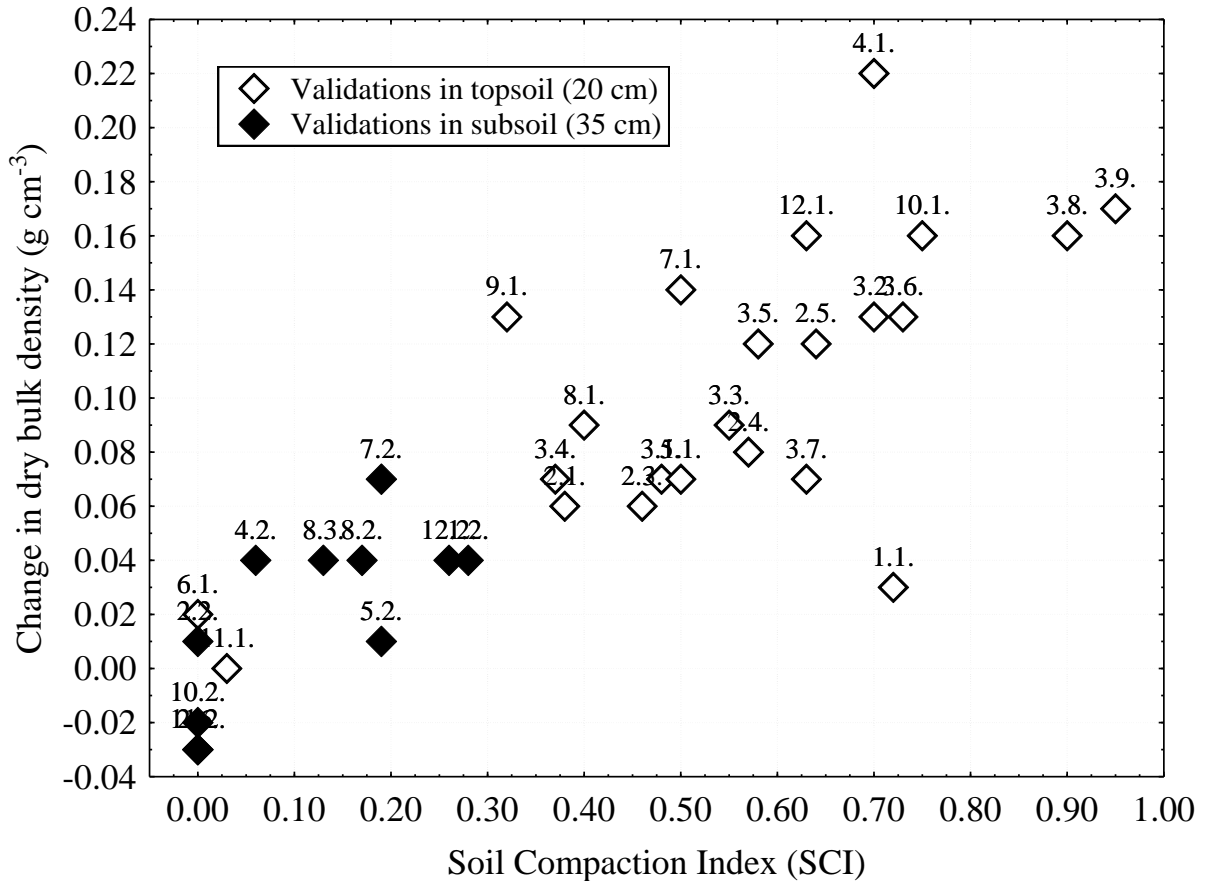


Figure 2.2.4. Relationship between calculated Soil Compaction Index and the change in dry bulk density at module validations; numbers indicate the site codes according to Table 2.2.1.

When considering the validations in detail it can be noted that, on some areas with multi-year calculation of the Soil Compaction Index on the field level, saturated hydraulic conductivity is sometimes slightly higher at the end of the observation period than at the beginning (e.g. site codes 10.2., 11.1., 12.2.), or that saturated hydraulic conductivity did not decrease quite as considerably as for a comparable Soil Compaction Index in other trials (e.g. site code 10.1.) (Fig. 2.2.3). Conversely, changes in dry bulk density at these sites follow the general trend from all the investigations (Fig. 2.2.4). One main reason for this is likely to be the fact that conservation tillage was performed throughout the entire period; it usually results in higher earthworm abundance (Ulrich et al., 2010) and, in turn, the increased formation of vertically oriented coarse pores. Additionally, pores created by roots and earthworms are not destroyed by soil cultivation. All vertically oriented pores are less susceptible to compaction (Hartge and Bohne, 1983), thus guaranteeing the preservation – or even the improvement – of saturated hydraulic conductivity while the degree of soil compaction remains the same. Other soil structure regeneration processes whose effects are more long-term, such as those caused by general climatic effects (Boizard et al., 2009) or frost (Frede, 1991), cannot be mapped by the module in *REPRO* either. On areas observed over a long period, these processes may cause variations between the actual

recorded changes in soil structure and the changes one might expect based on the calculated Soil Compaction Index.

The presence of vertically oriented pores that are not very susceptible to compaction is one reason why, in the subsoils, there is virtually no correlation between the Soil Compaction Index and the logarithmic change in saturated hydraulic conductivity. In addition, while the variability of individual values remains the same, the low correlation coefficient can also be explained mathematically by the fact that there is a much smaller range of Soil Compaction Indices calculated in the subsoil (0-0.28) than in the topsoil (0-0.95).

The change in dry bulk density at site 1.1. (Fig. 2.2.4) also deviates from the general trend of the correlation. Here a considerably greater increase in dry bulk density would have been expected. However, the change in saturated hydraulic conductivity reflects the high Soil Compaction Index well. This investigation is an example of the fact that, at very high soil water content levels and at the same time short stress periods (single pass by machinery), pore water pressure cannot be removed completely (Fazekas and Horn, 2005), rather resulting in shearing deformations and more restricted pore continuity than an increase in dry bulk density. Such processes cannot be adequately reflected in the *REPRO* module, which reduces the stress calculation, for example, to vertical stress. Be that as it may, a complete, three-dimensional description of the state of stress, including shear stress (Horn et al., 1992), would not be in keeping with the objective of requiring a low level of data input for the calculations.

2.2.3.3. Examples of module application

Below we present the risk of soil compaction in the subsoil (depth 35 cm) only. The preservation of an intact soil structure is particularly important here, because measures aimed at regenerating the subsoil – such as by tillage – are very complicated and generally not sustainable. The calculated Soil Compaction Indices turn out to be very low on the whole, and accordingly the assessments with the assessment function are also very good (Table 2.2.5). The Soil Compaction Indices are lower than the values determined during module validation. There are no considerable differences between passes along permanent traffic lanes and those with random traffic. When classifying the values it should however be noted that the occurrence of soil compaction, and in turn the calculated soil compaction risk, can increase considerably over a long period with recurring compaction events. For instance, investigations by Koch et al. (2008) on soils that were clearly susceptible to compaction at high soil water content levels, show ever greater compaction in the subsoil as a result of the land being repeatedly driven over each year with heavy agricultural machinery (sugar beet harvester). The two-year calculations presented here do not take effects such as these sufficiently into account. Even so, a tendency can at least be seen in that there is a slightly higher risk of soil compaction at farms 1, 3, 4, 14 and 15. Interpreting the values with great caution, these farms mostly have high proportions of maize and/or sugar beet. At the same time, four of the farms are located in regions with mean annual

rainfall higher than 700 mm, so their soil water content is presumably high all year round. Investigations by Capowiez et al. (2009) have already shown that crop systems with high levels of maize and sugar beet – especially those with reduced levels of soil tillage and where the crops are sown and harvested at times where the soil is very moist – result in higher dry bulk densities in the topsoil. These results have also been confirmed by Jacobs et al. (2013). Here, growing winter wheat in monoculture and with conservation tillage led to a more favourable soil structure (e.g. air capacity) in the topsoil compared with maize and sugar beet monoculture. However, most of the studies mentioned only show the effects of the crop system itself on the topsoil.

Table 2.2.5. Soil Compaction Indices calculated at 35 cm depth (subsoil) for the farms for the module application.

Farm No.	Soil Compaction Index			Assessment of SCI _{LEVEL} with the mark scale
	Passes along permanent traffic lanes (SCI _{PTL})	Passes with random traffic (SCI _{RT})	Total of arable land level (SCI _{LEVEL})	
1	0.00	0.09	0.09	0.78
2	0.04	0.00	0.00	1.00
3	0.00	0.05	0.05	0.88
4	0.00	0.07	0.07	0.83
5	0.05	0.03	0.03	0.93
6	0.00	0.01	0.01	0.98
7	0.00	0.02	0.02	0.95
8	0.08	0.02	0.03	0.93
9	0.05	0.01	0.01	0.98
10	0.03	0.00	0.01	0.98
11	0.03	0.01	0.04	0.90
12	0.07	0.01	0.01	0.98
13	0.00	0.03	0.03	0.93
14	0.03	0.07	0.07	0.83
15	0.12	0.14	0.14	0.65

Three of the farms with an increased Soil Compaction Index mostly practise conventional tillage with a plough, and all five farms apply conventional tillage methods at least partially. By driving along furrows, the soil stress from the tractor wheel is transferred directly into the subsoil. This stress is thus higher in the subsoil than it is when driving a machine with similar parameters (wheel load, inflation pressure, tyres) over the soil surface ('on-land pass') (Weisskopf et al., 2000). Considered together, therefore, the higher proportion of maize and/or sugar beet crops, the local climatic conditions and the tillage system result in the slightly higher

two-year Soil Compaction Indices seen for farms 1, 3, 4, 14 and 15. Based on previous literature however, one would have expected that farms that use machines with high wheel loads would display greater soil compaction risks due to the potentially higher soil stresses in the subsoil (Trautner and Arvidsson, 2003). Conversely, at the five farms mentioned above the wheel loads, inflation pressures and wheeled area of each pass rather correspond to the average, while farms with large machines (e.g. farms no. 9, 10 and 13) do not automatically display higher soil compaction risks in the subsoil in this study.

2.2.4. Conclusions

Steps should be taken to avoid soil compaction because targeted melioration of such damage is complex, costly and rarely long-lasting. Mathematical empirical models, specifically the *REPRO* software module presented here, are a promising way of performing situational analyses of the risk of soil compaction and subsequent assessment, up to farm level, that considers all main factors. However, accurate forecasts can only be guaranteed by extensively validating a model's algorithms. Taking all the validations performed for the *REPRO* software module together, the Soil Compaction Index – as a measure of the risk of compaction – represents a good way of reflecting changes in soil structure (changes in dry bulk density and saturated hydraulic conductivity) caused by mechanical stresses when the ground is driven over and during management activities. Thus overall it enables reliable analysis of the problems that a soil compaction risk poses for a wide range of site conditions. The module's application as part of consulting and certification systems also demonstrates the high practicality of its approach, even for the analysis of entire farms. It can thus be used as a tool to contribute to improving soil structure protection in the spirit of sustainable land management.

Acknowledgements

The authors wish to thank the state of Rhineland-Palatinate and the Deutsche Bundesstiftung Umwelt (DBU) for their financial support with the development and testing of the module during the various stages of the project. We thank Gabriele Hensel (Privates Institut für Nachhaltige Landbewirtschaftung GmbH, Halle/Saale) for software implementation, Jörg Weickel and Fritz Mossel (Dienstleistungszentrum Ländlicher Raum Rheinhessen-Nahe-Hunsrück, Bad Kreuznach) for their support with the research work and Martin Schmidt (German Weather Service, Leipzig) for providing us with climate data. Thanks also go to Heinz-Josef Koch (Institute of Sugar Beet Research, Göttingen), Gerhard Dumbeck (RWE Power AG, Erftstadt) and all the farmers who participated for allowing us to validate the module.

Appendix A 2.2.1. Abbreviations and symbols in the equations and their descriptions.

Abbreviation or symbol	Parameter description	Unit
A_{FIELD}	field size	ha
A_{GR}	wheeled area in the groups for calculation of Soil Compaction Index for random traffic	-
A_{PTL}	wheeled area of the permanent traffic lanes on the field	-
A_{RT}	wheeled area of the random traffic passes over the field	%/100
AD	aggregate density	g cm^{-3}
BD	dry bulk density	g cm^{-3}
GR	gravel content	volume %
e	Euler's number	-
$\log \sigma_{\text{P}}$	logarithm soil strength (logarithm of kPa values)	-
$\log \sigma_{\text{P}-6\text{kPa}}$	logarithm soil strength at -6 kPa matric potential (logarithm of kPa values)	-
$\Delta \log \sigma_{\text{P GR}}$	logarithm change in soil strength with increasing gravel content	-
$\Delta \log \sigma_{\text{P WC}}$	logarithm change in soil strength with decreasing water content	-
$\log \sigma_{\text{z}}$	logarithm major principal stress (logarithm of kPa values)	-
P	wheel load	kg
PD	packing density	-
p_i	inflation pressure	kPa
$\text{SCI}_{\text{FIELD}}$	Soil Compaction Index of the field	-
SCI_{GRM}	mean Soil Compaction Index in the groups for calculation of Soil Compaction Index for random traffic	-
$\text{SCI}_{\text{LEVEL}}$	Soil Compaction Index at different farm levels	-
SCI_{MAX}	maximum Soil Compaction Index for permanent traffic lanes	-
SCI_{MEAN}	average Soil Compaction Index for permanent traffic lanes	-
SCI_{PTL}	Soil Compaction Index of passes along permanent traffic lanes	-
SCI_{RT}	Soil Compaction Index of passes for random traffic	-
SCI_{SP}	Soil Compaction Index of single working steps	-
z	soil depth	cm
%FC	relative soil water content as a percentage of field capacity	%
v	concentration factor	-
σ_{z}	major principal stress	kPa

Appendix A 2.2.2. Example of the steps used to calculate the Soil Compaction Indices for a fictitious field with winter wheat: Wheeled area and calculation of Soil Compaction Index for single working steps; ¹ passes with random traffic, ² passes along permanent traffic lanes, * negative values were put to zero.

No.	Working step	Wheeled area	Logarithm soil stress (log σ_z)	Logarithm soil strength (log σ_P)	Soil Compaction Index for the single working steps (SCI _{SP})
1	First tillage ¹	0.25	1.95	2.10	0.00*
2	Second tillage ¹	0.25	2.30	2.00	0.30
3	Seedbed preparation ¹	0.20	2.00	1.95	0.05
4	Seeding ¹	0.20	1.90	1.90	0.00
5	Fertilizer application ²	0.05	2.30	1.80	0.50
6	Pesticide application ²	0.05	2.25	1.85	0.40
7	Fertilizer application ²	0.05	2.30	1.90	0.40
8	Pesticide application ²	0.05	2.20	2.05	0.15
9	Harvest ¹	0.25	2.35	2.20	0.15

Soil Compaction Index of the permanent traffic lanes calculated from table A 2.2.2 with equation (2.2.-8):

$$\begin{aligned}
 \text{SCI}_{\text{PTL}} &= (((0.50+0.40+0.40+0.15)/4)+0.50)/2+0.50/2 \\
 &= \underline{\underline{0.47}}
 \end{aligned}$$

Appendix A 2.2.3. Example of the steps used to calculate the Soil Compaction Indices for a fictitious field with winter wheat: Calculation of wheeled areas for the Soil Compaction Index with random traffic

Soil Compaction Index group	Mean Soil Compaction Index of the group (SCI _{GRM})	Working steps in example	Wheeled area in the group	Wheeled area in group reduced with factor 0.75 (A _{GR})
0.31-0.40	0.35	-	-	-
0.21-0.30	0.25	Second tillage	0.25	0.19
0.11-0.20	0.15	Harvest	0.25	0.19
0.00-0.10	0.05	First tillage, seedbed preparation, seeding	0.25+0.20+0.20 =0.65	0.49

Soil Compaction Index of random traffic calculated from table A 2.2.3 with equation (2.2.-9):

$$\begin{aligned} \text{SCI}_{\text{RT}} &= 0.25*0.19 + 0.15*0.19 + 0.05*0.49 \\ &= \underline{\underline{0.10}} \end{aligned}$$

Total Soil Compaction Index of the field calculated with equation (2.2.-10):

$$\begin{aligned} \text{SCI}_{\text{TOTAL}} &= 0.47*0.05 + 0.10*0.95 \\ &= \underline{\underline{0.12}} \end{aligned}$$

3. Detailed algorithms for determination of soil strength

3.1. A simple model to estimate change in precompression stress as a function of water content on the basis of precompression stress at field capacity

Published in: *Geoderma* 177-178 (2012), 1-7

Jan Rücknagel¹, Olaf Christen¹, Bodo Hofmann¹, Sebastian Ulrich¹

¹Institute of Agricultural and Nutritional Sciences, Department Agronomy and Organic Farming, University of Halle-Wittenberg, Betty-Heimann-Str. 5, 06120 Halle/Saale (Germany)

Abstract

Precompression stress is an important criterion in soil mechanics and is often determined at a water content equivalent to a matric potential of -6 kPa. In German-speaking countries, this matric potential corresponds to field capacity. Yet in order to assess the risk of compaction in arable soils, it needs to be known for a wide range of soil water content levels. The site-specific determination of relationships between precompression stress and matric potential or water content is, however, highly labour intensive. Furthermore, previous regression models can only deduce changes in precompression stress depending on water content to a limited extent and not for all values. Alternatively, these models do not directly include precompression stress at a matric potential of -6 kPa as the basis of calculation. Thus the derivation and validation of a simple model are to be presented, which can be used to predict any precompression stress for decreasing soil water content levels. This requires only an initial precompression stress for a matric potential of -6 kPa and the respective soil water content as a percentage of field capacity. The model is based primarily on an analysis of numerous studies in which precompression stress was determined for various matric potentials. Relationships between precompression stress at a matric potential of -6 kPa and the relative water content as a percentage of field capacity at a matric potential of -30 kPa were also derived in the laboratory. These data were used to develop a mathematical model for four soil texture classes, as well as “All texture classes” collectively. This model was tested by way of soil compression tests and the determining of precompression stress at 25 sites. All soil compression tests were initially carried out with a matric potential of -6 kPa. Tests were carried out in parallel to this with greater matric potentials (-10 to -1500 kPa). The accuracy of the modelling approach presented here is good, both in terms of the use of systems of equations for “All texture classes” and for differentiated soil texture classes. In comparison to the regression model for all texture classes, calculation according to soil texture class causes a reduction of the mean absolute errors from 0.15 to 0.11 and of the RMSE from 0.19 to 0.14. Simultaneously, the coefficient of determination and the index of agreement (IA) increase, from 0.54 to 0.67 and 0.92 to 0.95 respectively. Calculation

according to different soil texture classes is therefore particularly recommended in the case of applications with high accuracy requirements.

3.1.1. Introduction

Precompression stress is an important criterion for soil susceptibility to compaction. In numerous studies, it is determined for a matric potential of -6 kPa (e.g. Peth and Horn, 2006; Peng and Horn, 2008). In German-speaking countries, this matric potential corresponds to field capacity. Often the greatest risk of compaction exists at field capacity because this is the condition where the combined influence of buoyancy and capillary cohesion is smallest. As soil water content decreases, thus precompression stress increases and the overall risk of compaction also decreases. Over the course of the year, soil water content may be subject to considerable fluctuations. This means that for assessments of the risk of compaction in arable soils, and of how to manage these soils, estimates often need to be made of precompression stress for various matric potentials.

For the most part, soil compression tests have hitherto been carried out with various matric potentials, identifying site-specific relationships between precompression stress and matric potential (e.g. Arvidsson et al., 2003; Keller et al., 2004). These tests are highly labour intensive and thus only feasible for a limited number of sites. An alternative to this is the application of the regression functions by Horn and Fleige (2003), which permit a calculation of precompression stress for matric potentials of -6 and -30 kPa. These functions do not however include drier conditions, and a derivation for all values is not possible either. Both these methods, i.e. determining site-specific relationships between precompression stress and matric potential and applying the regression functions by Horn and Fleige (2003), are reliant upon the availability of site-specific water retention curves. If, however, as a reference value only the corresponding water content at field capacity (matric potential -6 kPa) is known, and if the actual water content is determined gravimetrically, for example using a disturbed soil sample, then this can only be stated as a percentage of field capacity. This practice is applied in agricultural and agrometeorological consulting, or in the carrying out of simple field tests. (Wendling 1986, Schäfer-Landefeld et al., 2004). What is more, commercial water balance models which are available to a wide range of users (such as that of the German Meteorological Service) tend to show water content as a percentage of field capacity or available field capacity.

The regression functions by Saffih-Hdadi et al. (2009) represent another method of identifying any precompression stress depending on water content. Using these, it is possible to calculate precompression stress for five soil texture classes by means of dry bulk density and the gravimetrically ascertained soil water content. However, studies performed by Arvidson and Keller (2004), Mosaddeghi et al. (2003) and Semmel and Horn (1995) showed that it is not possible to provide a reliable estimate of precompression stress using dry bulk density alone, because the latter does not allow any conclusions to be made concerning the aggregation within the soil. Thus it is better to use precompression stress at a matric potential of -6 kPa as a direct basis for

calculation, if it is only a change in precompression stress depending on water content that is to be identified. Furthermore, this is possible because in recent years numerous studies on precompression stress at field capacity have been carried out in various countries, and also because of the availability of comprehensive soil maps (Horn et al. 2002, Cavalieri et al., 2008). Thus there already exists a broad basis of data which can be used. In order to avoid the drawbacks mentioned of previous approaches, this paper shall therefore present the derivation and validation of a simple, innovative model which can be used to calculate any precompression stress for decreasing soil water content levels in various soil texture classes. This requires only the initial precompression stress for a matric potential of -6 kPa (field capacity) and the respective soil water content as a percentage of field capacity.

The model was deliberately developed to be a simplified, empirical model which would causally link the correlations described in the following sections with each other. As a result, it does not follow the customary mechanistic approach. Overall we feel that an empirical model is more robust. It should be available for use in practical applications, and indeed the model presented here is already widely used, in the *REPRO* software program (Rücknagel and Christen, 2010) module concerning the analysis of the risk of soil compaction, as well as in parts of the *CANDY* C/N simulation model (Franko et al., 2007) and in a testing concept used across Germany to detect the actual risk of compaction in agricultural soils (Lebert, 2010).

3.1.2. Materials and methods

3.1.2.1. Analysis of data from previous studies

The model is based primarily on an analysis of various scientific literature (e.g. Horn, 1986; Lebert, 1989; Nissen, 1998; Arvidsson, 2001; Arvidsson et al., 2003; Berli et al., 2003; Keller et al., 2004) where precompression stress was determined for a total of 160 samples of natural soils, of varying texture, at matric potentials of -6 and -30 kPa. This analysis serves to help determine the differences in precompression stresses between these two matric potentials.

3.1.2.2. Relationships between matric potential and water content

As well as for soil texture classes in the analysis of scientific literature, relationships were derived between precompression stress at a matric potential of -6 kPa and relative water content as a percentage of field capacity at a matric potential of -30 kPa, so that the change in precompression stress could be contrasted with a relative change in water content. The corresponding precompression stress levels were calculated according to Rücknagel et al. (2007) using dry bulk density and aggregate density. Examples shown in this paper are the results for a “Silt Loam” (240 g kg⁻¹ clay, 230 g kg⁻¹ sand), a “Sandy Loam” (80 g kg⁻¹ clay, 660 g kg⁻¹ sand) and a “Clay” (460 g kg⁻¹ clay, 170 g kg⁻¹ sand).

3.1.2.3. Soil compression tests

Soil compression tests at 21 sites with natural soils (Tab. 3.1.1) form the basis of the model validation. They come from the topsoil and the subsoil of normal arable land (site code 6.1.-15.2.) and two soil tillage experiments (site code 18.1.-19.3.). These are supplemented by four disturbed samples (site code 21.1.-24.1.). For these, the soil core samplers were filled with sieved, field-wet soil of <10 mm aggregate diameter. In the model tests, the clay content varies between 10 and 550 g kg⁻¹, while the sand content ranges between 30 and 960 g kg⁻¹, thus covering a very broad range of texture classes, even if the primary focus is on the soil texture class “Silt Loam”. This is due to the prevalence of the soil texture class “Silt Loam” in the soils from the regions studied.

Table 3.1.1. Description of the test sites for model validation; ¹ USDA classification scheme (Gee and Bauder, 1986); SOM - soil organic matter.

Site code	Site and depth (cm)	Texture (g kg ⁻¹)			Texture class ¹	SOM (g kg ⁻¹)
		Clay	Silt	Sand		
6.1.	Neurath III 45-48	150	800	50	Silt Loam	24
7.1.	Fortuna IV 32-35	160	810	30	Silt Loam	22
7.2.	Fortuna IV 55-58	170	790	40	Silt Loam	22
7.3.	Fortuna IV 85-88	130	830	40	Silt Loam	22
9.1.	Pesch 40-43	120	850	30	Silt Loam	7
10.1.	Quellendorf 10-13	110	290	600	Sandy Loam	16
11.1.	Herrengosserstedt I 18-21	220	650	130	Silt Loam	-
11.2.	Herrengosserstedt I 32-35	240	630	130	Silt Loam	-
11.3.	Herrengosserstedt II 12-15	440	440	120	Silty Clay	-
11.4.	Herrengosserstedt II 25-28	550	370	80	Clay	-
12.1.	Uchtdorf 19-22	30	140	830	Loamy Sand	19
12.2.	Uchtdorf 35-38	10	30	960	Sand	4
13.1.	Lossa 2-5	150	690	160	Silt Loam	17
14.1.	Hemleben I 9-12	460	370	180	Clay	-
15.1.	Rothenberga I 14-17	60	830	110	Silt	22
15.2.	Rothenberga II 17-20	130	820	50	Silt Loam	22
18.1.	Lückstedt I 17-20	40	210	750	Loamy Sand	13
18.2.	Lückstedt II 17-20	40	210	750	Loamy Sand	12
19.1.	Buttelstedt I 15-18	310	640	50	Silty Clay Loam	32
19.2.	Buttelstedt I 45-48	270	650	80	Silty Clay Loam	10
19.3.	Buttelstedt II 15-18	310	660	30	Silty Clay Loam	34
21.1.	Halle I 15-25	80	260	660	Sandy Loam	21
22.1.	Hemleben II 15-25	500	380	120	Clay	36
23.1.	Niestetal 15-25	130	800	70	Silt Loam	16
24.1.	Seehausen 15-25	120	450	430	Loam	22

The soil compression tests were initially performed for each sample at a matric potential of -6 kPa. Tests were carried out in parallel to this with greater matric potentials (-10 to -1500 kPa). The corresponding water contents are given as g kg^{-1} and as a percentage of field capacity (% FC) (Tab. 3.1.2). The loading steps 5, 10, 25, 50, 100, 200, 350 and 550 kPa (and in some cases 1200 and 2500 kPa) were applied in succession to the soil core samples. A relaxation phase occurred after each step. The tests took place in drained conditions with a loading time of 180 minutes per loading step and relaxation phases lasting 15 minutes. In previous tests on soils of similar texture classes, for loading times of up to 540 minutes in comparison to 180 minutes only very slight increases in settlement were measured. Therefore, settlement can be regarded as largely finished after 180 minutes. However, how matric potential changed during the soil compression tests was not measured. The stress/bulk density functions served to help numerous independent testing persons (Rücknagel et al., 2010) determine precompression stress using Casagrande's graphical method (1936).

3.1.2.4. Statistical analysis

The statistical analysis of the data was carried out using the software program Statistica (StatSoft, Inc., 2009). Calculations using the data from the analysis of previous studies, the derivation and validation of the regression model, and the determination of mean values from the replications carried out, are all based on logarithm precompression stress. This is because when the unit kPa was applied, the test parameter precompression stress displayed a frequency distribution with a skew to the right. This is demonstrated for example by the composition of the data records by Lebert (1989) and Nissen (1998). The mean absolute error (MAE), the root mean square error (RMSE), the coefficient of determination (R^2) and the index of agreement (IA) according to Willmott (1982) were used to evaluate the prognostic accuracy of the model.

3.1.3. Results and discussion

3.1.3.1. Principal changes in stress/strain behaviour

Figure 3.1.1 shows a typical example for stress/strain behaviour and the change in precompression stress with decreasing water content (site code 7.3., "Fortuna IV 85-88"). Here, the increase in precompression stress is based primarily on a shifting of the virgin compression lines towards greater stress. Larson et al. (1980) report on an approximately parallel shift with a virtually constant "Compression index" (corresponding to the change in the void ratio in relation to the logarithmic change in stress). In contrast, however, the slope of the virgin compression line also increases with decreasing water content at the "Fortuna IV 85-88" site.

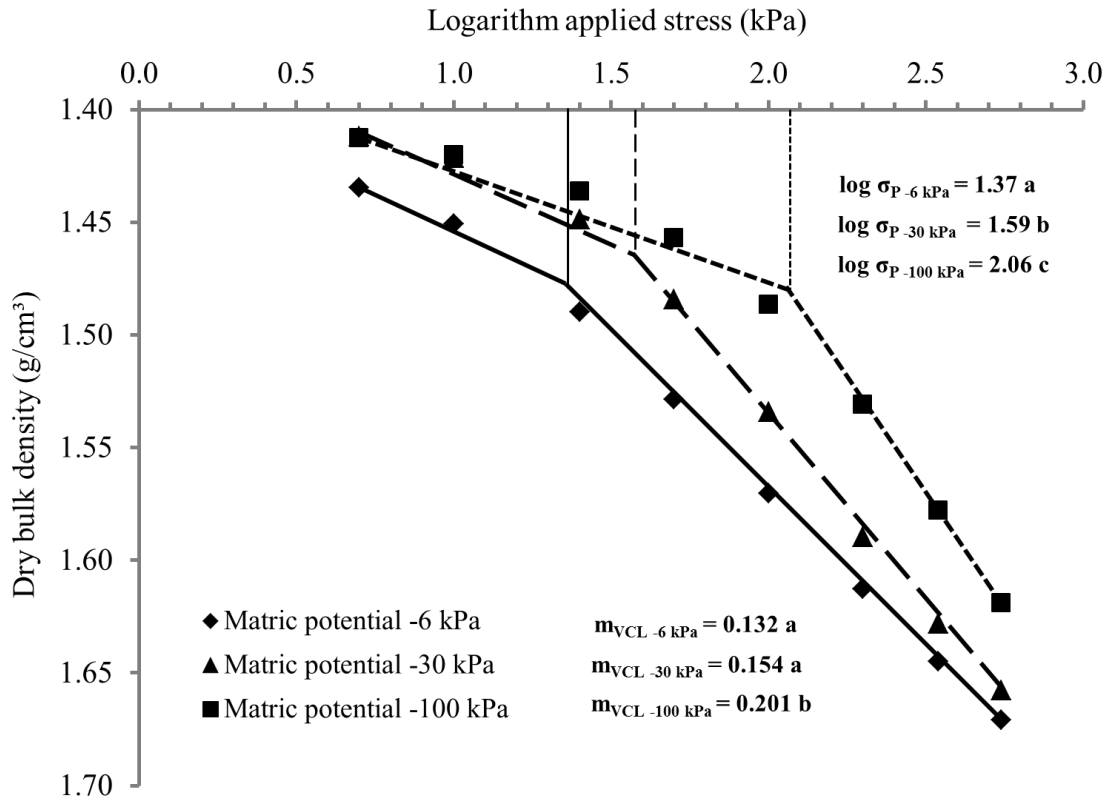


Figure 3.1.1. Logarithm stress/dry bulk density functions and precompression stress at different matric potentials for the example “Fortuna IV 85-88”, the different letters for precompression stress ($\log \sigma_P$) and slope of the virgin compression line (m_{VCL}) indicate significant values $p \leq 0.05$.

Taking the entire data record from the soil compression tests, it is evident that increasing pre-compression stress results from changes to both of the parameters which describe the virgin compression line (slope and position) (Tab. 3.1.2). Of a total of 36 soil compression tests carried out where water content was smaller than field capacity, 17 (47 %) nevertheless demonstrate a shifting of the virgin compression line towards greater stress. An example of this can be seen on the virgin compression lines by means of dry bulk density for the loading step of 350 kPa (BD_{350} in Table 3.1.2). In 9 tests (25 %) the position does not change and in only 10 tests (28 %) is there a shifting towards smaller stress. In the tests carried out, the slope of the virgin compression line plays a decisive role for the increase in precompression stress, as it increases with decreasing water content levels in 26 of the tests (72 %). This confirms the findings of Saffih-Hdadi et al. (2009), where an increase in the “Compression index” with decreasing water content was also observed. A shifting of the virgin compression line in combination with an increase in its slope can be observed in approximately half of the tests, similarly to the example of “Fortuna IV 85-88”. Yet using the tests presented here, it is not possible to deduce which soil conditions, such as soil texture or initial soil structure, are likely to lead to a shifting of or an increase in the slope of the virgin compression lines.

Table 3.1.2. Total pore volume (TPV, cm³/cm³), volumetric soil water content (vSWC, cm³/cm³) and gravimetric soil water content (gSWC, g kg⁻¹) with corresponding soil water content as a percentage of field capacity (SWC, % FC), logarithm precompression stress (log σ_P) and precompression stress in unit kPa (σ_P), slope of the virgin compression line (m_{VCL}), dry bulk density (BD) and dry bulk density (BD₃₅₀) at the 350 kPa loading step at the sites for the model validation.

Site-Code	Site and depth (cm)	Matric potential	TPV (cm ³ /cm ³)	vSWC (cm ³ /cm ³)	gSWC (g kg ⁻¹)	SWC (% FC)	log σ_P	σ_P (kPa)	m _{VCL}	BD (g cm ⁻³)	BD ₃₅₀ (g cm ⁻³)
6.1.	Neurath III 45-48	-6 kPa	0.35	0.33	193	100	2.39	245	0.088	1.73	1.85
		-30 kPa	0.35	0.28	162	83.9	2.44	275	0.113	1.74	1.85
		-100 kPa	0.34	0.27	155	80.3	2.43	269	0.093	1.76	1.89
7.1.	Fortuna IV 32-35	-6 kPa	0.43	0.45	294	100	1.84	69	0.130	1.54	1.73
		-30 kPa	0.44	0.33	217	73.8	1.75	56	0.119	1.51	1.68
		-100 kPa	0.43	0.28	185	62.9	1.85	71	0.142	1.53	1.69
		-1500 kPa	0.43	0.25	160	54.4	2.11	129	0.138	1.54	1.68
7.2.	Fortuna IV 55-58	-6 kPa	0.47	0.44	306	100	1.79	62	0.148	1.43	1.65
		-30 kPa	0.47	0.35	246	80.4	1.59	39	0.144	1.42	1.65
		-100 kPa	0.47	0.22	153	50.0	1.94	87	0.176	1.42	1.63
		-1500 kPa	0.48	0.14	101	33.0	2.15	141	0.149	1.39	1.50
7.3.	Fortuna IV 85-88	-6 kPa	0.48	0.38	272	100	1.37	23	0.132	1.40	1.65
		-30 kPa	0.48	0.30	215	79.0	1.59	39	0.154	1.40	1.63
		-100 kPa	0.48	0.20	144	52.9	2.06	115	0.201	1.40	1.58
9.1.	Pesch 40-43	-6 kPa	0.42	0.38	245	100	2.30	200	0.134	1.55	1.68
		-30 kPa	0.41	0.33	210	85.7	2.30	200	0.150	1.56	1.70
		-100 kPa	0.41	0.28	180	73.6	2.35	224	0.159	1.56	1.71

Table 3.1.2 (continuation). Total pore volume (TPV, cm³/cm³), volumetric soil water content (vSWC, cm³/cm³) and gravimetric soil water content (gSWC, g kg⁻¹) with corresponding soil water content as a percentage of field capacity (SWC, % FC), logarithm precompression stress (log σ_P) and precompression stress in unit kPa (σ_P), slope of the virgin compression line (m_{VCL}), dry bulk density (BD) and dry bulk density (BD₃₅₀) at the 350 kPa loading step at the sites for the model validation.

Site-Code	Site and depth (cm)	Matric potential	TPV (cm ³ /cm ³)	vSWC (cm ³ /cm ³)	gSWC (g kg ⁻¹)	SWC (% FC)	log σ_P	σ_P (kPa)	m_{VCL}	BD (g cm ⁻³)	BD ₃₅₀ (g cm ⁻³)
10.1.	Quellendorf 10-13	-6 kPa	0.34	0.26	149	100	2.16	145	0.148	1.72	1.89
		-30 kPa	0.34	0.22	127	85.1	2.16	145	0.143	1.73	1.89
		-100 kPa	0.34	0.21	124	83.4	2.12	132	0.163	1.72	1.89
11.1.	Herrengosserstedt I 18-21	-6 kPa	0.45	0.36	247	100	2.09	123	0.214	1.44	1.69
		-100 kPa	0.45	0.32	219	88.8	2.11	129	0.225	1.44	1.69
11.2.	Herrengosserstedt I 32-35	-6 kPa	0.40	0.34	216	100	2.24	174	0.182	1.56	1.75
		-100 kPa	0.41	0.30	195	90.4	2.32	209	0.203	1.55	1.73
11.3.	Herrengosserstedt II 12-15	-6 kPa	0.48	0.48	356	100	1.95	89	0.174	1.34	1.54
		-100 kPa	0.48	0.44	327	91.9	2.03	107	0.163	1.35	1.53
11.4.	Herrengosserstedt II 25-28	-6 kPa	0.48	0.47	343	100	1.96	91	0.166	1.38	1.58
		-100 kPa	0.49	0.37	271	78.9	2.21	162	0.171	1.35	1.51
12.1.	Uchtdorf 19-22	-6 kPa	0.42	0.17	114	100	1.76	58	0.142	1.52	1.74
		-10 kPa	0.40	0.17	109	95.3	1.85	71	0.137	1.55	1.75
12.2.	Uchtdorf 35-38	-6 kPa	0.36	0.10	62	100	1.60	40	0.074	1.68	1.86
		-10 kPa	0.36	0.10	57	92.6	1.49	31	0.067	1.69	1.84
13.1.	Lossa 2-5	-6 kPa	0.53	0.33	272	100	1.25	18	0.178	1.22	1.62
		-1000 kPa	0.53	0.15	126	46.2	2.02	105	0.277	1.23	1.49

Table 3.1.2 (continuation). Total pore volume (TPV, cm³/cm³), volumetric soil water content (vSWC, cm³/cm³) and gravimetric soil water content (gSWC, g kg⁻¹) with corresponding soil water content as a percentage of field capacity (SWC, % FC), logarithm precompression stress (log σ_P) and precompression stress in unit kPa (σ_P), slope of the virgin compression line (m_{VCL}), dry bulk density (BD) and dry bulk density (BD₃₅₀) at the 350 kPa loading step at the sites for the model validation.

Site-Code	Site and depth (cm)	Matric potential	TPV (cm ³ /cm ³)	vSWC (cm ³ /cm ³)	gSWC (g kg ⁻¹)	SWC (% FC)	log σ_P	σ_P (kPa)	m_{VCL}	BD (g cm ⁻³)	BD ₃₅₀ (g cm ⁻³)
14.1.	Hemleben I 9-12	-6 kPa	0.52	0.39	306	100	1.51	32	0.204	1.27	1.62
		-100 kPa	0.52	0.35	268	87.6	1.76	58	0.254	1.29	1.62
15.1.	Rothenberga I 14-17	-6 kPa	0.40	0.35	220	100	2.19	155	0.154	1.59	1.74
		-30 kPa	0.39	0.32	201	91.3	2.19	155	0.144	1.60	1.74
		-100 kPa	0.39	0.32	198	90.0	2.34	219	0.142	1.61	1.74
15.2.	Rothenberga II 17-20	-6 kPa	0.49	0.36	265	100	1.72	52	0.144	1.36	1.56
		-30 kPa	0.49	0.30	227	85.7	1.73	54	0.161	1.34	1.55
		-100 kPa	0.49	0.28	211	79.5	2.09	123	0.208	1.35	1.52
18.1.	Lückstedt I 17-20	-6 kPa	0.39	0.24	149	100	2.19	155	0.105	1.61	1.73
		-100 kPa	0.37	0.14	87	58.5	2.36	229	0.082	1.64	1.75
18.2.	Lückstedt II 17-20	-6 kPa	0.45	0.21	150	100	1.81	65	0.156	1.43	1.66
		-100 kPa	0.43	0.15	104	69.6	1.99	98	0.142	1.47	1.67
19.1.	Buttelstedt I 15-18	-6 kPa	0.53	0.33	272	100	1.28	19	0.223	1.21	1.59
		-30 kPa	0.54	0.31	261	96.0	1.23	17	0.231	1.19	1.62
19.2.	Buttelstedt I 45-48	-6 kPa	0.52	0.36	284	100	1.81	65	0.248	1.26	1.55
		-30 kPa	0.52	0.30	241	84.9	1.90	79	0.267	1.26	1.54

Table 3.1.2 (continuation). Total pore volume (TPV, cm³/cm³), volumetric soil water content (vSWC, cm³/cm³) and gravimetric soil water content (gSWC, g kg⁻¹) with corresponding soil water content as a percentage of field capacity (SWC, % FC), logarithm precompression stress (log σ_P) and precompression stress in unit kPa (σ_P), slope of the virgin compression line (m_{VCL}), dry bulk density (BD) and dry bulk density (BD₃₅₀) at the 350 kPa loading step at the sites for the model validation.

Site-Code	Site and depth (cm)	Matric potential	TPV (cm ³ /cm ³)	vSWC (cm ³ /cm ³)	gSWC (g kg ⁻¹)	SWC (% FC)	log σ_P	σ_P (kPa)	m_{VCL}	BD (g cm ⁻³)	BD ₃₅₀ (g cm ⁻³)
19.3.	Buttelstedt II 15-18	-6 kPa	0.47	0.37	266	100	1.72	52	0.224	1.38	1.60
		-30 kPa	0.47	0.29	212	79.9	2.05	112	0.319	1.38	1.64
21.1.	Halle I 15-25	-6 kPa	0.39	0.23	145	100	1.76	58	0.206	1.59	1.85
		-100 kPa	0.39	0.18	110	75.6	1.99	98	0.281	1.60	1.86
22.1.	Hemleben II 15-25	-6 kPa	0.56	0.38	326	100	1.62	42	0.289	1.17	1.55
		-1500 kPa	0.56	0.25	210	64.5	2.30	200	0.478	1.17	1.45
23.1.	Niestetal 15-25	-6 kPa	0.51	0.39	299	100	1.38	24	0.138	1.30	1.60
		-100 kPa	0.51	0.25	191	63.8	1.86	72	0.234	1.30	1.59
24.1.	Seehausen 15-25	-6 kPa	0.50	0.32	239	100	1.39	25	0.158	1.33	1.67
		-30 kPa	0.50	0.29	220	92.1	1.64	44	0.201	1.33	1.68
		-100 kPa	0.49	0.24	180	75.3	1.80	63	0.249	1.34	1.67

3.1.3.2. Derivation of the model

3.1.3.2.1. Change in precompression stress with matric potential

When matric potential changes from -6 to -30 kPa, the subsequent change in precompression stress is dependent on the level of the initial precompression stress at matric potential -6 kPa. This is demonstrated by the analysis of literature data (Fig. 3.1.2).

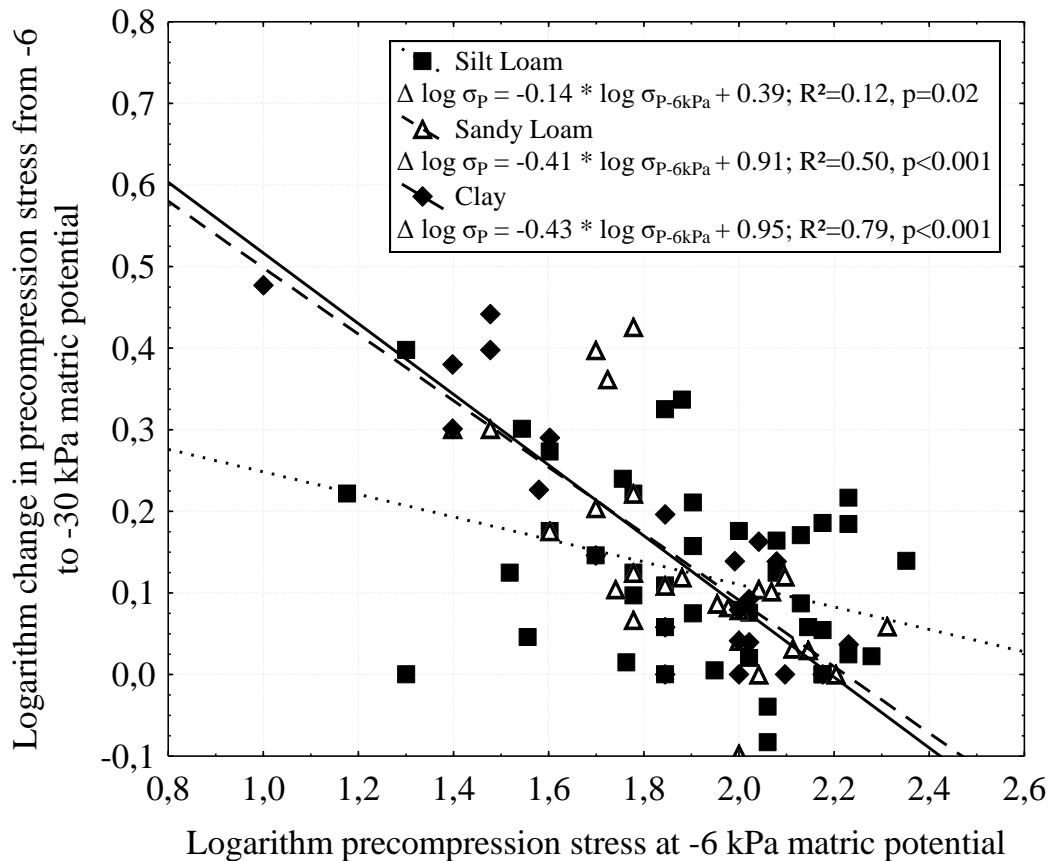


Figure 3.1.2. Logarithm change in precompression stress from -6 to -30 kPa matric potential using the example of soil texture classes “Silt Loam“, “Sandy Loam“ and “Clay“; combination of references Horn, 1986, Lebert, 1989, Nissen, 1998, Arvidsson, 2001, Arvidsson et al., 2003, Berli et al., 2003, Keller et al., 2004.

Moreover, this change decreases continuously as precompression stress increases. As a result, the soils can be divided into two groups. In the first are soils with a large increase in precompression stress from a small initial value when matric potential changes from -6 to -30 kPa. They are associated with a strong decline in this rise as precompression stress increases. This group includes the soil texture classes “Loam“, “Sandy Loam“, “Clay” and “Clay Loam“. The second includes the soil texture classes “Sand“, “Silt Loam” and “Silty Clay Loam“, which display a rather small increase in precompression stress from a small initial value when matric potential changes from -6 to -30 kPa. However, as initial precompression stress increases, these changes decrease less than in the first group. For all the texture classes not listed, it was not possible to make any deductions using the literature data. The individual values are generally

widely spread. In some cases, decreasing precompression stress levels were in fact measured as matric potential increased. Nonetheless the correlation is significant. The high variation of the literature data can be explained by the fact that soils with comparable precompression stress and soil texture can demonstrate differentiated structural properties and hence varying amounts of coarse pores (Arvidsson and Keller, 2004). Dehydrating these causes varying increases in stability. This effect is amplified by the range of clay, silt and sand contents which can also be present within a soil texture class, which contributes to further variation in the amount of coarse pores. Apart from pore size distribution, determining precompression stress according to Casagrande's method (1936) – applied in most of the studies used here – may contribute to a variation of the values, as this method is associated with a certain amount of subjectivity on the part of the observer (Rücknagel et al., 2010).

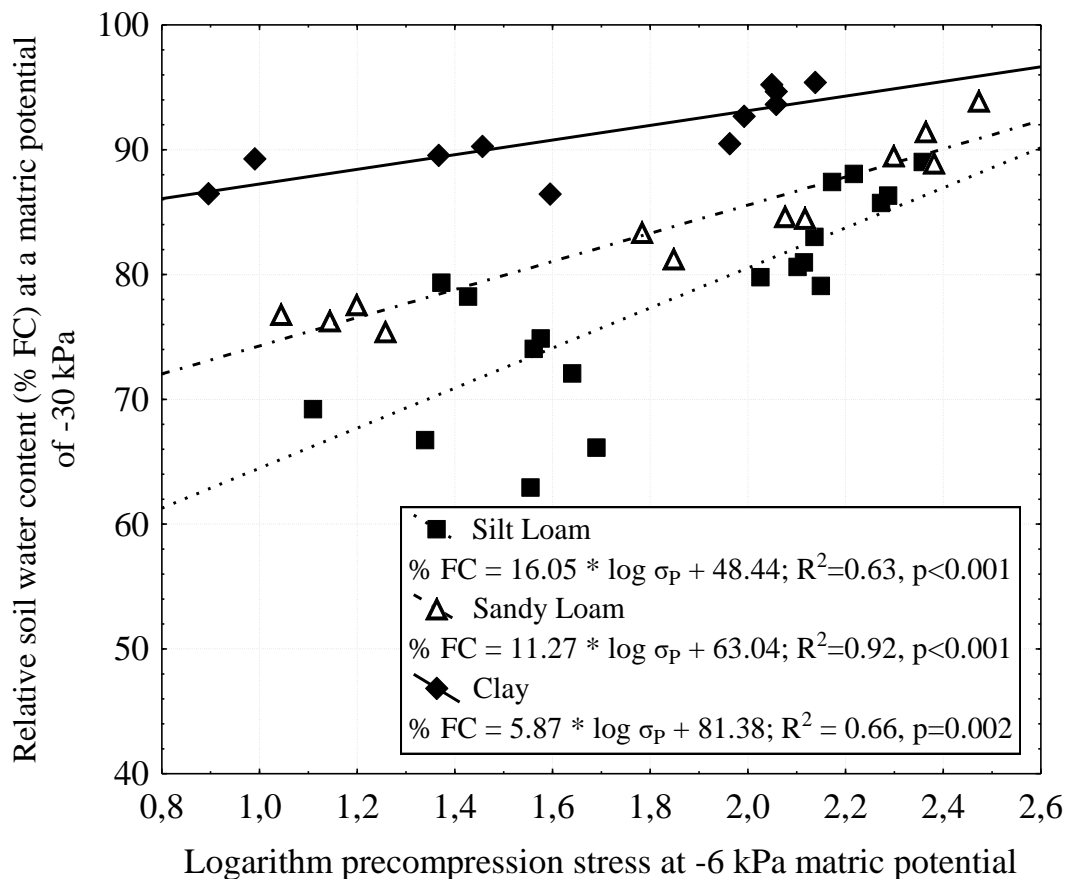


Figure 3.1.3. Relative soil water content at a matric potential of -30 kPa in comparison to the soil water content on a matric potential of -6 kPa (= 100 % FC) as a function of precompression stress at -6 kPa matric potential using the example of soil texture classes “Silt Loam“, “Sandy Loam“ and “Clay“.

Other factors which contribute to the large variation in individual values are the varying dimensions of the soil samples and the varying boundary conditions in the tests. For instance, the size of the soil core samples varies from 25 mm in height and 72 mm in diameter (e.g. Keller et al.,

2004) to 30 mm in height and 100 mm in diameter (e.g. Nissen, 1998) and the loading time per loading step is between 30 minutes (e.g. Berli et al., 2003) and 23 hours (e.g. Lebert, 1989).

3.1.3.2.2. Change in water content

In keeping with the aim of the paper, changes in precompression stress are to be calculated without the need for site-specific water retention curves when applying the model. Thus a relative water content (% FC) needs to be allocated to a matric potential of -30 kPa for different soils and depending on initial precompression stress. Examples of this procedure for a “Silt Loam”, a “Sandy Loam” and a “Clay” are depicted in Figure 3.1.3. As precompression stress increases, so does the relative water content at a matric potential of -30 kPa. This is due to an increasing dry bulk density, which also leads to an increase in precompression stress when aggregate density remains constant (Rücknagel et al., 2007). As dry bulk density increases, first the coarsest and most unstable pores are reduced in size. Coarse pores of $>50 \mu\text{m}$ are affected the most, but so are narrow coarse pores with a diameter of $10\text{-}50 \mu\text{m}$ (Lebert, 1989). The latter pore size range becomes dehydrated when matric potential is raised from -6 to -30 kPa. There are considerable differences between different texture classes. With comparable precompression stress, “Clay” in particular demonstrates a relatively lower water content than “Sandy Loam” and “Silt Loam”.

3.1.3.2.3. Principal approach in deriving the model

The principal approach used for the derivation of the regression function is depicted in Figure 3.1.4 for the example “All texture classes”:

1. For various initial precompression stress levels (-6 kPa matric potential), first the increase in precompression stress was determined when matric potential changed to -30 kPa. In the example of Figure 3.1.4, log initial precompression stress increases from 1.40 to around 1.70.
2. Now, the accompanying relative change in water content is missing. This is ascertained by way of the relationship between precompression stress at -6 kPa matric potential and the relative water content at -30 kPa matric potential. The relative water content is assigned to precompression stress at -6 kPa, because this is used in the model as an independent variable. In the example, water content corresponds to 80 % of water content at a matric potential of -6 kPa (=80 % FC).
3. This results in a first data point for the regression model. For an initial value at field capacity of log precompression stress 1.40 and a decrease in water content to 80% of field capacity, the increase in log precompression stress (dependent variable) amounts to 0.30: $0.30=f(1.40 \log \sigma_P; 80 \% \text{ FC})$. To work out a statistical model for all values, 15 data points were ascertained in this way (Table 3.1.3). An additional, satisfactory derivation of data points for

greater matric potentials using the literature data was not possible, therefore all data points which could not be identified from the relationships seen in Figures 3.1.1 and 3.1.2 were calculated via linear interpolation. Thus in the example the increase in log precompression stress at 90 % FC is 0.15, and at 70 % FC it is 0.45. This approach is a radical simplification, because the correlation between the relative change in water content and the change in pre-compression stress is not necessarily linear. However, the model in question is both simple and empirical and is intended for practical application; the aim is to achieve a high level of practicability.

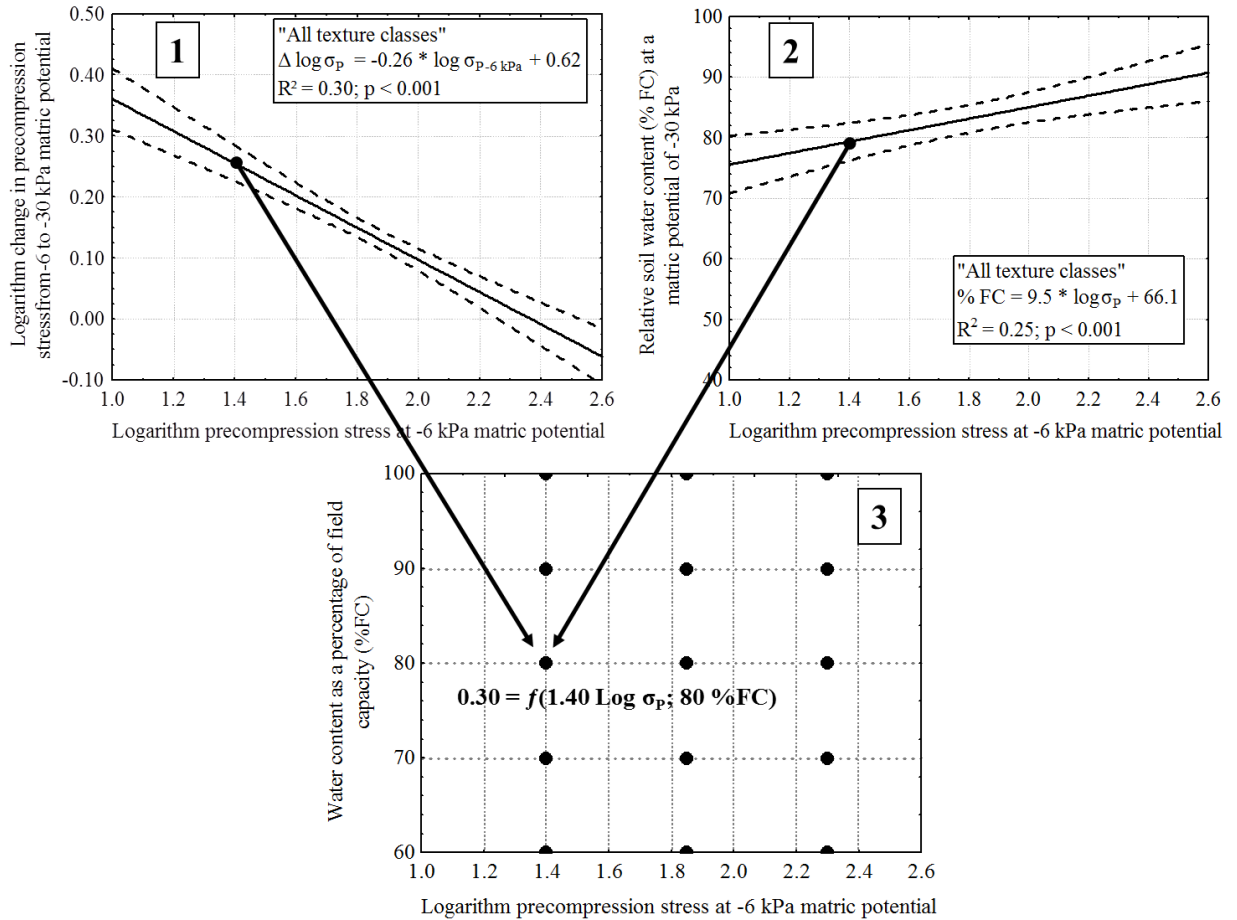


Figure 3.1.4. Depiction of model derivation for “All texture classes”: [1] Logarithm change in precompression stress from -6 to -30 kPa matric potential; [2] Relative soil water content at a matric potential of -30 kPa as a function of precompression stress at -6 kPa matric potential; [3] Matrix to derive regression function.

The matrices calculated in this way constitute the basis of a regression model (Fig. 3.1.5). The model calculates the increase z in precompression stress (logarithm) using the parameters of soil water content as a percentage of field capacity (% FC) and precompression stress at a matric potential of -6 kPa ($\log \sigma_{P-6\text{kPa}}$):

$$z = a + b * \log \sigma_{P-6\text{kPa}} + c * \% \text{ FC} + d * \% \text{ FC}^2 + e * \log \sigma_{P-6\text{kPa}} * \% \text{ FC} \quad (3.1.-1)$$

Precompression stress (logarithm) for any water content is then calculated according to:

$$\log \sigma_P = \log \sigma_{P-6kPa} + Z \quad (3.1.-2)$$

Table 3.1.3. Data points for increasing logarithm precompression stress used for the model “All texture classes”; $\log \sigma_{P-6kPa}$ logarithm precompression stress at -6 kPa matric potential.

Precompression stress ($\log \sigma_{P-6kPa}$)	Water content as a percentage of field water capacity				
	100	90	80	70	60
1.40	0.00	0.15	0.30	0.45	0.60
1.85	0.00	0.11	0.22	0.33	0.44
2.30	0.00	0.07	0.14	0.21	0.28

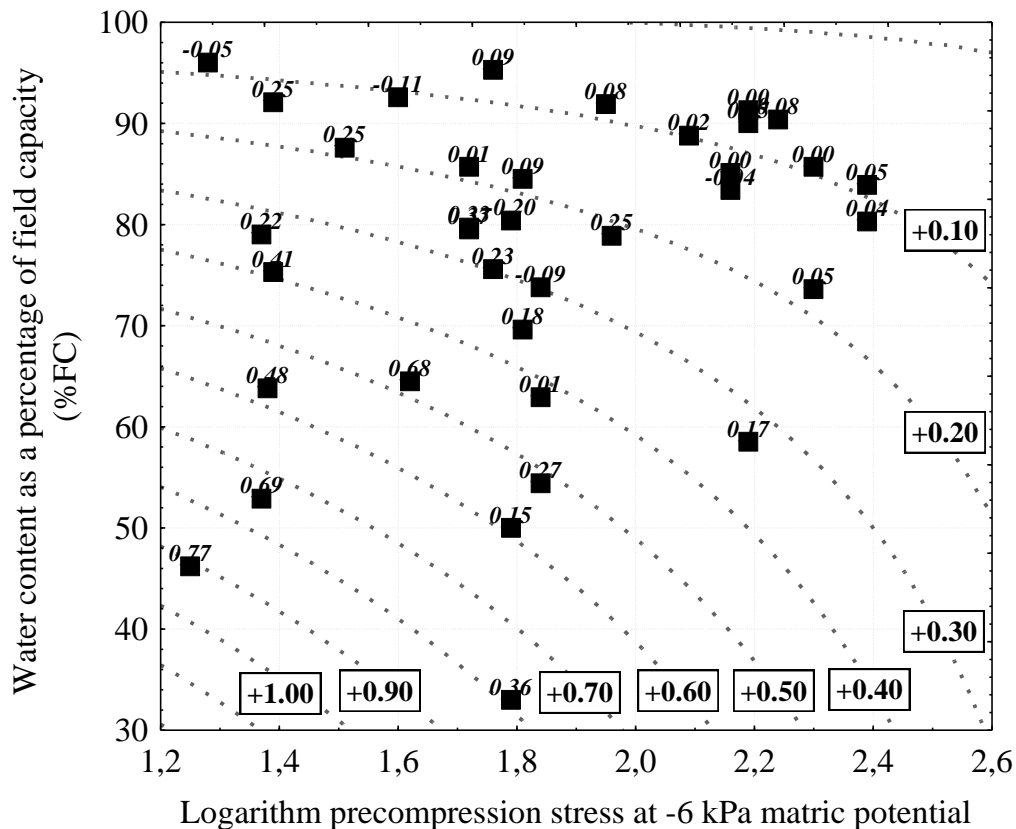


Figure 3.1.5. Regression model (“All texture classes”) for estimating change in precompression stress as a function of relative soil water content (%FC) and initial precompression stress at -6 kPa matric potential; the black squares shows the values of model validation.

3.1.3.2.4. Differentiating according to soil texture class

Bearing in mind the preceding sections, it becomes evident that very different changes in precompression stress and water content may occur in varying soils. Accordingly, one might suspect that differentiating the soils according to different soil texture classes may increase the

accuracy of the model. If the observations from Fig. 3.1.2 and 3.1.3 are linked, four groups of soils can be empirically differentiated from each other:

1. The increase in precompression stress when matric potential changes from -6 to -30 kPa is “great” and the relative change in water content is also “great”. This group includes the soil texture classes “Loam” and “Sandy Loam”.
2. The increase in precompression stress when matric potential changes from -6 to -30 kPa is “great”, but the relative change in water content is “slight”. This group includes the soil texture classes “Clay” and “Clay Loam”.
3. The increase in precompression stress when matric potential changes from -6 to -30 kPa is “slight” and the relative change in water content is also “slight”. This group includes the soil texture classes “Silty Clay Loam” and “Silty Clay”.
4. The increase in precompression stress when matric potential changes from -6 to -30 kPa is “slight”, but the relative change in water content is “great”. This group includes the soil texture classes “Sand”, “Silt Loam”, “Silt” and “Loamy Sand”.

In Tab. 3.1.4 the constants (a, b, c, d, e) are given for the calculation of the increase z according to equation (3.1.-1) for “All texture classes” and the different soil texture classes.

Table 3.1.4. Constants for “All texture classes” and different texture classes for estimating pre-compression stress as a function of soil water content based on field capacity data.

Texture classes	Constant				
	a	b	c	d	e
All texture classes	2.8335	-0.9271	-0.0279	$1.67 \cdot 10^{-7}$	0.00906
Loam, Sandy Loam	2.7833	-1.0000	-0.0278	$-116 \cdot 10^{-15}$	0.01000
Clay, Clay Loam	4.3056	-1.4444	-0.0431	$-537 \cdot 10^{-16}$	0.01440
Silty Clay Loam, Silty Clay	2.5333	-0.6667	-0.0253	$21 \cdot 10^{-14}$	0.00667
Sand, Silt Loam, Silt, Loamy Sand	1.7611	-0.5556	-0.0176	$4.11 \cdot 10^{-14}$	0.00556

3.1.3.3. Validation of the model

Concerning both the application of systems of equations for “All texture classes” and differentiated soil texture classes, the accuracy of the modelling approach presented here is good (Fig. 3.1.6). The statistical functions in the comparison of recorded and calculated values actually produce flatter slopes than the theoretical 1:1 line ($m=0.72$ for “All texture classes” and $m=0.59$ for the calculation for different soil texture classes) and intersect the abscissa a little above zero

($x_0=0.16$ for “All texture classes” and $x_0=0.11$ for the calculation for different soil texture classes). Thus the changes in precompression stress are somewhat overestimated in the slighter area, while they are underestimated in the greater area. In comparison to “All texture classes”, calculation according to soil texture class causes a reduction of the mean absolute errors (MAE) from 0.15 to 0.11 and of the RMSE from 0.19 to 0.14. The coefficient of determination and the index of agreement (IA) simultaneously increase, from 0.54 to 0.67 and 0.92 to 0.95 respectively. Calculation according to various soil texture classes is therefore particularly recommended in the case of applications with high accuracy requirements. In soils for whose soil texture class no constants could be identified (“Sandy Clay” and “Sandy Clay Loam”), changes in precompression stress must be calculated according to the constants for “All texture classes”. Nevertheless, application according to soil texture class is possible for a very wide range of sites.

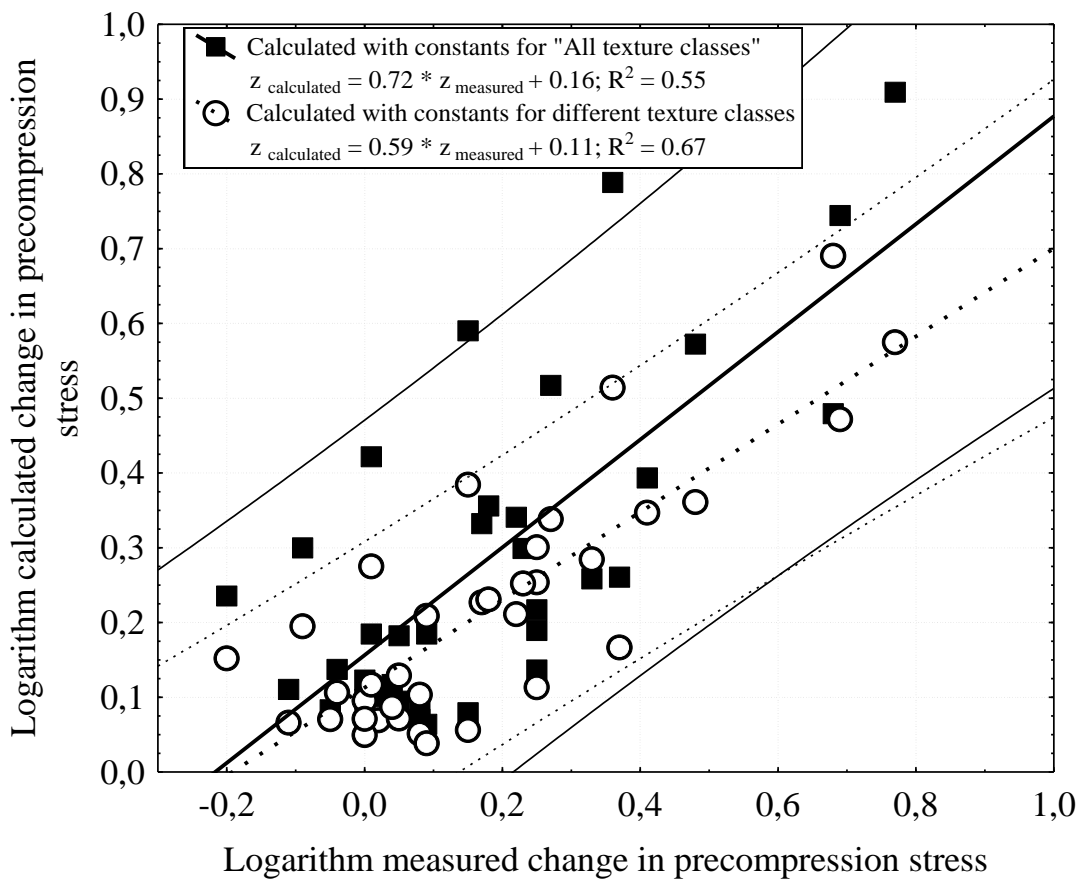


Figure 3.1.6. Measured change in precompression stress and values calculated with function (3.1.-1); constants for “All texture classes” (black square) and constants for different texture classes (empty circles). The area between the thin lines shows the calculated values at 95% probability.

Furthermore, the errors of this modelling approach are approximately comparable with the variations of values measured in the relationships of Arvidsson et al. (2003) and Berli et al. (2003) concerning matric potential and precompression stress. In some cases, similarly to with the literature data, decreasing precompression stress levels were measured with increasing matric

potential. The good validity of the modelling approach presented here generally underlines the high level of practicability in the model's derivation, despite the fact that the derivation is not always in keeping with a classical approach one might expect based on the fundamentals of soil physics.

Ranging between 18 (log 1.25) and 246 kPa (log 2.39), almost the entire breadth of precompression stress values measured in arable soils at a matric potential of -6 kPa is represented (Lebert, 1989). Water content levels of up to 33 % of field capacity in the tests ensure that a broad spectrum of moisture conditions can be covered.

3.1.4. Conclusions

The regression model presented here provides a simple, relatively accurate and widely usable tool for estimating precompression stress for small water contents. There are minimal requirements (precompression stress at matric potential of -6 kPa and relative water content as a percentage of field capacity) for the provision of input data. No labour-intensive soil compression tests are needed to determine the relationship between water content and precompression stress. These are the prerequisites for a practicable application in compaction models for the purposes of preventive soil protection.

Acknowledgement

The authors offer their heartfelt thanks to Dr. Thomas Keller (Agroscope Research Station ART, Switzerland) for checking the contents of this article most thoroughly.

3.2. The influence of soil gravel content on compaction behaviour and precompression stress

Published in: *Geoderma* 209-210 (2013), 226-232

Jan Rücknagel¹, Philipp Götze¹, Bodo Hofmann¹, Olaf Christen¹, Karin Marschall²

¹Institute of Agricultural and Nutritional Sciences, Department Agronomy and Organic Farming, University of Halle-Wittenberg, Betty-Heimann-Str. 5, 06120 Halle/Saale (Germany)

²Thüringer Landesanstalt für Landwirtschaft, Naumburger Str. 98, 07743 Jena (Germany)

Abstract

Many arable soils have significant horizon-specific gravel content levels. Just how these influence compaction behaviour, and in particular precompression stress as an important criterion of a soil's susceptibility to compaction, has yet to be sufficiently clarified. This article is intended to contribute towards answering this question.

Firstly, three different fine earths, from the "Clay", "Silt Loam" and "Sandy Loam" soil texture classes were mixed with staggered proportions (0, 10, 20, 30, 40 per cent by volume) of a quartz gravel (the shape of which was subrounded to rounded, average weighted diameter 6 mm). Soil core samplers were filled with the mixtures at a typical density for a natural site. In the case of the 30 per cent by volume variant only, in addition to the quartz gravel an angular to subangular limestone gravel with the same size graduation was also used. The tests were supplemented by 20 samples from a natural site; the gravel content of these varied between 0.1 and 23.5 per cent by volume. All of the disturbed and natural samples were adjusted to a water content at a matric potential of -6 kPa. Subsequently, an oedometer test was used to apply loads to them in stages (5-550 kPa). Precompression stress was calculated using the resulting stress/bulk density functions.

While fine earth bulk density remained constant, the staggered addition of quartz gravel led to an increase in the whole soil density after packing, and thus also to a vertical shift in overall stress/bulk density functions. However, the stress-density functions of the fine earth do show that the overall compaction of fine earth decreased as gravel content increased. In the case of low gravel content levels of no more than 10 per cent by volume, the increase in precompression stress (log) in the disturbed samples was, on the whole, very low. In the disturbed samples, however, as gravel content increased precompression stress (log) increased exponentially. Contrary to this, a continuous linear increase in precompression stress (log) could be observed with increasing gravel content in the natural samples. The angular to subangular shape of the gravel only resulted in greater precompression stress (log) in the "Silt Loam".

At gravel-rich sites, gravel content influences soil compaction behaviour and precompression stress very strongly. For this reason, it is essential that it be considered when assessing such sites' risk of compaction damage.

3.2.1. Introduction

Many soils contain varying horizon-specific amounts of gravel. A data-set by Batjes (1997) based on FAO-UNESCO soil units includes C-class (6-15 vol.%) gravel content levels for phaeozems and yermosols, M-class (16-40 vol.%) gravel content levels for lithosols, regosols and rankers as well as A-class (>41 vol.%) gravel content levels for rendzinas. Re-cultivated soils, for instance following an open-cast tunnel construction (Kaufmann et al., 2009), can also have average gravel content levels. The distribution of gravelly soils varies highly from region to region. In Western Europe, according to Poesen and Lavee (1994), it is mostly Mediterranean areas that are characterised by large amounts of gravelly soils, although gravelly soils can often also be found in Europe's low mountain ranges.

The external shape and the quantity of the gravel in these soils vary considerably. A distinction is made between angular, subangular, subrounded, rounded and well rounded shapes (Mitchell and Soga, 2005). Gravel includes all particles larger than 2 mm. In addition to actual gravel (USDA system: diameter of 2-76 mm), cobbles (USDA system: diameter up to 254 mm) can also be found at arable sites. Only in exceptional cases is arable farming practised on soils with a high proportion of stones larger than 254 mm in diameter. Apart from affecting root penetration behaviour (Babalola and Lal, 1977), infiltration properties (Brakensiek and Rawls, 1994) and the water retention curve (Ingelmo et al., 1994), gravel content in the soil matrix also has an impact on a soil's mechanical properties.

Until now, studies examining the impact of gravel content and its shape on the compaction behaviour of soils have largely only been conducted using Proctor tests, or modified procedures based on these (e.g., Donaghe and Torrey, 1994; Chinkulkijniwat et al., 2010). The purpose of most of these studies was to determine the maximum achievable dry bulk density and water content for optimum compaction of the soil material, for example in the context of construction work. As gravel content increases so does the maximum achievable dry bulk density, while the optimum water content for compaction drops (Chinkulkijniwat et al., 2010).

However in soil science, specifically as concerns protecting soil from compaction, it is important to know the maximum mechanical load capacity of a soil at which essential soil functions (e.g., hydraulic and air conductivity) are still adequately preserved. This question applies particularly to arable farming sites where agricultural machinery with a constantly increasing weight is used. Oedometer tests are thus performed in order to map a soil's stress/strain behaviour. In these experiments, the soil sample, which is adjusted to a specific matric potential (e.g., -6 kPa), is subjected in stages to increasing loads, and the resulting settlement accurately measured. Details about how these experiments are performed can be found in Bradford and Gupta (1986). The resulting stress/settlement curves identified in a semi-logarithmic graph, or indeed stress/dry bulk density curves or stress/void ratio curves of pre-compacted soils derived from these, can be used to determine precompression stress. In soil mechanics, this is a direct criterion of a soil's susceptibility to compaction (Arvidsson and Keller, 2004). According to Topp

et al. (1997), precompression stress corresponds to the maximum stress that has acted on the soil in the past, if it is determined under the same load conditions. In the topsoil layer, it results from pressure exerted when machinery is driven over the ground, from tillage activity aimed at loosening the soil and from the formation of microstructures caused by drying and shrinkage processes, the effects of frost and biogenic aggregate formation. In the subsoil, precompression stress is also due to the load from overlying soil layers as well as previous coverings of ice.

So far, there have been only very few results on the effect of soil gravel content on precompression stress, and at times these contradict each other. For example, Horn and Fleige (2003) report higher precompression stress as gravel content increases, whereas Kaufmann et al. (2009) describe a negative effect of gravel content in multiple regressions. The aim of this study is, therefore, to investigate the question of just how an increasing gravel content and different gravel shapes affect precompression stress and compaction behaviour in soils of different texture classes.

3.2.2. Materials and methods

3.2.2.1. Preparation of artificial samples

The experiments were based on artificial soil core samples with three fine earths from different soil texture classes (Tab. 3.2.1).

Table 3.2.1. Description of the test soils for the disturbed and naturally extracted samples, ¹USDA classification system (Gee and Bauder, 1986), ² mean values, ³ ranges of measured values.

Texture class ¹	Clay (g kg ⁻¹)	Silt (g kg ⁻¹)	Sand (g kg ⁻¹)	Organic carbon content (g kg ⁻¹)	CaCO ₃ content (g kg ⁻¹)
Disturbed samples					
Clay	460	370	170	28	3
Silt Loam	130	780	90	12	0
Sandy Loam	100	310	590	11	0
Natural samples					
Silt Loam	220 ² (150-280) ³	600 ² (410-740) ³	180 ² (70-350) ³	16 ² (11-21) ³	93 ² (3-210) ³

Only by preparing disturbed samples is it possible to exclude naturally occurring variability, particularly that of fine earth bulk density. The soil was extracted in the field using a small shovel. It was then carefully divided using a sieve with an opening size of 20 mm; until the experiments were carried out, the soil was stored in closed buckets and kept cool. Variants with a gravel content (GR) of 0, 10, 20, 30 and 40 per cent by volume were created for each soil type (8 soil core samplers per variant). According to Holtz and Lowitz (1957, as cited in Donaghe

and Torrey, 1994), gravel particle diameter in soil-gravel mixtures should not be larger than 1/5 to 1/6 of the compaction mold diameter. The soil core samplers used in this study (volume 220 cm³) have a height-to-diameter ratio of 1:3.6 (28 mm high, 101 mm in diameter). For this reason, a very fine quartz gravel (particle density 2.64 g cm⁻³) with an average weighted diameter of 6 mm was used (particle size distribution 65 g kg⁻¹ at a size of 8-10 mm, 714 g kg⁻¹ at a size of 5-8 mm and 221 g kg⁻¹ at a size of 2-5 mm). In this way the size ratio of the gravel – not only to the diameter but also to the height of the soil core samplers – is kept largely uniform. The shape of the gravel was subrounded to rounded (Fig. 3.2.1).

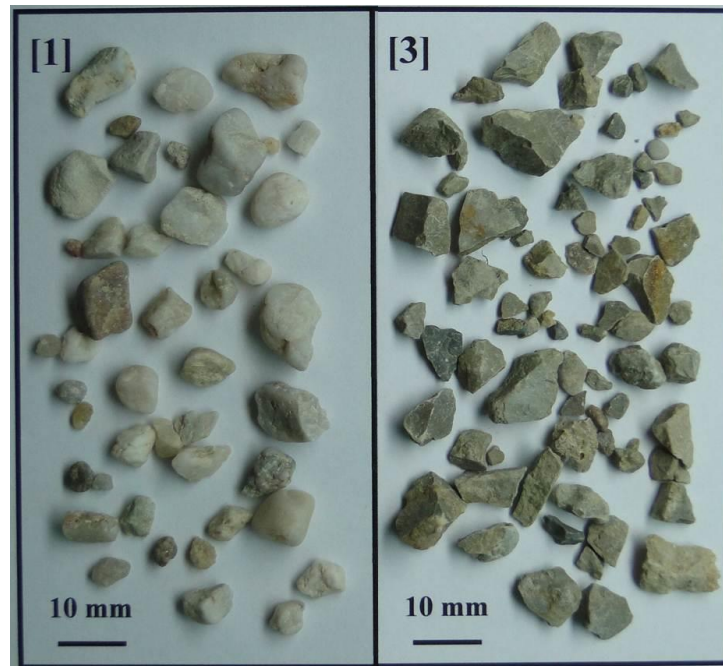


Figure 3.2.1. Shape and size distribution of the gravel for the tests with disturbed samples: [1] subrounded/rounded shapes, [3] angular/subangular shapes; each rectangle containing 10 g gravel.

Additionally, in the variant with 30 per cent gravel by volume, for all three fine earths soil core samples were created with limestone gravel (particle density 2.72 g cm⁻³), which has an angular to subangular form and the same size graduation as with the quartz gravel (Fig. 3.2.1). It was not possible to use the limestone gravel for all the gravel content variants, because not enough limestone gravel with the same properties was available.

At natural field water contents of 224 g kg⁻¹ (Clay), 226 g kg⁻¹ (Silt Loam) and 198 g kg⁻¹ (Sandy Loam), the fine earths were mixed uniformly with the dry quartz gravel or limestone gravel and then added to the soil core samplers. In keeping with previous studies on natural sites (Rücknagel et al. 2007, Rücknagel et al. 2012b), the fine earth density was 1.15 g cm⁻³ for the “Clay”, 1.30 g cm⁻³ for the “Silt Loam” and 1.40 g cm⁻³ for the “Sandy Loam”, and was the same for all of the gravel content variants within each texture class.

3.2.2.2. Extraction of naturally occurring samples

To verify the experiments on the disturbed samples, a total of 20 soil core samples were extracted from a naturally formed gravelly topsoil (9-12 cm) at an arable site in Rastenberg (Germany, Federal State of Thuringia). The average clay and sand contents in the samples were 220 g kg⁻¹ clay (150-280 g kg⁻¹) and 180 g kg⁻¹ sand (70-350 g kg⁻¹) (soil texture class “Silt Loam”), and the amount of soil organic carbon was 16 g kg⁻¹ (11-21 g kg⁻¹). In addition to the soil texture and the amount of organic carbon, the fine earth measuring <2 mm from each soil core sampler was examined for its calcium carbonate content and pH value. The site was chosen because, while the texture of the fine earth remains similar, the gravel content in the form of limestone gravel (angular to subangular shape) varies locally between 0.1 and 23.5 per cent by volume and the mean weighted diameter of the gravel is just 10 mm (particle size distribution 41 g kg⁻¹ at a size of 20-22 mm, 410 g kg⁻¹ at a size of 10-20 mm, 140 g kg⁻¹ at a size of 8-10 mm, 208 g kg⁻¹ at a size of 5-8 mm and 201 g kg⁻¹ at a size of 2-5 mm). This is the prerequisite for using standardised soil core samplers of the aforementioned size. After the soil compression tests and once the dry bulk density had been determined, wet screening was performed to determine the gravel content and size distribution. When taking the samples, special care was taken to minimise any disturbance to the natural soil structure caused by hammering the soil core samplers in. In the case of the samples with a high gravel content, it was not possible to simply hammer the soil sample rings into the ground. This was because non-visible gravel beneath the rings could have caused the soil to become loose. For this reason, a knife was used to cut the soil samples to a diameter of 100 mm (which corresponds to the diameter of the soil sample rings) so as not to loosen the gravel. A soil sample ring was then positioned around the soil sample, before the sample was removed from the ground and the top and bottom edges cut off cleanly. Since this procedure was not always successful straightaway, significantly more soil samples were prepared than could ultimately be used for the experiments.

3.2.2.3. Soil compression tests

The soil samples (disturbed or natural, extracted samples) were saturated and then adjusted to a matric potential of -6 kPa in a sand box. In German-speaking countries, this matric potential corresponds to field capacity. The soil samples in the core were subjected to pressures of 5, 10, 25, 50, 100, 200, 350 and 550 kPa successively in a fully automatic oedometer. After each loading step, a relaxation phase was included. Each loading step lasted 180 minutes and was followed by a relaxation phase lasting 15 minutes. In previous tests on soils of similar texture classes, for loading times of up to 540 minutes only very slight increases in settlement were measured in comparison to 180 minutes. Therefore, settlement can be regarded as largely finished after 180 minutes. However, just how matric potential changed during the soil compression tests was not measured. All tests took place under drained conditions. After drying the sample cores at 105 °C until the sample mass remained constant, the dry bulk density (BD) was determined after treatment in the oedometer.

Using the settlement (S) of the sample after each loading step compared to its initial height (H) as well as the density of the whole soil at the beginning of the experiment (BD_t), it is possible to calculate the resulting density of the whole soil for each loading step ($BD_{t\ xi}$):

$$BD_{t\ xi} = ((H - S)/H)^{-1} * BD_t \quad (3.2.-1)$$

In order to also be able to consider the deformation of the fine earth without the incompressible gravel content, the dry bulk densities of the fine earths (BD_{fe}) were calculated. This requires the fine earth mass per soil core sampler (m_{fe}) as well as the soil core sampler volume minus the volume of the gravel ($V_{GR\ cor.}$):

$$BD_{fe} = m_{fe} / V_{GR\ cor.} \quad (3.2.-2)$$

Mechanical precompression stress was determined according to Casagrande's (1936) graphical method, using the whole soil stress/bulk density functions and the stress/bulk density functions of fine earth in a semi-logarithmic graph. A tangent against the highest point of the curvature and a parallel to the abscissa are drawn. The point of intersection of the bisector of the angle between these two straight lines and the virgin compression line describes the precompression stress. Casagrande's (1936) graphical method involves a subjective assessment by the experimenter, who not only determines the point of the highest curvature visually but also decides which points should be used for generating the virgin compression line. Involving several independent persons can serve to further improve the variance values, and thus also the reproducibility and comparability of the obtained results (Rücknagel et al., 2010). For this reason, in this study precompression stress was determined by two independent experimenters. An average was calculated using the two logarithmic precompression stress values.

3.2.2.4. Statistical analysis

The program Statistica (StatSoft, Inc., 2009) was used for the variance analyses (ANOVA) and subsequent comparisons of mean values (Tukey's test or t-Test), the derivation of regression and correlation relationships, the calculation of standard deviations and the presentation of box plots. Significance levels of $p < 0.05$ are highlighted with different lower-case letters. The coefficient of determination and the p value are provided for the regression equations. The standard deviation (s) is calculated using the sum of the squared deviations (SQ) and the total number of repeated measurements (n) based on the following formula:

$$s = \sqrt{(SQ/(n-1))} \quad (3.2.-3)$$

Precompression stress was used in logarithmic form throughout, since the parameter of precompression stress displays a frequency distribution with a right skew when the unit 'kPa' is

employed. This is shown, for example, by combining the data sets by Lebert (1989) and Nissen (1998).

3.2.3. Results

3.2.3.1. Gravel content in disturbed soil samples

3.2.3.1.1. Stress/density curves

The impacts of different gravel contents on stress/density behaviour in the whole soil and on stress/density behaviour in the fine earth are explained in more detail here using the example of the “Clay” soil. Generally speaking, the other two fine earths used display similar effects. Adding 10, 20, 30 or 40 per cent quartz gravel by volume whilst keeping the fine earth’s dry bulk density at a level typical of a natural site (1.15 g cm^{-3}), initially results in increased dry bulk density in the whole soil, and thus to a downward shift of the entire stress/density functions (Fig. 3.2.2).

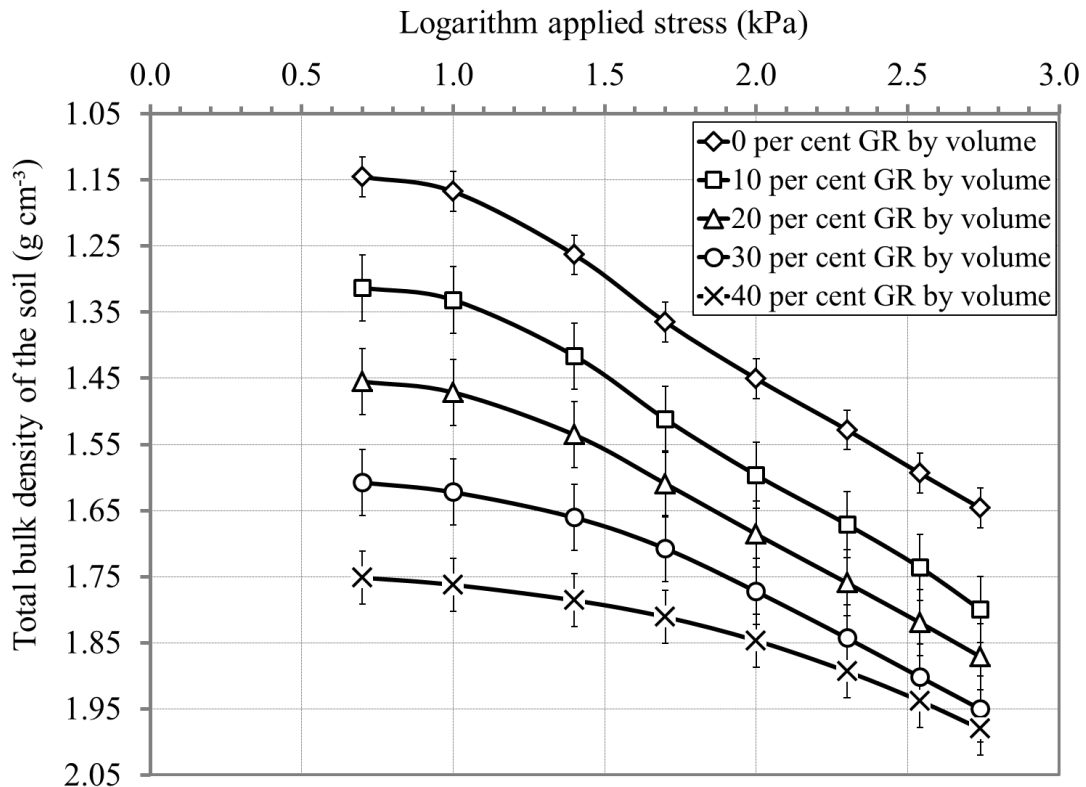


Figure 3.2.2. Mean logarithm stress/total bulk density functions at -6 kPa matric potential for the disturbed samples (8 replications) at different gravel contents (GR) and the fine earth texture class “Clay”, error bars show the standard deviation.

With increasing gravel content, a continuous change can be observed in the fundamental shape of the stress/density functions of the whole soil, moving from an S-shaped to a bi-linear curve

and, finally, to a rounded shape. Such changes can be observed in the case of fine earth as well (Fig. 3.2.3).

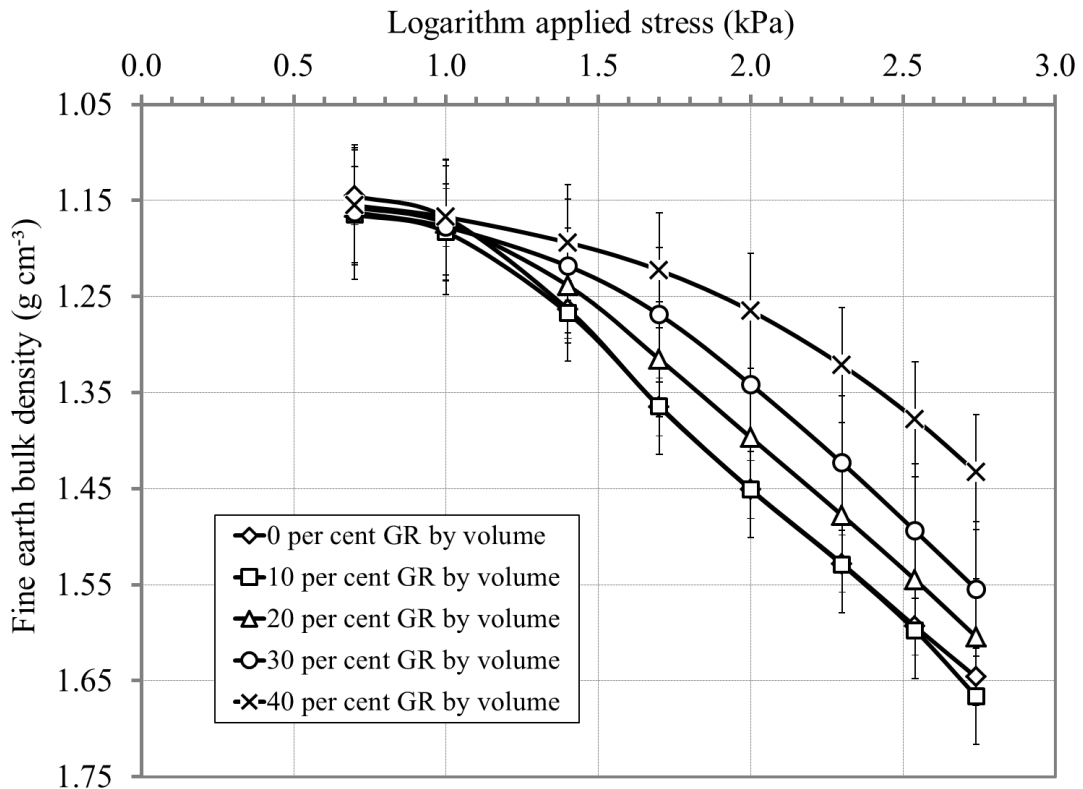


Figure 3.2.3. Mean logarithm stress/fine earth bulk density functions at -6 kPa matric potential for the disturbed samples (8 replications) at different gravel contents (GR) and the fine earth texture class “Clay”, error bars show the standard deviation.

The stress/density functions of both the whole soil and the fine earth can be divided up into a recompression portion and a virgin compression portion, enabling the calculation of mechanical precompression stress. However, they do show that the overall compaction of fine earth decreases as gravel content increases. For example, the fine earth densities decrease during the highest loading step (550 kPa), dropping from 1.65 g cm⁻³ (0 vol.% GR) and 1.67 g cm⁻³ (10 vol.% GR) to 1.60 g cm⁻³ (20 vol.% GR) and 1.55 g cm⁻³ (30 vol.% GR), and finally to 1.43 g cm⁻³ (40 vol.% GR). One exception here is the variant with a gravel content of 10 per cent by volume. Its stress/density function for the fine gravel does not differ from the gravel-free variant.

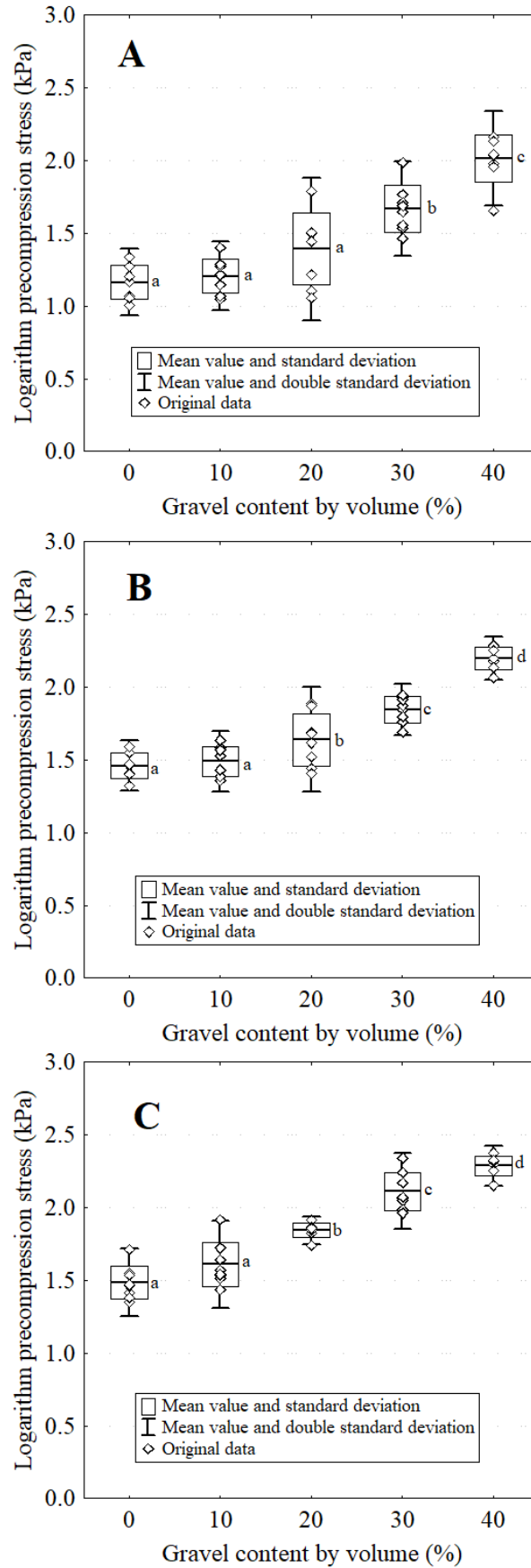


Figure 3.2.4. Logarithm precompression stress at different gravel contents and the fine earth texture classes “Clay” (A), “Silt Loam” (B), “Sandy Loam” (C); different small letters indicate significant differences between the gravel variants ($p < 0.05$).

3.2.3.1.2. Mechanical precompression stress

At 15 kPa (log 1.16) for the “Clay”, 29 kPa (log 1.46) for the “Silt Loam” and 30 kPa (log 1.48) for the “Sandy Loam”, the mechanical precompression stress levels in the samples which have no gravel are very low overall (Fig. 3.2.4). In all three textural classes of fine earth, gravel content levels of 10 per cent by volume merely result in a tendency towards increased precompression stress (+log 0.03 to 0.13). In the “Clay”, gravel content levels of 20 per cent by volume only result in a slight tendency towards increased precompression stress (+log 0.23), and in the “Silt Loam” and “Sandy Loam” they contribute significantly to an increase (+log 0.18 and 0.36 respectively). Not until gravel content levels of 30 and 40 per cent by volume does precompression stress increase considerably for all three textural classes of fine earth (+log 0.51 to 0.63 at 30 vol.% and +log 0.74 to 0.85 at 40 vol.%), and generally this increase is disproportionately higher than the increase in gravel content. In none of the fine earths textural classes used do the precompression stress values calculated for the whole soil and the fine earth differ from each other. For this reason, we have refrained from providing a separate presentation of the precompression stress determined using the stress-density functions of the fine earth.

For the three textural classes of fine earth in this study, the logarithmic change in precompression stress ($\Delta \log \sigma_P$) compared to the gravel-free soil can be estimated, depending on gravel content (GR) of up to a maximum of 40 per cent by volume, according to the following equations:

$$\text{Clay:} \quad \Delta \log \sigma_P = 0.0434 * e^{(0.0777 * GR)} \quad (3.2.-4)$$

$$R^2 = 0.75; p < 0.001$$

$$\text{Silt Loam:} \quad \Delta \log \sigma_P = 0.031 * e^{(0.083 * GR)} \quad (3.2.-5)$$

$$R^2 = 0.79; p < 0.001$$

$$\text{Sandy Loam:} \quad \Delta \log \sigma_P = 0.0772 * e^{(0.0631 * GR)} \quad (3.2.-6)$$

$$R^2 = 0.88; p < 0.001$$

Table 3.2.2. Logarithm precompression stress ($\log \sigma_P$) for different shapes of gravel and the different fine soil texture classes at 30 per cent gravel content by volume; different lower case letters indicate significant differences between the gravel shapes ($p < 0.05$).

Gravel shape	Clay	Silt Loam	Sandy Loam
Subrounded/rounded	1.67 a	1.84 a	2.11 a
Angular/subangular	1.63 a	2.14 b	2.06 a

In the “Silt Loam”, the shape of the added gravel influences precompression stress (Table 3.2.2). With an angular to subangular shape, precompression stress is significantly higher than

with a subrounded to rounded shape. In contrast, however, in the “Clay” and “Sandy Loam” precompression stress is not influenced by the shape of the gravel.

3.2.3.2. Gravel content in naturally structured soil samples

The experiments at the Rastenbergl site allow the disturbed samples to be compared with a natural context. Figure 3.2.5 demonstrates three typical stress/bulk density functions at -6 kPa matric potential with increasing gravel content. Similarly to the disturbed samples, the global shape also changes from an S-shape to a more bi-linear form.

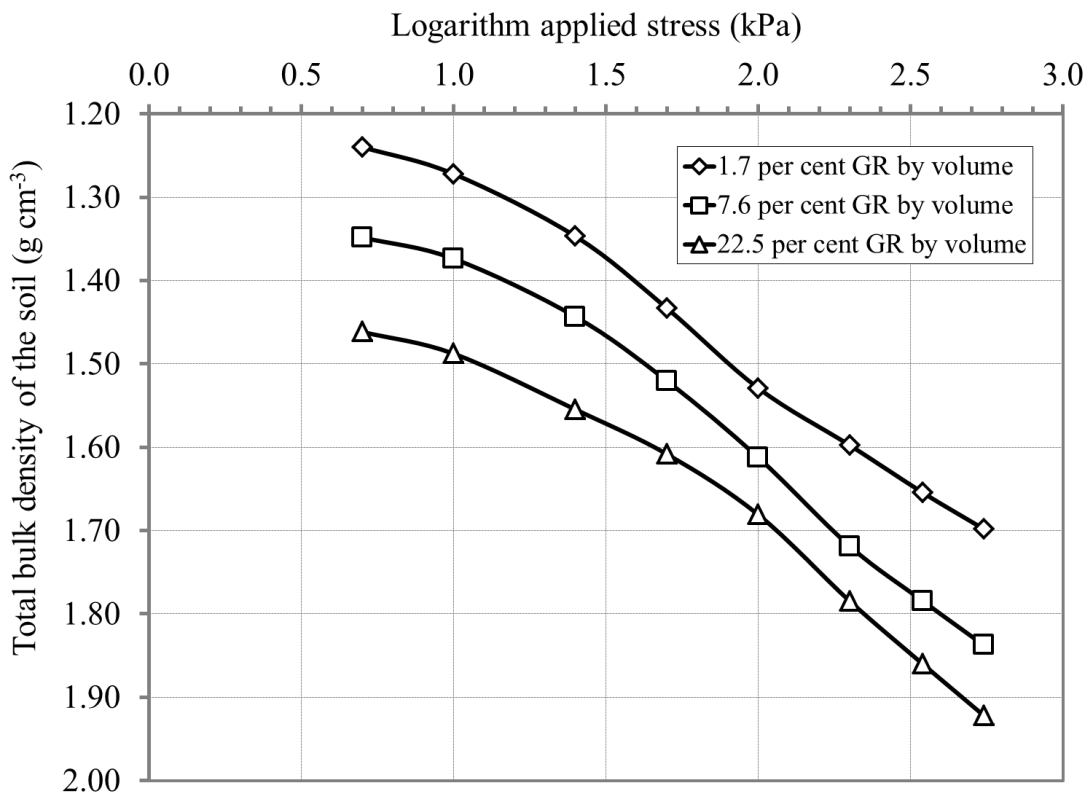


Figure 3.2.5. Examples of logarithm stress-total bulk density functions at -6 kPa matric potential for the naturally occurring samples at different gravel contents (GR) for the test site Rastenbergl.

The total bulk density of the soil, however, increases from an average of 1.18 g cm^{-3} (no gravel) to approximately 1.50 g cm^{-3} in the soil core samplers with the highest gravel contents (Fig. 3.2.6). Here, the bulk density of the fine earth remains constant at around 1.17 g cm^{-3} for the entire range of gravel content levels. While at the highest loading step the fine earth bulk densities in the disturbed samples decrease as gravel content rises, at the Rastenbergl site no change in fine earth bulk density can be observed. Unlike in the artificially produced samples, as the gravel content level increases there are also slight increases in sand content ($r=0.71$, $p=0.02$), organic carbon content ($r=0.57$, $p=0.08$), calcium carbonate content ($r=0.95$, $p<0.001$) and the pH value ($r=0.72$, $p<0.02$) of the fine earth. By contrast, fine earth silt levels drop as gravel content increases ($r=-0.64$, $p=0.05$).

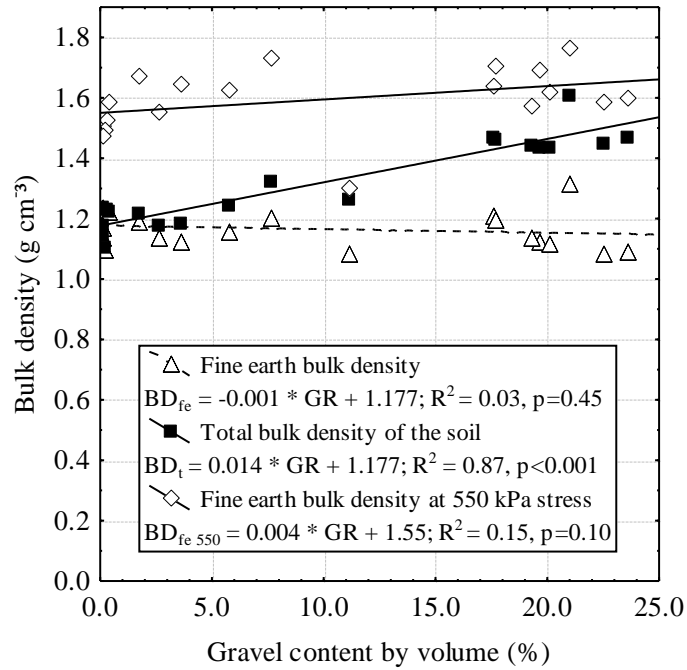


Figure 3.2.6. Relation between gravel content by volume (GR) and fine earth bulk density (BD_{fe}), total bulk density of the soil (BD_t) and fine earth bulk density at 550 kPa stress ($BD_{fe\ 550}$) for the test site Rastenbergl.

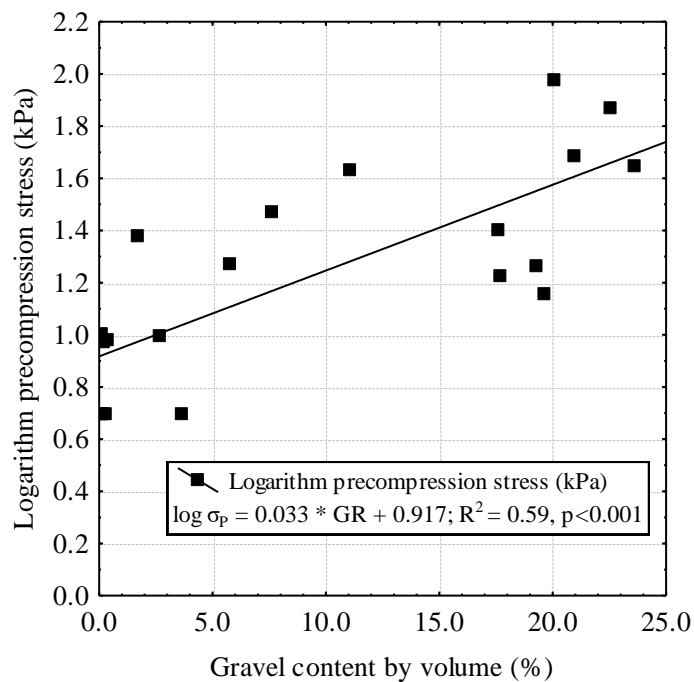


Figure 3.2.7. Relation between gravel content by volume (GR) and logarithm precompression stress ($\log \sigma_p$) at -6 kPa matric potential for the test site Rastenbergl.

Precompression stress in the whole soil also increases continuously with gravel content at the Rastenbergl site, from 8 kPa ($\log 0.92$) to 55 kPa ($\log 1.74$) (Fig. 3.2.7). The standard deviation of the measured precompression stress values from the regression function calculated in Figure

3.2.7 is $\log 0.25$. Thus overall it lies within the upper range of standard deviations that were identified for each of the gravel content levels in the disturbed samples ($\log 0.05$ to $\log 0.25$) (see Fig. 3.2.4 B). Moreover, at comparable gravel content levels of up to 30 per cent by volume in the soil type “Silt Loam”, precompression stress in the disturbed samples increased in a non-linear manner, and only by around $\log 0.30$. As was the case with the disturbed samples, there are no differences between the precompression stress levels of the fine earth and those of the whole soil.

3.2.4. Discussion

3.2.4.1. Bulk density of the fine earth and of the whole soil

With its natural soil structure, the experiments at the Rastenberg site showed that, up to a gravel content of around 25 per cent by volume, fine earth bulk density remained virtually constant while the total bulk density of the soil steadily increased. The increase in the dry bulk density of the whole soil can, therefore, be explained solely by the higher particle density of the gravel compared to the bulk density of the fine earth. As silt content decreased and sand content increased in the fine earth, an increase in fine earth bulk density might even have been expected (Kaufmann et al., 2010), although this is not seen here. In the tests on disturbed samples the increase in the dry bulk density of the whole soil as gravel content rises can be explained solely by the gravel’s higher particle density in comparison to the bulk density of the fine earth. Overall, this paper confirms studies by Poesen and Lavee (1994) which also describe constant fine earth bulk densities and increasing whole soil bulk densities up to a gravel content of approximately 30 per cent by mass (which corresponds to around 20 per cent by volume). Beyond these gravel content levels, both fine earth bulk density and whole soil bulk density drop again (Poesen and Lavee, 1994). Gravel contents of above 25 per cent by volume were not, however, found at the Rastenberg site. Poesen and Lavee (1994) discuss various causes for the drop in fine earth bulk density when gravel content is high. For instance, the presence of gravel can cause soil organic matter to become concentrated in the finer soil. The higher proportion of organic matter with a comparatively low matter density thus reduces the bulk density of the fine earth. At the Rastenberg site, no evidence was found of a correlation between fine earth bulk density and the level of organic matter, although the amount of organic matter identified in the fine earth measuring <2 mm tended to increase with gravel content. This is confirmed by the higher concentration in the fine earth. A mixture of two different particle sizes made of fine earth and gravel can also react in different ways to expansion and contraction, for example during cycles of drying and re-moistening (Poesen and Lavee, 1994). This causes the active formation of microstructures, but only in the fine earth. There is no indication of this at the Rastenberg site.

In the trials using disturbed soil samples, levels of soil organic carbon as well as the fine earth bulk densities were kept equal in all variants of the respective soil textural class, and processes of structural formation may be ruled out here. Nevertheless, the higher the gravel content level,

as the compressive stress increases compaction decreases in the fine earth. This is presumably caused by the direct effect gravel has on reducing compaction, because, as gravel content increases, the loads applied to the soil are transferred more and more through the contact points in the gravel. The gravel thus acts as a supporting frame, helping to distribute stress throughout the soil. In the case of very high gravel content levels, this is facilitated by the fact that there is no longer enough fine earth in the spaces between the gravel particles to become more heavily compacted. Saini and Grant (1980) as well as Ravina and Magier (1984) have already reported on similar effects of reducing compaction that accompany an increased gravel content.

3.2.4.2. Precompression stress

Only a small number of compaction damage concepts and model estimates of precompression stress incorporate gravel content into their evaluation. Regardless of soil textural classes and the initial level of precompression stress, in their evaluation approach Horn and Fleige (2003) ascertain additions to precompression stress in a stone-free soil of 30 kPa at 10-25 vol.% gravel, 60 kPa at 25-50 vol.% gravel, 90 kPa at 50-75 vol.% gravel and 120 kPa at more than 75 vol.% gravel. The article lacks measurement data that underlie these additions as well as any indication of their origins. Compared to the results presented here, giving details of these additions using the unit 'kPa' seems disadvantageous, because precompression stress with the unit 'kPa' does not increase in a linear manner as gravel content levels rise. On the other hand, a uniform approach with no differentiation according to different soil types seems justified. This is because in the trials presented here – for the disturbed samples, at least – there are also only slight differences in the soils' fundamental behaviour. In our experiments, differentiations only exist in the case of significant effects above 20 or 30 per cent by volume as well as in the extent of the continued increase in precompression stress (exponential instead of linear increase).

However, in multiple regressions Kaufmann et al. (2009) find a negative correlation of gravel content level and precompression stress. They reason that if gravel content increases but the void ratio remains constant, then this leads to a higher void ratio in the fine-textured soil. The fine earth thus becomes less stable; according to Kaufmann et al. (2009), only when the gravel content is high enough and distributed evenly does this lead to an increase in precompression stress, by way of a 'lattice effect'. However, at a maximum of 13.7 per cent by mass, the gravel content levels in the experiments by Kaufmann et al. (2009) were too low overall. The results presented here show significant increases in precompression stress for gravel content levels above approximately 15-20 vol.%. It is only then that the gravel content can act as a supporting framework, taking on part of the stress applied to the soil without the soil becoming compacted. However, when comparing these results with those of Kaufmann et al. (2009) it should be noted that in our study just gravel content is variable, while other factors, such as void ratio in the fine-textured soil, were variable in Kaufmann et al. (2009).

Ultimately, in order to use regression models to estimate precompression stress for soils containing gravel, it is probably worth using fine earth density for such a calculation. On this basis, the effect of gravel can be calculated separately, for instance using equations 3.2.-4 – 3.2.-6.

Overall, the increasing precompression stress seen as gravel content levels rise can largely be attributed to the stress/bulk density functions – particularly the virgin compression lines – shifting towards higher stresses. This is especially apparent for the stress/bulk density functions of the fine earth. Here, there is an analogy between the changed stress/strain behaviour and the increase in precompression stress when soil water content decreases. The latter is often also associated with a shift of the virgin compression lines, and moreover with a change in their slopes, or a combination of the two (Rücknagel et al., 2012a).

The study presented here cannot sufficiently answer the question of the extent to which a gravel's shape can influence precompression stress for equal gravel content levels and size distributions. Hamidi et al. (2011) found higher shear resistance of angular gravel shapes when compared to rounded shapes. Hence a higher compressive stress would be necessary to move the angular corners of the limestone gravel. As a result, the point of greatest curvature of the stress/bulk density function should shift towards higher stress, with precompression stress thus increasing. However, this was only observed in the "Silt Loam". Accordingly, gravel shape only seems to have an effect depending on the particular type of fine earth.

Finally, from a methodological perspective it should be noted that the mean weighted diameter of the gravel in the natural samples from the Rastenberg site is slightly greater than in the experiments carried out on the disturbed samples. Therefore the size ratio specified by Holtz and Lowitz (1957, as cited in Donaghe and Torrey, 1994) of the gravel diameter – in particular to the height of the soil core sampler – is not quite achieved. It follows that the linear increase in precompression stress (log) and its variation at the Rastenberg site could also have been influenced by the size of the soil core samplers. The low height of the soil core samplers may have led to reduced soil settlement, because the stones were less able to shift downwards. Consequently, the stones' supporting effect in the soil core sampler would likely be greater than it would otherwise be in a natural setting. Also, although the greatest care was taken when extracting the samples, it is not possible to completely rule out structural disturbances, particularly in those soil core samplers with higher gravel contents.

At the Rastenberg site, the fine earth properties are not constant as gravel content increases. For instance, sand content, the level of soil organic carbon and the pH value of the fine earth increase with gravel content. By contrast, fine earth silt levels drop. Experiments by Imhoff et al. (2004) and Saffih-Hdadi et al. (2009) have shown that textural properties and, above all, clay content, influence precompression stress. But the variation at the Rastenberg site is so slight that all of the samples were classified as the soil type "Silt Loam". The amount of soil organic carbon, however, has no significant influence on precompression stress (Imhoff et al., 2004), and increasing pH values (Chaplain et al., 2011) tend to result in a reduction of precompression stress. At natural sites, it is not always possible to clearly separate the effects mentioned of

these soil properties from the influence of gravel. Nonetheless, overall the natural samples confirm the change in precompression stress with gravel content.

3.2.5. Conclusions

High gravel content levels of more than 15-20 per cent by volume act as a supporting framework, thus protecting the fine earth considerably from compaction, and they also increase precompression stress substantially. For these soils with higher gravel content, at least, consideration should be given to gravel content when assessing their susceptibility to compaction damage. Failure to do so could otherwise result in miscalculations of mechanical load capacity. On the other hand, in soils with low gravel contents of less than 10 per cent by volume, the gravel's effect of reducing compaction requires somewhat less consideration. With regard to the impact of a gravel's shape on precompression stress, no clear conclusions can be drawn from these experiments. Here there appears to be considerable interdependency with the texture of the fine earth, and future investigations should aim to shed light on this.

Acknowledgement

The authors would like to thank the "Agrargenossenschaft Rastenberg e.G." for allowing them to take the natural samples at the Rastenberg site.

3.3. Uniaxial compression behaviour and soil physical quality of topsoils under conventional and conservation tillage

Published in: *Geoderma* 286 (2017), 1-7

Jan Rücknagel¹, Anne Rademacher², Philipp Götze¹, Bodo Hofmann¹, Olaf Christen¹

¹Institute of Agricultural and Nutritional Sciences, Department Agronomy and Organic Farming, University of Halle-Wittenberg, Betty-Heimann-Str. 5, 06120 Halle/Saale (Germany)

²Research Institute for Post-Mining Landscapes FIB e. V., Brauhausweg 2, 03228 Finsterwalde (Germany)

Abstract

Considering conventional tillage with a mouldboard plough and conservation tillage with a cultivator or disc harrow, this study analysed whether structural differences in the soil of the lower topsoil led to any difference in this layer's susceptibility to compaction, and also how density changed – in the whole soil and also in the individual aggregates – during the compaction process in both tillage variants. To this end, soil samples were taken from the lower topsoil of seven medium-term and long-term soil tillage trials conducted in Central Europe. Compression tests were performed on these samples and they were also used to determine dry bulk density, aggregate density, air capacity and saturated hydraulic conductivity. The stress/bulk density functions as well as the stress/strain functions from the compression tests were analysed and the precompression stress determined. At two test sites, compaction behaviour was analysed for whole soil and for aggregates separately. In the case of conservation tillage, the soil structure demonstrated higher dry bulk density as well as lower air capacity and saturated hydraulic conductivity. Aggregate density was mostly similar. It increased relatively slowly during compaction, and often not before high loading steps. This is why higher precompression stress values in the variants under conservation tillage were mostly the result of a dense compaction of aggregates, and indicated higher stability against mechanical loads. However, for both variants the virgin compression section of the stress/bulk density functions displayed similar compression behaviour; and generally higher settlement for conventional tillage in the compression test did not result in higher dry bulk densities than with conservation tillage. Stability against mechanical loads in the conservation tillage variants should therefore not be overestimated.

3.3.1. Introduction

Traditional primary tillage using a plough, also called “conventional tillage”, usually involves turning the whole of the topsoil. This fully works any crop residues into the soil. Besides this system, around the world tillage methods have become established which refrain from turning the soil in this way, and often also from loosening the whole of the topsoil. Crop residues are only worked into the soil close to the surface (e.g. mulch tillage and reduced tillage). It is also

possible to dispense with loosening the soil altogether (no-tillage). These methods are known collectively as “conservation tillage” systems (FAO, 1993).

One important reason for using conservation tillage systems is that they cost less (Ndaeyo, 2010), but usually result in comparable yield levels under temperate climate conditions like those of Western or Central Europe (Rücknagel et al., 2004; Brennan et al., 2014). Apart from this, environmental aspects also play a role. Factors associated with conservation tillage include a higher energy output / input ratio (Borin et al., 1997), the enrichment of soil organic carbon near the soil surface in particular (Six et al., 1999; Tebrügge and Düring, 1999), and reductions in sediment loss and nutrient loss through erosion (Chichester and Richardson, 1992).

Conservation tillage is also seen as a preventive way to protect the soil against compaction damage (Brunotte et al., 2013). Among other reasons, this is because conventional tillage with a plough commonly involves the tractor wheel driving in the furrow. On-land ploughing, which involves all wheels of the tractor driving on top of the soil, is recommended but not common practice. In the case of conventional tillage with driving in the furrow, the wheel induced stress is transferred directly into the subsoil (Weisskopf et al., 2000). By contrast, conservation tillage involves driving on the surface of the soil. By shifting the tyre-soil contact area to the surface, there is a greater reduction in stress down to the subsoil, in turn decreasing the risk of plough sole compaction. In addition, differences in physical soil properties as a result of conservation tillage mean that, when driving over the land with agricultural machinery, the soil stress in the topsoil and subsoil can be reduced (Zink et al., 2010).

As regards soil physical properties, there are particularly striking differences between conventional and conservation tillage in the lower topsoil, an area which is no longer tilled regularly and thus often more densely layered (Rasmussen, 1999; Deubel et al., 2011). Particularly where conservation tillage is practised in the long term, a continuous, vertically oriented pore system with higher saturated hydraulic conductivity may form (Azooz and Arshad, 1996). These vertically oriented pores are comparatively less susceptible to compaction (Hartge and Bohne, 1983). However, there are indications that, in conservation tillage soils, the layers below the reduced tillage depth display air-filled porosity, air diffusivity and permeability levels which lie below the critical ranges for favourable plant growth (Schjonning, 1989; Götze et al., 2013). Compacted and displaying high dry bulk density and low porosity, these soil layers are described as the “no-till pan” (Reichert et al., 2009).

For the lower topsoil in particular, the question thus arises as to whether different physical soil conditions in the tillage variants lead to different sensitivity to compaction in this layer. The uniaxial compression test is well suited to this analysis, because it allows the application of defined increasing soil pressures and comparable matric potentials to soil samples taken directly from this layer. Using the stress/strain or stress/bulk density function derived from this, it is possible to identify not only the compression index but also the precompression stress. Soil precompression stress is a key criterion for the soil’s stability when subjected to mechanical loads (Horn and Rostek, 2000). Once it is exceeded, this leads to irreversible changes in soil functions. As yet, however, it remains unclear to what extent precompression stress levels of

the whole soil and of aggregates are dependent on various textural and structural conditions. Therefore a further aim was to investigate how density changed – in the whole soil and also in the individual aggregates – during the compaction process in the conventional and conservation tillage variants. Based on this, it is possible to determine the maximum pressure load which will not cause aggregate compaction, and consequently the highest load under which the soil is able to regenerate a sufficient macropore or inter-aggregate pore system. In order to answer these questions, this article analysed compression tests from the lower topsoil of seven medium-term and long-term soil tillage trials in Central Europe.

3.3.2. Materials and methods

3.3.2.1. Test sites and variants

The trials were located at seven different sites in Germany (Table 3.3.1) which are characterised by a moderate continental climate with mean annual temperatures of between 8.5 and 9.5 °C as well as mean annual precipitation of between 460 and 640 mm. Each test site included a medium-term or long-term tillage experiment with the variants “conventional tillage” with a mouldboard plough (tillage depth 25 cm) and “conservation tillage” with a cultivator or disc harrow (tillage depth 8-15 cm). In the tillage trials, the clay content in the topsoil varied between 40 and 310 g kg⁻¹, while the sand content ranged between 40 and 750 g kg⁻¹, thus covering a very broad range of soil textures. The total organic carbon content varied between 7 and 20 g kg⁻¹. On all sites, the gravel content was below 20 g kg⁻¹.

3.3.2.2. Soil compression tests

For each site and tillage variant, horizontally oriented soil core samples (n = 4-8) were extracted from the topsoil (soil depth 15 ... 22 cm) at four different places; these samples were taken for subsequent soil compression tests. With the exception of the Warin site, all samples were taken in the spring (March until May). Ploughing and seedbed preparation already occurred in the autumn of the previous year. At the Warin site, sampling took place during autumn approximately two months after ploughing and seedbed preparation. The soil cores used in the compression tests had a diameter of 100 mm and a height of 28 mm. After collecting the soil, the samples were saturated and then adjusted to a matric potential of -6 kPa in a sand box. This matric potential corresponds to field capacity. The loading steps 5, 10, 25, 50, 100, 200, 350 and 550 kPa were applied in succession to the soil core samples. The tests took place in drained conditions with a loading time of 180 minutes per loading step and relaxation phases lasting 15 minutes. In previous tests on soils of similar textural classes, for loading times of up to 540 minutes only very slight increases in settlement were measured in comparison to 180 minutes.

Table 3.3.1. Experimental sites with texture and total organic carbon (TOC) in the topsoil layer; ¹ FAO soil classification, ² USDA classification scheme (Gee and Bauder, 1986), ³ Conventional tillage, ⁴ Conservation tillage, ⁵ Content not differentiated between the tillage variants.

Site name	Federal state	Trial duration (years)	Taxonomy ¹	Texture (g kg ⁻¹)		Texture class ²	TOC (g kg ⁻¹)	
				Clay	Sand		Conv. ³	Cons. ⁴
Bad Kreuznach	Rhineland-Palatinate	6	Haplic Luvisol	240	230	Silt Loam	14	13
Bernburg	Saxony-Anhalt	7	Chernozem	190	110	Silt Loam	16	15
Buttelstedt	Thuringia	3	Chernozem	310	40	Silty Clay Loam	19	20
Görzig	Saxony-Anhalt	8	Chernozem	240	220	Silt Loam	15 ⁵	
Lückstedt	Saxony-Anhalt	4	Gleyic Cambisol	40	750	Loamy Sand	7	8
Warin	Mecklenburg-Western Pomerania	6	Cambisol	100	590	Sandy Loam	-	
Zschortau	Saxony	17	Haplic Planosol	130	560	Sandy Loam	7	10

Therefore, settlement can be regarded as largely finished after 180 minutes. However, just how matric potential changed during the soil compression tests was not measured. The oedometer applied (Bradford and Gupta, 1986) was fully automatic, and the settlement (S) was recorded to an accuracy of 0.01 mm. After drying the sample cores at 105 °C until the sample mass remained constant, the dry bulk density at the beginning of the experiment (BD_t) was determined after treatment in the oedometer. Using the settlement (S) of the sample after each loading step compared to its initial height (H) as well as the density of the whole soil at the beginning of the experiment (BD_t), it was possible to calculate the resulting density of the whole soil for each loading step ($BD_{t\ xi}$):

$$BD_{t\ xi} = ((H - S)/H)^{-1} * BD_t \quad (3.3.-1)$$

The stress/bulk density functions as well as the stress/strain functions from the compression tests were analysed separately. Taking the last three loading steps of the compression tests, these were used to identify the respective slopes of the virgin compression lines (m_{VCL}). This involved calculating the change in settlement and dry bulk density from 200 kPa (S_{200kPa} or BD_{200kPa}) to 550 kPa (S_{550kPa} or BD_{550kPa}) in relation to the logarithmic change in stress from 200 kPa ($\sigma_{z\ \log 200kPa}$) to 550 kPa ($\sigma_{z\ \log 550kPa}$):

$$m_{VCL} = (S_{550kPa} - S_{200kPa}) / (\sigma_{z\ \log 550kPa} - \sigma_{z\ \log 200kPa}) \quad (3.3.-2)$$

$$m_{VCL} = (BD_{550kPa} - BD_{200kPa}) / (\sigma_{z\ \log 550kPa} - \sigma_{z\ \log 200kPa}) \quad (3.3.-3)$$

At the Görzig site, calculations were performed using different values of 160 and 500 kPa. Only the stress/bulk density functions served to help numerous independent testing persons (Rücknagel et al., 2010) determine precompression stress using Casagrande's graphical method (1936).

At two test sites, compaction behaviour was analysed for whole soil and for aggregates separately. Contrary to the procedure described above, we used five (Görzig site) and eight (Warin site) loading steps (5, 16, 50, 160, 500 kPa and 5, 10, 25, 50, 100, 200, 350, 550 kPa respectively), with three (Görzig site) and six (Warin site) replications at each loading step. Only one loading step was applied to each individual soil core. Afterwards, the samples were carefully broken up and aggregates measuring 8-10 mm sieved out. These were then used to directly measure aggregate density. For each loading step, the results provide the resulting dry bulk density and aggregate density caused by the loading. It was possible to use this information to create a function of stress and dry bulk density, or of stress and aggregate density. These functions were also used to determine the precompression stress using Casagrande's graphical method (1936).

3.3.2.3. Determination of soil physical parameters

Parallel to core sampling for the compression tests, disturbed soil samples were collected from the same depths and variants to determine aggregate density. Only at the Lückstedt site was it not possible to extract soil with aggregates due to the high sand content. For the test sites Görzig and Warin, aggregate density was determined for each individual soil core after the compression test. The soil material was carefully broken up using a screen of 20 mm slot diameter, and then the aggregates measuring 8-10 mm in size were separated. The aggregates were saturated in a sand box and adjusted to the same matric potential (-6 kPa) as used in the samplers of the compression test. In the box, the aggregates were arranged in rings of 50 mm diameter in such a way that each aggregate was in contact with the sand. Saturation occurred through capillary suction by the aggregate pores, with the water supplied by a film of water in the sand box about 1 mm thick. Higher water levels would have increased the danger of aggregate crumbling. When the matric potential was equalized (one day later), the water content was determined in a portion of each sample (about 10-15 g) by drying it at 105 °C. The second part of the sample (another 10-15 g) was weighed, placed in a fine mesh screen and dipped in vegetable oil. The soaked aggregates were spread on filter paper, allowing excess oil to run off. The aggregate was thus coated by a thin, water-repellent film which had little effect on the volume. Having been prepared in this way, the aggregates were then completely immersed in water. The volume of water displaced corresponded to the aggregates' own volume (Archimedes' principle). The mass of water displaced was measured to an accuracy of 0.01 g. At a water density of 1.0 g cm⁻³, it corresponded to the volume of the weighed aggregates. The aggregate density (AD) was determined using the mass of the dry aggregates and their volume. The AD/BD ratio was calculated as the quotient of aggregate density and dry bulk density. The ratio does not have a physical dimension and is a yardstick for the expression of the inter-aggregate pore system and thus also for density heterogeneity within the soil structure. A classification of the values calculated was possible on the basis of Rücknagel et al. (2007).

As a difference between field capacity (matric potential of -6 kPa) and total pore volume, air capacity was determined on the same soil core as for the compression tests. Air capacity is an important factor in soil ecology, and it covers pores with an equivalent diameter of >50 µm, in which water moves in accordance with gravity (unit vol.%). Determination occurs in a sand box (German laboratory standard DIN ISO 11274, 1998).

Additionally to the soil core sampling for the compression test, soil cores with a volume of 250 cm³ (n=8-12) were collected in order to determine saturated hydraulic conductivity for each tillage variant. Saturated hydraulic conductivity is the parameter of Darcy's law applied to saturated water movement within the soil as a measure of the hydraulic permeability of water-saturated soil (unit cm d⁻¹). Apart from size and shape, soil permeability for water is influenced heavily by pore continuity. Determination takes place in a stationary facility according to the principle described by Klute and Dirksen (1986).

3.3.2.4. Statistical analysis

The statistical analysis for each individual test site was carried out with an ANOVA and a subsequent comparison of mean values (t-test) with the software program Statistica (StatSoft, 2009). Significances with an error probability of $p < 0.05$ are shown in different lower-case letters. Beforehand, the data sets were tested for normal distribution using the Shapiro-Wilk test. The saturated hydraulic conductivity and precompression stress values were then calculated in logarithmic form in the variance analysis.

3.3.3. Results and discussion

3.3.3.1. Soil physical parameters

In the case of conservation tillage, the lower topsoil displayed higher dry bulk density at all sites compared to conventional tillage (between $+0.06$ and $+0.27 \text{ g cm}^{-3}$) (Table 3.3.2). At the Buttstedt and Warin sites, however, this difference in dry bulk density was not statistically significant. Conversely, the air capacity values for the lower topsoil in the conservation tillage variants were generally significantly lower than in the conventional variants (between -7.2 and $-14.1 \text{ vol.}\%$). Only at the Warin site did both tillage variants display similar air capacity. Numerous publications describe higher dry bulk densities and/or decreasing coarse pore volumes and air capacities in the lower topsoil if it is not tilled, or tilled at irregular intervals, as part of long-term conservation tillage (Rasmussen, 1999; Tebrügge and Düring, 1999; Deubel et al., 2011; Götze et al., 2013). Direct drilling in particular results in soil layers known as “no-till pans”, which have higher dry bulk density and are less porous (Reichert et al., 2009). Even so, in this article there were only indications of such a compact zone at the Görzig and Zschortau sites, where the minimum of $8 \text{ vol.}\%$ air capacity (Werner and Paul, 1999) for an intact soil structure was not reached.

Results in the literature differ with regard to saturated hydraulic conductivity. Tebrügge and Düring (1999) described comparable or higher saturated hydraulic conductivity levels when conservation tillage was practised. This was primarily attributable to higher levels of earthworm activity (Ulrich et al., 2010) and the continuous macropores formed by plant roots (Angers and Caron, 1998). According to Aura (1988, cited in Rasmussen, 1999), however, ploughed soils with a higher proportion of macropores had higher saturated hydraulic conductivity. The trials presented here also painted an inconsistent picture with regard to saturated hydraulic conductivity. In the conservation tillage variant, this parameter was significantly lower than under conventional tillage at the Bad Kreuznach and Görzig sites, and also at least slightly lower at the Bernburg, Buttstedt, Lückstedt and Zschortau sites. By contrast, the conservation tillage variant at the Warin site displayed marginally higher saturated hydraulic conductivity. However, Buttstedt was the only site where the minimum requirement of 10 cm d^{-1} (Werner and Paul, 1999) for an intact soil structure was not reached.

Table 3.3.2. Air capacity (AC), saturated hydraulic conductivity (k_s), dry bulk density (BD), aggregate density (AD), aggregate density/dry bulk density ratio (AD/BD ratio), logarithm precompression stress ($\log \sigma_P$), dry bulk density at the 350 kPa loading step (BD_{350}), strain at the 350 kPa loading step (S_{350}), slope of the virgin compression line in the stress/bulk density diagram ($m_{VCL(BD)}$) and slope of the virgin compression line in the stress/strain diagram ($m_{VCL(S)}$) for the different sites and tillage variants; different lower-case letters indicate significant differences between the tillage variants at the same test site ($p < 0.05$); ¹ Conventional tillage, ² Conservation tillage, ³ loading step 500 kPa, ⁴ according to Paul (2010).

Site name	Tillage variant	AC (vol.%)	k_s (cm d ⁻¹)	BD (g cm ⁻³)	AD (g cm ⁻³)	AD/BD ratio	$\log \sigma_P$ (log kPa)	BD_{350} (g cm ⁻³)	S_{350} (mm)	$m_{VCL(BD)}$ (g cm ⁻³ /1 log σ_z)	$m_{VCL(S)}$ (mm/1 log σ_z)
Bad Kreuznach	Conv. ¹	21.1 a	355 a	1.31 a	1.63 a	1.24	1.33 a	1.70 a	6.82 a	0.22 a	2.96 a
	Cons. ²	12.3 b	12 b	1.50 b	1.62 a	1.08	1.88 b	1.72 a	3.96 b	0.23 a	3.58 b
Bernburg	Conv. ¹	18.9 a	63 a	1.24 a	1.55 a	1.25	1.12 a	1.63 a	6.69 a	0.21 a	2.80 a
	Cons. ²	11.7 b	25 a	1.41 b	1.55 a	1.10	1.86 b	1.63 a	3.95 b	0.22 a	3.51 b
Buttelstedt	Conv. ¹	20.6 a	66 ⁴	1.21 a	1.62 a	1.34	1.28 a	1.60 a	6.72 a	0.22 a	2.97 a
	Cons. ²	12.4 b	7 ⁴	1.35 a	1.62 a	1.20	1.72 b	1.60 a	4.51 a	0.22 a	3.25 a
Görzig	Conv. ¹	20.4 a	142 a	1.26 a	1.59 a	1.26	1.57	1.76 a ³	8.87 a ³	0.23 a	6.48 a
	Cons. ²	7.2 b	42 b	1.53 b	1.71 b	1.12	1.75	1.81 a ³	4.28 b ³	0.18 a	2.50 b
Lückstedt	Conv. ¹	23.2 a	51 a	1.44 a	-	-	1.81 a	1.66 a	3.81 a	0.16 a	2.28 a
	Cons. ²	14.6 b	32 a	1.61 b	-	-	2.19 b	1.73 b	1.97 b	0.10 b	1.56 b
Warin	Conv. ¹	16.4 a	18 a	1.58 a	1.77 a	1.12	1.25	1.85 a	3.95 a	0.17 a	2.25 a
	Cons. ²	16.5 a	28 a	1.64 a	1.83 b	1.12	1.51	1.86 a	3.46 a	0.16 a	1.90 a
Zschortau	Conv. ¹	21.8 a	116 a	1.31 a	1.69 a	1.29	1.21 a	1.63 a	5.56 a	0.17 a	2.33 a
	Cons. ²	7.7 b	23 a	1.56 b	1.63 b	1.05	1.80 b	1.77 b	3.21 b	0.17 a	2.32 a

At the Bad Kreuznach, Bernburg and Buttstedt sites the aggregate densities did not vary between the tillage variants. At the Görzig and Warin sites, conservation tillage displayed significantly higher aggregate densities than conventional tillage. By contrast, conservation tillage at the Zschortau site resulted in lower aggregate density than conventional soil tillage. Nevertheless, the differences in aggregate density between the tillage variants were much smaller overall than the differences between the dry bulk densities. With the exception of the Warin site, therefore, for conservation tillage there was always a lower AD/BD ratio than for conventional tillage. According to the classification by Rücknagel et al. (2007), the AD/BD ratios are low to mean under conservation tillage, while they are high to very high for conventional soil tillage. Based on the lower AD/BD ratios seen in conservation tillage, it can ultimately be concluded that the compact settlement of the lower topsoil can be explained by a reduced inter-aggregate pore volume, with increased support between individual aggregates.

3.3.3.2. Stress/strain and stress/bulk density behaviour

Figure 3.3.1 uses the conventional and conservation tillage variants at the Bernburg site as an example, presenting the stress/strain and stress/bulk density behaviour for the lower topsoil. Apart from the lowest loading step (5 kPa), settlement was significantly higher for conventional than for conservation tillage for the entire loading range up to 550 kPa. By contrast, up to the third loading step (25 kPa) the dry bulk density in the stress/bulk density diagram was significantly lower for conventional tillage than for conservation tillage. At the higher loading steps (50-550 kPa) the dry bulk densities in the two variants were almost identical.

In the stress/strain diagram for the Bernburg site, the slope of the virgin compression line for conservation tillage ($m=3.51$) is significantly steeper than for conventional tillage ($m=2.80$), while it is similar in the stress/bulk density diagram ($m=0.22$ and $m=0.21$ respectively). This difference in the slopes of the soil tillage variants' virgin compression lines between the stress/strain diagram and the stress/bulk density diagram can be explained by the non-linear relationship between settlement and dry bulk density. A similarly non-linear relationship which affects the gradient of the compaction curve, and also the level of precompression stress, exists between dry bulk density and void ratio (Mosaddeghi et al., 2003; Rücknagel et al., 2010). Overall, both tillage variants have almost the same virgin compression line in the stress/bulk density diagram.

For characterising soil compression curves, the shapes can be divided into rounded, bi-linear and S-shaped (Chaplain et al., 2011; Rücknagel et al., 2013b). In both the stress/strain diagram and the stress/ bulk density diagram, there is typical bi-linear compression behaviour for conservation tillage at the Bernburg site. In the case of conventional soil tillage, however, and in particular in the stress/strain diagram, the settlement function is slightly S-shaped. At $\log \sigma_p = 1.86$ (72 kPa), precompression stress was significantly higher for conservation tillage than for conventional tillage ($\log \sigma_p = 1.12$, 13 kPa).

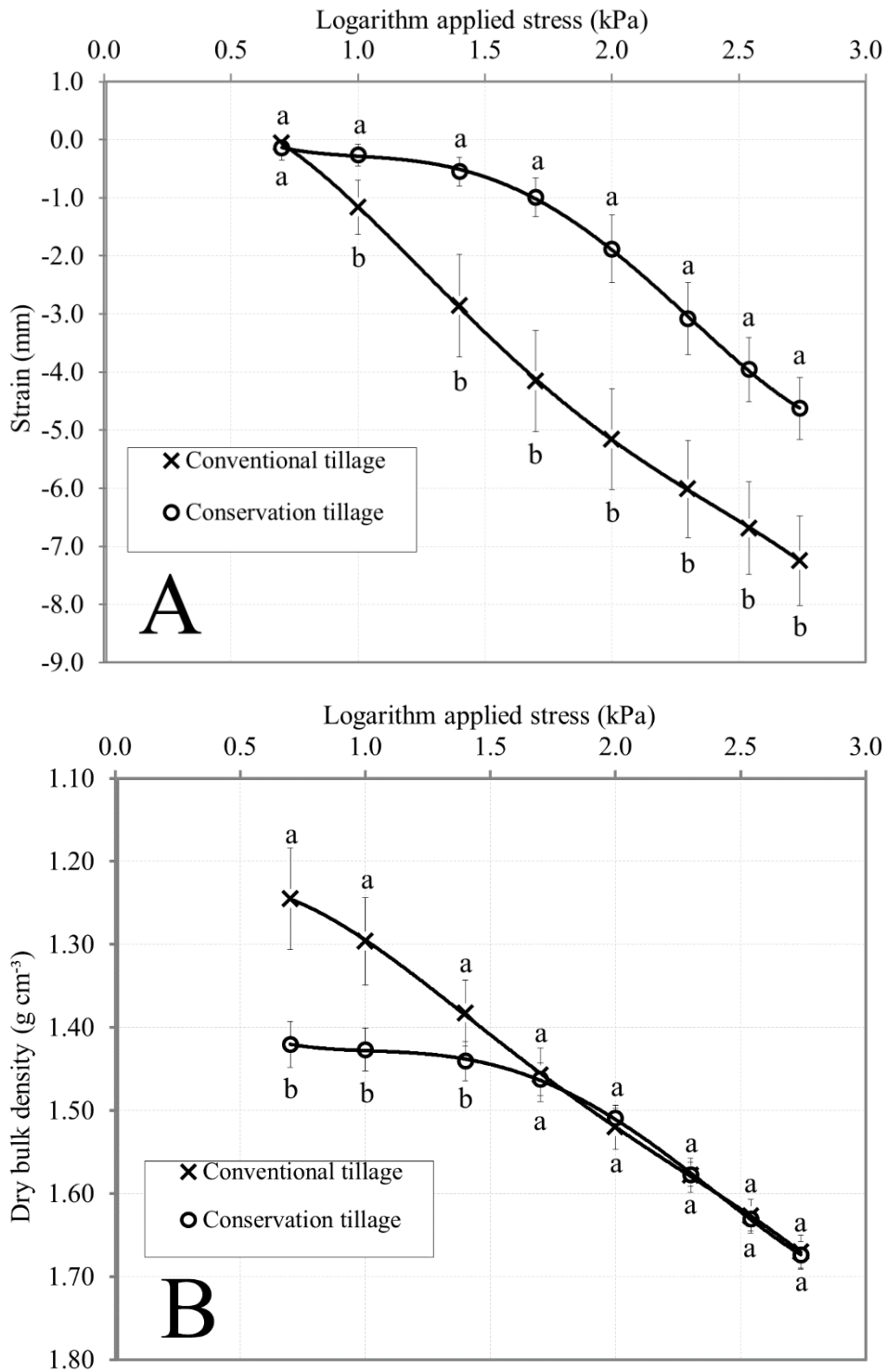


Figure 3.3.1. Stress/strain [A] and stress/bulk density functions [B] for the tillage variants at the test site Bernburg (depth 19-22 cm); error bars shows standard deviation and different lower-case letters indicate significant differences between the tillage variants at the same loading step ($p < 0.05$).

At most of the seven soil tillage trials, the overall picture was generally similar to that seen at Bernburg. In the stress/strain diagram, settlement (loading step 350 kPa shown as an example

in Table 3.3.2) was higher overall for conventional soil tillage than conservation tillage. At the Buttelstedt and Warin sites, however, this difference was not significant. In contrast to this, for the 350 kPa loading step in the compression test, dry bulk density for conservation tillage was slightly higher at the Bad Kreuznach, Görzig and Warin sites, and also significantly higher at the Lückstedt and Zschortau sites, than for conventional tillage. Only at the Bernburg and Buttelstedt sites were the dry bulk densities of both tillage variants equally high for the 350 kPa loading step. Paz and Guerif (2000) showed on soil samples with different aggregate packing densities that the final density after a compressive load was also higher when the initial packing density was higher. The lower topsoils of the conservation tillage variants studied here displayed not only higher initial dry bulk densities, but also, as described earlier, lower AD/BD ratios than in the conventionally tilled variants. The AD/BD ratio in turn correlated negatively with packing density (Rücknagel et al., 2013a). Therefore the dry bulk densities in the virgin compression area were often higher for conservation tillage than conventional tillage. The higher settlement seen in the compression test for conventionally tilled soils also explains the observation from agricultural practice that, under comparable textural and soil water content conditions, wheeling depth is considerably greater on conventionally tilled land. However, the trials illustrate that it is not possible to draw any firm conclusions as to the level of soil compaction based solely on settlement or wheeling depth. As such, sensor systems which work based on settlement or wheeling depth measurements (Nolting et al., 2006) can only provide very limited information about the actual compaction effect of passing over the soil with agricultural machinery. When transferring the results of the uniaxial compression tests in the oedometer to field level, it should certainly be remembered that driving over the soil with agricultural machinery actually results in three-dimensional stress distribution (Horn et al., 1992). Whereas beneath the centre line of the wheel – similarly to in the uniaxial compression test – the stresses and thus the soil movements are primarily vertical in nature, towards the outer edge of the wheel tracks in particular there may be increased shear stress, which would raise the likelihood of a change in pore continuity (Berisso et al., 2013). Therefore the findings from the oedometer tests mainly apply to the behaviour of the soil under the centre line of the wheel.

In the stress/strain diagram, the slope of the virgin compression lines is significantly lower at the Bad Kreuznach and Bernburg sites, and slightly lower in Buttelstedt, for conventional tillage when compared to conservation tillage. The reverse can be seen at the other trial sites. Here, for conventional soil tillage the slope of the virgin compression lines in the stress/strain diagrams is higher than or comparable with that of conservation tillage. On the other hand, apart from the Görzig and Lückstedt sites, the slopes of the virgin compression lines in the stress/bulk density diagram are the same for both tillage variants. In Görzig and Lückstedt, the slope of the virgin compression lines is lower for conservation tillage than for conventional tillage. This is consistent with the results of da Veiga et al. (2007), who found lower slopes of the virgin compression lines in the stress/void ratio diagram for no-till than for conventional tillage. In addition to the initial dry bulk density and void ratio (Keller et al., 2011), the slope of the virgin compression lines is often also determined by the clay content (Larson et al., 1980). Nevertheless,

in the experiments presented here there was no clear influence of initial dry bulk density or clay content.

In these experiments, the precompression stress in the variants with conventional tillage was very low over all, at $\log \sigma_P$ 1.12-1.81 (13-64 kPa). All trial sites had in common the fact that precompression stress was higher – sometimes considerably so – in the lower topsoil when conservation tillage was practised ($\log \sigma_P$ 1.51-2.19, 32-155 kPa). These higher precompression stress values were directly related to the lower AD/BD ratio seen in the conservation tillage variants, because decreasing AD/BD ratios led to increasing precompression stress values (Rücknagel et al., 2007). In principle, the higher precompression stress levels for conservation tillage confirm the results of da Veiga et al. (2007) and Peng and Horn (2008). On the other hand, Wiermann et al. (2000) found lower precompression stress values for conservation tillage at soil depths of 10 and 30 cm. Especially at a soil depth of 30 cm, this can be explained by a higher cohesion of the soil and a decline in macroporosity in the conventional treatments.

Conservation tillage, or no-tillage, can result in an increase in organic carbon content, especially in the upper topsoil (Six et al., 1999; Tebrügge and Düring, 1999). However, even in the presence of higher differences in organic carbon content in a long-term fertilization trial, Arthur et al. (2013) recorded only slight differences in precompression stress and the compression index, concluding that organic carbon content has no direct influence on a soil's resistance to compaction. In the experiments presented here, the differences in total organic carbon content between the tillage variants were very small, and the conservation tillage variants not ever displayed higher total organic carbon content levels (Table 3.3.1), meaning these presumably do not affect precompression stress or the slope of the virgin compression line.

3.3.3.3. Stress/bulk density behaviour of whole soil and aggregates

Since each soil core sample from the Görzig and Warin sites was only subjected to one loading step, and also only five loading steps were applied for the Görzig site, the stress/density functions had a less favourable goodness of fit when compared to the application of steadily increasing loading steps. The standard deviations of the resulting dry bulk density were higher at the individual loading steps, particularly at the Warin site. This is one disadvantage in the interpretation of mechanical soil properties. Nevertheless, for each of the tillage variants and sites, the stress/bulk density functions of the whole soil followed the typical development for over-consolidated soil with a rounded shape (Chaplain et al., 2011), (Figs. 3.3.2 and 3.3.3). When precompression stress is exceeded, the recompression section – which demonstrates only a slight increase in dry bulk density – is followed by a more pronounced plastic deformation in the virgin compression section. Overall, the precompression stress values of the whole soil were low (Görzig $\log \sigma_P$ 1.57-1.75 and 37-56 kPa, Warin $\log \sigma_P$ 1.25-1.51 and 18-32 kPa). The conservation tillage variants did, however, demonstrate slightly higher precompression stress than the conventional tillage variants. Be that as it may, these differences could not be statistically verified. In Görzig, the higher precompression stress levels for the conservation tillage variant

could be explained by the considerably closer AD/BD ratio, and in Warin by the higher dry bulk density for a comparable AD/BD ratio in the initial structure (Rücknagel et al., 2007).

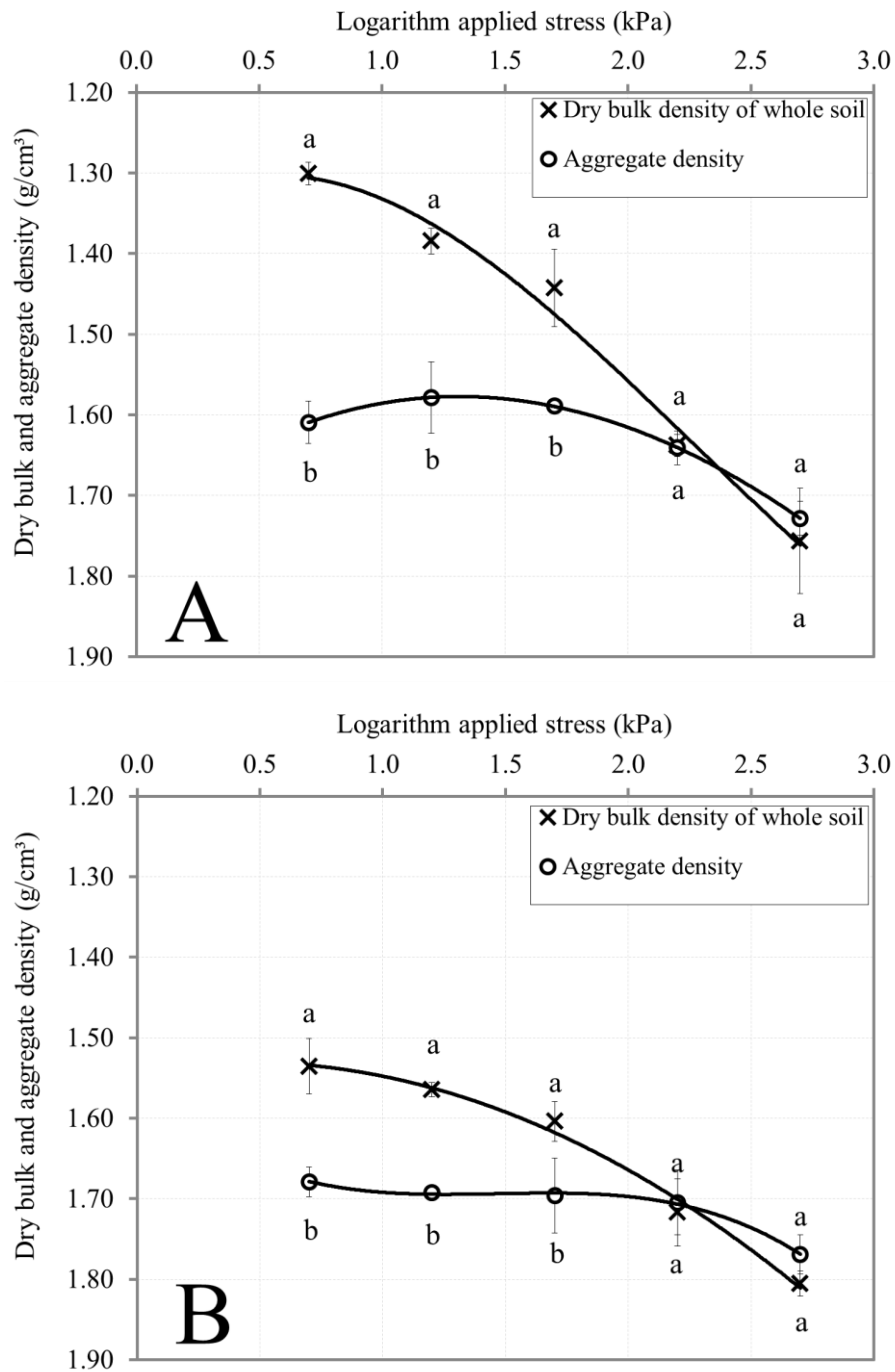


Figure 3.3.2. Stress/bulk density functions of whole soil and aggregates for the Görzig site (depth 19-22 cm) – [A] conventional tillage, [B] conservation tillage; error bars shows standard deviation and different lower-case letters indicate significant differences between dry bulk density and aggregate density at the same loading step ($p < 0.05$).

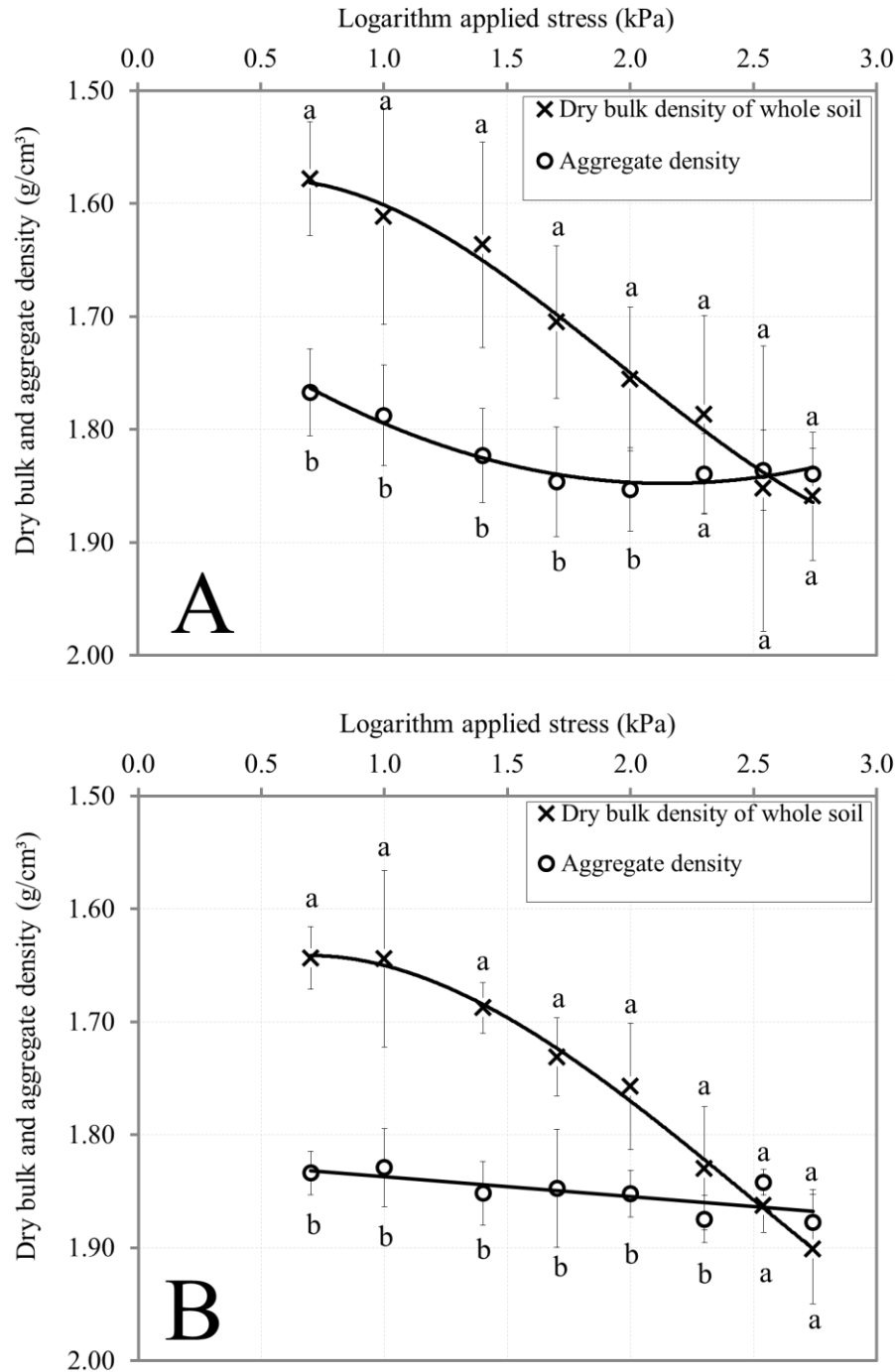


Figure 3.3.3. Stress/bulk density functions of whole soil and aggregates for the Warin site (depth 15-18 cm) – [A] conventional tillage, [B] conservation tillage; error bars shows standard deviation and different lower-case letters indicate significant differences between dry bulk density and aggregate density at the same loading step ($p < 0.05$).

The stress/aggregate density functions presented a different picture. At the Warin site, they followed a linear (conservation tillage) or asymptotic (conventional tillage) pattern. Here, for conservation tillage aggregate density increased only slightly, and not significantly, between the lowest and the highest loading steps. For conventional tillage at the Warin site, only the 5 kPa loading step showed significant differences compared to the 50, 100, 200, 350 and 550 kPa

loading steps. Precompression stress could not be determined. For both tillage variants at the Görzig test site, only for the highest loading step did aggregate density demonstrate a significant increase compared to the values for lower stress levels. Here, too, it was not possible to reliably calculate precompression stress. It can however be presumed that its value lay somewhere between the final two loading steps ($\log \sigma_p$ 2.20-2.70, 160-500 kPa). Thus it lay considerably above the precompression stress levels of the whole soil. All of the variants examined had in common the fact that aggregate density and dry bulk density equalled each other in the highest loading steps. As a measure of density heterogeneity, the AD/BD ratios decreased only slightly below the precompression stress level of the whole soil, and beyond it they reduced quite considerably, reaching a value of approximately 1.0 (completely closed aggregate arrangement) at the highest loading steps (Tables 3.3.3 and 3.3.4).

Table 3.3.3. AD/BD ratios for the different tillage variants and loading steps at Görzig site; ¹Conventional tillage, ² Conservation tillage.

Tillage variant	AD/BD ratio at loading step (kPa)				
	5	16	50	160	500
Conv. ¹	1.24	1.15	1.10	1.00	0.98
Cons. ²	1.09	1.08	1.06	0.99	0.98

Table 3.3.4. AD/BD ratios for the different tillage variants and loading steps at Warin site; ¹Conventional tillage, ² Conservation tillage.

Tillage variant	AD/BD ratio at loading step (kPa)							
	5	10	25	50	100	200	350	550
Conv. ¹	1.12	1.11	1.11	1.08	1.06	1.03	0.99	0.99
Cons. ²	1.12	1.11	1.10	1.07	1.05	1.02	0.99	0.99

The reason for the differentiated stress/bulk density behaviour is the frequency distribution of grain contacts, which has two maxima in aggregated soil (Hartge and Sommer, 1982). The average number of grain contacts between the aggregates is lower, as is the number of grain contacts within the aggregates. When low loading steps are applied, the number of grain contacts barely increases until the precompression stress level of the whole soil is reached. When this whole-soil precompression stress level is exceeded, first the number of contacts between aggregates increases and these are pushed together. If during this phase aggregate stability is exceeded, this can cause aggregates to break without there being any considerable change to their density. It is not until greater stress is applied that the number of contacts within the aggregates can increase, which is linked to an increase in aggregate density. The frequency distribution of the grain contact points can also help to explain how the precompression stress levels of the whole soil and of the aggregates differ depending on the respective density heterogeneity.

3.3.4. Conclusions

The differences in soil structure in the lower topsoil between the two tillage variants considered were at times very large, and the soil physical quality was better in conventional tillage than in conservation tillage. When conservation tillage was practised, indications of the existence of a compacted “no-till pan” were only seen at isolated sites. Almost always higher precompression stress values in the conservation tillage variants indicated higher stability against mechanical loads. In the virgin compression area of the stress/bulk density functions, however, both variants displayed similar compression behaviour, and the generally higher settlement levels for conventional tillage did not result in higher dry bulk densities than for conservation tillage. Stability against mechanical loads in the conservation tillage variants should therefore not be overestimated. Moreover, it is evident that it is not possible to draw conclusions about the final state of compaction based on the degree of settlement or, in agricultural practice, on the depth of the wheel track.

Aggregate density increased relatively slowly during the compaction process, and often not before high loading steps, and the high precompression stress values seen in the lower topsoil in the conservation tillage variants mostly resulted from a lower AD/BD ratio. The restoration of a sufficient macropore volume does therefore seem possible in compacted topsoils where conservation tillage is practised, as long as the aggregates do not become compacted.

Acknowledgements

The authors would like to thank Joachim Bischoff (Landesanstalt für Landwirtschaft, Forsten und Gartenbau; Bernburg), Bernhard Loibl (Südzucker AG; Mannheim/Ochsenfurt), Rainer Paul (Thüringer Landesanstalt für Landwirtschaft; Jena) and Stefan Weimar (Dienstleistungszentrum Ländlicher Raum Rheinhessen-Nahe-Hunsrück; Bad Kreuznach) for allowing them to take the soil samples at the tillage trials.

3.4. Visual structure assessment and mechanical soil properties of re-cultivated soils made up of loess

Published in: *Soil Use and Management* 29 (2013), 271-278

Jan Rücknagel¹, Gerhard Dumbeck², Tamas Harrach³, Eva Höhne¹, Olaf Christen¹

¹ Institute of Agricultural and Nutritional Sciences, Department Agronomy and Organic Farming, University of Halle-Wittenberg, Betty-Heimann-Str. 5, 06120 Halle/Saale (Germany)

² RWE Power AG, Rekultivierung Land- und Forstwirtschaft, Friedrich-Ebert-Str. 104, 50374 Erftstadt (Germany)

³ Justus-Liebig-Universität Giessen, Institut für Bodenkunde und Bodenerhaltung, Heinrich-Buff-Ring 26-32, 35392 Gießen (Germany)

Abstract

Re-cultivated soils (previously-piled soils used as the final surface cover in renovation of open cast mine sites) are particularly susceptible to compaction, which is why a simple estimate of mechanical strength is necessary for land management. In this study, therefore, precompression stress (-6 kPa matric potential) was determined for a total of 20 soil layers from 9 repeatedly cultivated areas of arable land in North Rhine-Westphalia (Germany), along with the aggregate density/dry bulk density ratio (as a measure of density heterogeneity) and air capacity (as a soil ecological parameter). These results are contrasted with the determination of packing density. Packing density (PD) is an integrated parameter that combines various properties (aggregate size, cohesion of the soil structure, root distribution, biogenic macropores, aggregate arrangement) and is assessed visually in the field. Packing density levels range between 1 (very loose soil) and 5 (very highly compacted). There is a strongly negative relationship between packing density and both the aggregate density/dry bulk density ratio and air capacity. Conversely, mechanical precompression stress increases with packing density. Ranges of the individual parameters can be assigned to each of the packing density levels. Packing density level 3 represents an optimisation with regard to mechanical soil stability whilst maintaining minimum air capacity requirements (5-8 vol.%).

3.4.1. Introduction

Soil structure is a major factor for all transport processes and nutrient dynamics in soils. It thus affects rooting depth, availability of nutrients and the amount of plant available water, consequently having a considerable impact on plant growth and development (e.g. Ball and Robertson, 1994; Horn and Rostek, 2000). Re-cultivated soils (previously-piled soils used as the final surface cover in renovation of open cast mine sites) in particular demonstrate very specific characteristics and soil structure depending on the tillage tool applied and subsequent husbandry techniques (Dumbeck, 2000; Kaufmann et al., 2009; Krümmelbein et al., 2010). As a rule, re-

cultivated soils are very susceptible to soil compaction. There are various laboratory parameters – such as dry bulk density, air capacity and saturated water conductivity – as well as mechanical parameters, such as precompression stress, which can be used to estimate soil microstructure and the susceptibility to compaction of soils, including re-cultivated soils. All physical and mechanical parameters share the common limitation that determining them is highly time-consuming and costly. For this reason, their widespread application in agricultural practice is virtually impossible, especially given that soil structure is often subject to considerable temporal and spatial fluctuations. In this context, straightforward evaluation methods are intended to assist in providing a comprehensive overall impression of a soil's structure. These involve using sensory data obtained directly in the field to determine parameters such as root distribution, aggregate size, aggregate arrangement, degree of compaction, structural form and macropore distribution. A chunk of soil extracted with a spade is often used for these methods. The visual soil structure assessment is a simple and important tool used to identify structural damage. There are often good relationships between the results of visual soil structure assessment and physical soil parameters, such as dry bulk density, as well as the yield of arable crops (Mueller et al., 2009; Höhne et al., 2011). An important method used in Germany to assess soil structural properties in the field is the measurement of the packing density (PD) (DIN 19682-10, 2007). With this technique the degree of compactness or looseness of a particular soil horizon is defined. Increases or decreases in packing density in soils are mainly due to associated changes in the proportion of secondary pores. Unlike primary pores, which are caused by differences in soil texture, these secondary pores are affected by processes such as loosening, shrinking, frost and biological processes. On the other hand, the precompression stress of the soil is taken as an important indicator of stability against mechanical stress (Horn and Rostek, 2000). Stress which exceeds a certain precompression stress level leads to irreversible changes in the soil functions. Precompression stress is affected by the inter-aggregate pore system and thus the density heterogeneity within the soil structure, which is in itself defined by the aggregate density/dry bulk density ratio (AD/BD ratio), (Rücknagel et al. 2007). Precompression stress is therefore determined by altering parameters that are also key in determining packing density. Thus the main emphasis of this work was to quantify the relationship between the morphological characterisation of the soil with the method of packing density and soil mechanical properties such as AD/BD ratio and precompression stress. However, the primary goal of land management is not the maximisation of mechanical stability, but rather an optimisation of mechanical stability whilst maintaining an intact soil structure. That is why in this study we incorporated air capacity into the assessment. For an analysis of compaction processes and the analysis of change in aggregate arrangement it is useful to differentiate between the behaviour of the bulk soil and of aggregates. An example for this is also shown in this paper for a site subject to recultivation.

3.4.2. Materials and methods

3.4.2.1. Data acquisition

The data of the studies were based on 20 samples with 4-5 replications each, collected in the years 2008-2010 in different topsoil and subsoil layers of 9 re-cultivated fields in North Rhine-Westphalia (Germany), (Table 3.4.1). The soils examined varied little in terms of texture (130-210 g kg⁻¹ clay, 20-180 g kg⁻¹ sand) and could be assigned to the soil textural classes “Silt” and “Silty loam” in the USDA classification scheme. Due to their low level of variation, a detailed representation of the individual sites’ textural values is not given here. The organic carbon content varied between just 5 and 7 g kg⁻¹.

Table 3.4.1. Dry bulk density (BD), aggregate density at -6 kPa matric potential (AD), AD/BD ratio, logarithm precompression stress at -6 kPa matric potential ($\log \sigma_P$) and packing density (PD) for the test sites.

Site code	Site and depth (cm)	BD (g cm ⁻³)	AD (g cm ⁻³)	AD/BD ratio	$\log \sigma_P$	PD
1.1.	Neurath I 35-38	1.61	1.79	1.11	1.89	3
1.3.	Neurath I 80-83	1.71	1.69	0.99	2.47	4
2.1.	Neurath II 35-38	1.51	1.73	1.15	1.85	3
2.2.	Neurath II 55-58	1.54	1.68	1.09	2.27	2
2.3.	Neurath II 80-83	1.49	1.73	1.16	1.74	2
3.1.	Fortuna II 17-20	1.56	1.70	1.09	2.21	3
3.2.	Fortuna II 35-38	1.49	1.74	1.17	1.61	2
3.3.	Fortuna II 80-83	1.40	1.78	1.27	1.16	1
4.1.	Fischbach I 30-33	1.63	1.79	1.10	2.30	3
5.1.	Frechen 35-38	1.57	1.77	1.13	2.06	3
5.2.	Frechen 55-58	1.51	1.68	1.11	1.63	3
5.3.	Frechen 80-83	1.54	1.70	1.10	1.76	3
6.1.	Neurath III 45-48	1.73	1.77	1.02	2.39	5
7.1.	Fortuna IV 32-35	1.54	1.64	1.06	1.84	3
7.2.	Fortuna IV 55-58	1.43	1.59	1.11	1.79	2
7.3.	Fortuna IV 85-88	1.40	1.66	1.19	1.37	1
8.1.	Königshofen III 35-38	1.72	1.77	1.03	2.47	4
9.1.	Fortuna 19-22	1.39	1.61	1.16	1.20	2
9.2.	Fortuna 33-36	1.47	1.68	1.14	1.47	3
9.3.	Fortuna 49-51	1.49	1.66	1.11	1.46	2

3.4.2.2. Soil compression tests

The soil cores used in the compression tests had a diameter of 100 mm and a length of 28 mm. After collecting the soil, the samples were saturated and then adjusted to a matric potential of -6 kPa in a sand box. In many countries, this matric potential corresponds to field capacity. The difference between the total porosity of the soil and field capacity corresponds to the air capacity. This is an important factor in soil ecology. The soil samples in the core were exposed to pressures of 5, 10, 25, 50, 100, 200, 350 and 550 kPa (and in some cases 1200 and 2500 kPa) successively in a fully automatic oedometer (Bradford and Gupta, 1986). After each loading step, a relaxation phase was included. Each loading step lasted 180 minutes and was followed by a relaxation phase lasting 15 minutes. In previous tests on soils of similar texture classes, for loading times of up to 540 minutes in comparison to 180 minutes only very slight increases in settlement were measured. Therefore, settlement can be regarded as largely finished after 180 minutes. However, exactly how matric potential changed during the soil compression tests was not measured. All tests were performed under drained conditions. After drying the sample cores at 105 °C until the sample mass remained constant, the dry bulk density (BD) was determined after treatment in the oedometer. The stress/bulk density functions served to help numerous individuals (Rücknagel et al., 2010) determine precompression stress using Casagrande's graphical method (1936).

At one test site, (Neurath II, site code 2.1.: 160 g kg⁻¹ clay, 30 g kg⁻¹ sand), compaction behaviour was analysed for whole soil and for aggregates separately. Contrary to the procedure described above, a total of 15 soil cores were extracted from a depth of 35-38 cm and then adjusted to a matric potential of -6 kPa in a sand box. In the oedometer, pressure was applied to 3 samples each for each of the following loading steps: 5, 16, 50, 160 and 500 kPa (loading time 180 minutes, relaxation phase 15 minutes). Afterwards, the samples were carefully broken up and aggregates measuring 8-10 mm sieved out. These were then used to directly calculate aggregate density. For each loading step, the results provide the resulting dry bulk density and aggregate density caused by the loading. This information can be used to create a function of stress and dry bulk density, or of stress and aggregate density.

3.4.2.3. Determination of aggregate density

Parallel to core sampling for the oedometer tests, disturbed soil samples were collected from the same depths for determining the aggregate density (AD). In a sand box, the aggregates with a size of 8-10 mm were saturated and adjusted to the same matric potential (-6 kPa) as used in the samples from the compression test. When the matric potential was equalised, the water content was determined in a portion of each sample by drying it at 105 °C. The second part of the sample was weighed, placed on a fine-meshed screen and dipped in vegetable oil. The soaked aggregates were spread out on filter paper to let excess oil run off. The aggregates were thus coated with a thin water-repellent film, which had a negligible effect on their volume and their volume determined by water displacement. For the method applied here, previous studies

have not yielded any statistically sound correlation between aggregate density and the selected size fraction. Aggregates measuring 8-10 mm in size were chosen, in particular because they are very practical when it comes to determining aggregate density.

Each determination of aggregate density was performed with 3 replications for each site and depth. The AD/BD ratio was calculated as the quotient of aggregate density and dry bulk density. The ratio does not have a physical dimension and is a yardstick for the expression of the inter-aggregate pore system and thus also for the density heterogeneity within the soil structure. A classification of the values calculated is possible on the basis of Rücknagel et al. (2007), (Table 3.4.2).

Table 3.4.2. Classification of aggregate density/dry bulk density ratios (AD/BD ratio) according to Rücknagel et al. (2007).

Classification	Very low	Low	Mean	High	Very High
AD/BD ratio	< 1.05	1.05-1.10	1.10-1.15	1.15-1.20	> 1.20

3.4.2.4. Determination of packing density

Packing density (PD) is an integrated parameter which combines various soil structural properties affected by the degree of compaction and is assessed visually in the field (DIN 19682-10, 2007).

Table 3.4.3. Estimation of packing density (PD) according to German Industry Standard (DIN 19682-10, 2007), ¹ mean importance for assessment, ² high importance for assessment, ³ very high importance for assessment.

PD	Aggregate size ¹	Cohesion of soil structure ¹	Aggregate arrangement ²	Quantity of biogenic macropores ²	Root distribution ³
very low PD 1	very fine (1-2)	very low (1)	bulky (1)	very high (1)	regular (1)
low PD 2	fine (1-3)	low (2)	open (2)	high (2)	regular (2)
mean PD 3	mean (2-4)	mean (3)	half open (3)	mean (3)	almost regular (3)
high PD 4	coarse (3-5)	high (4)	half closed (4)	low (4)	irregular (4)
very high PD 5	very coarse (4-5)	very high (5)	closed (5)	very low (5)	very irregular (5)

It should give an indication of a number of important soil functions, such as water and air porosity as well as root resistance. The assessment of packing density is based on the following macroscopic properties, divided into five steps (Table 3.4.3), in the different soil horizons:

1. Aggregate size
2. Cohesion of the soil structure, assessed with a falling test
3. Aggregate arrangement as an indication of the properties of the aggregate space
4. Proportion of biogenic macropores (root and earthworm channels)
5. Root distribution in the different soil horizons

If for a characteristic, such as aggregate size, a wide range of aggregates of differing sizes are found, then the most common size class is used for assessment. Aggregate form is not considered when determining packing density. The packing density levels are intended to represent the following soil structure conditions: At packing density levels 1 and 2, the soil is loose, the water and air conductivity are high or very high and the rooting characteristics are excellent (for example see picture 3.4.1).



Picture 3.4.1. Re-cultivated loess soil with fine aggregate size and bulky aggregate arrangement at packing density level 1.



Picture 3.4.2. Re-cultivated loess soil with high cohesion of soil structure and closed aggregate arrangement at packing density level 4.

At packing density level 3, the soil is less loose but not compacted. There are hardly any negative effects on the ecological functions. At packing density levels 4 and 5, the soil is compacted and the ecological functions are severely impaired (for example see picture 3.4.2).

The determination of packing density in the study presented here was performed horizontally in each case on prepared soil profiles in spring (March-April), with comparable water content levels near field capacity. The development of the crop plants grown (usually winter wheat) also allowed a comparative evaluation of root distribution in the soil.

3.4.2.5. Statistical analysis

To be able to represent the relationships of the individual test parameters with the visually determined packing density scores in mathematical terms, a Spearman's rank correlation (correlation coefficient r_s) was calculated according to the following formula:

$$r_s = 1 - \frac{6 \sum_i d_i^2}{n(n^2 - 1)} \quad (3.4.-1)$$

where

$$d_i = rg(x_i) - rg(y_i) \quad (3.4.-2)$$

d_i = difference of ranks of x and y of an observation

n = number of value pairs

$rg(x_i)$ = the rank of x

$rg(y_i)$ = the rank of y

In addition to correlation coefficients, here the standard deviations are calculated based on the sum of squares (SQ) and the number of all replicated measurements (n) using the equation:

$$s = \sqrt{(SQ/(n-1))} \quad (3.4.-3)$$

All calculations were based on logarithm precompression stress. This is because when the unit kPa was applied, the test parameter precompression stress displayed a frequency distribution with a skew to the right. This is demonstrated for example by the composition of the data records by Lebert (1989) and Nissen (1998).

3.4.3. Results and discussion

3.4.3.1. Morphological characterisation of soil structure and soil mechanical properties

The soil layers examined covered the entire range of packing density levels. However, the largest cluster lies with levels 2 ($n = 6$) and 3 ($n = 9$), while there were fewer soil layers of levels 4 and 5 or level 1 (Table 3.4.1). The range of the AD/BD ratio was correspondingly broad, varying between 0.99 (very low) and 1.27 (very high). Most readings, however, were between 1.10 and 1.15 (mean). As shown in Figure 3.4.1, for the soils in this experiment a good estimate of the AD/BD ratio can be obtained from the different packing density levels (correlation coefficient $r_s = -0.75$). For packing densities 1 to 4 the standard deviation was around ± 0.03 . The good relationship between packing density and AD/BD ratio was not surprising, since aggregate arrangement is a highly significant structural characteristic for determining packing density and can be recorded quite easily when assessing soil structure.

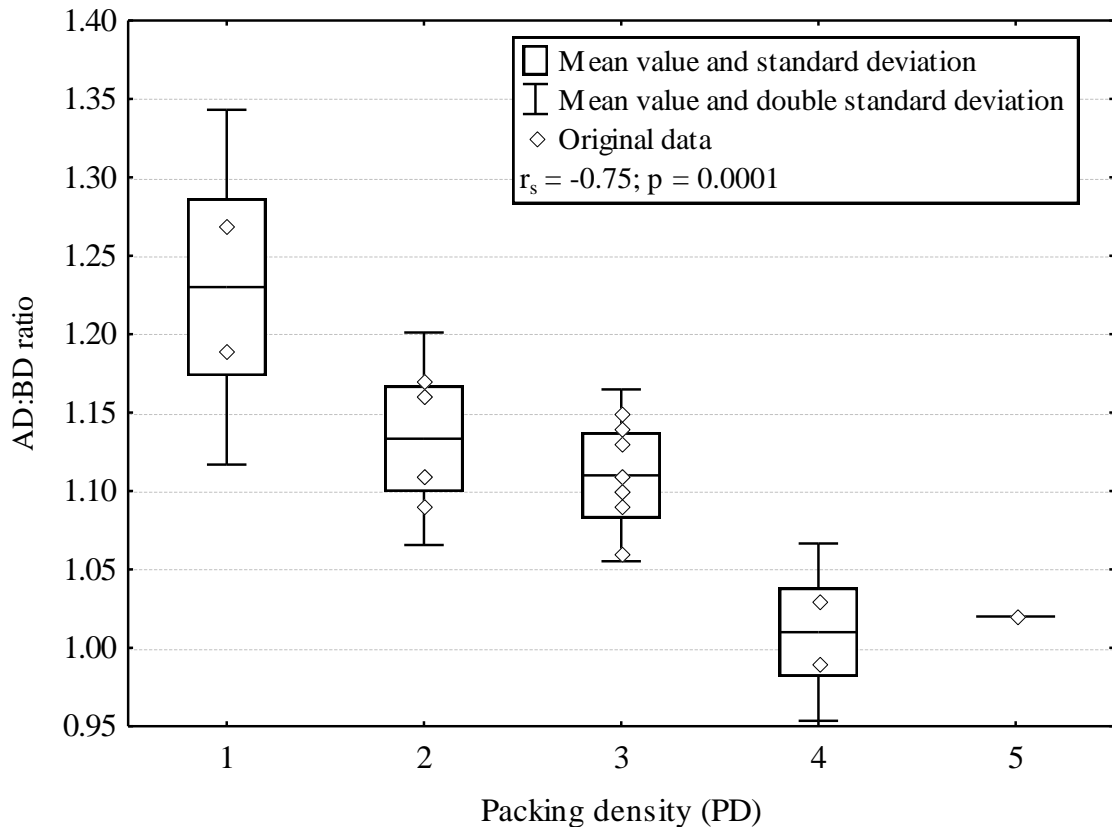


Figure 3.4.1. Relationship and correlation coefficient (r_s) between packing density (PD) and aggregate density/dry bulk density ratio (AD/BD ratio).

Along the lines of the various AD/BD ratios, the different levels of packing density can thus also be assigned to different ranges of precompression stress (Fig. 3.4.2). Extraordinarily low measurements for precompression stress were detected in horizons with a very large AD/BD ratio e.g. “Fortuna II 35-38” (site code 3.2.) and “Fortuna II 80-83” (site code 3.3.). With decreasing AD/BD ratio, the precompression stress increased (correlation coefficient $r_s = 0.76$),

showing the largest values in horizons with a coherent structure such as “Neurath I 80-83” (site code 1.3.). However, the standard deviation of precompression stress varies highly between the individual packing density levels. Levels 2 and 3 in particular demonstrate somewhat higher standard deviations. The mean standard deviation of all packing density levels in the logarithmic scale was around ± 0.20 . In addition to aggregate arrangement, which is reflected directly in the AD/BD ratio, aggregate size is a further parameter used for determining packing density.

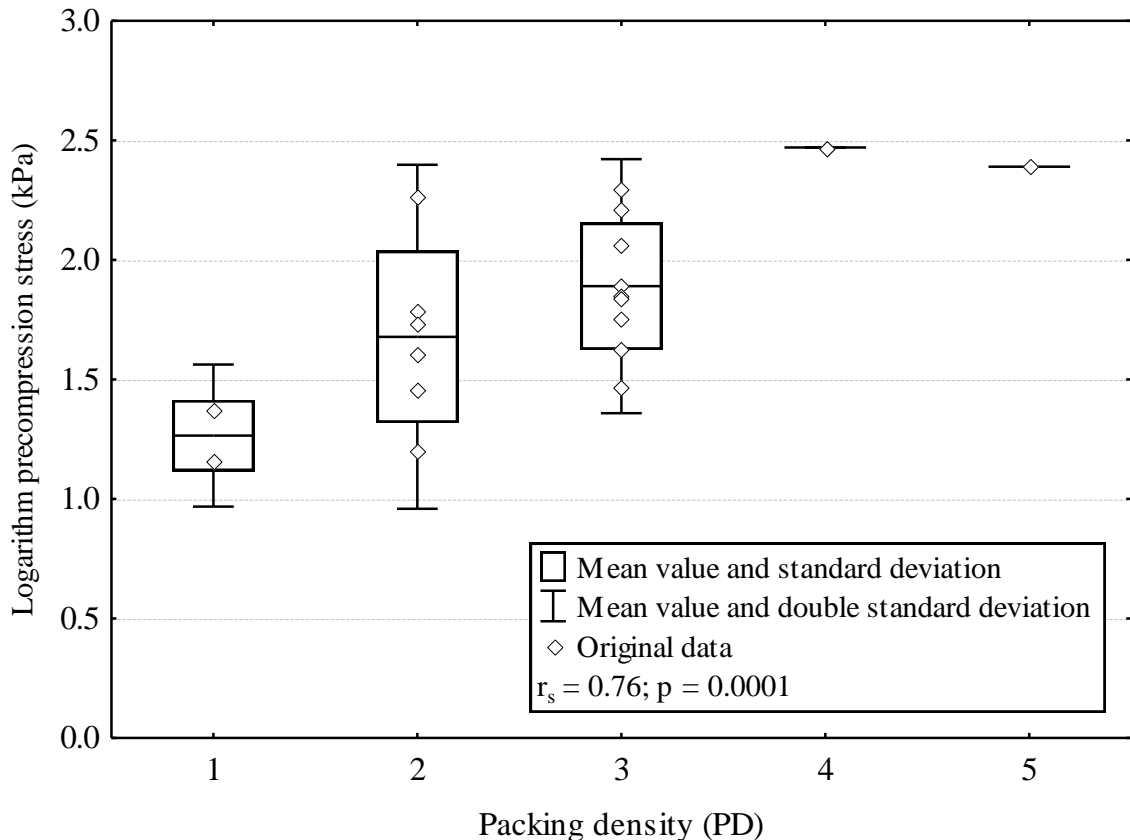


Figure 3.4.2. Relationship and correlation coefficient (r_s) between packing density (PD) and precompression stress (logarithm kPa).

In this study, it was recorded qualitatively according to Table 3.4.3 and thus also has an indirect influence on the positive relationship between packing density and precompression stress. However, this contradicts tests by Keller et al. (2011), in which no direct relationship between aggregate size and precompression stress was found. Furthermore, Horn and Fleige (2009) noted a clear tendency that aggregate formation was related to precompression stress. Soils with blocky to (sub)angular structures in particular demonstrated higher levels of precompression stress than those with prismatic to coherent structures. When determining packing density according to DIN 19682-10 (2007), however, structural form is not considered at all. Nevertheless, this method too results in good relationships with precompression stress. Thus various methods of visual assessment appear to provide highly similar results. Overall, it is thus possible to make an approximate estimate of precompression stress, as an important soil mechanical

criterion, based on packing density level, and to use it, for example, for subsequent calculations in models to estimate the risk of compaction (e.g. Keller et al., 2007; Rücknagel et al., 2012b). An overall assessment of the status of a soil with a subsequent optimisation based solely on precompression stress is not sufficient. For this reason, different levels of packing densities are assigned to the respective air capacities (Fig. 3.4.3). Air capacity decreases with increasing packing density (correlation coefficient $r_s = -0.66$) and shows, approximately, figures below 5 to 8 vol.% at level 3, which have been postulated by Houskova (2002), Lebert et al. (2004) and Paul (2004) as minimum requirements. For each of the levels 1-3, however, standard deviation was equal to approximately 4 vol.% air capacity. The soil layers of packing density levels 4 and 5 possess almost no more air capacity whatsoever. With respect to mechanical strength and soil ecological requirements, the optimum soil structure for the soil samples included in this project would be a packing density at level 3. At this level the logarithm of precompression stress at field water capacity (-6 kPa matric potential) averages at 1.89 (78 kPa). Apart from the air capacity, the continuity of the pores measured by the air or water conductivity is important for the functionality of the soil structure (Topp et al., 1997). Measurements of those conductivity parameters, however, were not possible in the cores taken during this project.

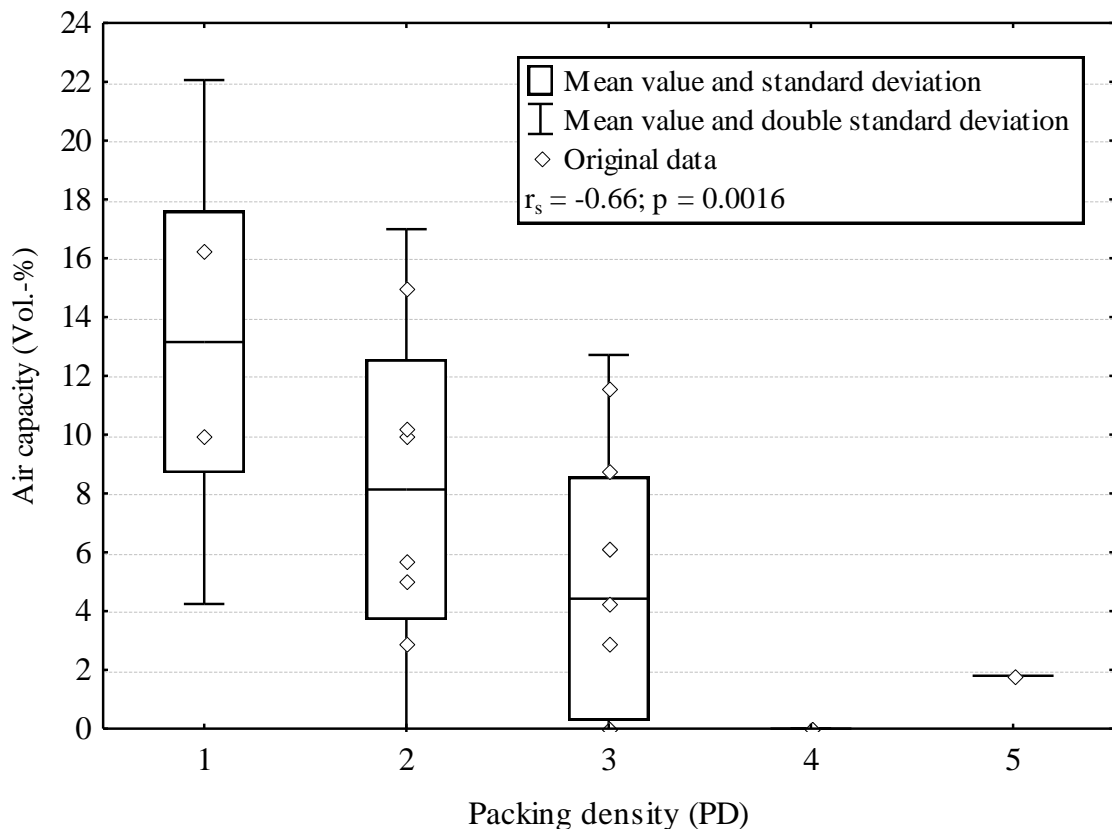


Figure 3.4.3. Relationship and correlation coefficient (r_s) between packing density (PD) and air capacity (vol.%).

One considerable advantage of the visual method of structural assessment presented is the possibility it offers of examining soil for practical purposes (e.g. soil conservation) on a small scale, rapidly, and with comparatively little effort. This could reduce costs and the time required for

laboratory analyses. All of the individual characteristics are, however, subject to a certain amount of subjectivity on the part of the person analysing them. Based on this aspect alone, the correlations of the packing density scores with the physical test results should be classified as strong. What is more, if tests are not performed on dried soils or on young crops with underdeveloped roots, then the method's margins of error can largely be limited.

3.4.3.2. Stress/bulk density behaviour of whole soil and aggregates

The analysis of compaction processes where a distinction is made between the behaviour of the bulk soil and that of aggregates was exemplified by the site "Neurath II 35-38" in Figure 3.4.4. Changes in the dry bulk density and aggregate density are not normally synchronic. On the recompression line of the whole soil, the dry bulk density increased slightly, whereas no changes to the densities were detectable on the recompression line of aggregates.

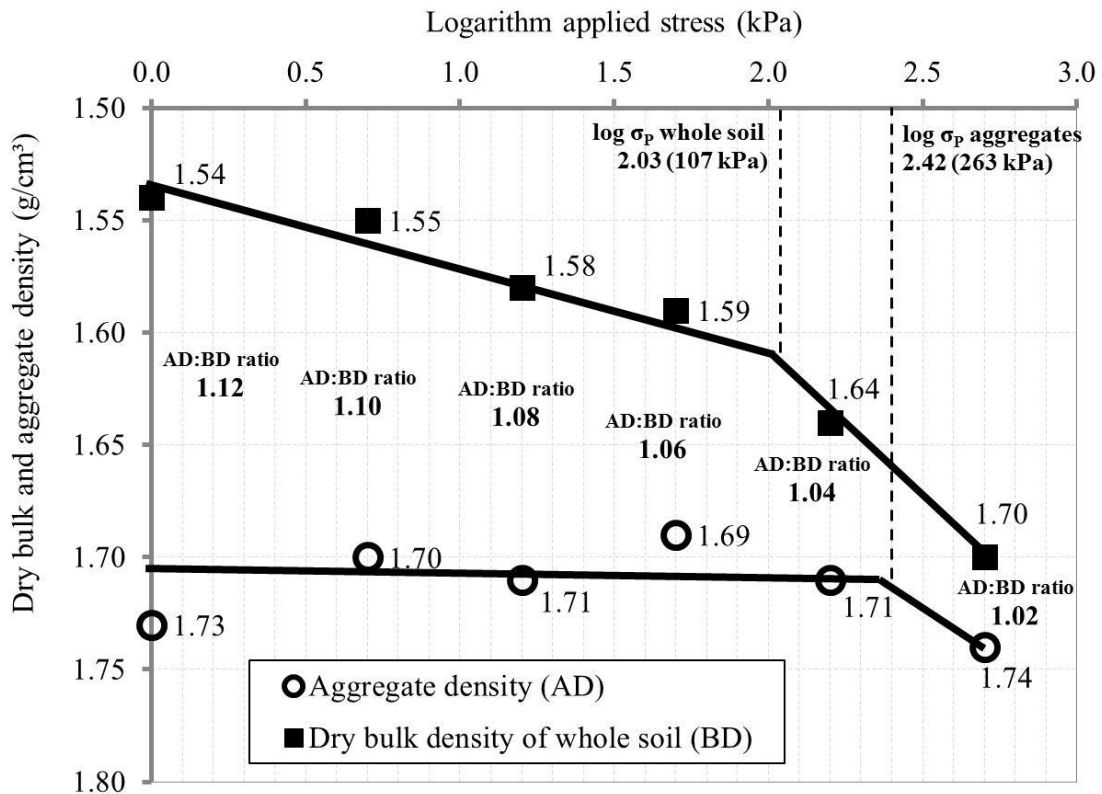


Figure 3.4.4. Stress/bulk density functions and logarithm precompression stress ($\log \sigma_p$) of whole soil and aggregates for the example "Neurath II 35-38".

The logarithm precompression stress of the aggregates, at 2.42 (263 kPa), was much greater compared with the value in the bulk soil of only 2.03 (107 kPa). Exceeding the precompression stress of the bulk soil (close to the virgin compression line) depends on the load and leads to a sharp increase in dry bulk density. On the other hand, the aggregate density was only detectable at the highest loading step and was similar to the density of the bulk soil for this load. In the whole compaction process, the AD/BD ratio was reduced to a closed aggregate arrangement.

In keeping with Figure 3.4.1, the reduction of the AB/BD ratio during the compaction process can also explain the increase in packing density seen in compacted soils.

The reason for the differentiated stress/bulk density behaviour is the frequency distribution of grain contacts, which has two maxima in aggregated soil (Hartge and Sommer, 1982). The average number of grain contacts between the aggregates is smaller, as is the number of grain contacts within the aggregates. At low loading steps the number of grain contacts between aggregates increases, however with higher loads the number of grain contacts within the aggregates is increased and this increases the aggregate density.

3.4.4. Conclusions

This study can be used to demonstrate that a negative relationship exists between packing density and the AB/BD ratio as well as air capacity. Conversely, mechanical precompression stress increases with packing density. Thus packing density is, on the whole, an easy-to-use instrument in field soil science which is also suitable for deriving soil mechanical parameters. Packing density level 3 represents an optimisation with regard to mechanical soil stability whilst maintaining the minimum air capacity requirements for re-cultivated loess soils.

Acknowledgement

The authors would like to thank Joachim Spilke from the Biometrics and Informatics in Agriculture group of the Martin Luther University Halle-Wittenberg for his valuable input regarding the statistical alignment of the data presented in this study.

4. Applications of the module concept

4.1. Impact on soil physical properties of using large-grain legumes for catch crop cultivation under different tillage conditions

Published in: *European Journal of Agronomy* 77 (2016), 28-37

Jan Rücknagel¹, Philipp Götze¹, Barbara Koblenz¹, Nora Bachmann¹, Stefanie Löbner¹, Sarah Lindner¹, Joachim Bischoff², Olaf Christen¹

¹Institute of Agricultural and Nutritional Sciences, Department Agronomy and Organic Farming, University of Halle-Wittenberg, Betty-Heimann-Str. 5, 06120 Halle/Saale (Germany)

²Landesanstalt für Landwirtschaft, Gartenbau und Forsten, Strenzfelder Allee 22, 06406 Bernburg (Germany)

Abstract

In Central Europe, various plant species including large-grain legumes and their mixtures are grown as catch crops, particularly between grains harvested early and subsequent summer crops. This article investigates the question of how soil structure in the topsoil is influenced when catch cropping with large-grain legumes (experimental factor A: without catch crop, with catch crop) under different ploughless tillage conditions during catch crop seeding (experimental factor B: deep tillage / 25-30 cm, shallow tillage / 8-10 cm). Five one-year trials were performed using standard machinery at various sites in Germany. Soil core samples extracted from the topsoil in the spring after catch crop cultivation served to identify air capacity, saturated hydraulic conductivity and precompression stress. The above-ground and below-ground biomass yields of the catch crops were also determined at most of the sites. In addition, the soil compaction risk for the working steps in the experiments was calculated using the *REPRO* model.

The dry matter yield of the catch crops varied considerably between the individual trial sites and years. In particular, high levels of dry matter were able to form in the case of early seeding and a sufficient supply of precipitation. The soil structure was only rarely affected positively by catch crop cultivation, and catch crops did not contribute in the short term to loosening already compacted topsoils. In contrast, mechanical soil stresses caused by driving over the ground and additional working steps used in cultivating catch crops often led to lower air capacity in these treatments. This is consistent with the soil compaction risks calculated using the *REPRO* model, which were higher in the treatments with catch cropping. Catch crop cultivation also only resulted in improved mechanical stability at one location. The positive effect of deep ploughless tillage on air capacity and saturated hydraulic conductivity, however, became more clearly evident regardless of catch crop cultivation. In order for catch crop cultivation with large-grain legumes to be able to have a favourable impact on soil structure, it is therefore important that cultivating them does not result in any new soil compaction. In the conditions

evaluated, deep tillage was more effective at loosening compacted topsoil than growing catch crops.

4.1.1. Introduction

In Central Europe, various plant species are grown as cover crops in winter and catch crops sown in July/August, particularly between species of grain harvested early and subsequent summer crops like sugar beets (*Beta vulgaris* subsp. *vulgaris*), maize (*Zea mays* L.) and spring barley (*Hordeum vulgare* L.) (Lütke Entrup, 2000). Cover crops such as rye (*Secale cereale* L.) and common vetch (*Vicia sativa* L.) cover the soil during winter and are tolerant of frost. Their above-ground biomass can be used in the spring after seeding as animal feed or in anaerobic digestion plants. By contrast, species with rapid juvenile growth are preferred for use as catch crops in summer; these species are killed by frost under the prevailing climatic conditions in the winter months. Their above-ground biomass is only used as green manure. White mustard (*Sinapis alba* L.), oil radish (*Raphanus sativus* var. *oleiformis*) and phacelia (*Phacelia* Juss.) are particularly popular as catch crops (Buhre et al., 2014). Currently, however, more and more farms are considering using large-grain legumes such as field beans (*Vicia faba* L.).

The cultivation of both cover crops and catch crops is supposed to serve a wide range of functions. Particularly when combined with direct or mulch seeding, catch crops reduce the risk of soil erosion when cultivating the subsequent crop (Bechmann et al., 2009) as well as associated nutrient losses (Ulen, 1997). Non-leguminous catch crops, but also mixtures of non-leguminous and leguminous catch crops, reduce the nitrate concentration in soil solutions, thus preventing mineral nitrogen from shifting down into deeper soil layers during winter (Hooker et al., 2008; Rinnofner et al., 2008). On the other hand, by fixing biological nitrogen in the soil, leguminous catch crops can serve as a source of nitrogen, particularly in systems like organic farming which do not use mineral nitrogen (Watson et al., 2002; Rinnofner et al., 2008). Catch crop plant growth serves as an essential source of food for earthworms (Schmidt et al., 2003; Reeleder et al., 2006) and can thus contribute to increasing soil biodiversity. Cover crops can raise the soil organic carbon content (Higashi et al., 2014) and change its characteristic composition (Ding et al., 2006).

In addition to – and also sometimes in interaction with – the functions mentioned, one general advantage of cultivating catch crops is the improvement of soil structure. Previous studies have focused mainly on the water stability of soil aggregates (Breland, 1995; Ball-Coelho et al., 2000), measuring soil strength using a penetrometer (Folorunso et al., 1992; Raper et al., 2000) and identifying dry bulk density (Breland, 1995). Furthermore, the above-mentioned studies considered the effect of cover crops on soil structure. Very few documented studies have investigated these questions using catch crops. But catch crops may also contribute to improving soil structure – particularly those which have strong taproot systems, provide extensive and longer-term shade and produce high levels of above-ground and below-ground biomass. In principal,

legumes are more effective at stabilising the soil structure than non-legumes (Cochrane and Aylemore, 1994 cited in Hamza and Anderson, 2005).

For economic reasons, catch crops are often grown using ploughless tillage. The depth of tillage can be very shallow (<8-10 cm) but also include the whole topsoil (25-30 cm). Varying tillage intensity impacts upon physical soil properties (Tebrügge and Düring, 1999), and combined with catch crop cultivation this in turn may affect soil structure.

Therefore this study investigates the question of how important physical and mechanical soil properties in the topsoil are influenced when cultivating large-grain legumes as catch crops, with varying depths of ploughless tillage. In order to describe the effects of cultivation techniques on soil structure and to characterise soil performance, Horn and Kutilek (2009) recommend also using an intensity-based parameter (e.g., saturated hydraulic conductivity) in addition to a capacity parameter (e.g., air capacity). In the topsoil, an intact soil structure displays air capacity of at least 8 % by volume and saturated hydraulic conductivity of 10 cm d^{-1} (Werner and Paul, 1999). Additionally, mechanical precompression stress is an important, direct mechanical criterion of a soil's susceptibility to compaction (Arvidsson and Keller, 2004).

In this article, the investigation of physical and mechanical soil properties was deliberately conducted shortly after seeding of the main crops, because under the prevailing conditions in Central Germany the roots of summer crops like spring barley (*Hordeum vulgare* L.) and sugar beets (*Beta vulgaris* subsp. *vulgaris*) reach depths of more than 30 cm – and hence the transitional layer between the topsoil and subsoil – just 30-40 days after seeding (Damm et al., 2013). Also bearing in mind the tillage technique, potential effects on soil structure in the topsoil of cultivating catch crops are therefore particularly relevant shortly after the main crop has been sown and during its juvenile growth period. One particular aspect of the study presented here is how it considers catch crops in the context of practical cultivation methods and the calculated soil compaction risk for the individual working steps, because only in this way is it possible to identify and evaluate the sum of all factors which influence soil structure.

4.1.2. Materials and methods

4.1.2.1. Site description and precipitation data

The experiments took place over five years at farms at various sites in Central Germany. Site-specific soil texture details are given in Table 4.1.1. The soil type according to the FAO classification (FAO, 1998) was a Haplic Planosol at Bergzow, a Chernozem at Andisleben I and Andisleben II and an Albic Luvisol at Rothenberga I and Rothenberga II.

The climate in this region is moderate, with cold winter months and relatively warm summers and mean annual temperatures of between 8.5 and 9.0 °C as well as mean annual precipitation of between 500 and 550 mm. Data on precipitation during the trial period – from when the catch crops were sown (July) until the subsequent main crops were sown (April) – and compared to the long-term average are shown in Figure 4.1.1.

Table 4.1.1. Experimental sites with texture and soil organic matter (SOM) in the topsoil layer (0-25 cm depth); ¹ USDA classification scheme (Gee and Bauder, 1986).

Site	Year	Texture (g kg ⁻¹)		Texture class ¹	SOM (g kg ⁻¹)
		Clay	Sand		
Bergzow	2008/2009	200	520	Sandy Loam	22
Andisleben I	2009/2010	270	70	Silty Clay Loam	30
Andisleben II	2010/2011	330	50	Silty Clay Loam	30
Rothenberga I	2011/2012	170	110	Silt Loam	19
Rothenberga II	2013/2014	150	70	Silt Loam	18

Precipitation volumes were above average in the July shortly before the catch crops were sown at the four experimental sites Bergzow, Andisleben I, Andisleben II and Rothenberga I (+17 to +62 mm), while at the site Rothenberga II very little rain fell during this period (-30 mm). During the autumn months (September, October, November), overall precipitation rates were very high in Andisleben I and II in particular (+112 mm and +84 mm respectively), but also in Bergzow (+11 mm), while they were average in Rothenberga II and considerably low in Rothenberga I (-59 mm). The period before main crop cultivation, particularly the months of March and April, was somewhat too dry at all five locations (-25 mm to -68 mm).

4.1.2.2. Treatments and experimental conditions

The experimental treatments in the two-factorial experiments at the sites Andisleben I and II as well as Rothenberga I and II were the cultivation of catch crops (experimental factor A: without catch crop, with catch crop) as well as soil tillage depth prior to seeding (experimental factor B: deep tillage / 25-30 cm, shallow tillage / 8-10 cm). At the Bergzow site, the experiment was only set up to include cultivation with and without a catch crop. This was sown in Bergzow using direct seeding. Ploughless tillage was generally also performed at the other sites. The catch crops grown at Bergzow were blue lupins (*Lupinus angustifolius* L.), and at Rothenberga I field beans (*Vicia faba* L.), with seeding rates of 100 and 55 germinable seeds per m² respectively. At Andisleben I and II as well as Rothenberga II, a mixture of field beans (*Vicia faba* L.) (15-20 germinable seeds per m²), field peas (*Pisum sativum* L. convar. *speciosum* (Dierb.) Alef.) (15-20 germinable seeds per m²) and vetch (*Vicia sativa* L.) (30-40 germinable seeds per m²) was used. Following Lütke Entrup (2000), the large-grain legume species used (and mixtures of these) are well suited to the respective locations.

In order to ensure cultivation was as realistic as possible, the experimental treatments were set up as large plots 9-18 m wide. Each treatment was replicated four times at the sites Bergzow, Andisleben I, Andisleben II and Rothenberga II, and twice at Rothenberga I. The catch crops were cultivated in accordance with customary procedures, details of which are given in Table 4.1.2.

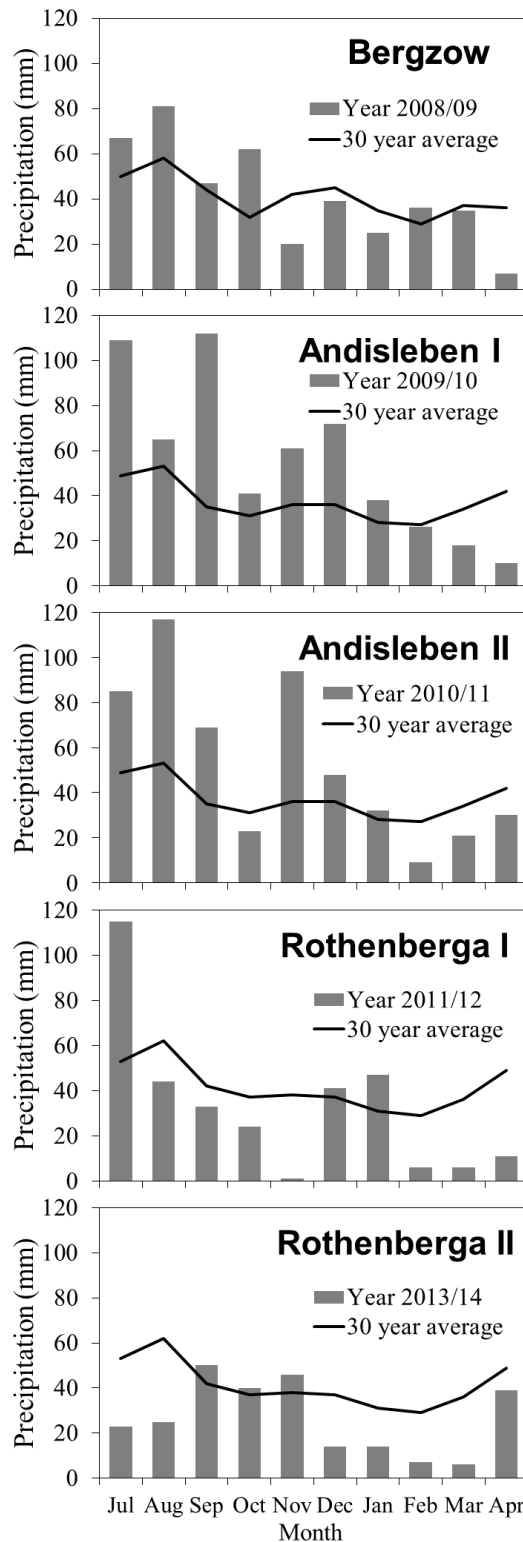


Figure 4.1.1. Monthly cumulative precipitation (July-April) for the experimental sites and years.

As a rule, the catch crops were sown between late July and early August immediately after the previous crops had been harvested (winter wheat (*Triticum aestivum* L.) or winter barley (*Hordeum vulgare* L.)). These freeze and die during the winter months at the trial locations. In some cases, additional working steps were performed in order to shred catch crop plant growth.

Table 4.1.2. Working steps and machinery characterisation for calculating the Soil Compaction Index between harvest of main crop and soil core sampling at the experimental sites for all treatments, and additional steps for the catch crop treatments; WL = wheel load of the axle with the highest load, IP = inflation pressure of the axle with the highest load, WA = wheeled area of single pass as a percentage (%) of the total area divided by 100; ¹ catch crop seed was combined with tillage, ² permanent traffic lanes were not included in the soil sampling area and calculation of the Soil Compaction Index.

Site	All treatments		Only in catch crop treatments	
	Working steps	Machinery characterisation	Working steps	Machinery characterisation
Bergzow			Catch crop seed (at the end of July 2008)	-
	Seedbed preparation (at the end of March 2009)	-		
Andisleben I	Tillage, different depth in the treatments (31 th July 2009) ¹	WL (kg): 2820 IP (kPa): 80 WA (%/100): 0.27		
			Rolling (1 st August 2009)	WL (kg): 2480 IP (kPa): 80 WA (%/100): 0.15
	Herbicide application (18 th August 2009) ²	-		
			Mulching (7 th December 2009)	WL (kg): 2600 IP (kPa): 70 WA (%/100): 0.22
	Tillage, 8 cm depth (14 th December 2009)	WL (kg): 7740 IP (kPa): 60 WA (%/100): 0.23		
	Tillage, 8 cm depth (23 th March 2010)	WL (kg): 7740 IP (kPa): 60 WA (%/100): 0.23		
	Seedbed preparation, 4-6 cm depth (25 th March 2010)	WL (kg): 3480 IP (kPa): 80 WA (%/100): 0.30		
Sugar beet seed (31 th March 2010)	WL (kg): 1610 IP (kPa): 235 WA (%/100): 0.11			

Table 4.1.2 (continuation). Working steps and machinery characterisation for calculating the Soil Compaction Index between harvest of main crop and soil core sampling at the experimental sites for all treatments, and additional steps for the catch crop treatments; WL = wheel load of the axle with the highest load, IP = inflation pressure of the axle with the highest load, WA = wheeled area of single pass as a percentage (%) of the total area divided by 100; ¹ catch crop seed was combined with tillage, ² permanent traffic lanes were not included in the soil sampling area and calculation of the Soil Compaction Index.

Site	All treatments		Only in catch crop treatments	
	Working steps	Machinery characterisation	Working steps	Machinery characterisation
Andisleben II	Tillage, different depth in the treatments (30 th July 2010) ¹	WL (kg): 3090 IP (kPa): 110 WA (%/100): 0.30		
	Herbicide application (7 th August 2010) ²	-		
			Mulching (15 th December 2010)	WL (kg): 2600 IP (kPa): 70 WA (%/100): 0.22
	Tillage, 8 cm depth (17 th December 2010)	WL (kg): 7740 IP (kPa): 60 WA (%/100): 0.23		
	Tillage, 8 cm depth (16 th February 2011)	WL (kg): 7740 IP (kPa): 60 WA (%/100): 0.23		
	Seedbed preparation, 4-6 cm depth (25 th March 2011)	WL (kg): 3480 IP (kPa): 80 WA (%/100): 0.30		
	Sugar beet seed (28 th March 2011)	WL (kg): 1610 IP (kPa): 235 WA (%/100): 0.11		

Table 4.1.2 (continuation). Working steps and machinery characterisation for calculating the Soil Compaction Index between harvest of main crop and soil core sampling at the experimental sites for all treatments, and additional steps for the catch crop treatments; WL = wheel load of the axle with the highest load, IP = inflation pressure of the axle with the highest load, WA = wheeled area of single pass as a percentage (%) of the total area divided by 100; ¹ catch crop seed was combined with tillage, ² permanent traffic lanes were not included in the soil sampling area and calculation of the Soil Compaction Index.

Site	All treatments		Only in catch crop treatments	
	Working steps	Machinery characterisation	Working steps	Machinery characterisation
Rothenberga I	Tillage, different depth in the treatments (2 th August 2011)	-		
			Catch crop seed combined with seedbed preparation, 4-6 cm depth (3 th August 2011)	WL (kg): 2500 IP (kPa): 80 WA (%/100): 0.45
	Herbicide application (21 th August 2011) ²	-		
	Herbicide application (16 th September 2011) ²	-		
	Fertilizer application (17 th March 2012) ²	-		
			Mulching (22 th March 2012)	WL (kg): 2200 IP (kPa): 80 WA (%/100): 0.42
	Spring barley seed combined with seedbed preparation, 4-6 cm depth (23 th March 2012)	WL (kg): 2500 IP (kPa): 80 WA (%/100): 0.45		
	Rolling (24 th March 2012)	WL (kg): 1900 IP (kPa): 80 WA (%/100): 0.16		

Table 4.1.2 (continuation). Working steps and machinery characterisation for calculating the Soil Compaction Index between harvest of main crop and soil core sampling at the experimental sites for all treatments, and additional steps for the catch crop treatments; WL = wheel load of the axle with the highest load, IP = inflation pressure of the axle with the highest load, WA = wheeled area of single pass as a percentage (%) of the total area divided by 100; ¹ catch crop seed was combined with tillage, ² permanent traffic lanes were not included in the soil sampling area and calculation of the Soil Compaction Index.

Site	All treatments		Only in catch crop treatments	
	Working steps	Machinery characterisation	Working steps	Machinery characterisation
Rothenberga II	Tillage, different depth in the treatments (15 th August 2013)	-		
			Catch crop seed combined with seedbed preparation, 4-6 cm depth (15 th August 2013)	WL (kg): 2500 IP (kPa): 80 WA (%/100): 0.45
	Herbicide application (7 th September 2013) ²	-		
	Herbicide application (1 th October 2013) ²	-		
			Mulching (24 th February 2014)	WL (kg): 2200 IP (kPa): 80 WA (%/100): 0.42
	Fertilizer application (4 th March 2014) ²	-		
	Spring barley seed combined with seedbed preparation, 4-6 cm depth (4 th March 2014)	WL (kg): 2500 IP (kPa): 80 WA (%/100): 0.45		
	Rolling (5 th March 2014)	WL (kg): 1900 IP (kPa): 80 WA (%/100): 0.16		

4.1.2.3. Crop and soil sampling

With the exception of the Bergzow site, the catch crops' above-ground growth was determined on one sampling date in November of the seeding year at the end of the vegetation period. On that date, one quarter of a square metre was harvested in all replications of each combination of treatments. The proportions of field beans, field peas and vetch were weighed in the seed mixtures at Andisleben I and II as well as Rothenberga II. At the sites Rothenberga I and II, root mass was also determined in parallel to the above-ground biomass. To this end, the soil beneath the harvest areas used to determine the above-ground biomass was dug up along with the roots of the catch crops, down to a depth of 25 cm. Following the method described by Böhm (1979), the roots were washed from the soil in the lab using water and a fine-meshed screen. In order to determine the amount of dry matter, the plants and roots were dried at 105 °C until their mass remained constant.

In the experiments at Andisleben I and II as well as Rothenberga I and II, soil core samples were taken no later than four weeks after the main crops (sugar beet (*Beta vulgaris* subsp. *vulgaris*) or spring barley (*Hordeum vulgare* L.)) were sown. At the Bergzow site, soil core samples were already taken shortly before the main crop was sown (sugar beet (*Beta vulgaris* subsp. *vulgaris*)). In each replication, 3 soil core samples (Rothenberga I 6 soil core samples) per depth (n=12), each with a volume of 250 cm³, were taken at the depths 6-12 cm and 16-22 cm, in order to determine air capacity and saturated hydraulic conductivity. The selection of these physical soil parameters was based on a proposal by Lebert et al. (2004) for identifying soil compaction damage as well as the use of an intensity-based parameter in addition to a capacity parameter following Horn and Kutilek (2009). The air capacity is air-filled porosity expressed in % on a volumetric basis at -6 kPa matric potential. It is an important factor in soil ecology, and it covers pores with an equivalent diameter of >50 µm, in which water moves in accordance with gravity. It is determined in a sandbox (German laboratory standard DIN ISO 11274, 1998). Saturated hydraulic conductivity is the parameter of Darcy's law applied to saturated water movement within the soil as a measure of the hydraulic permeability of water-saturated soil (unit cm d⁻¹). Apart from pore size and shape, soil permeability for water is influenced heavily by pore continuity. This parameter is determined in a stationary facility according to the principle described by Klute and Dirksen (1986).

Soil core samples (2 per replication at the sites Andisleben I and Rothenberga II and 3 per replication at the site Rothenberga I, volume 220 cm³, height 28 mm) were also extracted for soil compression tests and the subsequent determination of precompression stress at a depth of 9-12 cm at the sites Andisleben I, Rothenberga I and Rothenberga II. Precompression stress was selected because it can provide evidence of the extent to which catch crop cultivation has a mechanically stabilising effect on the soil structure in combination with different tillage techniques. After collecting the soil, the samples were saturated and then adjusted to a matric potential of -6 kPa in a sandbox. The soil samples in the core were exposed to pressures of 5, 10, 25, 50, 100, 200, 350 and 550 kPa successively in a fully automatic oedometer (Bradford and

Gupta, 1986). Each loading step lasted 180 minutes and was followed by a relaxation phase lasting 15 minutes. All tests were performed under drained conditions. After drying the sample cores at 105 °C until the sample mass remained constant, the dry bulk density was determined after treatment in the oedometer. The precompression stress was determined from the stress/bulk density functions using Casagrande's graphical method (1936). This involves a subjective assessment by the experimenter. For this reason, in this work separate individuals determined precompression stress independently in order to improve the reproducibility of the results (Rücknagel et al., 2010).

4.1.2.4. Calculation of Soil Compaction Index

The risk of soil compaction was modelled based on the method by Rücknagel et al. (2015) using the modelling program *REPRO* (*REPRO*duction of soil fertility, Hülsbergen 2003; Küstermann et al. 2010), at 20 cm soil depth for the sites Andisleben I and II and Rothenberga I and II. For this, the soil strength (logarithm precompression stress σ_p) in the soil structure was contrasted with the vertical soil stress (logarithm major principal stress σ_z) at the respective soil depth for each machinery pass. Soil strength was adjusted depending on the soil water content as a percentage of field capacity (Rücknagel et al. 2012a). This study used soil water content levels calculated by the German Meteorological Service (DWD) for the weather station Halle/Saale. If the vertical soil stress exceeds the soil strength of the soil structure, this results in a dimensionless index, the Soil Compaction Index (SCI), which reflects the risk of soil compaction. Values greater than 0 indicate a plastic deformation (increase in dry bulk density) of the soil. This can be characterised by the slope of the so-called virgin compression line on the stress/bulk density diagram. The slope was 0.20 on average (ranges of measured values 0.10-0.30), and was determined from numerous soil compression tests (Rücknagel et al., 2007; Rücknagel et al., 2012a). Accordingly, in theory it is to be expected that for every time the soil strength is exceeded by 0.10 there will be an average increase in dry bulk density of 0.02 g cm⁻³. Taking into account the wheeled area of the individual passes, an overall index was aggregated. Since soil strength was not examined when the individual experiments presented here were set up, the SCI calculations are based on standard soil strength values in the model, which are related to soil type and tillage depth. It was thus assumed that the deep-tillage treatments at 20 cm had a soil strength of log 1.59 (39 kPa) at a base water content with a matric potential of -6 kPa, while log 1.91 (81 kPa) was assumed for the shallow-tillage treatments. The axle load and tyre inflation pressure from the working steps listed in Table 4.1.2 were used when calculating vertical soil stress.

4.1.2.5. Statistical analysis

For the statistical analyses, a variance analysis was performed using the program SAS (SAS Institute, 2008). Before this, the data sets were tested for normal distribution by performing the

Shapiro-Wilk test in the program Statistica (Statsoft, 2009). Then the logarithmic form of the saturated hydraulic conductivity values was used in the variance analysis. Precompression stress was also used in its logarithmic form, because when using the unit kPa the parameter displays a right-skewed frequency distribution.

A mixed statistical model was used with the fixed effects tillage depth, catch crop cultivation and tillage depth * catch crop cultivation. The plots sampled and measurement values within the plots in the respective year of the study were included in the model as random effects and repeated measures. An independent analysis was performed for each location and year. Significance levels with a probability of error $p < 0.05$ have been marked with different letters.

4.1.3. Results

4.1.3.1. Catch crop yield

The above-ground catch crop plant biomass varied at the individual sites between 2.33 t and 7.88 t dry matter (DM) ha^{-1} (Table 4.1.3). Root biomass, which ranged between 0.60 and 1.56 t DM ha^{-1} , was far lower at the sites Rothenberga II than at Rothenberga I.

Table 4.1.3. Above-ground biomass (DM) and root dry mass (0-25 cm) of the catch crops measured at the end of vegetation; different lower-case letters indicate significant differences between the tillage depths ($p < 0.05$).

Site	Above-ground biomass (DM) (t ha^{-1})		Root dry mass (t ha^{-1})	
	Tillage depth	Tillage depth	Tillage depth	Tillage depth
	25-30 cm	8-10 cm	25-30 cm	8-10 cm
Andisleben I	3.66 a	3.52 a	-	-
Andisleben II	3.73 a	3.06 a	-	-
Rothenberga I	7.88 a	6.65 a	1.56 a	1.46 a
Rothenberga II	2.58 a	2.33 a	0.60 a	0.62 a

Calculation of the weight proportions of the constituent crops in the seed mixture at the sites Andisleben I and II as well as Rothenberga II showed that field beans accounted for 40-55 %, field peas 45-55 % and vetch just 2-7 % of dry mass. The latter was thus almost completely suppressed by the other two constituents of the seed mixture. There was no evidence of any differences between tillage depths with regard to mixture composition.

4.1.3.2. Air capacity and saturated hydraulic conductivity

At none of the experimental sites was there any interaction between tillage and catch crop cultivation for the parameters air capacity and saturated hydraulic conductivity. Therefore it was

possible to consider the average effects of tillage across the catch crop treatments, and the average effect of catch crop cultivation across tillage treatments (Table 4.1.4). Catch crop cultivation only significantly affected the physical soil properties at a depth of 16-22 cm at Rothenberga II. Air capacity was lower here with catch crop cultivation than without. When comparing deep tillage to shallow tillage, the former had a significantly positive impact on air capacity and saturated hydraulic conductivity at depths of 6-12 cm and 16-22 cm at the site Andisleben II, and on saturated hydraulic conductivity at a depth of 16-22 cm at Andisleben I. At Rothenberga II, though, at a depth of 16-22 cm the deeper tillage did result in significantly lower air capacity and lower saturated hydraulic conductivity.

The lowest air capacity levels were identified for the Bergzow site (Table 4.1.4). These did not fulfil the minimum requirements for an intact soil structure in the topsoil of 8 % by volume. Air capacity levels were also mostly below the critical value in the shallow tillage treatment at the Andisleben I site and at a depth of 16-22 cm in the shallow tillage treatment at Andisleben II. At a depth of 6-12 cm, air capacity values at Andisleben II were considerably higher at 10 % by volume. Higher values could be seen for deep tillage at Andisleben II. Air capacity was highest at the sites Rothenberga I and Rothenberga II at a depth of 6-12 cm. The saturated hydraulic conductivity values basically displayed analogies to those for air capacity, in such a way that the lowest values were measured at the Bergzow site. With the exception of 6-12 cm depth in the treatment with deep tillage, at the site Andisleben I the saturated hydraulic conductivity levels were also all in the critical region $<10 \text{ cm d}^{-1}$. At Andisleben II, however, only the depth 16-22 cm in the shallow tillage treatment was characterised by such low values. At all other sites and depths, saturated hydraulic conductivity levels were higher than 10 cm d^{-1} , sometimes considerably so.

Taking all sites and depths into consideration, cultivating catch crops in the treatments where soil had been loosened deeply led to an overall decline in air capacity (median -3.0 % by volume; range -5.2 to +2.8 % by volume) (Fig. 4.1.2A). This decrease in air capacity with catch crop cultivation was less pronounced in the treatments where loosening was more shallow (median -0.8 % by volume; range -3.4 to +2.6 % by volume). There was however no negative impact of catch crop cultivation on the median saturated hydraulic conductivity (Fig. 4.1.2B). Ultimately, positive and negative values cancelled each other out here. By contrast, if one considers all sites and depths then deeper tillage – both with and without catch crop cultivation – had a positive impact on air capacity and saturated hydraulic conductivity (Fig. 4.1.3A and 4.1.3B). In the case of deep tillage with catch crop cultivation, the median air capacity was around 2.5 % by volume (range -3.0 to +9.4 % by volume) higher than for shallow tillage, and the median saturated hydraulic capacity approximately 13.8 cm d^{-1} (range -42.8 to +63.1 cm d^{-1}) higher. Without catch crop cultivation the positive effect of tillage was actually slightly greater (median +3.2 % by volume air capacity and 30.0 cm d^{-1} saturated hydraulic capacity).

Table 4.1.4. Air capacity and saturated hydraulic conductivity in the topsoil measured in the spring at different tillage depths and probability values from F-test of the fixed effects tillage and catch crop (no interaction was observed between tillage and catch crop); numbers in bold indicate significant p-values ($p < 0.05$); ¹ No tillage was performed at the Bergzow site before seeding the catch crop.

Site	Depth (cm)	Air capacity (vol.%)						Saturated hydraulic conductivity (cm d ⁻¹)					
		Tillage depth treatment			Catch crop treatment			Tillage depth treatment			Catch crop treatment		
		8-10 cm	25-30 cm	p-value	With	Without	p-value	8-10 cm	25-30 cm	p-value	With	Without	p-value
Bergzow	6-12	- ¹	- ¹	- ¹	4.0	2.8	0.26	- ¹	- ¹	- ¹	2.0	1.9	0.89
	16-22	- ¹	- ¹	- ¹	3.4	4.2	0.53	- ¹	- ¹	- ¹	3.2	5.7	0.40
Andisleben I	6-12	7.3	11.1	0.06	9.7	8.7	0.60	6.4	10.7	0.47	8.2	7.5	0.78
	16-22	6.9	7.5	0.77	8.5	5.9	0.09	2.5	6.0	0.04	4.4	3.5	0.51
Andisleben II	6-12	10.0	16.6	0.03	11.9	14.7	0.24	28.2	155.9	0.01	46.0	95.5	0.19
	16-22	5.0	14.5	<0.01	8.9	10.6	0.43	6.5	76.2	<0.01	20.9	23.5	0.83
Rothenberga I	6-12	19.4	20.0	0.57	19.1	20.3	0.23	123.2	136.1	0.61	130.3	128.6	0.94
	16-22	9.2	13.8	0.06	9.7	13.3	0.11	46.6	121.6	0.06	64.6	87.7	0.42
Rothenberga II	6-12	19.3	20.6	0.36	18.6	21.4	0.06	67.3	95.7	0.27	88.0	73.2	0.55
	16-22	15.0	12.1	0.01	12.2	14.8	0.02	81.8	38.0	0.05	59.4	52.4	0.72

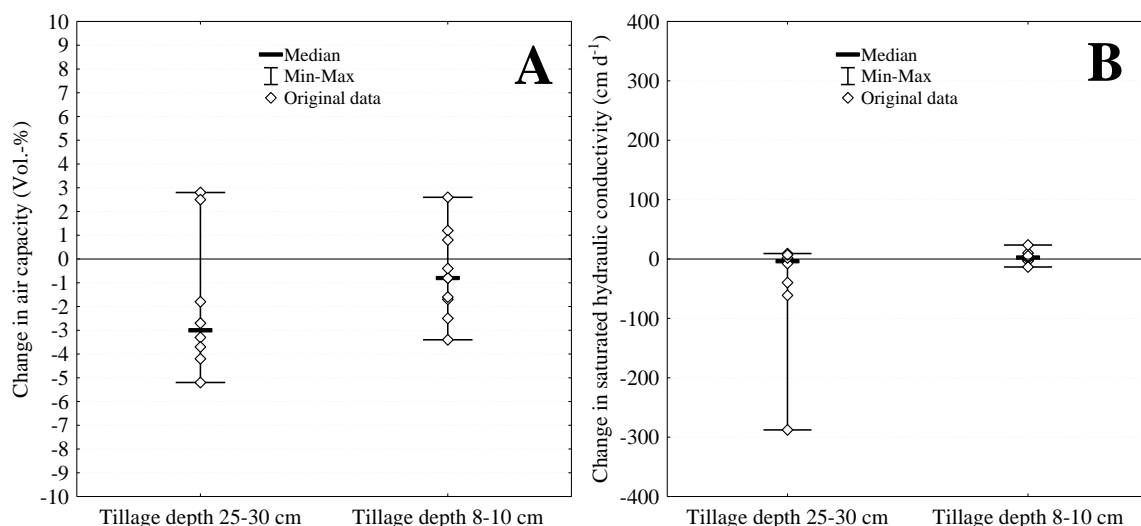


Figure 4.1.2. Change in air capacity (A) and in saturated hydraulic conductivity (B) across all sites and tested depths in the treatment with catch crop compared to the treatment without catch crop at different tillage depths.

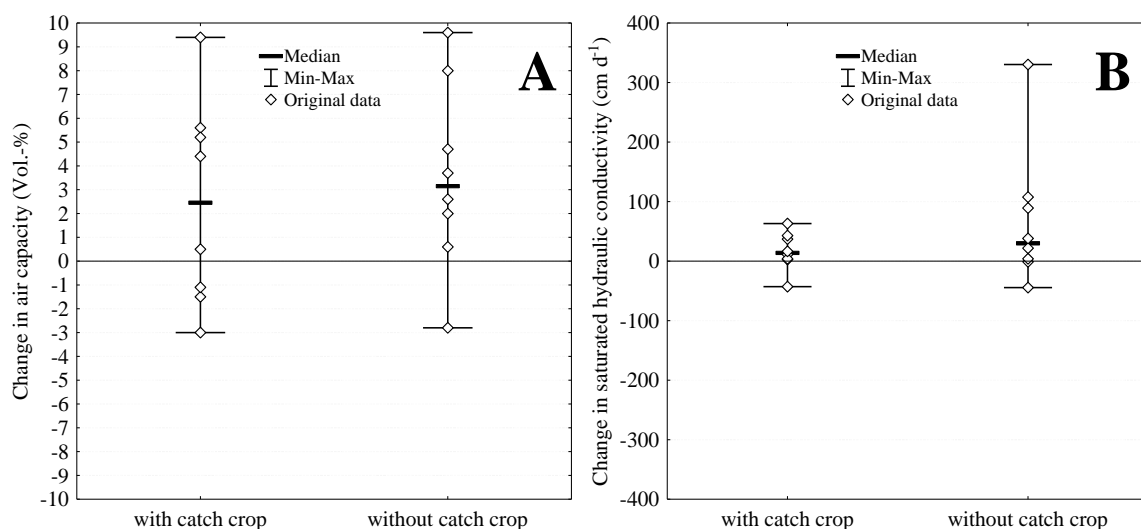


Figure 4.1.3. Change in air capacity (A) and in saturated hydraulic conductivity (B) across all sites and tested depths in the treatment with 25-30 cm tillage depth compared to the treatment with 8-10 cm tillage depth for the treatments with and without catch crop.

4.1.3.3. Precompression stress

The precompression stress values were very low in all of the trials, especially at the Rothenberga I site (Table 4.1.5). Only at the experimental site Andisleben II was there an interaction between tillage and catch crop cultivation for the parameter precompression stress. Deep tillage with catch crop cultivation was associated with significantly higher precompression stress. However, dry bulk density was also higher. This was in turn related to the air capacity and saturated hydraulic conductivity values at the Andisleben II site. Furthermore, there were no

effects of catch crop cultivation on precompression stress. At Andisleben II, deep tillage without catch crop cultivation resulted in a reduction in precompression stress. On the other hand, at Rothenberga I and II the depth of soil tillage did not have any impact on precompression stress.

Table 4.1.5. Logarithm precompression stress ($\text{Log } \sigma_P$) (kPa values in brackets) and dry bulk density (BD) in the topsoil (9-12 cm) measured in the spring at different tillage depths and for different treatments with and without catch crop cultivation; different lower-case letters indicate significant differences between the catch crop treatments at the same tillage depths, and capital letters indicate significant differences between tillage depth treatments for the same catch crop treatment ($p < 0.05$).

Site	Soil physical parameter	Tillage depth 25-30 cm		Tillage depth 8-10 cm	
		With catch crop	Without catch crop	With catch crop	Without catch crop
Andisleben II	$\text{Log } \sigma_P$	1.35 (22) aA	1.00 (10) bA	1.40 (25) aA	1.46 (29) aB
	BD	1.16 aA	1.07 aA	1.27 aA	1.24 aB
Rothenberga I	$\text{Log } \sigma_P$	0.83 (7) aA	0.78 (6) aA	0.84 (7) aA	0.78 (6) aA
	BD	1.13 aA	1.13 aA	1.16 aA	1.11 aA
Rothenberga II	$\text{Log } \sigma_P$	1.06 (12) aA	0.98 (10) aA	0.92 (8) aA	1.00 (10) aA
	BD	1.11 aA	1.11 aA	1.13 aA	1.16 aA

4.1.3.4. Soil Compaction Index

Because of the different soil strengths assumed in the *REPRO* model, the calculated Soil Compaction Indices were far higher overall for deep tillage than for shallow tillage (Table 4.1.6).

Table 4.1.6. Soil Compaction Indices calculated at 20 cm depth for the different tillage and catch crop treatments.

Site	With catch crop		Without catch crop	
	Tillage depth 25-30 cm	Tillage depth 8-10 cm	Tillage depth 25-30 cm	Tillage depth 8-10 cm
Andisleben I	0.36	0.09	0.29	0.08
Andisleben II	0.36	0.07	0.28	0.07
Rothenberga I	0.27	0.03	0.16	0.02
Rothenberga II	0.26	0.03	0.16	0.02

With deep tillage and catch cropping, the calculated Soil Compaction Indices were considerably higher at all four experimental sites than deep tillage without catch cropping. In the case of

shallow tillage with catch cropping, the calculated Soil Compaction Indices were only marginally higher than shallow tillage without catch crops.

4.1.4. Discussion

4.1.4.1. Catch crop yield

The dry mass growth of the catch crops varied considerably between the individual trial locations and years. As seen at Rothenberga I, if catch crops were sown early and there was sufficient precipitation to allow rapid sprouting, then comparatively high dry mass levels could accumulate. By contrast, late seeding and dry conditions at the Rothenberga II site led to comparatively low dry mass yields. Rinnofner et al. (2008) also describe very high fluctuations in dry mass of catch crop growth depending on moisture conditions. In their experiment with a leguminous catch crop (mixture of field pea, common vetch and chickling vetch) under moderately dry conditions, they identified around 2.6 t DM ha⁻¹ of above-ground biomass and 0.9 t DM ha⁻¹ of below-ground biomass, levels which are similar to those in the trials presented here. The below-ground biomass values identified at Rothenberga I and Rothenberga II were fairly consistent with the values indicated by Klimanek (1997).

4.1.4.2. Air capacity, saturated hydraulic conductivity and Soil Compaction Index

According to Angers and Caron (1998), plants can have a positive influence on soil structure by means of various mechanisms, e.g. when plant roots form macropores which improve the root penetration of subsequent crops and also transport water. However, such structural change can take several years, which is why it is particularly common when perennial fodder crops are cultivated (Meek et al., 1989; Kautz et al., 2010; Uteau et al., 2013).

Past studies have shown highly differentiated impacts on soil structure when cultivating cover crops with a vegetation period of around 8 months, primarily in the uppermost layer in the topsoil (0-10 cm) (Wilson et al., 1982). For example, there have been reports on a reduction in soil strength measured using a penetrometer (Folorunso et al., 1992; Raper et al., 2000) as well as trends towards slightly reduced dry bulk densities (Breland, 1995). On the other hand, Carof et al. (2007) found no major differences in the effect of three cover crops on hydraulic conductivity and porosity. However, larger functional pores and more tubules were identified when cover crops were grown using direct sowing. In terms of catch cropping with oil radish (*Raphanus sativus* var. *Oleiformis*), only Glab and Kulig (2008) describe a decline in dry bulk density and an increase in the number of macropores at a soil depth of 0-10 cm when combined with reduced tillage.

The vegetation period of the leguminous catch crops is only around 2-3 months, which is considerably shorter than when growing the same species as main crops and shorter than for cover crops. In addition, unlike when growing main crops, catch crop cultivation is followed immediately by winter and a cessation of biological activity. In this study, these general conditions

may have restricted a demonstrably positive effect of the leguminous catch crops on soil structure. In contrast to the investigations by Stirzaker and White (1995), there is therefore certainly no way that compacted soil layers – like those at the Bergzow site – could stand any chance of amelioration by using leguminous catch crops. Although the dead roots of catch crop plants are able to create continuous macropores, the actual gain in macropores is still rather low. If it is assumed that the fresh root biomass recorded for the catch crops in late autumn at the trial locations Rothenberga I and II only left behind macropores $>50\ \mu\text{m}$ after degradation by microorganisms, then air capacity in the topsoil would have only increased by 0.2-0.5 % by volume. For this calculation we assumed that the dry matter content in the fresh root biomass was 12 % and the density of the fresh root biomass was $1.0\ \text{g cm}^{-3}$, and also a topsoil depth of 25 cm. However, cold winter conditions mean that it is unlikely that all roots would have been broken down by the spring when samples were taken. This is one reason why it can hardly be expected that the roots make a direct, measurable contribution to improving air capacity. In fact it is more likely that the dead roots result in continuous pores, which have a higher saturated hydraulic conductivity. This is at least supported by the fact that, at all sites and depths, similarly high saturated hydraulic conductivities were identified with catch crop cultivation than without, although air capacity was lower overall with catch crop cultivation. Furthermore, the catch crops' short vegetation period mostly does not allow a stronger drying of the soil compared to the bare fallow in Central Germany (Böttcher et al., 2014). According to Dexter (1998) such wetting and drying cycles can contribute significantly to structural formation.

The cultivation of catch crops and the improved food source this creates would presumably result in an increase in the earthworm population (Curry and Schmidt, 2007), although this was not explicitly investigated in this study. Dry conditions like those seen in the autumn at the sites Rothenberga I and Rothenberga II for example, can inhibit earthworm activity (Whalen et al., 1998). It is therefore unlikely that any improvement in soil structure would be caused by earthworm activity.

In contrast to the potential positive effects the plants have directly or indirectly on soil structure, growing crops implies driving, more or less regularly, over the soil with agricultural machinery (Kroulik et al., 2012). This necessity was taken into account in this study, by establishing the trials in large, realistic plots, recording information on individual working steps and calculating the Soil Compaction Index using the *REPRO* model. As a rule, cultivating catch crops requires additional working steps. Compared with the plots without catch crop cultivation, catch cropping involved one or two additional working steps for sowing and for shredding the catch crop plant growth. The latter was usually necessary to facilitate main crop seeding. Depending on the tyres used, the inflation pressure, wheel load and how much of the ground is driven over, using such agricultural machinery can lead to the deterioration of soil structure (Schäfer-Landefeld et al., 2004; Rücknagel et al., 2012b; Berisso et al., 2013). High soil water content levels, which were present at the trial sites when the catch crops were tilled and mulched in the winter or early spring, also promote soil compaction (Rücknagel et al., 2015). This can be understood by means of the Soil Compaction Indices calculated with the *REPRO* model; with catch crops

SCI was considerably higher for deep tillage and slightly higher for shallow tillage when compared to the treatments without catch cropping. However, in the experiments presented here no direct measurements of soil physical parameters were taken for single passes or in zones which were not driven over.

Ultimately, the expected overall effect in the cropping system of catch crop cultivation on soil structure depends on which is more influential: the effects of the plants, or the mechanical stress caused by driving over the soil. In the trials presented here, where soil structure was investigated shortly after the main crops were sown, the SCI calculation using the *REPRO* model suggests that the impacts of mechanical soil stresses seem to outweigh the benefits in the case of catch crop cultivation. The fact that sampling occurred when it did means that any longer-term effects on soil structure were not taken into account. It should also be noted that crop rotation practices in Central Europe mean that catch crop cultivation can usually only take place every three to five years. In the case of large-grain legumes, the time interval before the next round of cultivation should be long where possible, in order to minimise the occurrence of crop rotation pathogens. This makes long-term or even cumulative effects of cultivating leguminous catch crops on soil structure rather unlikely.

Compared with the effect of catch crops, the higher depth of tillage often had a positive influence on air capacity and saturated hydraulic conductivity in the trials presented. Carof et al. (2007) also draw similar conclusions; in their investigations, more intensive conventional tillage led to higher hydraulic conductivities when compared with no tillage. The effect of soil tillage on hydraulic conductivity was always greater than the impact of the cover crop.

4.1.4.3. Precompression stress

Higher precompression stress levels with an intact pore system allow higher resistance to mechanical soil stresses. For example, under a low stress of 40 kPa Trükmann (2011) found that plant roots on grassland had the effect of stabilising the soil against mechanical stresses. In the study presented here, the oedometer tests began with a stress of 5 kPa, and all precompression stress values were lower than 40 kPa. Even so, an increase in precompression stress was only seen in the case of catch crop cultivation with deep tillage at the Andisleben II site. But this in turn was associated with increased dry bulk density, and as such was probably not due to the impact of catch crop plants and their roots. The increase in dry bulk density resulted in stronger support between aggregates, and thus also an increase in precompression stress (Rücknagel et al., 2013a). The formation of a similarly extensive and stabilising root system to those seen on grassland does not occur in the case of catch crop cultivation. At 3-12 t DM ha⁻¹ (Klimanek, 1997), below-ground biomass of perennial grasses in the topsoil is considerably higher than the catch crop root masses found here.

Lafond et al. (1992) identified higher precompression stress levels below various crop types when compared with fallow land. These were however due to the sometimes significantly higher water contents on fallow land, and not the presence of plant roots. In the study presented

here, the oedometer tests were carried out at a matric potential of -6 kPa for all treatments, meaning an increase in precompression stress as water content decreases (Rücknagel et al., 2012a) can be ruled out.

4.1.5. Conclusions

In the trials presented, the positive tendencies of the catch crop plants for soil structure were mostly counteracted by the negative tendencies of mechanical soil stresses caused when cultivating them. Catch crop cultivation did not improve mechanical stability either. If growing catch crops with large-grain legumes is supposed to have a positive impact on soil structure, it is therefore important that cultivation does not cause any new soil compaction. This means it is important to sow catch crops under dry conditions and, if possible, without any additional working steps, for example in combination with soil tillage. It would be best to avoid shredding catch crop plant growth in an additional working step, and the subsequent seeding of the main crop should in turn be performed on well-dried soil in one combined working step incorporating both seedbed preparation and sowing. The leguminous catch crops in the trials presented, however, hardly contribute in the short term to loosening compacted topsoils for the subsequent main crop. Tillage is more effective here; its effect on soil loosening became more clearly visible in this study, independent of catch cropping.

Acknowledgement

The authors wish to thank the farms S & W Agrar GmbH Bergzow and Geratal Agrar GmbH & Co. KG Andisleben for providing the land and performing the catch crop trials in accordance with customary operating procedures, and M. Schmidt of the German Meteorological Service (DWD) for providing precipitation data.

4.2. Impact on soil compaction of driving agricultural machinery over ground frozen near the surface

Published in: *Cold Regions Science and Technology* 70 (2012), 113-116

Jan Rücknagel¹, Sandra Rücknagel¹, Olaf Christen¹

¹Institute of Agricultural and Nutritional Sciences, Department Agronomy and Organic Farming, University of Halle-Wittenberg, Betty-Heimann-Str. 5, 06120 Halle/Saale (Germany)

Abstract

The compaction of arable soils caused by driving over them with agricultural machinery poses a serious problem in numerous agricultural regions across temperate climate zones. The risk of compaction is particularly high in early spring or late autumn when soils are wet. This is why driving over soils frozen near the surface is recommended in some cases in temperate climate zones to prevent soil compaction. However, no findings have been available about the thickness of frozen soil required to effectively prevent compaction when the soil is driven over. In one experiment, soil physical measurements were carried out on the topsoil after a single pass with a tractor (4100 kg wheel load, 80 kPa inflation pressure) over an unfrozen variant, a variant with 2-3 cm frost covering and a variant with 5-7 cm frost covering, with comparisons made with a control variant that had not been driven over. Driving over the unfrozen variant led to a significant compaction of the whole of the topsoil. By contrast, the frozen surfaces were able to significantly buffer the compaction. No appreciable differences were detected between the two depths of frost penetration. A depth of frost penetration of as little as 2-3 cm was therefore sufficient to reduce the risk of compaction with a wheel load of approximately 4000 kg and appropriately adjusted inflation pressure.

4.2.1. Introduction

Compaction of arable soils caused by agricultural machinery is a significant problem on arable land subject to intensive cultivation, particularly in the temperate climate area of Central and Eastern Europe (e.g. Fulajtár, 2000). Compaction severely restricts a number of important ecological soil functions. Air capacity decreases and gas exchange is restricted (Ball and Robertson, 1994; Horn and Rostek, 2000). Another likely consequence of soil compaction and the establishment of platy and coherent soil structure is reduced water infiltration with water runoff and erosion (Horn et al., 1995). In some cases even yield decrease has been observed (Voorhees, 2000). In early spring and late autumn, the water content of arable soils is in most cases near the field capacity and there is therefore a high risk of compaction if driven over (Arvidsson et al., 2003). In addition to numerous preventive measures, such as reducing the wheel load and internal tyre pressure or using specialised chassis, a recommended practice in Central European

agriculture involves driving over soil which is frozen near the surface. This option is available for several agronomical measures, such as the timely spreading of mineral fertiliser early on in the year or the tillage of unused arable land during the winter, particularly in agricultural areas of Central Europe's temperate climate zone. During years with particularly wet spells of autumn weather, part of the grain maize harvest also occurs on ground which is slightly frozen, in order to guarantee the ability to drive over it. All of the measures named here make use of weather situations where a light frost (usually >-2 °C) occurs at night and by day temperatures above freezing (usually >5 °C). Hence this does not concern prolonged periods of frost, rather solely ground frozen near the surface for only a few hours. From an agricultural point of view this is necessary to ensure, for example, the solubility of mineral fertilisers in the soil, which by day is not frozen.

It is already known from other scientific disciplines that the strength of frozen soils overall can be very high (Yang et al., 2010), up to the point where crushing occurs. There are, however, no findings concerning the depth of frost penetration required to effectively prevent compaction when the soil is driven over by agricultural machines. The results of a field trial carried out in March 2010 to answer this question are set out below.

4.2.2. Materials and methods

The test site was located in Central Germany on the north-eastern edge of the federal state of Thuringia. The soil type (FAO soil classification) was an Albic Luvisol of the soil textural class silt loam (90 g kg⁻¹ sand, 130 g kg⁻¹ clay) and located in the topsoil. The organic carbon content in the topsoil was equal to 12 g kg⁻¹. The soil water contents in the topsoil at the time of the test were 0.31-0.33 m³/m³. This corresponds to ~95 % of soil field capacity. In autumn 2009 before the tests were carried out, a cultivator was used to prepare the entire test area at a depth of 25 cm. At the time of the experiment, there were still no cultivated plants growing on the test area. The precompression stress (Rücknagel et al., 2007; Rücknagel et al., 2010) of the loosened soil at a depth of 20 cm was 21 kPa (logarithm 1.32).

A tractor with a seedbed combination with drill served as a test device. Each variant was driven over once with the tractor. The wheel load of the rear wheels (tyre size 680/75 R 32) was 4100 kg with an inflation pressure of 80 kPa. Apart from the control (1) that was not driven over, the test variants comprised a variant with no frost (2), a variant with 2-3 cm depth of frost penetration (3) and a variant with 5-7 cm depth of frost penetration (4). The frost depths were determined by breaking open the frozen layers for each variation at various points and then measuring the respective strength (Picture 4.2.1). Each variant was replicated four times. The variant with no frost was created by covering the tracts of land to be tested with a fleece cover on the evening before the frost (lowest temperature on the day of the test -5 °C at 7.00 am). The variant with a depth of frost penetration of 2-3 cm was created by removing the fleece cover during the night, while the variant with a depth of frost penetration of 5-7 cm soil was created by leaving the soil uncovered. Dry bulk density, air capacity and saturated hydraulic conductivity were

determined from soil cores (n=12) taken at depths 7-13 cm and 17-23 cm following the single pass (Picture 4.2.2).



Picture 4.2.1. Determinations of the frost depths by breaking open the frozen layers for each variation at various points and measuring the respective strength.



Picture 4.2.2. The physical soil parameters were determined using soil core samplers.

The dry bulk density corresponds to the quotient of the dry mass of a naturally deposited soil sample and its total volume (unit g cm^{-3}). It is a measure of the state of soil compaction. The air capacity is equivalent to soil air content as a volume fraction at field capacity (-6 kPa matric potential). It is an important factor in soil ecology, and in German-speaking countries it covers pores with an equivalent diameter of $>50 \mu\text{m}$, in which water moves in accordance with gravity (unit vol.%). Determination occurs in a sandbox (German laboratory standard DIN ISO 11274). Saturated hydraulic conductivity is the parameter of Darcy's law applied to saturated water movement within the soil as a measure of the hydraulic permeability of water-saturated soil (unit cm/d). Apart from size and shape, soil permeability for water is influenced heavily by pore continuity. Determination takes place in a stationary facility according to the principle described by Klute and Dirksen (1986).

The vertical principal stress at 20 cm depth of soil for the passing over of the unfrozen variant was calculated at the same time using the *REPRO* model (Rücknagel and Christen, 2009). The calculation of the vertical principal stress σ_z (unit kPa) using wheel load (P, unit kg) and inflation pressure (q, unit kPa) at a soil depth z (unit cm) is based on Koolen et al. (1992):

$$\sigma_z = 2 * q * (1 - \cos^k (\arctan ((1/z) * (P/(\pi * 2 * q/100))^{1/2}))) \quad (4.2.-1)$$

The concentration factor (k, no unit) in formula (4.2.-1) was calculated with a linear regression model with logarithm of precompression stress ($\log \sigma_p$, Logarithm of unit kPa) and water content in percent of field capacity (FC):

$$k = -2.0 * \log \sigma_p + 0.03 * FC + 3.2 \quad (4.2.-2)$$

Furthermore, the depth of the rut driven in was identified for the individual variants. In addition, the depth of tyre sinkage across the tyre width was measured at intervals of 5 cm and using a level staff with 4 replications per variant. The control variant that was not driven over was also included as a reference level, in order to rule out any natural unevenness in the ground.

The statistical analysis of the data was carried out with an ANOVA and a subsequent comparison of mean values (Tukey-Test). Significances with an error probability of $p < 0.05$ are shown in different lower case letters. The variation coefficient (s%) was also calculated for the depth of tyre sinkage. In addition to this, the standard deviation (s) and the mean value ($\bar{\phi}$) of the respective tyre sinkage is needed:

$$s\% = s/\bar{\phi} * 100 \quad (4.2.-3)$$

High coefficients indicate an increasing variability of the characteristic recorded. The standard deviation is calculated here from the sum of squares (SQ) and the number of all replicated measurements (n) using the equation:

$$s = \sqrt{(SQ/(n-1))} \quad (4.2.-4)$$

4.2.3. Results and discussion

A low depth of tyre sinkage is primarily to be regarded as a horticultural quality criterion. It also provides initial indications of changes in the soil structure. The mean tyre sinkages amounted to 3.2 cm (no frost), 1.4 cm (depth of frost penetration 2-3 cm) and 1.1 cm (depth of frost penetration 5-7 cm), (Fig. 4.2.1). However, the different depths of frost penetrations do not differ significantly from each other. The tyre sinkage was distributed increasingly unevenly over the track width with a decreasing depth of frost penetration, especially in the variant without frost. This can also be seen in the variation coefficients calculated amounting to 51% (no frost), 49% (depth of frost penetration 2-3 cm) and 43% (depth of frost penetration 5-7 cm). The reason for this is the sinking of the lugs which characterised the appearance of the track especially in the variant with no frost. In a light frost the lug impressions were clearly less pronounced and at a depth of frost penetration of 5-7 cm the tyre sinkage was relatively evenly distributed over the width of the track. In the latter case the sinking of the wheel was associated with a fracture of the entire frozen surface, with the load being transmitted via the spaces between the lugs. There are analogies here with the fracture of strong plough pans in the subsoil where the strength of the plough pans is exceeded (Peth et al., 2006).

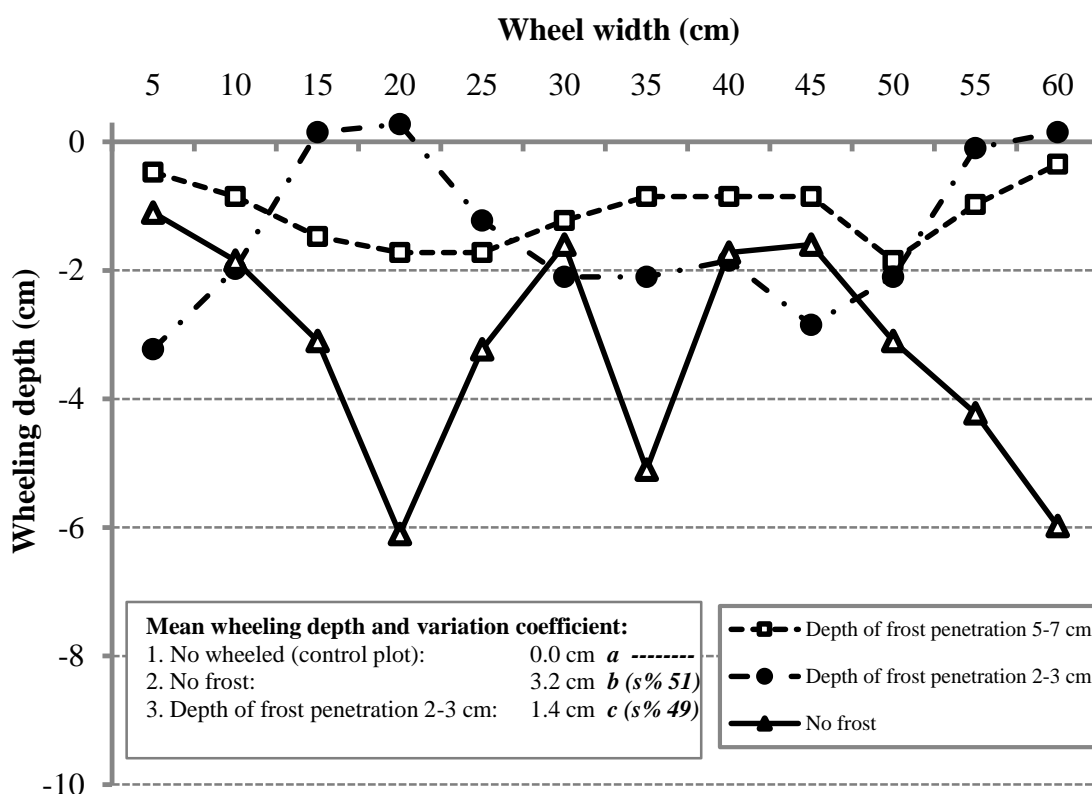


Figure 4.2.1. Tyre sinkage over the tyre width in the experimental variants.

Because of the intensive tillage in the autumn before the test was carried out, the soil structure before being passed over was very porous with high air capacities and a very high saturated

hydraulic conductivity (Table 4.2.1). Driving over the soil that was not frozen led to a significant compaction of the entire topsoil which was reflected in the increase in dry bulk density and conversely in the decrease of air capacity and saturated hydraulic conductivity. This is also to be expected with the vertical principal stress of 135 kPa, calculated for a depth of 20 cm, which is present when driving over the unfrozen variant. The height of the ground pressure calculated here corresponds approximately to Arvidsson and Keller's (2007) measurement results for similar agricultural technology (70 kPa inflation pressure, 3300 kg wheel load) and water content equivalent to field capacity on clay soil at 30 cm depth. Overall, ground pressure exceeds pre-compression stress in the experiment presented here by a factor of approximately 6. In some cases, Keller and Lamandé (2010) observe lasting consolidation at ground pressure levels which correspond to precompression stress. In their investigations, precompression stress was exceeded by factor 3 at most. Very pronounced soil consolidation was recorded here.

Table 4.2.1. Dry bulk density, air capacity and saturated hydraulic conductivity of the experimental variants; different small letters indicates significant differences between the experimental variants ($p < 0.05$).

	Experimental variant			
	No wheeled (control plot)	No frost	Depth of frost penetration 2-3 cm	Depth of frost penetration 5-7 cm
Depth 7-13 cm				
Dry bulk density (g cm ⁻³)	1.13 a	1.32 b	1.26 c	1.25 c
Air capacity (vol.%)	22.1 a	8.1 b	13.1 c	14.8 c
Saturated hydraulic conductivity (cm/d)	322 a	4 b	36 c	91 ac
Depth 17-23 cm				
Dry bulk density (g cm ⁻³)	1.26 a	1.39 b	1.34 c	1.32 c
Air capacity (vol.%)	17.5 a	10.0 b	13.8 c	13.4 c
Saturated hydraulic conductivity (cm/d)	143 a	11 b	104 a	63 a

At a depth of 7-13 cm the minimum requirements of an intact soil structure required by Lebert et al. (2004) and Paul (2004) (8.0 vol.% air capacity and 10 cm/d saturated hydraulic conductivity) were not met in some cases. While the frozen variants were able to significantly buffer

the compressive stress when passed over, they could not completely prevent changes in soil structure. At both depths, however, the minimum requirements of a functional soil structure were definitely maintained. No appreciable differences were detected between the depths of frost penetrations. A depth of frost penetration of as little as 2-3 cm is therefore sufficient to reduce the risk of compaction with a wheel load of 4000 kg and appropriately adjusted inflation pressure (80 kPa).

In agricultural practice, tractors and other agricultural machines with high wheel loads and internal tyre pressure are often employed (see for example Schäfer-Landefeld et al., 2004). However, it remains doubtful whether ground frozen near the surface can also buffer the ground pressures which occur when subject to such machinery, which sometimes amount to 400 kPa at a depth of 30 cm (Trautner and Arvidsson, 2003).

The low depths of frost penetration of no more than 7 cm also ensure favourable conditions for shallow soil tillage. A greater depth of frost penetration would presumably increase the necessary tractive force and decrease the quality of work.

Appendix A 4.2.1. Abbreviations and symbols in the equations and their descriptions.

Abbreviation or symbol	Parameter description	Unit
FC	water content in percent of field capacity	%
k	concentration factor	-
$\log \sigma_p$	logarithm of precompression stress (logarithm of kPa values)	-
n	number of all replicated measurements	-
P	wheel load	kg
q	inflation pressure	kPa
s	standard deviation	-
SQ	sum of squares	-
s%	variation coefficient	-
z	soil depth	cm
$\bar{\sigma}$	mean value	-
σ_z	major principal stress	kPa

4.3. Environmental impacts of different crop rotations in terms of soil compaction

Published in: Journal of Environmental Management 181 (2016), 54-63

Philipp Götze^{1,2}, Jan Rücknagel¹, Anna Jacobs², Bernward Märländer², Heinz-Josef Koch², Olaf Christen¹

¹Institute of Agricultural and Nutritional Sciences, Department Agronomy and Organic Farming, University of Halle-Wittenberg, Betty-Heimann-Str. 5, 06120 Halle/Saale (Germany)

²Institute of Sugar Beet Research, Holtenser Landstrasse 77, 37079 Göttingen (Germany)

Abstract

Avoiding soil compaction caused by agricultural management is a key aim of sustainable land management, and the soil compaction risk should be considered when assessing the environmental impacts of land use systems. Therefore this project compares different crop rotations in terms of soil structure and the soil compaction risk. It is based on a field trial in Germany, in which the crop rotations (i) silage maize (SM) monoculture, (ii) catch crop mustard (Mu)_sugar beet (SB)-winter wheat (WW)-WW, (iii) Mu_SM-WW-WW and (iv) SB-WW-Mu_SM are established since 2010. Based on the cultivation dates, the operation specific soil compaction risks and the soil compaction risk of the entire crop rotations are modelled at two soil depths (20 and 35 cm). To this end, based on assumptions of the equipment currently used in practice by a model farm, two scenarios are modelled (100 and 50 % hopper load for SB and WW harvest). In addition, after one complete rotation, in 2013 and in 2014, the physical soil parameters saturated hydraulic conductivity (k_s) and air capacity (AC) were determined at soil depths 2-8, 12-18, 22-28 and 32-38 cm in order to quantify the soil structure. At both soil depths, the modelled soil compaction risks for the crop rotations including SB (Mu_SB-WW-WW, SB-WW-Mu_SM) are higher (20 cm: medium to very high risks; 35 cm: no to medium risks) than for those without SB (SM monoculture, Mu_SM-WW-WW; 20 cm: medium risks; 35 cm: no to low risks). This increased soil compaction risk is largely influenced by the SB harvest in years where soil water content is high. Halving the hopper load and adjusting the tyre inflation pressure reduces the soil compaction risk for the crop rotation as a whole. Under these conditions, there are no to low soil compaction risks for all variants in the subsoil (soil depth 35 cm). Soil structure is mainly influenced in the topsoil (2-8 cm) related to the cultivation of Mu as a catch crop and WW as a preceding crop. Concerning k_s , Mu_SB-WW-WW (240 cm d⁻¹) and Mu_SM-WW-WW (196 cm d⁻¹) displayed significantly higher values than the SM monoculture (67 cm d⁻¹), indicating better structural stability and infiltration capacity. At other soil depths, and for the parameter AC, there are no systematic differences in soil structure between the variants. Under the circumstances described, all crop rotations investigated are not associated with environmental impacts caused by soil compaction.

4.3.1. Introduction

Indicator based assessments of the environmental impact of land use systems often do not include their influence on soil structure and the soil compaction risk (Castoldi and Bechini, 2010; Gaudino et al., 2014; Paracchini et al., 2015). However, soil structure is an important criterion of soil fertility (Mueller et al., 2010) since it determines the water and air balance as well as the rootability (Hartge, 1994) and the habitat quality for soil organisms (Birkás et al., 2004). Accordingly, soil compaction has a negative impact on the essential soil functions, resulting in increased environmental impacts (Nawaz et al., 2013). Preserving a functional soil structure and avoiding soil compaction are therefore important aspects of sustainable agriculture. Preventive measures, from using adapted chassis and tyres which protect the soil right up to Controlled Traffic Farming (CTF), are preferable since they are less expensive than taking subsequent remedial action (Chamen et al., 2015). Another method of preventive soil protection is to consider the effect of crop species on the formation of soil structure – as well as the soil compaction risk associated with cultivating these species – when planning the crop rotation.

Cultivating a crop can influence the soil structure by a number of factors. Aspects of root morphology and physiology are often discussed in this context, as well as the impact of harvest residues (Bronick and Lal, 2005; Blanco-Canqui and Lal, 2009). However, the effect of the crop or of the crop rotation on soil structure is often masked by the tillage method (Malhi et al., 2008) or by different levels of mechanical stress when driving over the soil with agricultural machinery (Boizard et al., 2002; Capowiez et al., 2009). A positive influence on soil structure is attributed to legumes and perennial forage crops. Specifically, cultivating them can result in increased macroporosity and hydraulic conductivity (McCallum et al., 2004) as well as aggregate stability (Reid and Goss, 1981), while dry bulk density and penetration resistance can decrease (Chan and Heenan, 1996).

Cultivating crops for bioenergy use aims to reduce environmental impacts, especially greenhouse gas emissions. Therefore crop rotations including crops with the lowest energetic input-output ratio are advantageous. In terms of biogas production under the conditions in Central Europe, silage maize (SM, *Zea mays* L.) and sugar beet (SB, *Beta vulgaris* L.) are suitable due to their high methane yields (Amon et al., 2007; Weiland 2010, Brauer-Siebrecht et al., 2016). However, aspects concerning the impact on soil structure should be considered for the cultivation of crops for bioenergy use and only few results have been published on the impact of SB and SM on soil structure (Boizard et al., 2002; Deumelandt et al., 2010; Głąb et al., 2013; Jacobs et al., 2014). Therefore, this paper aims to identify the impacts of cultivating SB and SM in crop rotations with winter wheat (WW, *Triticum aestivum* L.) as well as of SM monoculture on soil structure. Due to the numerous factors which influence soil structure and the way they interact, it is expedient to integrate several methodological approaches to compare the soil structure related to different cultivation practices. To this end, physical soil parameters are recorded in a crop rotation experiment, in order to, first of all, present the crop-specific impact on soil structure under field trial conditions. Furthermore, model calculations are used to derive the

soil compaction risk associated with common cultivation methods used for the entire crop rotation. This is based on a model farm which is assumed to use modern, standard equipment and refers to the operations and respective dates performed during the field trial. The validity of the model used is tested by field investigations into physical soil parameters. Finally, the results of both methods are used to assess the environmental impacts by soil compaction for different crop rotations.

4.3.2. Materials and methods

4.3.2.1. Field site and experimental design

A crop rotation field trial set up in 2010 in Aiterhofen (Germany, Lower Bavaria, 48°85' N; 12°63' E) forms the basis of these investigations. In this field trial, soil samples were taken in order to identify physical soil parameters and the soil structure. The field trial's cultivation dates (driving dates) as well as site information serve to model the soil compaction risk.

The soil type is classified as a Luvisol (FAO, 2014), and the soil texture at a depth of 0-45 cm is that of a silt loam (205 g kg⁻¹ clay, 128 g kg⁻¹ sand). Long-term (1981-2010) average annual precipitation is 757 mm, and the mean annual temperature 8.6°C (Straubing station, DWD, 2014). The field trial tests four crop rotations, containing SB, SM and WW as well as mustard as a catch crop (Mu, *Sinapis alba* L.) (Table 4.3.1). The field trial has a block design with four replications, with each crop rotation field being sown every year on a separate plot. Every replication comprises 10 plots, each of them 420 m² in size.

Primary tillage is performed as conservation tillage in the autumn, using a cultivator at a soil depth of 18 cm (working width 3 m). For SM, seedbed preparation is performed using a rotary harrow (working width 3 m, working depth 10 cm) and for SB using a seedbed cultivator (working width 5.6 m, working depth ≤5 cm). For WW, seedbed preparation is performed using a rotary harrow (working width 3 m, working depth ≤10 cm) in combination with the seeder. For the spring crops SB and SM which follow WW, the catch crop Mu is sown in combination with primary tillage in August after WW harvest. Additionally, nitrogen fertilization is carried out using 40 kg N ha⁻¹ UAN (solution of urea and ammonium nitrate). Nitrogen fertilization for the main crops is performed using UAN depending on the amount identified as optimal for each particular year. Work performed at the field trial uses machinery typically employed in practice; special trial equipment is only used for sowing SB (three-row plot drill). SB are harvested using a six-row self-propelled SB harvester. The WW harvest is performed using a self-propelled combine harvester. A self-propelled forage harvester is used to harvest SM, with the harvested crop transferred onto a transport vehicle during operation.

4.3.2.2. Investigations into soil structure at the field trial Aiterhofen

After having completed the entire rotation on each plot, in May 2013, samples were taken from those plots with the first crop rotation field (Table 4.3.1) of all crop rotations. The sampling

was repeated in 2014 for the same crop rotation fields which were than cultivated on different plots, except the SM monoculture.

Table 4.3.1. Schemata for the crop rotations per replication at field site Aiterhofen (SB – sugar beet; WW – winter wheat; SM – silage maize; Mu – mustard catch crop, Mi – millet); ¹ plots with investigations into soil structure, ² Mi was cultivated because of regional quarantine regulations.

Crop rotation No.	Plot	Year				
		2010	2011	2012	2013	2014
1	1.1	SM	SM/Mi ²	SM	SM ¹	SM ¹
2	2.1	Mu_SB	WW-1	WW-2	Mu_SB ¹	WW-1
	2.2	WW-1	WW-2	Mu_SB	WW-1	WW-2
	2.3	WW-2	Mu_SB	WW-1	WW-2	Mu_SB ¹
3	3.1	Mu_SM	WW-1	WW-2	Mu_SM ¹	WW-1
	3.2	WW-1	WW-2	Mu_SM	WW-1	WW-2
	3.3	WW-2	Mu_SM	WW-1	WW-2	Mu_SM ¹
4	4.1	SB	WW-1	Mu_SM	SB ¹	WW-1
	4.2	WW-1	Mu_SM	SB	WW-1	Mu_SM
	4.3	Mu_SM	SB	WW-1	Mu_SM	SB ¹

The Sampling was conducted after the emergence of SB and SM. Undisturbed soil core samples (250 cm³, height 6 cm, n = 4 per plot and depth) from soil depths 2-8 cm, 12-18 cm, 22-28 cm and 32-38 cm were saturated and then adjusted to a matrix potential of -6 kPa in a sand box in order to determine air capacity (AC) (ISO 11274:1998). Subsequently, the same soil cores were used to determine saturated hydraulic conductivity (k_s) in a stationary system (percolation time 4 h) (ICS 13.080; 65.060.35).

4.3.2.3. Modelling the soil compaction risk

4.3.2.3.1. Model structure

The soil compaction risk is modelled based on the method by Rücknagel et al. (2015) and is performed using the modelling software *REPRO* (*REPRO*duction of soil fertility, Hülshberger, 2003). In this model, the soil strength (precompression stress σ_p) at two soil depths (lower top-soil at 20 cm and subsoil at 35 cm) is contrasted with the vertical soil stress (major principal stress σ_z) at the respective soil depth. Soil strength is adjusted depending on the water content (Rücknagel et al., 2012a). If the vertical soil stress exceeds the soil strength of the soil structure,

this results in a dimensionless Soil Compaction Index (SCI). The SCI reflects the soil compaction risk using the categories (i) low ($SCI \leq 0.10$), (ii) medium ($SCI 0.11-0.20$); (iii) high ($SCI 0.21-0.30$), (iv) very high ($SCI 0.31-0.40$) and (v) extremely high ($SCI > 0.40$). The input parameters required are: (i) Technical specifications of the machinery used as well as (ii) the dates on which they were driven over the soil; (iii) mechanical precompression stress at both soil depths for a matrix potential of -6 kPa; (iv) soil water content.

The SCIs are first modelled annually for the single crop specific operations: (i) Tillage (comprises primary tillage, stubble tillage and seedbed preparation); (ii) seeding; (iii) fertilization (comprises N and P/K fertilization); (iv) pesticide application; (v) harvest; (vi) field transport during SM harvest. This serves to identify the level of the soil compaction risk for single operations in individual years. In a second step, the SCIs are modelled for entire crop rotations. For that, all operations performed each crop rotation plot in the reference period are sorted in descending order of their modelled SCI. Then, according to the proportion of wheeled area, these SCIs are summed until a proportion of 100 % wheeled area is reached. The maximum modelled SCIs for single operations, in combination with their proportion of wheeled area, are thus crucial to model the SCI for entire rotations. For a more detailed explanation see Rücknagel et al. (2015).

4.3.2.3.2. Input parameters

Technical parameters and husbandry – model farm Aiterhofen

In order to validate the model (see chapter 4.3.2.3.3), the soil compaction risk is only modelled based on the equipment actually used in the field trial. However, not all of this equipment represents the current state of the art and SB is sown using special field trial equipment. Therefore, the estimation of the soil compaction risk of entire crop rotations is based on a model farm of 75 ha which is a typical size for the region. The technical equipment typically used in modern practice to manage the four crop rotations is set for a farm of this size. The cultivation dates from the field trial are used to model the soil compaction risk for each crop rotation plot in each year. The technical data required for modelling (axle load and tyres of the heaviest axle) are taken from the machines' respective operating manuals and are listed in appendix A 4.3.1. For harvesting WW and SB, it is assumed that the harvested crop is transferred to the transport vehicle or a beet storage clamp at the edge of the field. The parallel harvesting method is used for SM, with the SM forage transferred to the transport vehicle whilst driving. In the case of SB harvest, diagonal steer is assumed, where the wheels of the rear axle run next to the wheel tracks of the front axle. Depending on the actual axle loads, the tyre inflation pressures are adjusted to the lowest technically permissible pressures for field work conditions, although these are never below 0.8 bar. A full hopper is assumed for fertilization and the application of pesticides as well as for transporting the SM. Two scenarios are modelled for harvesting WW and SB. In the first scenario, the SCIs are modelled for a hopper that is 100 % full. In the second scenario, in

years when SCIs >0.10 were identified in the first scenario, the hopper load is reduced to 50 % and the tyre inflation pressure adjusted.

In order to obtain representative results for the soil compaction risks of the individual crop rotations, all operations performed on the crop rotation plots over a period of three rotations (2004 until 2012) are considered. Since cultivation dates from the field trial are available for the years 2010, 2011 and 2012 only, these dates are applied to the foregoing years. Using the first plot of crop rotation 2 (Mu_SB-WW-WW) as an example, appendix A 4.3.2 shows the operations performed in the field trial with the corresponding machinery or machinery combinations from the model farm. To estimate the soil compaction risk of one crop rotation plot, all operations following the harvest of the preceding crop until the harvest of the observed crop are taken into account.

Soil strength at -6 kPa matric potential

In the field trial, soil samples were taken in the year 2013 and used to determine the mechanical precompression stress using the method by Rücknagel et al., (2007), which is based on the ratio of aggregate density to dry bulk density. The precompression stress is $\log 1.91$ (= 81.3 kPa) for the topsoil (20 cm) and $\log 1.86$ (= 72.4 kPa) for the subsoil (35 cm), and is only included as a typical site specific value when modelling the soil compaction risk for the model farm.

Soil water content during wheeling

Soil water content (% field capacity – % FC) is modelled on a daily basis (period 2004 to 2012) by the German Meteorological Service (GMS) for the 0-60 cm soil layer (Straubing station, texture silt loam, 38 vol.% FC) and for the crops SB, SM and WW. Generally, for all three crop types, a decrease in soil water content can be observed as the vegetation period commences in the spring, and thus evapotranspiration increases until the respective crop is harvested (Fig. 4.3.1). In the period considered, soil water content levels at harvest vary considerably. At the time of harvest, the mean soil water content is 63 % FC for WW, 77 % FC for SM and 59 % FC for SB. However, the values vary between 35 and 85 % FC for WW, 44 and 97 % FC for SM and 41 to 79 % FC for SB depending on the respective year. After harvest and declining evapotranspiration in the autumn, the average soil water content increases up to field capacity until spring time for all crops.

4.3.2.3.3. Model validation

In order to test the validity of the model, the SCIs modelled for the crop rotations are compared with the actual changes in AC as a physical soil parameter. To this end, in the year 2013, soil cores (220 cm³, h = 2.8 cm, n = 5) were taken from the soil depths 20 cm and 35 cm from an adjacent field whose soil structure was comparable to that of a ploughed topsoil and thus reflected the initial soil conditions before the field trial began.

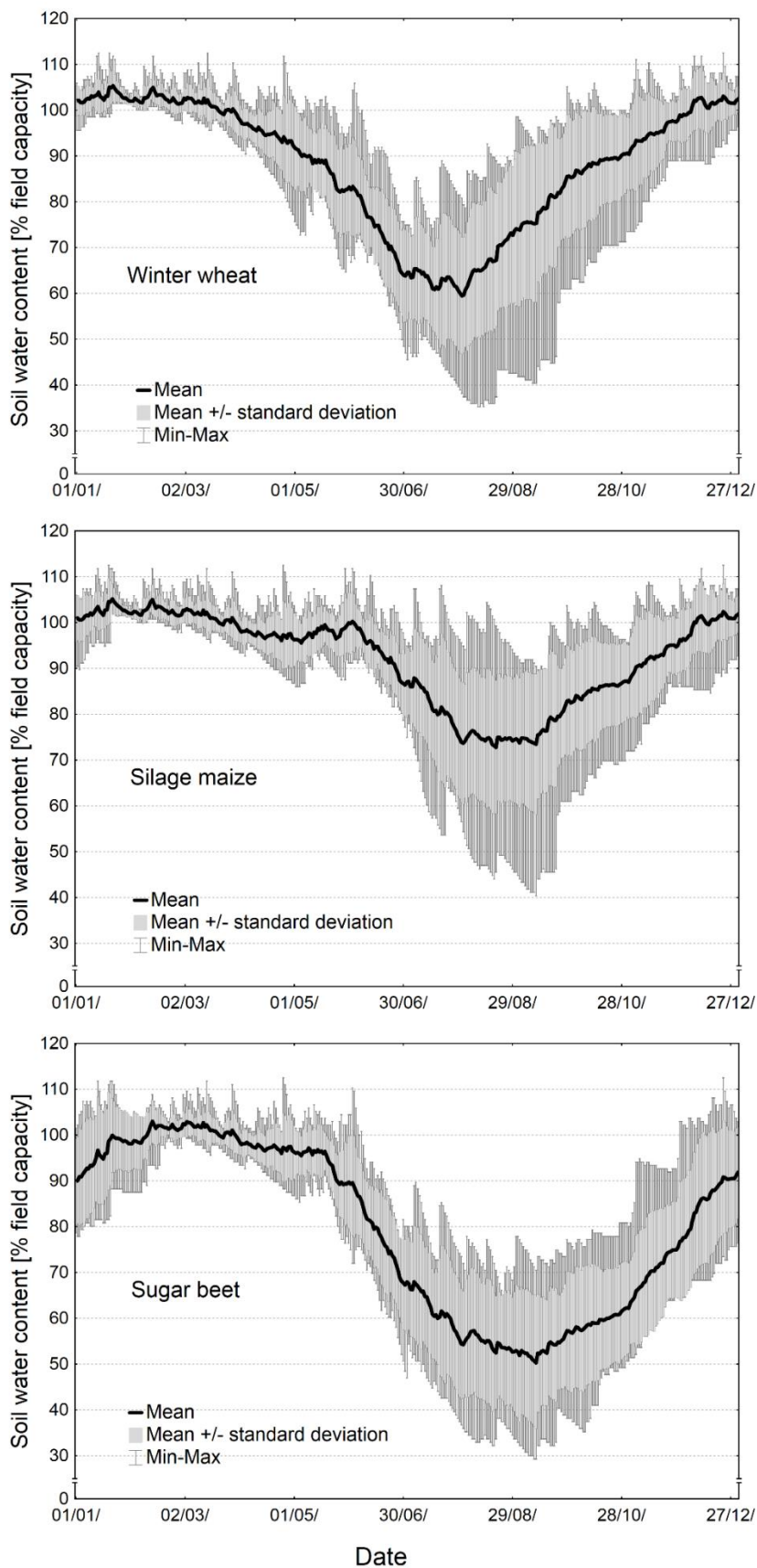


Figure 4.3.1. Seasonal course and annual variation in soil water content for the crops investigated, modelled for the 0-60 cm soil depth by the German Meteorological Service (Straubing station, period 2004 to 2012).

These soil cores were saturated and then adjusted to a matrix potential of -6 kPa in a sand box in order to determine AC according to ISO 11274:1998. After subsequent soil compression tests, Casagrande's (1936) graphical methods were used by two experts working independently of each other to determine the mechanical precompression stress (Rücknagel et al., 2010). This is log 1.58 (38.0 kPa) for the topsoil (20 cm) and log 1.72 (52.5 kPa) for the subsoil (35 cm). For validating the model, these latter values are used as initial values before the trial was set up. Based on the machinery used in reality during the field trial, the SCI is modelled for the areas of the plots which were sampled in 2013 and 2014. Therefore, operations involving driving along permanent traffic lanes, such as fertilizer and pesticide application, are not considered.

The change in AC is calculated based on the values from the trial plots and those from the adjacent field. The AC values at 20 cm in the adjacent field are compared to the trial plot values from 22-28 cm, and the AC values at 35 cm from the adjacent field against the trial plot values from 32-38 cm.

4.3.2.4. Statistical analysis

An analysis of variance is carried out using the program SAS (SAS Institute, 2008) in order to statistically evaluate the parameters AC and k_s . Prior to this, the data set for k_s was logarithmized and the data sets of the soil parameters k_s and AC were checked for normal distribution by a Shapiro-Wilk test with the program Statistica (Statsoft, 2014). A mixed statistical model is used, in which the effects crop rotation, year, crop rotation*year, replication and replication*block are recognised as fixed effects. The plots sampled in the respective years of the investigation and the soil cores per plot are included in the model as random effects and repeated measures. Thus, $n = 16$ values are allocated per crop rotation, sampling depth and year. The degrees of freedom are estimated according to Kenward and Roger (1997). An F-test is conducted to test the fixed effects for significance ($\alpha = 5\%$) by using the SAS procedure MIXED. Due to unbalanced data sets, the pairwise comparison of means (Tukey-Kramer method) is performed using adjusted means and the LS MEANS procedure.

The descriptive evaluation of soil compaction risks is performed using the Statistica software (Statsoft, 2014). Box-and-whisker plots serve to identify the soil compaction risk for the individual operations. The location parameter used is the median. The 25 % and 75 % percentiles as well as the minimum and maximum values indicate the spread and variation; the sample size is $n = 9$ years. In order to evaluate the soil compaction risk of the entire crop rotations, the median, minimum and maximum are provided. These values indicate the SCIs identified for the individual crop rotation plots of a crop rotation. The exception is SM monoculture, because this consists of just one plot and therefore only one value can be provided.

Validation is performed by correlating the SCIs identified for the field trial and the change in AC from the years 2013 and 2014 for both soil depths separately using the program Statistica (Statsoft, 2014). Thus, $n = 8$ pairs of values are calculated for each depth. Additional an F-test

to test the effects soil depth, year and year*soil depth for significance ($\alpha = 5\%$) is performed for both, the change in AC and the SCIs modelled, by using the SAS procedure GLM. Thus, $n = 8$ values are allocated per soil depth.

4.3.3. Results

4.3.3.1. Measured soil structure for the field trial Aiterhofen

The crop rotation has a significant impact on the soil structural properties in the topsoil (2-8 cm) (Table 4.3.2). For the parameter AC, the crop rotation*year interactions is significant at this soil depth, meaning the two sampling years are considered individually for the pairwise comparison of means. There are no significant interactions at the other soil depths (12-18, 22-28 and 32-38 cm) or for the parameter k_s (all soil depths).

Table 4.3.2. Probability values from F-test of fixed effects for the parameter air capacity (AC) and saturated hydraulic conductivity (k_s) at different soil depths at the field trial Aiterhofen (sampling years 2013 and 2014); values below the significance threshold of $\alpha = 5\%$ are shown in bold italics.

Effect	AC [vol.%]				k_s [cm d ⁻¹]			
	Soil depth [cm]				Soil depth [cm]			
	2-8	12-18	22-28	32-38	2-8	12-18	22-28	32-38
Crop rotation (CR)	<i>0.014</i>	0.359	0.156	0.332	<i>0.001</i>	0.657	0.094	0.513
Year (Y)	<i>< 0.001</i>	0.362	0.876	0.862	0.825	0.821	0.395	0.548
CR * Y	<i>0.018</i>	0.664	0.632	0.691	0.400	0.854	0.464	0.802
Replication (R)	0.068	0.467	0.193	0.804	0.090	0.693	0.162	0.507
R * Block	0.572	0.811	0.211	0.579	0.644	0.966	0.744	0.901

Therefore, sampling years are considered not individually for the pairwise comparison of means. In 2013, the crop rotation SB-WW-Mu_SM reveals a significantly lower AC value compared with the crop rotation Mu_SM-WW-WW while the rotations SM monoculture and Mu_SB-WW-WW are intermediate (Table 4.3.3). In 2014, the differences between the variants are not significant. For the parameter k_s , the highest values are observed in the topsoil (2-8 cm) in variants where Mu is cultivated as a catch crop and WW as a preceding crop (Mu_SB-WW-WW, Mu_SM-WW-WW). This effect is statistically sound when compared with the SM monoculture. At the other soil depths, no considerable differences can be discerned between the different crop rotations for AC and k_s .

Table 4.3.3. Crop rotation effects on air capacity (AC) and saturated hydraulic conductivity (k_s) at the field trial Aiterhofen (sampling years 2013 and 2014). Different lower-case letters show significant differences for $p \leq 0.05$ (Mu – mustard catch crop, SB – sugar beet, SM – silage maize, WW – winter wheat). ¹ both sampling years separated, as significant Crop rotation * Year interaction present, ² means across both sampling years, as no significant Crop rotation * Year interactions present.

Parameter	Soil depth [cm]	Crop rotation			
		SM monoculture	Mu_SB-WW-WW	Mu_SM-WW-WW	SB-WW-Mu_SM
AC	2-8 ¹ 2013	24.6 ab	22.8 ab	26.5 a	18.6 b
[vol.%]	2-8 ¹ 2014	18.7	16.8	20.1	19.6
	12-18 ²	13.6	10.7	12.3	11.0
	22-28 ²	9.2	10.6	10.7	8.4
	32-38 ²	6.2	6.7	8.2	6.9
k_s	2-8 ²	67 a	240 b	196 b	108 ab
[cm d ⁻¹]	12-18 ²	52	33	64	36
	22-28 ²	25	42	74	20
	32-38 ²	11	19	36	23

4.3.3.2. Soil compaction risk modelled for the model farm Aiterhofen

4.3.3.2.1. Model validation

For the modelled SCIs and the change in AC at the respective soil depth, the range of values is small. Thus, there are no significant correlations between these parameters (20 cm: $r = 0.41$, $p = 0.32$; 35 cm: $r = -0.06$, $p = 0.89$). However, the changes in AC for the topsoil (20 cm) are significantly higher than those for the subsoil (35 cm), as well as the modelled SCIs for the topsoil are significantly higher than those for the subsoil (35 cm) (Fig. 4.3.2). Therefore, greater differences in the level of soil compaction, in terms of changes in AC, can be detected by the modelled SCIs.

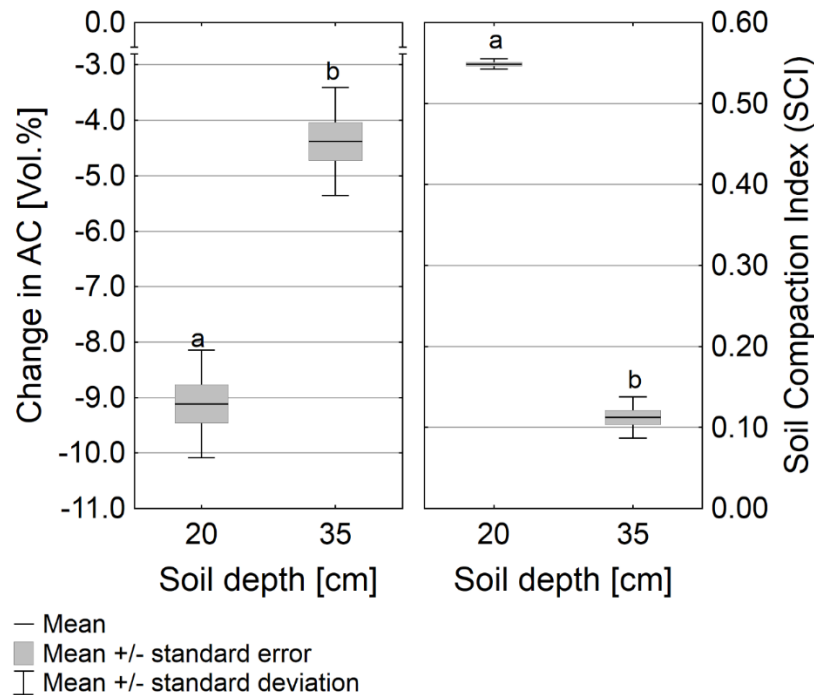


Figure 4.3.2. Box-plots of the change in air capacity (AC) and the modelled Soil Compaction Index (SCI) for two soil depths at the field trial Aiterhofen (sampling years 2013 and 2014); different lower-case letters show significant differences for $p \leq 0.05$ ($n = 8$).

4.3.3.2.2. Soil Compaction Index for crop - specific operations

In the lower topsoil (20 cm), the medians of the modelled SCIs are below 0.10 for all crop-specific operations (Fig. 4.3.3). The soil compaction risk can therefore be classified as low. However, far higher SCIs, and thus higher soil compaction risks, can be observed in individual years: For example, in the observation period, the SB and WW harvesting methods result in the highest SCIs and very high soil compaction risks. Further, the fertilizer application is associated with high soil compaction risks, regardless of the cultivated crop. Using the forage harvester for SM harvest showed either a small soil compaction risk or none at all. However, the field transport of SM during harvest leads to medium soil compaction risks in individual years. The maximum modelled SCIs determined for tillage, sowing and pesticide application operations are far lower than for the harvesting methods and fertilization. For the spring crops SM, Mu_SM, SB and Mu_SB, the soil compaction risks of the operations involving soil tillage and the application of pesticides are higher than for the WW crop rotation fields. Sowing generally has a minor influence or none at all (SM cultivation) on the soil compaction risk.

In the subsoil (35 cm), an SCI >0.00 is only present in individual years. Here, SB harvest displays the highest soil compaction risks, which are classified as "medium", followed by WW harvest and fertilization. The other operations result in low or no soil compaction risk at this soil depth.

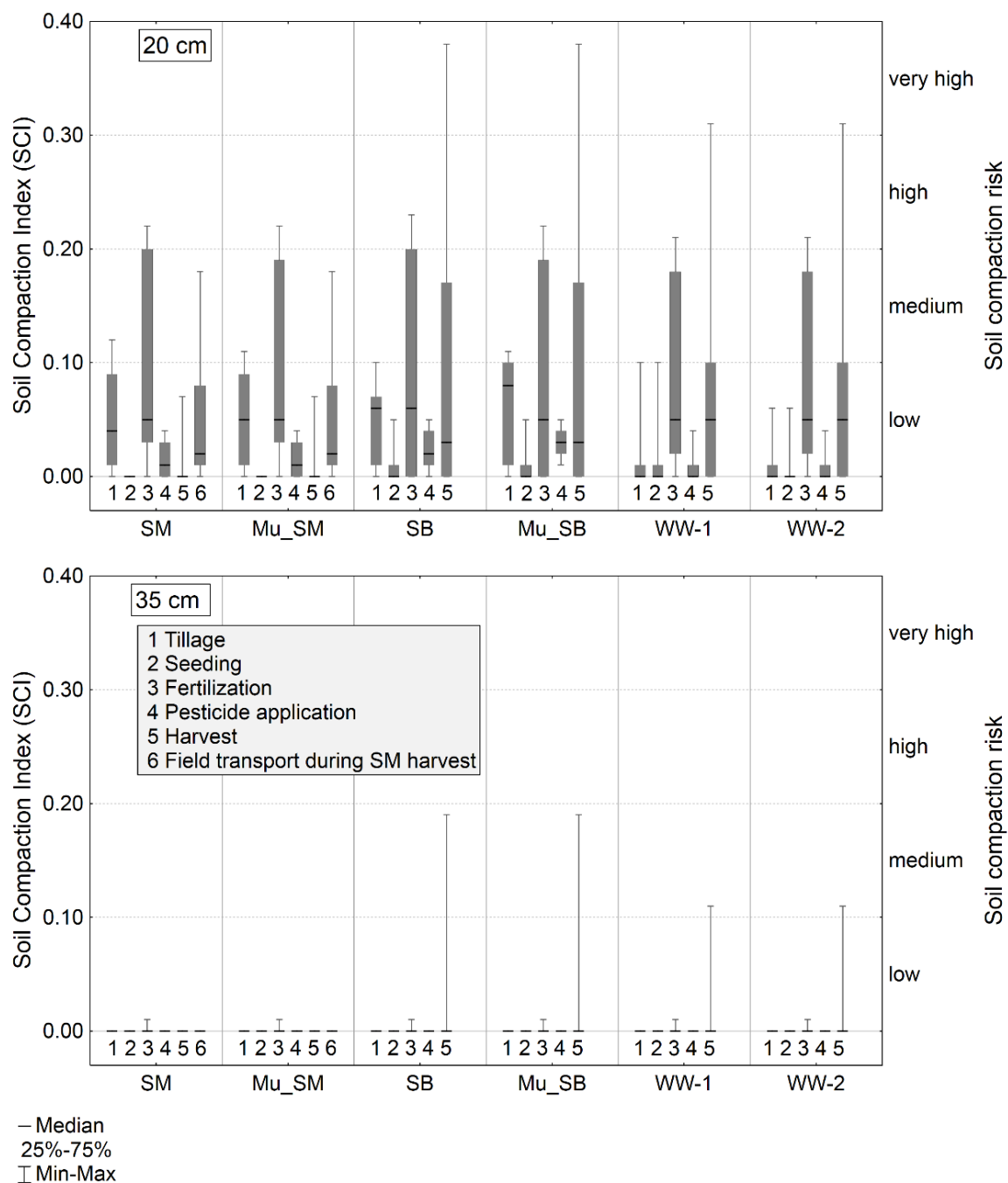


Figure 4.3.3. Box-plot of the modelled Soil Compaction Index (SCI) and the respective soil compaction risk modelled annually for each crop-specific operation conducted for the weather conditions of 2004-2012 at two soil depths (20 and 35 cm) for the model farm Aiterhofen. ‘Tillage’ comprises the operations primary tillage, stubble cultivation and seedbed preparation. ‘Fertilization’ comprises the operations N and P/K fertilization (SB – sugar beet; SM – silage maize, Mu – mustard catch crop, WW – winter wheat).

At both soil depths, halving the hopper load and adjusting the tyre inflation pressure during WW and SB harvest reduces the maximum modelled SCI (Fig. 4.3.4). In accordance with the classification of the modelled SCI, for the SB harvest the maximum soil compaction risk drops

from very high to high (20 cm) and from medium to low (35 cm), and for the WW harvest from very high to medium (20 cm) and from medium to low (35 cm).

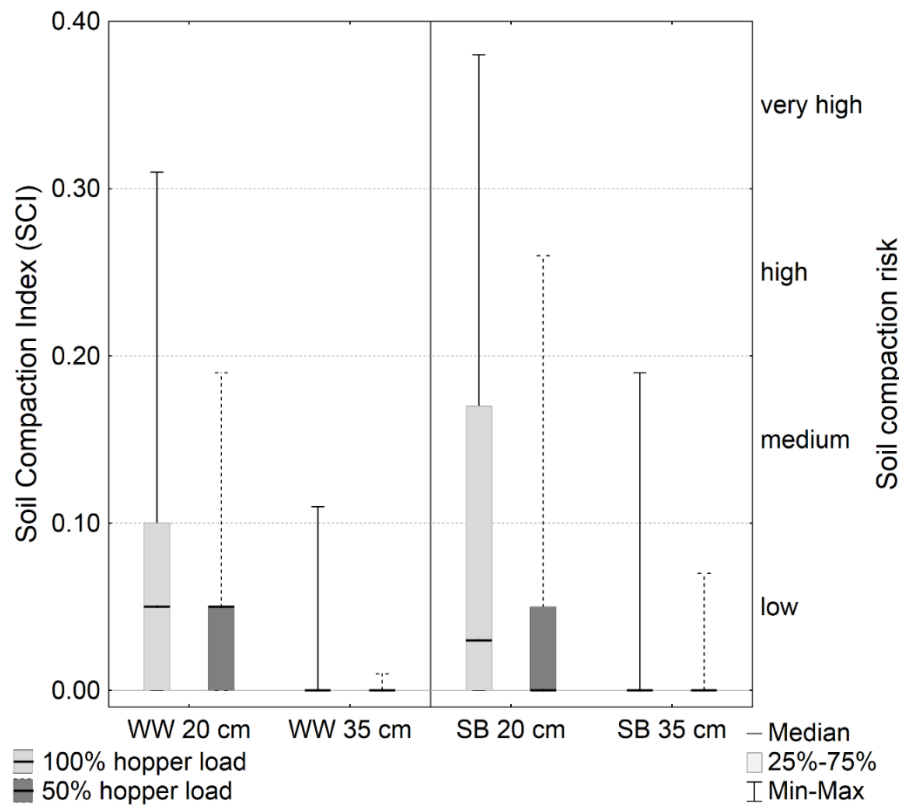


Figure 4.3.4. Modelled Soil Compaction Index (SCI) and the respective soil compaction risk conducted for the weather conditions of 2004-2012 at two soil depths (20 and 35 cm) for the harvesting of sugar beet (SB) and winter wheat (WW) with reduced hopper load and adjusted tyre inflation pressure for those years in which an SCI >0.10 is indicated for hopper load of 100 % (n = 9) (model farm Aiterhofen).

4.3.3.2.3. Soil compaction risk of entire crop rotations

Across the whole period of 9 years, both, the highest soil compaction risks and the highest variation exist for the crop rotations including SB (Mu_SB-WW-WW, SB-WW_SM) (Fig. 4.3.5). Reducing the hopper load at SB and WW harvest and adjusting the tyre inflation pressure reduces the soil compaction risk at both soil depths. At both soil depths and for both hopper loads, the differences between the crop rotations including SB are very small, although the crop rotations Mu_SB-WW-WW and SB-WW-Mu_SM vary in terms of their proportions of WW and SM cultivation.

Compared to SM in monoculture, cultivating SM in crop rotations with twofold WW (Mu_SM-WW-WW) reduces the soil compaction risk in the lower topsoil (20 cm) only (Fig. 4.3.5). In the subsoil (35 cm), there are no soil compaction risks for SM monoculture, while Mu_SM-WW-WW displays no to low soil compaction risks. These can thus be attributed to the low to

medium soil compaction risk when harvesting WW. In crop rotations with WW and SB, the soil compaction risk can be reduced by halving the hopper load and adjusting the tyre inflation pressure during harvest.

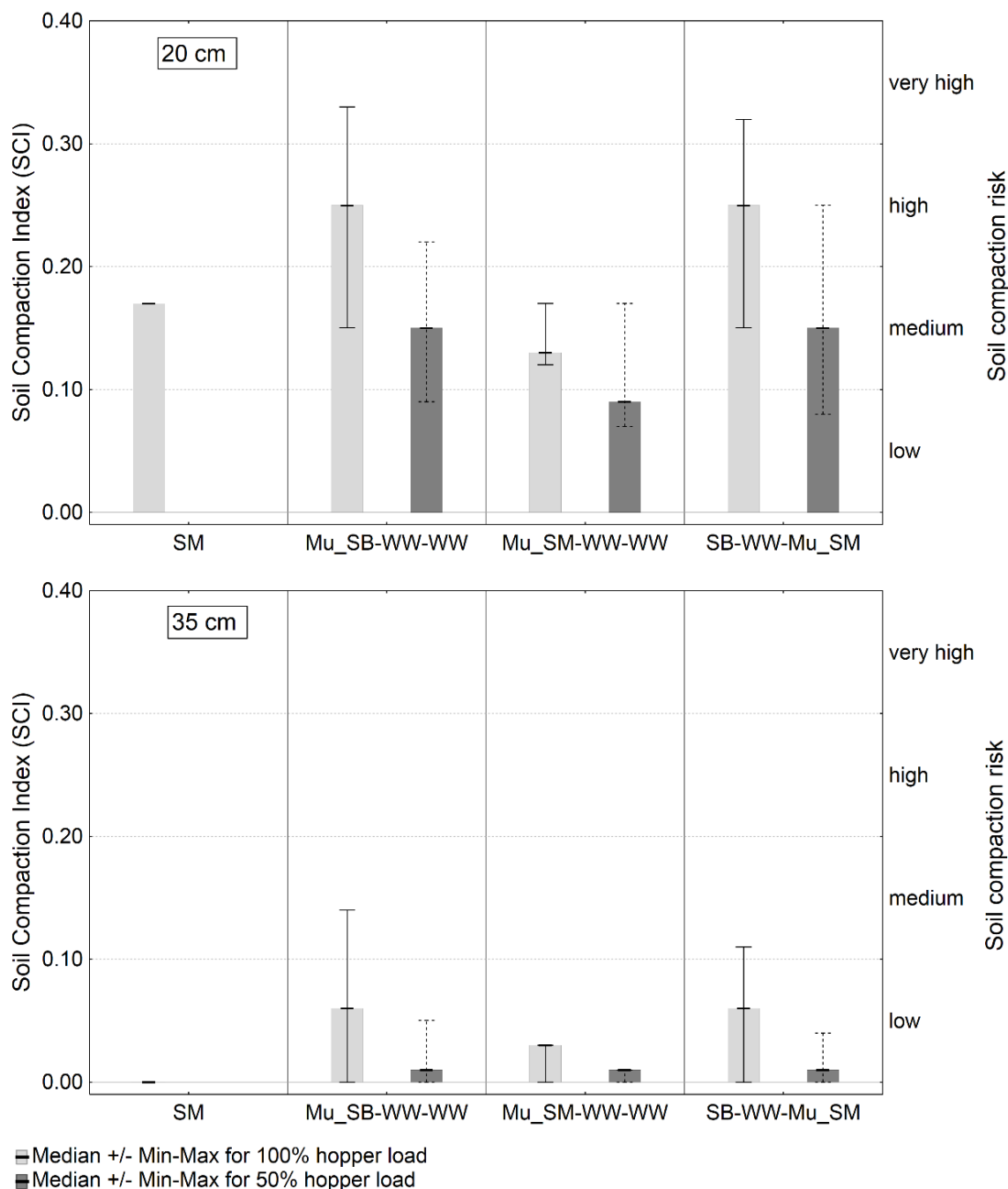


Figure 4.3.5. Modelled Soil Compaction Index (SCI) and the respective soil compaction risk for entire crop rotations conducted for the weather conditions of 2004-2012 at two soil depths (20 and 35 cm) for the model farm Aiterhofen (SB – sugar beet, SM – silage maize, Mu – mustard catch crop, WW – winter wheat).

4.3.4. Discussion

4.3.4.1. Soil structure measured at the field trial Aiterhofen

In the literature, threshold values for a functioning soil structure are specified as 8 vol.% AC and 10 cm d⁻¹ k_s in the topsoil as well as 5 vol.% AC and 10 cm d⁻¹ k_s in the subsoil (Werner and Paul, 1999; Lebert et al., 2004). The values in this investigation do not drop below these thresholds, and as such the physical soil parameters studied do not suggest a functional restriction of soil structure at any soil depth or for any crop rotation.

The differences in soil structure found in this trial are restricted to the topsoil (2-8 cm). At this depth, for the parameter AC the only significant effect of the crop rotation is a reduction in 2013 in the SB-WW-Mu_SM rotation compared to Mu_SM-WW-WW. After SM was cultivated as a preceding crop, the soil probably became compacted and, when preparing the seedbed for the following SM in the SM monoculture, it was loosened more than for SB. There was a higher soil compaction risk when harvesting SM compared to WW in 2012. For the equipment used in the field trial the estimated SCI for the forage harvester during SM harvest was 0.54 while the SCI for WW harvest was 0.00 (data not shown). This means that the investigations into soil structure in 2013 would presumably show lower AC in all plots with SM as a preceding crop. However, in 2013, the soil under SB cultivated after SM as a preceding crop, tends to higher ACs than under SM monoculture. This is due to the fact that SM seedbed preparation is performed using a rotary harrow at a soil depth of 10 cm, while for SB only a shallow seedbed (<5 cm) is prepared using a cultivator.

With regard to the parameter k_s, the differences are probably influenced by the combination of preceding crops. The higher k_s values in the topsoil (2-8 cm) of the variants where Mu is cultivated as a catch crop and WW as a preceding crop (Mu_SB-WW-WW, Mu_SM-WW-WW) may be the result of improved structural and aggregate stability, and in turn the reduced susceptibility to surface capping. In situations where WW harvest residues are left on the soil surface, as in our trial, aggregate stability and the water infiltration rate of the soil increase (Ghuman and Sur, 2001). Also, cultivating catch crops under reduced tillage can result in higher macroporosity in the topsoil (Głąb and Kulig, 2008), which contributes heavily to k_s (Beven and Germann, 1982).

At the other soil depths, there are only minor differences in soil structure or none at all. Unfavourable soil structure conditions are especially critical in the subsoil, as it is costly to rectify such problems and they are often persistent (Alakukku, 1996). Subsoil compaction is usually only observed if soils are subjected to stress from high wheel loads when their water content is high or, additionally, if the frequency of wheeling increases (Koch et al., 2008). However, the machinery used in the trial investigated is unlikely to cause compaction of this extent. Furthermore, crop-related loosening of the soil structure in the topsoil is often only observed in crops with strong taproot systems, such as alfalfa (*Medicago spp.*) (Oquist et al., 2006; Uteau et al., 2013), and is unlikely to occur with the crops investigated here.

4.3.4.2. Soil compaction risk modelled for the model farm Aiterhofen

A number of models are described which serve to predict the soil compaction risk (O’Sullivan et al., 1999; Horn and Fleige, 2003; van den Akker, 2004; Keller et al., 2007). These models can be used to estimate and depict the site-related soil compaction risk (van den Akker and Hoogland, 2011; D’Or and Destain, 2014), for individual machinery passes or operations (Arvidsson et al., 2003; Défossez et al., 2003; Trautner and Arvidsson, 2003; Lozano et al., 2013), or for a combination of both (Duttmann et al., 2014). Compared to these models, the model used here can quantify and assess the soil compaction risk of entire crop rotations up to the farm level. The model can be integrated into the software *REPRO*, making all necessary input parameters available. For example, this means that the soil compaction risks and greenhouse gas or energy balances can be modelled on the basis of the same farm machinery. By using the standardisation function presented by Rücknagel et al. (2015), it is possible to incorporate this information into sustainability assessments of farming systems.

Rücknagel et al. (2015) validated the model based on measurements of dry bulk density and k_S . Like the results presented, Rücknagel et al. (2015) found that the modelled SCIs and changes in dry bulk density are lower for the subsoil (35 cm) than for the lower topsoil (20 cm). In this trial, for the soil depths 22-28 cm and 32-38 cm, which are used to validate the model, there are only slight differences in soil structure between crop rotations measured. Similarly, the crop rotation SCIs modelled for the trial-specific machinery differ only marginally. When differences in the modelled SCIs increases, as it is for the subsoil (35 cm) comparing to the topsoil (20 cm), higher changes in AC are measured. Thus, the model delivers valid results for the Aiterhofen site.

Models represent a simplified version of reality, and as such they all have limitations. The soil water contents included for modelling in this study are for the soil depth 0-60 cm and not considered individually for both soil depths (20 cm, 35 cm) evaluated. Spatial and temporal variability of soil water content in fields are possible. Furthermore, applying the cultivation dates from the field trial to previous years is associated with inaccuracies in terms of the cultivation dates and the respective soil water content. There are no real cultivation dates for the years 2004 to 2009, because the field trial was not set up before 2010. However, a longer period needs to be considered to ensure representative modelling of the soil compaction risk. Another limitation of the model is that it assumes static hopper load levels for sowing, pesticides, fertilization, SB and WW harvest and SM transport. So, the modelled SCI – and the soil compaction risk – only apply to the part of the field driven over with a full hopper load (or with half a hopper load for the second scenario). However, in order to identify machinery and/or operations which pose high soil compaction risks, the maximum possible axle load must be used, since this condition also occurs in practice even if for small areas only.

The results of modelling the soil compaction risks for individual operations and for the entire crop rotations are in keeping with past studies. Based on the contact pressure, the proportion of area driven over and the product of the wheel load and the distance travelled, Chamen et al.

(1992) ascribe a high soil compaction risk to the operations of soil tillage and harvest in the case of root and forage crops, like SB and SM. Even so, it is possible to reduce the soil compaction risk by sowing SB and SM later and harvesting them earlier, when soil water contents are usually lower (Boizard et al., 2002; Capowiez et al., 2009). As water content increases, the soil's compactability also increases (Rücknagel et al., 2012a), and the risk of causing soil compaction, even at greater soil depths, increases.

Accordingly, operations involving driving over soils with high axle loads at times when soil water content is high, display a high soil compaction risk. When comparing entire crop rotations, the model uses all operations in the period considered of 9 years to model the SCI. Therefore, high modelled SCIs which only appear in one year have an impact on the soil compaction risk of the entire period considered. In the investigations presented, this applies mainly to the harvesting operations. While it is true that, taking the annual average, soil water contents at the time of harvest are far below those when fertilizing in the spring, in individual years soil water contents which are approximately 20 % FC above the average for the period considered are observed for all three crops. In such years, there are two reasons why the harvesting operations have a high soil compaction risk. Firstly, the axle loads are very high for WW and SB harvest, particularly when the hopper is full. Secondly, the working width is very small. In the case of SB harvest, for example, it was 3 m and when using diagonal steer, as in the model assumptions, the wheels of the rear axle run next to the wheel tracks of the front axle. Thus, almost the entire area is driven over.

Tillage operations for the spring crops SM and SB display a greater soil compaction risk than for WW. So far, more unfavourable soil structure conditions have been found when cultivating SB and SM compared to WW (Jacobs et al., 2014), after cultivating spring crops compared to winter rape and winter cereals as preceding crops (Götze et al., 2013) and in crop rotations with a higher proportion of spring crops (Boizard et al., 2002; Capowiez et al., 2009). The authors attribute these findings in part to higher soil compaction risks during tillage and spring crop cultivation.

The results presented also show that, in years with an increased soil compaction risk, halving the hopper load and respective reduction of tire inflation pressure during the SB and WW harvest decreases soil compaction risks. In Germany, this approach is recommended as part of 'good agricultural practice' as a practical, weather-adjusted strategy of preventive soil protection when harvesting SB (Brunotte et al., 2013). However, this does require that the field lengths are sized accordingly so that the hopper load does not exceed 50 % at the end of the field. When harvesting SB, halving the hopper load reduces the axle load by around 20 %, and decreasing the tyre inflation pressure from 2.7 bar to 2.0 bar is technically acceptable. This reduces contact pressure (Koolen et al., 1992) and the propagation of pressure at greater depths (Söhne, 1953), and the soil compaction risk decreases both for the lower topsoil (20 cm) and for the subsoil (35 cm).

4.3.5. Conclusions

Under the experimental conditions at the field trial, following a complete rotation there are no differences in soil structure as a result of SM or SB cultivation. Cultivating WW and Mu as preceding crops for SB and SM increases k_s (196 cm d⁻¹ to 240 cm d⁻¹) compared to SM as a preceding crop (67 cm d⁻¹ to 108 cm d⁻¹), indicating better structural stability and infiltration capacity, and should therefore be preferred. To assess the soil compaction risks of entire crop rotations, it is necessary to distinguish between soil depths. If the intention is to permanently refrain from loosening the topsoil in a cropping system (no-till or minimum tillage), the soil compaction risk at a soil depth of 20 cm is decisive for the choice of cropping system. For the model conditions, cultivating SM (medium soil compaction risks) will presumably lead to less adverse effects in the soil structure at 20 cm depth compared to SB (medium to very high soil compaction risks). Even when the topsoil is loosened, the soil compaction risk at a soil depth of 35 cm is crucial for the evaluation. Compaction in this depth cannot be rectified, or doing so is highly costly, and as such any compaction should be avoided. Provided that the hopper load is halved and the tyre inflation pressure is adjusted in years with a high soil compaction risk when harvesting SB and WW, there are only slight differences in the subsoil (35 cm) between the variants. Under these circumstances, the crop rotations investigated caused no to low soil compaction risks and are therefore not associated with environmental impacts caused by soil compaction.

Acknowledgements

The project was funded by the Federal Ministry of Food and Agriculture by decision of the German Bundestag and via the Fachagentur Nachwachsende Rohstoffe e.V. within the joint project “The sugar beet as an energy crop in crop rotations on highly productive sites - an agronomic / economic system analysis”. We gratefully thank the technical staff of the Institute of Sugar Beet Research, Alfons Griesbauer and family and the team of the ARGE Regensburg for their help in conducting the field trial.

Appendix A 4.3.1. Technical data of the machinery used at the 75 ha model farm Aiterhofen (SB – sugar beet, WW – winter wheat, SM – silage maize, TIP – tyre inflation pressure). ¹ axle with highest load, ² hopper load, ³ equal to mustard sowing.

Operation	No.	Machinery used	Working width [m]	Tractor ¹			Trailer ¹		
				Axle load [kg]	Tyre size	TIP [bar]	Axle load [kg]	Tyre size	TIP [bar]
Primary tillage ³	1	Tractor 120 kW + cultivator	3.0	5506	650/65 R 42	0.8			
Seedbed preparation	2	Tractor 120 kW + rotary harrow	3.0	4620	650/65 R 42	0.8			
Stubble tillage	3	Tractor 120 kW + cultivator	3.0	5506	650/65 R 42	0.8			
SB seeding	4	Tractor 83 kW + 12 row precision drill	6.0	3480	420/85 R 38	0.8			
SM seeding	5	Tractor 67 kW + 8 row precision drill	6.0	3410	420/85 R 34	0.8			
WW seeding	6	Tractor 120 kW + rotary harrow + drill	3.0	5526	650/65 R 42	0.8			
Pesticide application	7	Tractor 67 kW + sprayer 2200l	21.0	3316	420/85 R 34	0.8	3812	420/85 R 38	0.8
N fertilization	8	Tractor 67 kW + sprayer 2200l	21.0	3404	420/85 R 34	0.8	4164	420/85 R 38	0.8
P,K fertilization	9	Tractor 67 kW + spreader 1500l	21.0	5848	420/85 R 34	1.4			
SB harvest 100 % ²	10a	6 row self-propelled, two axles	3.0	26180	1050/50 R 32	2.7			
SB harvest 50 % ²	10b	6 row self-propelled, two axles	3.0	20790	1050/50 R 32	2.0			
SM harvest	11	6 row self-propelled forage harvester	4.5	7764	650/75 R 32	1.0			
SM transport	12	Tractor 120 kW + trailer 40000 l	4.5	6466	650/65 R 42	0.8	8500	600/55 R 22.5	1.6
WW harvest 100 % ²	13a	Combine harvester 200 kW, 8000l	6.0	16400	710/75 R 34	2.0			
WW harvest 50 % ²	13b	Combine harvester 200 kW, 8000l	6.0	14000	710/75 R 34	1.4			
Rolling	14	Tractor 67 kW + roll	10.25	2520	420/85 R 34	0.8			

Appendix A 4.3.2. Management operations performed in the field trial Aiterhofen and corresponding machinery of the model farm Aiterhofen (no. see appendix A1) for modelling the soil compaction risk, using the first plot of crop rotation 2 (2.1, Mu_SB-WW-WW) (Mu – mustard, SB – sugar beet, WW – winter wheat) as an example; ¹ in combination with mustard sowing.

2010: Mu_SB			2011: WW-1			2012: WW-2		
Date	Operation	No.	Date	Operation	No.	Date	Operation	No.
25/08/2009	N fertilization	8	13/10/2010	Primary tillage	1	26/08/2011	Stubble tillage	3
26/08/2009	Primary tillage ¹	1	13/10/2010	WW seeding	6	27/09/2011	Primary tillage	1
26/03/2010	Pesticide application	7	23/02/2011	P,K fertilization	9	30/09/2011	WW seeding	6
07/04/2010	Seedbed preparation	2	12/03/2011	N fertilization	8	20/03/2012	N fertilization	8
08/04/2010	SB seeding	4	09/04/2011	Pesticide application	7	21/03/2012	Rolling	14
10/04/2010	N fertilization	8	11/04/2011	N fertilization	8	19/04/2012	Pesticide application	7
24/04/2010	Pesticide application	7	28/04/2011	Pesticide application	7	23/04/2012	N fertilization	8
30/04/2010	Pesticide application	7	20/05/2011	N fertilization	8	26/04/2012	Pesticide application	7
24/05/2010	Pesticide application	7	20/05/2011	Pesticide application	7	15/05/2012	N fertilization	8
05/06/2010	Pesticide application	7	31/05/2011	N fertilization	8	24/05/2012	N fertilization	8
14/07/2010	Pesticide application	7	11/08/2011	WW harvest	13	02/06/2012	Pesticide application	7
11/08/2010	Pesticide application	7				13/07/2012	Pesticide application	7
06/09/2010	Pesticide application	7				01/08/2012	WW harvest	13
12/10/2010	SB harvest	10						

5. Synthesis and general discussion

5.1. Suitability of precompression stress as a parameter for soil strength

This scientific work focuses on precompression stress as a central parameter of soil strength. This takes into account the original idea of Casagrande (1936) that precompression stress can be used to divide the stress/strain curve, of clay soils in particular, into a recompression section with minimal, reversible compaction, and a virgin compression section with plastic compaction behaviour. One significant advantage of precompression stress, including for the model concept presented in *REPRO*, is that it is expressed as a stress value, often in kPa. This means that soil stresses, mostly determined as vertical stresses in the load axis of agricultural machines, can be directly compared with precompression stress (Schjonning et al., 2012). Using precompression stress as a parameter for maximum soil strength also ensures that an existing soil structure remains largely unaffected in its pore volume and pore geometry. In addition, when agricultural machinery is driven over the soil, minimal soil movement and compaction reduces rolling resistance and thus energy consumption (Carman, 2002; Volk, 2018).

In principle, however, the scientific field of agricultural soil mechanics discusses whether precompression stress, and the methodological procedure used to determine it, are actually suitable for determining soil strength in agricultural soils (Vorderbrügge and Brunotte, 2011a, b, c). In this context, it is also discussed whether the values determined in uniaxial laboratory tests can be used to predict soil strength in the field (Keller et al., 2012). In addition, numerous methodological differentiations already exist in terms of how soil compression tests are conducted, for example with different loading times, with and without a subsequent relaxation phase, or with varying sizes of soil core samples (Salire et al., 1994; Keller et al., 2011; DIN 18135, 2012; Schjonning and Lamande, 2018). The tests are evaluated using either the stress/strain curves, the stress/void ratio curves or the stress/dry bulk density curves, with a variety of graphical and mathematical methods for determining the precompression stress (e.g. Dias Junior and Pierce, 1995; Cavalieri et al., 2008; Lamande et al., 2017). All of these methodological variations can lead to different precompression stress values, which are not necessarily comparable with each other or with the values determined graphically according to Casagrande (1936), as described in detail in chapter 2.1. Consequently, however, the methodological differences should not lead to a general rejection of this parameter, but rather to the definition and harmonisation of international standards. A contribution to this is made by this study, in that uniform, internationally common conditions across all partial investigations were used to conduct the soil compression tests (uniaxial, restricted lateral expansion, drained, loading time 180 minutes – 15 minutes relaxation) and evaluate the stress/dry bulk density function. This also ensures comparability within the work. In all chapters, precompression stress was always determined by several independent persons using stress/dry bulk density functions according to the Casagrande method (1936). This reduces the subjective margin of error and the results are more reproducible. Nevertheless, one criticism is that comparability with other work in the scientific field of agricultural soil mechanics is probably not always possible due to the variety of methods described.

Focusing on soil texture, Casagrande (1936) writes in his essay: “From a large number of tests on different types of soils it was found that for the majority of clays the pre-consolidation load can be derived with a satisfactory degree of accuracy by means of the empirical method shown [...]” However, not all soils seem to permit this method with the classical division of the stress/strain curve into a recompression and a virgin compression section, and the associated ability to derive the precompression stress. Schanz (2007), for example, shows a more or less linear stress/strain behaviour in the area of soil mechanics, especially for “granular” soils, with a very flat slope overall, depending on the dry bulk density of the soil. There was no such stress/strain behaviour in the agricultural soils examined in this work, even at sites with very low clay or very high sand contents such as “Uchtdorf 19-22” and “Uchtdorf 35-38” (site code 12.1. and 12.2., chapter 3.1.). But even on soils whose stress/strain behaviour can be divided into a recompression and a virgin compression section, there can be bi-linear-shaped, rounded or rather S-shaped variations (Chaplain et al., 2011), which complicates the graphical or mathematical derivation of the precompression stress. Examples of these varying curve shapes can be found in chapters 3.2., 3.3. and others.

An even more central point of criticism regarding the use of precompression stress as a parameter for maximum soil strength is its lack of relation to other important soil properties and functions (Stahl et al., 2005). Besides physical soil functions as a prerequisite for filtering, buffering and transformation, according to *Bundesbodenschutzgesetz* (“Germany’s Federal Soil Protection Act”) (BBodSchG, 1998) these also include the soil’s function as a habitat and its agricultural production function for the production of biomass. If only precompression stress is taken into account, it can on the one hand be the case that compacted soils with a high precompression stress may be subjected to high stresses, which in turn complicates the regeneration of the soil. On the other hand, on very loose soils with low precompression stress, a loosened soil structure is protected more than is necessary. This has hardly any advantages for plant growth, for example (Pöhlitz, 2019). On the question of how high the critical stress values of four sample soils of different main soil groups, Pöhlitz (2019) determined not only the grain and straw yield of spring barley (*Hordeum vulgare* L.), but also the biological macropores created by *Lumbricus terrestris*, the macroporosity and pore continuity as well as the precompression stress. The results of the study showed that the critical stress values of individual parameters in the four sample soils did indeed differ, but that for all soils they ranged between 50 and 100 kPa. Of particular interest, however, is the observation by Pöhlitz (2019) that precompression stress also lies within the median of this range. In the context of the results presented in this paper, this finding supports the use of precompression stress as a suitable parameter for soil strength. In chapter 3.4. it was also possible to derive a clear relationship between precompression stress and packing density as quality parameters for the soil structure. On the other hand, the stress values for the individual parameters in Pöhlitz (2019) can be found in such a limited range that general stress values of approximately 80-100 kPa are conceivable, regardless of the soil texture.

5.2. Categorisation of precompression stress values

The data set of all precompression stress values at a matric potential of -6 kPa, which were determined in the context of the individual subchapters of this study, allows an empirical categorisation and classification of the values (Fig. 5.2.1). A primary differentiation is made between topsoils and subsoils. For the latter, a further distinction is made between naturally occurring soils and soils resulting from re-cultivation. The topsoils are divided into locations with conservation tillage (all methods without ploughing) or conventional primary tillage with a plough. All of the field trials on soil tillage (chapter 3.3.), catch cropping (chapter 4.1.) and the artificially produced samples (chapters 3.1. and 3.2.) are not taken into account, because they do not allow a real assessment to be made of the naturally occurring conditions on arable land.

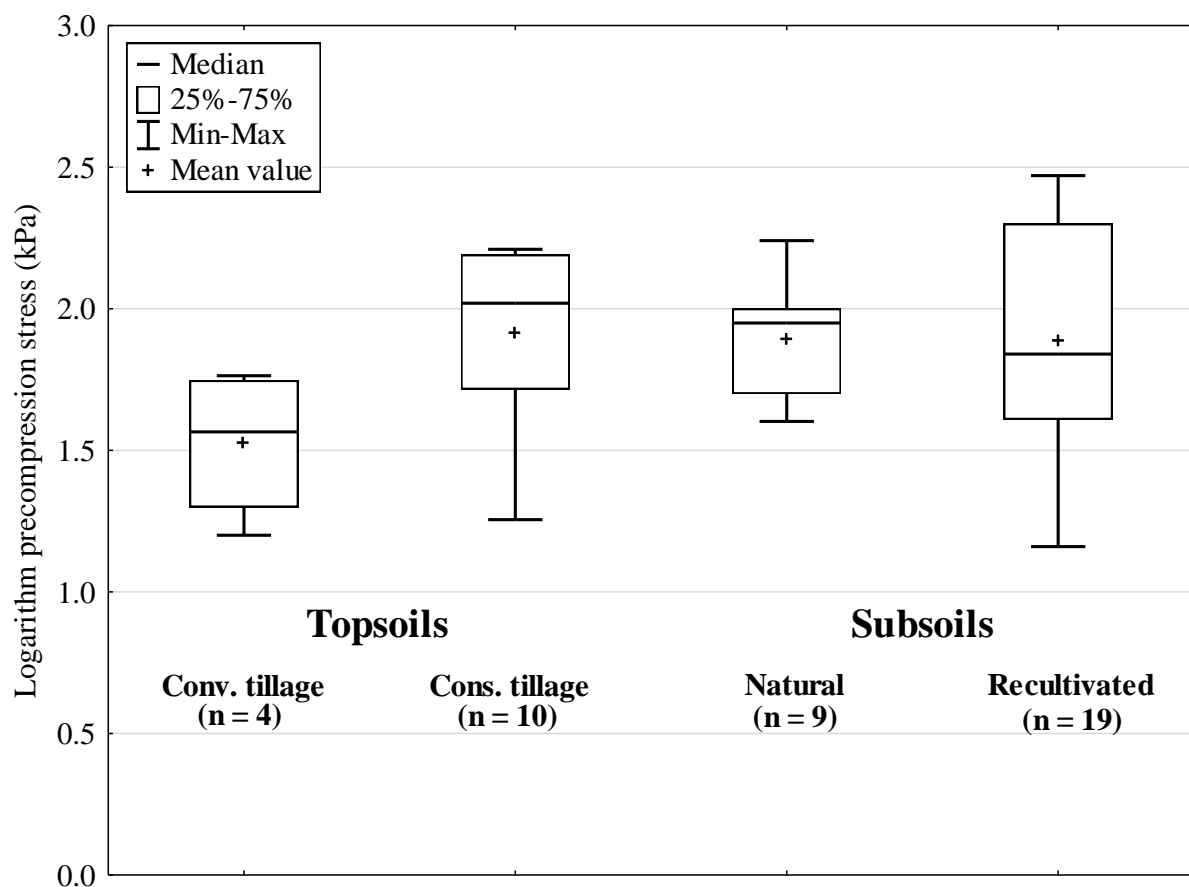


Figure 5.2.1. Empirical categorization of precompression stress values (Conv. - conventional, Cons. - conservation).

In the topsoil, the mean precompression stress values of the field sites with conservation tillage are 81 kPa (log 1.91), with a fairly large range of 18 kPa (log 1.26) to 162 kPa (log 2.21). One of the reasons for this range is that conservation tillage methods of varying intensity and sampling depths within the topsoil are combined here. Studies by da Veiga et al. (2007) also show differences in precompression stress values depending on the intensity of the conservation tillage and the sampling depth. At 33 kPa (log 1.52) and with a range of 16 kPa (log 1.20) to

58 kPa (log 1.76), the mean precompression stress values for conventional tillage are significantly lower. In principle, this result is in line with the results of the soil tillage experiments in chapter 3.3. and other investigations in which the precompression stress is higher with conservation soil tillage in less intensively loosened topsoil than with conventional soil tillage (Stahl et al., 2005; Peng and Horn, 2008). It should be noted, however, that the comparability of the sites here is limited due to the different number of conventional and conservation tilled sites and textural conditions. Soil types with a higher clay or lower sand content are more common on the fields with conservation soil tillage than on those with conventional soil tillage.

In the naturally occurring subsoils examined (30–45 cm depth), the mean precompression stress was 78 kPa (log 1.89), with a maximum range between 40 kPa (log 1.60) and 174 kPa (log 2.24). In the literature, distinctions are often made according to different soil texture groups. However, the small volume of data means that such differentiations are difficult and subject to certain caveats here. At 102 kPa (log 2.01), the mean precompression stress on the subsoils classifiable as clay soils according to the *Bodenkundliche Kartieranleitung* (Ad-Hoc Arbeitsgruppe Boden, 2005) is slightly higher than on the silt soils, at 76 kPa (log 1.88). Fleige et al. (2002) also report similar precompression stress values in subsoils of about 90 kPa, albeit without differentiating between clay soils and silt soils. The compilation of precompression stress data sets by Vorderbrügge and Brunotte (2011a) shows a larger range and higher values overall. There, precompression stress for clay soils and silt soils is between 78 kPa and 137 kPa. At this juncture, it should be noted that, even with similar textural properties in the subsoil, it is not only in this study that larger precompression stress ranges can be found as a function of soil structural properties, such as the aggregate shape, aggregate arrangement or other visual characteristics of the soil structure (Fleige et al., 2002; Rücknagel et al., 2007; Horn and Fleige, 2009; Höhne et al., 2013). In the topsoils, as already described, the influence of texture on precompression stress is also obscured by the type of tillage and thus in turn by the formation of the soil structure. It is therefore questionable whether texture is suitable at all as the sole criterion for classifying precompression stress.

Re-cultivated fields created as a result of open-cast lignite mining can consist of very different and in some cases mixed geological materials (Schröder, 1988; Sächsisches Staatsministerium für Umwelt und Landwirtschaft, 2018). Nevertheless, the precompression stress of the subsoils examined here, which were re-cultivated from loess substrate, was 78 kPa (log 1.89), an identical mean level to that of the natural sites. However, the maximum range of 14 kPa (log 1.16) to 295 kPa (log 2.47) is higher, which is probably attributable in part to the changing re-cultivation methods over time. All in all, the precompression stress values here are clearly above those of the re-cultivated subsoils in Krümelbein et al. (2010). Their investigations, however, took place on soils with sandy pit substrates.

5.3. Integration of algorithms in the *REPRO* software package

The different individual algorithms were implemented in the *REPRO* model, in the module for assessing the risk of soil compaction. In the user interface, the algorithms are mainly found in the table “*Standortgrunddaten*” (Fig. 5.3.1).

Schlag	Nr.	Teilschlag	Nr.	Jahr	Größe	V-Gefährdung	Tiefe	Grobbodenanteil	Rohdichte
In der Hasenmühle	1	In der Hasenmühle / 1	1	2019	2,0000		0	10,00	1
In der Hasenmühle	1	Hasenmühle / 2	2	2019	3,0000		0	25,00	1
In der Hasenmühle	1	Hasenmühle / 3	3	2019	6,0000		0	5,00	1
In der Hasenmühle	1	In der Hasenmühle / 4	4	2019	1,0000		0	0,00	1
In der Hasenmühle	1	In der Hasenmühle / 5	5	2019	4,0000		0	5,00	1

Klassenzeichen der Bodenschätzung | Bodenform | Ackerkrume/Unterboden | Wasser | Relief | mit Prüfungen

Tiefe **Grobbodenanteil** % **Trocken-Rohdichte** g/cm³ kein Überschreiben der TRD
 % g/cm³ eigene Vorbelast./Spatendiag.
 Belastbarkeit = Vorbelastung

Belastbarkeit pF **Vorbelastung (log)** pF 1,8 **Packungsdichte** **Aggregat-Dichte (pF 1,8)** g/cm³ g/cm³
 pF 1,8 g/cm³

Bodengruppe **Stufe der Verdichtungsgefährdung**

- 1 Table to choose the field
- 2 Table to choose the level of packing density (PD)
- 3 Display or input boxes for precompression stress values
- 4 Input boxes for dry bulk density and aggregate density
- 5 Input boxes for gravel content

Figure 5.3.1. User interface to assign the parameters of soil strength in the *REPRO* model at 20 and 35 cm depth.

In this table, site parameters that do not depend on the time of the individual pass are assigned to individual partial fields. A partial field can be defined as a section of a farm, especially in the context of the whole farm evaluation, or in the context of scientific questions as a single test variant or plot. In principle, the allocation of the site parameters is independent of the soil type and its profile structure at the depths 20 cm and 35 cm. Other model concepts similarly identify the risk of soil compaction for specified depths, e.g. in *TERRANIMO® light* (Stettler et al., 2014), or they identify a soil depth up to which there is a risk of soil compaction, e.g. in *TASC*

(Diserens, 2010). In *REPRO*, the depth of 20 cm represents the lower topsoil, for which it is important to assess the risk of soil compaction – especially in the case of long-term conservation tillage. This makes sense because investigations of the soil structure in arable soils subjected to many years of very shallow soil tillage or direct sowing have, in some cases, revealed considerable compaction of the lower topsoil at a depth of around 20 cm, since this layer is no longer disturbed (Reichert et al., 2009; Götze et al., 2013). A depth of 35 cm is used to determine the risk of soil compaction at the point of transition to the subsoil. Preventing soil compaction in the subsoil is particularly important, because compaction at this depth persists for a very long time (Alakukku, 1996; Berisso et al., 2012). Improving subsoil compaction is very costly and often only effective for a few years (Werner and Reich, 1993; Canarache et al., 2000).

The user interface is divided into the list with the individual partial fields at the top (Fig. 5.3.1 [1](#)) and the allocation of the site parameters at the bottom. To begin with, it is possible to select the precompression stress at -6 kPa matric potential, on the basis of the packing density determined in the field, using present levels of 1 to 5 (Fig. 5.3.1 [2](#)). The values specified in chapter 2.2. are stored for the individual packing density levels. However, it must be pointed out that these precompression stress values were derived from a data set with a limited textural range and exclusively on re-cultivated soils. Despite this fact, studies by Höhne et al. (2013) on numerous loam, silt, sand and clay soils show essentially similar results. Soil parameters determined visually have so far rarely found their way into the models used to calculate the compaction risk, although these parameters can quickly and easily provide information about the current soil structural condition. They also take into account the dynamics of the soil structure in terms of location and time, and are relatively easy to record. Besides the algorithms presented here, the *TASC* model is the only one in which visual methods can be used to define the topsoil strength in the stages “solid”, “semi-solid” and “soft” by way of the so-called “screwdriver test” (Diserens and Steinmann, 2002; Diserens and Spiess, 2004). However, this method presents an inseparable link between soil strength and soil water content, whereas the packing density derives only the precompression stress from the condition of the soil structure at constant soil water content (here at -6 kPa matric potential).

In addition, it is possible to input directly available precompression stress values at -6 kPa matric potential (Fig. 5.3.1 [3](#)), e.g. from measurements or mappings, or the precompression stress at -6 kPa matric potential can be estimated according to a regression approach by Rücknagel et al. (2007) with the formula 2.2.-1 (chapter 2.2.) using dry bulk density and aggregate density (Fig. 5.3.1 [4](#)). If there are no data available for aggregate density and dry bulk density, the calculations can be performed with standard values that are stored in the master data of the model. Dry bulk density and aggregate density are linked here to the soil texture class according to *Bodenschätzung* (BoSchätzG, 1970), because this information is also widely available for practical agriculture in Germany. The standard values in the topsoil (20 cm) are made dependent on the type of primary tillage (Table 5.3.1) and were derived from the tillage trials in chapter 3.3. To this end, the soil tillage trials were divided into two site groups, on the one hand with the soil textures Sand, Loamy Sand and Sandy Loam and on the other hand with the soil textures

Loam, Clay Loam and Clay, and mean values of aggregate density and dry bulk density were formed from them. The values of similar soil textures were adopted for soil textures for which no measured data were available.

Table 5.3.1. Standard values of dry bulk density (BD) and aggregate density (AD) in the *REPRO* model for topsoil (20 cm) derived from tillage trials in chapter 3.3; ¹ soil texture class according to BoSchätzG (1970), ² according to tillage trials in chapter 3.3., ³ conventional tillage, ⁴ conservation tillage, n.d. not determined.

Soil texture class ¹	Standard value and site name ²	AD ³ (g cm ⁻³)	AD ⁴ (g cm ⁻³)	BD ³ (g cm ⁻³)	BD ⁴ (g cm ⁻³)
Sand (anlehmiger Sand [Sl])	Standard value	1.73	1.73	1.45	1.62
Loamy Sand (lehmiger Sand [IS], stark lehmiger Sand [SL])	Standard value Lückstedt	1.73 n.d.	1.73 n.d.	1.45 1.44	1.62 1.61
Sandy Loam (sandiger Lehm [sL])	Standard value Warin Zschortau	1.73 1.77 1.69	1.73 1.83 1.63	1.45 1.58 1.31	1.62 1.64 1.56
Loam (Lehm [L])	Standard value Bad Kreuznach Bernburg Görzig	1.61 1.63 1.55 1.59	1.61 1.62 1.55 1.71	1.25 1.31 1.24 1.26	1.45 1.50 1.41 1.53
Clay Loam (schwerer Lehm [LT])	Standard value Buttelstedt	1.61 1.62	1.61 1.62	1.25 1.21	1.45 1.35
Clay (Ton [T])	Standard value	1.61	1.61	1.25	1.45

Across all soil tillage trials, the aggregate density does not differ between the soil tillage variants, which is why no distinction is made in the standard values. By contrast, dry bulk density is 0.18 g cm⁻³ higher with conservation tillage than with conventional tillage in all trials. Higher dry bulk densities in the lower topsoil under conservation tillage are also described in other publications, e.g. Tebrügge and Düring (1999), Deubel et al. (2011), Schlüter et al. (2018). For the two site groups, based on the standard values given in Table 5.3.1 the regression model of Rücknagel et al. (2007) shows – at -6 kPa matric potential and a depth of 20 cm – precompression stress values of 15 and 40 kPa (log 1.18 and log 1.60 respectively) for conventional tillage and 72 and 126 kPa (log 1.86 and log 2.10 respectively) for conservation tillage. These values are also more or less in line with the results for different soil tillage at the field sites investigated (Fig. 5.2.1). Essentially, the different precompression stress in *REPRO* indicated here is relevant for the calculation of vertical soil stress, since the concentration factor in formula 2.2.-6 (chapter 2.2.) is made dependent on precompression stress. Consequently, under otherwise

comparable conditions, the vertical soil stress is lower with conservation tillage than with conventional tillage. Zink et al. (2010) also arrive at similar results from the direct measurement of vertical soil stress.

2019: Anwendungsbeispiel

Schlag	Nr.	Teilschlag	Nr.	Größe	AZ	Jahr	1. Hauptfrucht	2. Frucht	3. Frucht	4. Frucht
In der Hasenmühl	1	In der Hasenmühl	1	2.0000	50	2019	Winterweizen (A)			
In der Hasenmühl	1	In der Hasenmühl	1	3.0000	55	2019	Winterweizen (A)			
In der Hasenmühl	1	In der Hasenmühl	1	6.0000	70	2019	Winterweizen (A)			
In der Hasenmühl	1	In der Hasenmühl	4	1.0000	55	2019	Winterweizen (A)			

Fruchtart Verfahren zusammen ausgebrachte Mittel nicht anzeigen nach Fruchtarten sortiert

Fruchtart	Verfahrensabschnitt	Gerät	Datum	Diesel l/ha
Winterweizen (A)	Bodenbearbeitung	Stoppelgrubbern flach 3,0 m, 120 kW	20.08.2018	11,88
Winterweizen (A)	Bodenbearbeitung	Stoppelgrubbern flach 3,0 m, 120 kW	10.09.2018	11,88
Winterweizen (A)	Bodenbearbeitung	Stoppelgrubbern flach 3,0 m, 120 kW	10.10.2018	11,88
Winterweizen (A)	Bestellung	Feinsaat mit Kreiselegge und Sämaschine 3,0 m, 120 kW	15.10.2018	17,44
Winterweizen (A)	Hauptproduktternte	Mähdrusch, Wintergetreide 7,5 m, 200 kW	10.08.2019	16,80

Verfahrensabschnitt Tag Monat Jahr
Hauptproduktternte Korn Originalsubstanz 10 8 2019

Gerät und Bedingungen
Mähdrusch, Wintergetreide | 7,5 m, 200 kW

Verfahrensangaben | Diesel/Ökonomie | Gesamt | Bemerkung | Belastungsindex (BI)

Auswahl der Bereifung	Bereifung 1		Bewertung mit langj. Bodenfeuchte	Bereifung 1		
	20 cm	35 cm		20 cm	35 cm	
Konzentrationsfaktor	4	1,64	1,69	3	2,18	2,15
Bodendruck Traktor/AM	5	2,42	2,16	6	0,24	0,01
Bodendruck Anhänger/Transp.		0,00	0,00		0,00	0,00

neue Maßnahme
Musterverfahren
Maßnahme löschen
Standardwerte
OK
Abbruch
Ende

- 1 Table to choose the field
- 2 Table with the working steps on the field
- 3 Display boxes of calculated soil strength (logarithm of kPa value)
- 4 Display boxes of calculated concentration factor
- 5 Display boxes of calculated vertical stress (logarithm of kPa value)
- 6 Display boxes of calculated Soil Compaction Index (SCI)

Figure 5.3.2. User interface for calculation of concentration factor, vertical stress, soil strength and Soil Compaction Index (SCI) for the time of single passes in the *REPRO* model at 20 and 35 cm depth.

By entering the soil gravel content by volume in the left part of the “*Standortgrunddaten*” user interface (Fig. 5.3.1 [5]), the precompression stress at -6 kPa matric potential is adjusted to reflect the gravel content using the formulae 3.2.-4 to 3.2.-6 from chapter 3.2. Since these investigations were carried out only by way of example on three fine soil textures, the other soil texture classes are also assigned according to *Bodenschätzung* (BoSchätzG, 1970). The calculation for Clay Loam and Clay is carried out with the formula 3.2.-4, for Sandy Loam and Loam

with the formula 3.2.-5, and for Sand and Loamy Sand with the formula 3.2.-6. This procedure is justifiable from a scientific point of view, because the mathematical relationships for the soils studied are essentially very similar and can generally be described for all soils using the formula 2.2.-2 in chapter 2.2.

The adjustment of the soil strength to account for soil water content is carried out based on the databases stored in the “*Bodenwassergehalt*” user interface for individual climate stations, with daily values of the soil water content as a percentage of field capacity (%FC) (not shown here). On this basis, the soil strength is modified for the day of the actual pass in the “*Verfahren*” user interface. In the middle part of this user interface, each partial field (Fig. 5.3.2 [1]) is first chronologically assigned the individual working steps (Fig. 5.3.2 [2]). For each of the working steps, the current soil strength is adjusted with formula 3.1.-1 from chapter 3.1. (Fig. 5.3.2 [3]). The constants from Table 3.1.4. (chapter 3.1.) are used for this purpose. For all soils for which there are no constants, the constants for “all texture classes” are used. Calculation of the concentration factor with formula 2.2.-6 (chapter 2.2.) (Fig. 5.3.2 [4]), of vertical soil stress with formula 2.2.-5 after Koolen et al. (1992) (Fig. 5.3.2 [5]), and of the Soil Compaction Index (SCI) for the individual passes with formula 2.2.-7 (Fig. 5.3.2 [6]) is also performed in the “*Verfahren*” interface. It is possible to specify some machinery parameters, with the allocation of tyres, tyre inflation pressures and axle loads, in a separate interface (called “*Arbeitsgängen-tamm-Auswahl* → *Reifenzuordnung*”; not shown here).

5.4. Application of algorithms in other model concepts and sustainability assessments

First of all, it is worth mentioning that the methodological aspects described in chapter 2.1. for determining precompression stress using the graphical method according to Casagrande (1936) have already been taken up by numerous other authors (e.g. Chaplain et al., 2011; Lamande et al., 2017; Ledermüller et al., 2018).

In addition, the algorithms and regressions described in this work have been implemented, or are in the process of being implemented, in other models, concepts and practical guides besides *REPRO*. Examples include the *SaSCiA* model (Kuhwald et al., 2018), the guidebook *Boden unter Druck* (Rücknagel, 2014) and the forthcoming DWA leaflet from the DWA-M 920 series on the assessment and evaluation of the risk of compaction of arable soils (DWA, 2019).

Particularly in the *SaSCiA* model, a freely usable implementation in “R” (R Core Team, 2017), there are numerous parallels to the soil compaction module in *REPRO*, especially with regard to the calculation of soil strength. The change in soil strength as soil water content decreases is calculated according to the method described in chapter 3.1., on the basis of precompression stress at -6 kPa matric potential and the soil water content as a percentage of field capacity. The adjustment of soil strength in soils with a significant gravel content is also carried out using the equations in chapter 3.2. In addition, the *SaSCiA* model applies formulae for calculating the concentration factor and the Soil Compaction Index (SCI) and its classification (chapter 2.2.).

Some of the algorithms have been included in the guidebook *Boden unter Druck* in a more simplified form and geared towards the information requirements of agricultural practice. This concerns primarily the derivation of soil strength as a function of soil water content (chapter 3.1.), the influence of conservation and conventional tillage on soil structure and soil strength (chapter 3.3.) as well as the calculation of soil stress and the overall risk of soil compaction (chapter 2.2.).

In addition to the results presented in chapter 2.2., the complete soil compaction module in *REPRO* has now been used on numerous other farms in German-speaking countries within the scope of the *Deutsche Landwirtschaftsgesellschaft* (“German Agricultural Society”) certification (INL, 2019). In addition to answering fundamental scientific questions, it thus also contributes to assessing the overall sustainability of farms and improving their environmental impact.

5.5. Discussion of module accuracy in general

Apart from the individual algorithms in the subchapters of this work, the entire *REPRO* module for assessing the risk of compaction has also been validated in numerous tests. This validation gives further indirect indications concerning the accuracy of the algorithms, as well as of those which were not tested individually (e.g. the calculation of vertical stress in the load axis), but also about how these interact in the overall context of the module in *REPRO*.

If the soil stress exceeds the precompression stress in the calculations, a permanent plastic deformation should be expected. In the commonly used semilogarithmic diagram, this deformation is a linear function for some soil properties, such as dry bulk density or void ratio, and is described by the compression index or by the slope of the virgin compression line (Bradford and Gupta, 1986; Arvidsson and Keller, 2004; DIN 18135, 2012). On this basis, the logarithmic amount by which the calculated soil stress exceeds the precompression stress can be shown as the Soil Compaction Index (SCI) in this model concept. Irrespective of the initial soil strength, this should always result in the same changes in soil properties. This makes it possible to compare the changes in soil properties across different trials, sites or depths as a function of the calculated Soil Compaction Index (SCI), as described in chapter 2.2. The prerequisite for this is that the soils exhibit similar virgin compression behaviour. The average slope of the virgin compression lines of the stress/dry bulk density diagrams (matric potential -6 kPa) of all the investigations in this study is 0.18 g cm^{-3} per change of a unit of stress $\log \sigma_z$, with a range of between 0.07 and 0.29 g cm^{-3} per change of a unit of stress $\log \sigma_z$. In addition to the clay content (Larson et al., 1980) and the dry bulk density or void ratio (Keller et al., 2011), there are indications that the water content also has an influence on the slope of the virgin compression line (chapter 3.1.). The actual compression effect in the field can therefore be slightly different, depending on the factors mentioned, even with the same calculated Soil Compaction Index (SCI). This certainly explains part of the variance in module validation (chapter 2.2.). On the whole, the mean slope of the virgin compression lines can be used to map the change in dry

bulk density as a function of the Soil Compaction Index (SCI) quite well across all module validations (Fig. 2.2.4, chapter 2.2.). Similar to the mean slope of all of the virgin compression lines, a regression line in this relationship would have a slope of 0.18 g cm^{-3} per unit of Soil Compaction Index (SCI) at an intersection with the ordinate close to zero.

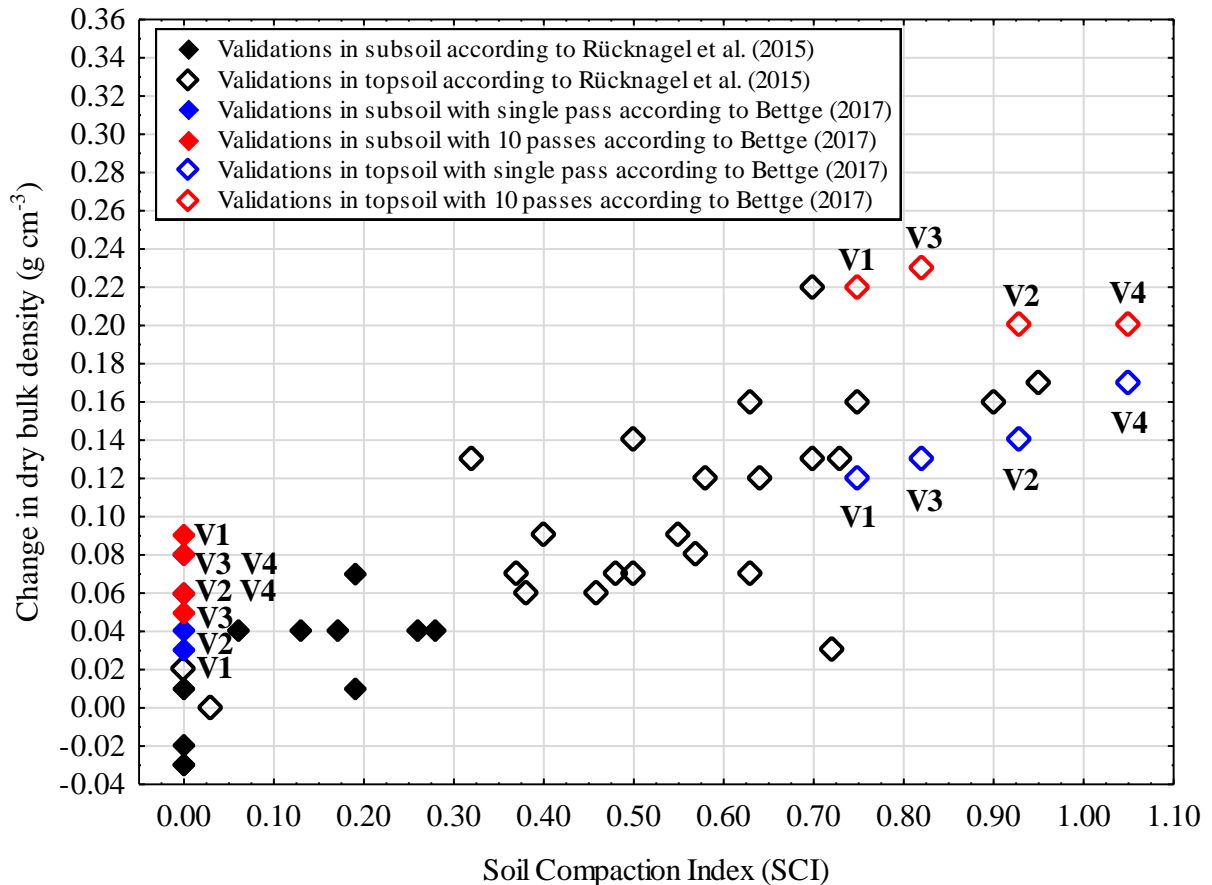


Figure 5.5.1. Relationship between calculated Soil Compaction Index (SCI) and the change in dry bulk density at module validations of Rücknagel et al. (2015, chapter 2.2.) and Bettge (2017) with treatments V1: 2.4 t wheel load and 80 kPa inflation pressure, V2: 2.4 t wheel load and 160 kPa inflation pressure, V3: 4.5 t wheel load and 80 kPa inflation pressure, V4: 4.5 t wheel load and 160 kPa inflation pressure.

In a more recent experiment to validate the module by Bettge (2017), however, there are indications that multiple passes that take place on the same day will have a stronger compression effect than single passes, with the same calculated Soil Compaction Index (SCI) (Fig. 5.5.1 and 5.5.2). Locations 7.1. (“Fortuna II 20”) and 7.2. (“Fortuna II 35”) from the previous module validation, both of which involve multiple passes along permanent traffic lanes, also fit in with this trend (chapter 2.2.). The higher overall compaction effect with multiple passes is supported firstly by the associated longer loading time in the field (Fazekas and Horn, 2005). On the other hand, the soil compression tests which serve as the basis of the algorithms described here were

carried out with a relatively long loading time of 180 minutes, which should result in consolidation. The more intensive vertical stress propagation in the soil in the case of multiple passes may also be of importance (Horn et al., 2003), although this has not yet been taken into account in the model algorithms. The modelling does not take into account dynamic effects and shear stress components, which increase in the case of multiple passes and can also lead to a significant increase in the compression effect (Lebert et al., 1987; Horn et al., 2003; Peth et al., 2010).

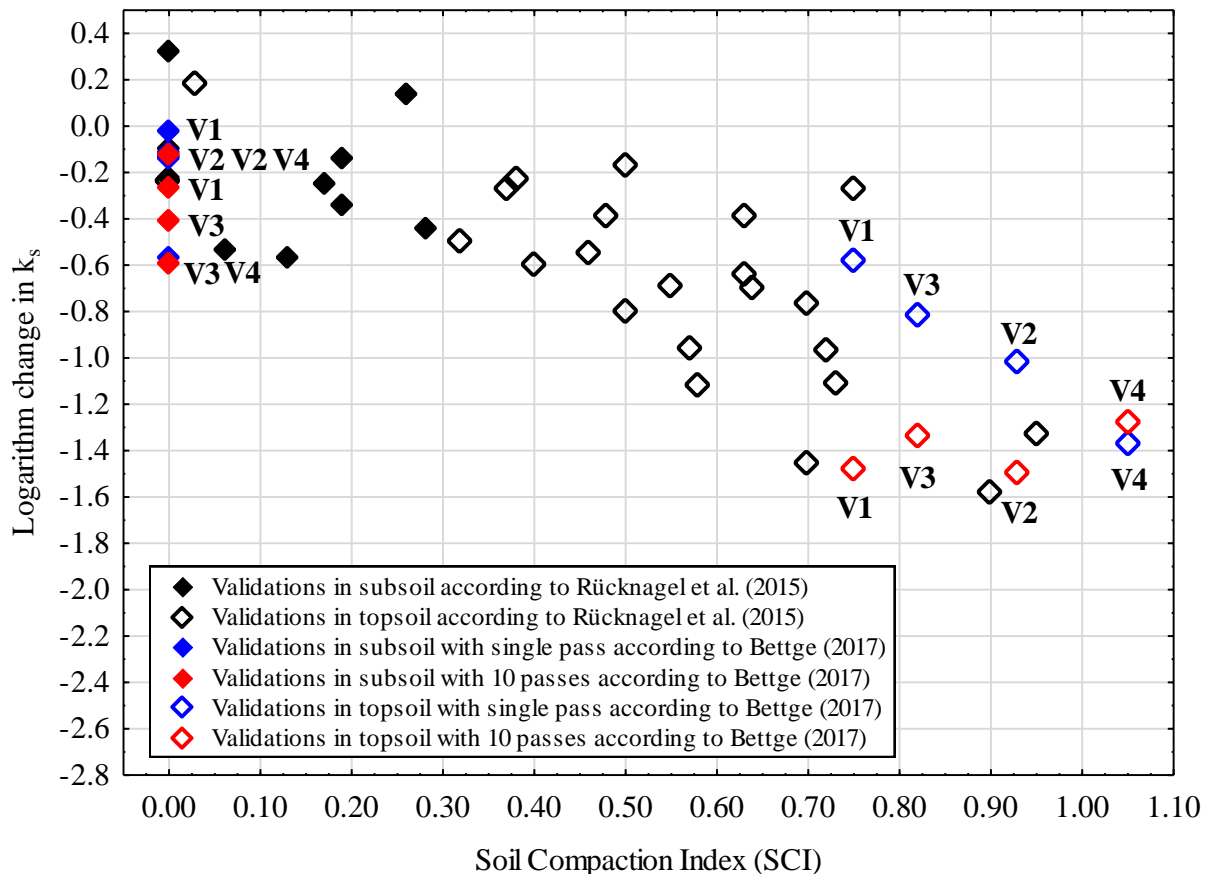


Figure 5.5.2. Relationship between calculated Soil Compaction Index (SCI) and the logarithm change in saturated hydraulic conductivity (k_s) at module validations of Rücknagel et al. (2015, chapter 2.2.) and Bettge (2017) with treatments V1: 2.4 t wheel load and 80 kPa inflation pressure, V2: 2.4 t wheel load and 160 kPa inflation pressure, V3: 4.5 t wheel load and 80 kPa inflation pressure, V4: 4.5 t wheel load and 160 kPa inflation pressure.

In the investigations by Bettge (2017), it also becomes apparent, particularly in the topsoil (20 cm depth), that the frequency of passes masks the effect of increasing wheel loads and tyre inflation pressures. For example, a similar increase in dry bulk density, or a decrease in saturated hydraulic conductivity, was observed in all variants that were driven over ten times, regardless of wheel load and tyre inflation pressure. An explanation for this could lie in the rather high overall compression effect in the variants with multiple passes. All of these have air capacities of only 4.5 to 5.2 vol.% after the passes, i.e. most of the remaining pore space is filled

with water. In connection with the primary consolidation of the soil, however, the pore water pressure is only slowly reduced during loading (Fazekas and Horn, 2005), which means that the theoretically expected higher compression effect of higher wheel load and higher tyre inflation pressure no longer applies. The observations suggest that further systematic trials, with staggered frequencies of vehicle passes in interaction with machine parameters, different site characteristics and soil water contents, should be carried out in order to introduce a correction factor for the frequency of vehicle passes or to adjust the algorithms accordingly.

However, including the experimental results of Bettge (2017) in the module validation, including the multiple passes, has only a minimal effect on the correlation coefficients in the context of the calculated Soil Compaction Index (SCI) and the change of the soil physical parameters. They are $r = 0.81$ ($p < 0.001$) between the Soil Compaction Index (SCI) and the changes in dry bulk density (previously $r = 0.83$; $p < 0.001$) and $r = -0.80$ ($p < 0.001$) between the Soil Compaction Index (SCI) and the change in saturated hydraulic conductivity (previously $r = -0.77$; $p < 0.001$).

5.6. Discussion of applications of the module concept

Most model concepts and PC-based compaction models, such as *TERRANIMO*® (Stettler et al., 2019) or *TASC* (Diserens, 2010), lack any relation to specific cultivation systems or crop rotations, and nor is there any concrete link between the annual cycle of soil water content and the actual date when the machines are used, which is why they do not adequately consider the conditions of complex agricultural systems. The module in *REPRO*, on the other hand, allows a historical as well as current and preventive assessment of the risk of soil compaction from individual machines, cultivation systems, crop rotations or even farms up to a complex scale, without the need to conduct extensive measurements. On this basis, the model concept can be used to plan crop rotations at farm level, or to schedule the use and investment of machinery, including from a soil protection perspective. The analysis and evaluation examples in chapters 4.1. to 4.3. should also be viewed in this context. They represent an application of the algorithms developed before, with special attention paid to plant cultivation issues. By combining classical wheeling or field trials with the modelling, it is thus possible to map and verify the interactions between the use of machinery and the crop rotation or crop type, taking into account various climatic conditions with regard to the risk of compaction. In chapter 4.1., for example, by modelling the risk of compaction it is possible to explain the at times less favourable soil structure beneath catch crops in practice as a result of the additional working steps required in catch cropping. This has never been considered in previous work on the effect of catch crops on the soil structure (Carof et al., 2007). As a consequence, however, it may also be possible to derive recommendations for agricultural practice for the design of agro-environmental programmes, in order to make better use of the positive effects of catch crop plants on the soil structure, e.g. refraining from operations to break up catch crop plants in early spring. On the other hand, the example in chapter 4.2. shows how a slightly frozen soil surface can reduce the risk of soil

compaction, which would in turn be beneficial for the shredding of catch crop plants in early spring. Chapter 4.2. is also a very specific example of the use of a module component.

Chapter 4.3. contains an analysis of the compaction risk for entire crop rotations and a model farm. By comparing soil physical measurements with the calculated Soil Compaction Indices (SCI), this section of the study also represents a further validation of the overall module. Taking into account the seasonal soil water contents and typical machinery used in the field, it is possible to identify all procedures and equipment presenting a high risk of compaction, and concrete recommendations for reducing the risk of compaction can be made and their effectiveness determined. In addition to the obvious high-risk methods such as sugar beet harvesting (Arvidsson, 2001), which have been identified by previous studies, it is also possible to identify methods that do not appear to have a medium to high risk of causing soil compaction, such as fertilization and cereal harvesting. Using the example of a site (Adenstedt) and date (7 August 2016), Kuhwald et al. (2018) also report large areas at a depth of 20 cm and 35 cm with a medium to extremely high risk of soil compaction for cereals, which in this case is presumably related to the cereal harvesting operation. For the Aiterhofen model farm, however, no more than an average compaction risk is reported for the winter wheat harvest. Consequently, in chapter 4.3. halving the hopper load and simultaneously adjusting the tyre inflation pressure during the sugar beet and winter wheat harvest are identified as a particularly effective measure to reduce the compaction risk. In an expert-based approach by Lorenz et al. (2016) to a soil-conserving use of machinery, which used various example sites and methods in Germany, including the sugar beet harvest, the positive effect of halving the hopper load is, however, not always so clear. While in the topsoil halving the hopper load did actually result in an increase in the number of so-called trafficability days, of between 3 and 24 days at 5 of the 9 example sites, for the subsoil the number of trafficability days increased at just 2 sites, by 7 and 23 days respectively. Overall, at many sites the estimates of the number of trafficability days is very high, at 91 out of a maximum of 91 possible days.

Even more aggregated is the calculation of the risk of soil compaction over a period of two years in the past for 15 complete farms in chapter 2.2. Distributed throughout Germany, the farms cover a total area of about 9600 ha and generally have a low Soil Compaction Index (SCI) of < 0.10 at a depth of 35 cm, which means that the risk of soil compaction is low. Based on the literature, it is not easy to categorise this compaction risk, because in most cases analyses are not as aggregated as those presented in this paper; other result parameters are indicated or there is a lack of spatial and temporal comparability. However, against the backdrop of the 10–20 % (UBA, 2013) share of compacted arable land in Germany estimated by experts from soil protection and agricultural administrations, these low Soil Compaction Indices (SCIs) do seem plausible, even though the complex method of calculating the Soil Compaction Index (SCI) on farms does not in itself allow specific compacted areas to be identified directly. Using algorithms very similar to those in the soil compaction module in *REPRO*, the *SaSCiA* model also calculates the risk of soil compaction for two regions in northern Germany, taking into account the cultivation systems and crop rotations (Kuhwald et al., 2018). On the whole, the results

show a higher spatial and temporal variability of the compaction risk, but are unfortunately not aggregated to an overall result at farm level.

Common to all of the application examples in this study is the fact that they essentially show no more than low to medium compaction risks at the different levels of the summarised Soil Compaction Indices (SCI). On the one hand, this underlines how soil compaction can be one of the most important causes of possible soil degradation, especially in countries with highly mechanised agriculture (Hamza and Anderson, 2005). On the other, however, it also emphasises that an exaggeratedly populist assessment of the problem, such as that of Beste (2015) or BUND (2019), is not appropriate for developing objective solutions.

5.7. Options for further validations and development

Of the 16.7 million ha of agricultural land in Germany alone, 11.8 million ha are used as arable land (Federal Statistical Office, 2018). The algorithms presented here for deriving soil strength, and the *REPRO* module for predicting the risk of soil compaction, were developed and validated especially for these sites and farming conditions. During this development and validation phase, however, it was not possible to include the entire range of texture properties or TOC contents found on arable land. For this reason, it will be necessary in future to take into account less common arable sites as well, in order to enable universal application of the modelling concept without site-related restrictions. High priority should also be given to conducting validations on arable sites, particularly in view of the uncertainties already described with regard to the impact of multiple passes.

In principle, the algorithms would also be suitable for calculating zones with varying degrees of compaction on arable land from GPS-supported records of the lanes left by agricultural machinery, as for example in Kroulik et al. (2012), and for then deriving maps for zone-specific tillage of the topsoil. Lubetzki (2013) has already carried out some preliminary work in this regard.

In addition to arable land, there is a considerable proportion of permanent grassland in Germany, totalling some 4.7 million ha (equivalent to approx. 28 % of all agricultural land) (Statistisches Bundesamt, 2018). Grassland farming with agricultural machinery induces high soil stresses in the topsoil in particular (Stahl et al., 2009), which is why it is also useful to use mathematical algorithms and models such as *REPRO* to estimate the risk of compaction on grassland soils. Grassland sites, however, have a number of significant characteristics. In contrast to arable land, they feature constant vegetation with perennial plant species, especially grasses, but also herbs and legumes, and thus extensive, multi-layered rooting year-round. This root penetration can contribute to an altered stability of the soil structure (Trückmann, 2011). Grassland soils are partly characterised by a higher gravel content (Stahl et al., 2009) and higher organic carbon contents (BMEL, 2018). Compared to arable land, grassland sites often display more diversified site conditions with different soil water contents, ground surface and forms of

use (Opitz von Boberfeld, 1994). Given all these characteristics, applying the algorithms described in this study, or the entire *REPRO* module, may lead to an inaccurate or limited calculation of the risk of soil compaction on grassland sites. For this reason, it would be useful to continue this work by examining the individual algorithms, such as the relationship between visual evaluation of the soil structure and soil strength, the change in soil strength with decreasing water content, and the calculation of the vertical soil stress in the load axis, as well as the entire *REPRO* module, for grassland sites specifically – and to adapt these if necessary.

Similar validations and adjustments are also necessary for any application to forest sites, as widespread forest soil types also have a number of site-specific characteristics. These include shallow and gravel-rich rendzinas, brown earths, podzols and pseudogley soils with a wide pH range, varying water balance and a superficial layer of organic matter (Dalhäuser, 1998). Forest soils are sometimes located on extreme slopes and are permanently rooted with strongly woody but also fine roots. Moreover, similar to grassland soils, forest soils cannot be treated to loosen compaction, which is why there is a greater need here to minimise the risk of compaction in the topsoil than in arable soils. Since forestry involves the creation of logging roads, which are used for all traffic, especially during harvesting, a high number of vehicle passes often occur in forests. On the whole, it would be very important to be able to estimate the risk of compaction in forest soils using model concepts like *REPRO*, because increasingly heavy forestry machines induce high vertical soil stresses (Riggert et al., 2016) and soil compaction in forest soils has numerous negative effects on biological soil properties as well as tree growth. In addition, the risk of soil erosion and increasing greenhouse gas emissions is increasing (Cambi et al., 2015). This is particularly relevant because forests, at 10.6 million ha, cover an extraordinarily large area in Germany (Statistisches Bundesamt, 2019).

Ultimately, in view of the broad application of the compaction module in *REPRO*, it would be advantageous to make it available online. By combining the soil compaction module with weather forecasts, up-to-date soil water contents or soil water balance models, it would even be possible to predict the compaction risk a few days in advance. This would allow short-term operational estimates regarding the use of agricultural equipment, and it could be used to estimate the current risk of compaction. The younger generation of users in particular are more inclined to use online or PC-based models (Mauer, 2015). The *Terranimo*® model (Stettler et al., 2019) is certainly something of a role model in this regard.

6. General conclusions

In the following, a number of basic conclusions are drawn with regard to the framework described at the outset and the objectives of this study.

Methodological aspects, model conception and validation

First of all, the methodical investigations for the determination of precompression stress as a parameter for soil strength make it clear that above all the graphical method for deriving the precompression stress is in principle suitable for determining reproducible values. Furthermore, all arable sites investigated show more or less typical stress/strain behaviour, even at sites with very low clay or very high sand contents. Numerous methodological differences on the international level should therefore not lead to a general rejection of the parameter “precompression stress”, but rather contribute to further defining and standardising international standards. The results of the study also show that precompression stress is related to other important soil properties and functions, such as packing density as a quality parameter for the soil structure, and that precompression stress is therefore fundamentally suitable as a guideline for soil strength in comparison with other soil structure parameters.

The entire *REPRO* module for assessing the risk of compaction was successfully validated in numerous tests. This overall validation provides further indirect indications as to the accuracy of the individual algorithms, as well as those that were not specifically tested and their interaction in the overall context. The logarithmic amount by which the calculated soil stress exceeds the soil strength is shown as the Soil Compaction Index (SCI) and is thus closely related to the average slope of the virgin compression lines in the stress/dry bulk density diagram. This relationship between the SCI and the change in dry bulk density can be mapped very well across all module validations. In addition, the change in the saturated hydraulic conductivity also shows a close relationship with the calculated SCI. Overall, the SCI thus allows a comparison of the risk of compaction across different trials, sites and depths. In addition, the model validation tests make it clear that the precompression stress values determined in the uniaxial laboratory test can certainly be used to derive the soil compaction risk in the field. However, there are indications that multiple passes by machinery on the same day, despite no changes to the calculated SCI, actually have a higher compaction effect than single passes, although the soil compression tests on which the algorithms are based were performed with a relatively long load duration until consolidation. There are also indications that the frequency of vehicle passes is more important than the effect of increasing wheel loads and tyre inflation pressures. As a consequence of the observations, additional systematic experiments with staggered traffic frequencies – in interaction with machine parameters, different site properties and soil water contents – should be carried out in order to modify the algorithms if necessary.

Algorithms for determination of soil strength

The various innovative individual algorithms developed within the framework of this research, such as the adjustment of the precompression stress at -6 kPa matric potential to reflect the

actual water content at the time of wheeling, the adjustment of the precompression stress at -6 kPa matric potential to reflect the gravel content in soil, the standard values for the precompression stress derived from the tillage trials, and the derivation of the precompression stress at -6 kPa matric potential on the basis of the packing density determined in the field, were implemented in the *REPRO* model in the module for assessing the risk of soil compaction, and were successfully validated in each case.

Applications of the module concept

From the modelling examples relevant to crop cultivation, it can first be generally deduced that general wheel load limits alone do not adequately address the complex conditions of different cultivation systems. Nonetheless, it should be ensured that wheel loads on farms do not increase any further or, depending on the cultivation system, that they are even reduced. The examples also show that the module can be used to assess the risk of soil compaction not only for individual agricultural machines, but also on an aggregated basis for crop rotations, complex cultivation systems or entire farms. On this basis, the model concept can be useful for planning crop rotations at farm level, or for scheduling the use and investment of machinery, including from a soil protection perspective, or for addressing scientific questions concerning soil compaction. More globally, the model concept can help decision-makers in agricultural and environmental policy to plan and review specific agro-environmental measures. As such, the concept differs significantly from other model approaches not only in terms of small details.

Synthesis and general discussion

Overall, there is considerable variation in the precompression stresses determined in the course of this work on different soils at comparable matric potential, depending on the intensity of soil tillage, sampling depth, and general soil structure properties, such as for example aggregate shape or aggregate arrangement. These factors are more important than texture, which is why soil texture should be viewed critically as a sole criterion for classifying precompression stress. Some algorithms and regressions have found their way into other models, concepts and practical guides besides *REPRO*, which testifies to their validity and practicability.

If this work were to be continued, however, it would make sense to test the individual algorithms for less common arable sites and adjust them if necessary, in order to make it possible to apply them universally without site restrictions. On arable land, one conceivable option for further development would be to use the model algorithms to derive maps for zone-specific tillage of the topsoil. In addition, the whole *REPRO* module should be specially tested, and adjusted if necessary, for typical grassland and forest sites, because preventing soil compaction in these areas is also a major challenge. Ideally, the module would be made available online, allowing users to predict individual compaction risk a few days in advance.

7. References

- Ad-Hoc Arbeitsgruppe Boden, 2005. *Bodenkundliche Kartieranleitung*. 5. Auflage. Stuttgart, Schweizerbart'sche Verlagsbuchhandlung.
- Alakukku, L., 1996. Persistence of soil compaction due to high axle load traffic. II. Long-term effects on the properties of fine-textured and organic soils. *Soil & Tillage Research* 37, 223-238.
- Amon, T., Amon, B., Kryvoruchko, V., Machmüller, A., Hopfner-Sixt, K., Bodiroza, V., Hrbek, R., Friedel, J., Pötsch, E., Wagentristsl, H., Schreiner, M., Zollitsch, W., 2007. Methane production through anaerobic digestion of various energy crops grown in sustainable crop rotations. *Bioresource technology* 98, 3204-3212.
- Angers, D.A., Caron, J., 1998. Plant-induced changes in soil structure: Processes and feedbacks. *Biogeochemistry* 42, 55-72.
- Arthur, E., Schjonning, P., Moldrup, P., Tuller, M., de Jonge, L.W., 2013. Density and permeability of a loess soil: Long-term organic matter effect and the response to compressive stress. *Geoderma* 193-194, 236-245.
- Arvidsson, J., 2001. Subsoil compaction caused by heavy sugarbeet harvesters in southern Sweden. I. Soil physical properties and crop yield in six field experiments. *Soil & Tillage Research* 60, 67-78.
- Arvidsson, J., Keller, T., 2004. Soil precompression stress I. A survey of Swedish arable soils. *Soil & Tillage Research* 77, 85-95.
- Arvidsson, J., Keller, T., 2007. Soil stress affected by wheel load and tyre inflation pressure. *Soil & Tillage Research* 96, 284-291.
- Arvidsson, J., Sjöberg, E., van den Akker, J.J.H., 2003. Subsoil compaction by heavy sugarbeet harvesters in southern Sweden III. Risk assessment using a soil water model. *Soil & Tillage Research* 73, 77-87.
- Arvidsson, J., Trautner, A., van den Akker, J.J.H., 2000. Subsoil compaction-risk assessment and economic consequences. *Advances in GeoEcologie* 32, 3-12.
- Azooz, R.H., Arshad, M.A., 1996. Soil infiltration and hydraulic conductivity under long-term no-tillage and conventional tillage systems. *Canadian Journal of Soil Science* 76, 143-152.
- Babalola, O., Lal, R., 1977. Subsoil gravel horizon and maize root growth. I. Gravel concentration and bulk density effects. *Plant and Soil* 46, 337-346.
- Ball, B.C., Robertson, E.A.G., 1994. Effects of uniaxial compaction on aeration and structure of ploughed or direct drilled soils. *Soil & Tillage Research* 31, 135-148.
- Ball-Coelho, B.R., Roy, R.C., Swanton, C.J., 2000. Tillage and cover crop impacts on aggregation of a sandy soil. *Can. J. Soil Sci.* 80, 363-366.
- Batjes, N.H., 1997. A world dataset of derived soil properties by FAO-UNESCO soil unit for global modelling. *Soil Use and Management* 13, 9-16.
- Baumgartl, T., Köck, B., 2004. Modeling volume change and mechanical properties with hydraulic models. *Soil Sci. Soc. Am. J.* 68, 57-65.
- BBodSchG, 1998. Gesetz zum Schutz vor schädlichen Bodenveränderungen und zur Sanierung von Altlasten (Bundes-Bodenschutzgesetz - BbodSchG). Bundes-Bodenschutzgesetz vom 17. März 1998 (BGBl. I S. 502), das zuletzt durch Artikel 3 Absatz 3 der Verordnung vom 27. September 2017 (BGBl. I S. 3465) geändert worden ist.
- Bechmann, M., Stalnacke, P., Kvaerno, S., Eggstad, H.O., Oygarden, L., 2009. Integrated tool for risk assessment in agricultural management of soil erosion and losses of phosphorus and nitrogen. *Science of the Total Environment* 407, 749-759.
- Berisso, F.E., Schjonning, P., Keller, T., Lamande, M., Etana, A., de Jonge, L.W., Iversen, B.V., Arvidsson, J., Forkmann, J., 2012. Persistent effects of subsoil compaction on pore size distribution and gas transport in a loamy soil. *Soil & Tillage Research* 122, 42-51.
- Berisso, F.E., Schjonning, P., Keller, T., Lamande, M., Simojoki, A., Iversen, B.V., Alakukku, L., Forkman, J., 2013. Gas transport and subsoil pore characteristics: Anisotropy and long-term effects of compaction. *Geoderma* 195-196, 184-191.
- Berisso, F.E., Schjonning, P., Lamande, M., Weisskopf, P., Stettler, M., Keller, T., 2013. Effects of the stress field induced by a running tyre on the soil pore system. *Soil & Tillage Research* 131, 36-46.
- Berli, M., Kirby, J.M., Springmann, S.M., Schulin, R., 2003. Modelling compaction of agricultural subsoils by tracked heavy construction machinery under various moisture conditions in Switzerland. *Soil & Tillage Research* 73, 57-66.

- Berli, M., Kulli, B., Attinger, W., Keller, M., Leuenberger, J., Flühler, H., Springmann, S. M., Schulin, R., 2004. Compaction of agricultural and forest subsoils by tracked heavy construction machinery. *Soil & Tillage Research* 75, 37-52.
- Beste, A., 2015. Intensivfeldbau: Industrielle Landwirtschaft mit Zukunftsproblemen. In: Chemnitz, C., Weigelt, J., (Eds.). *Bodenatlas 2015*, 4. Auflage, 18-19.
- Bettge, E., 2017. Auswirkung von Radlast, Reifeninnendruck und Überrollhäufigkeit auf bodenphysikalische und mechanische Parameter vor der Aussaat von Sojabohnen (*Glycine max* [L.] Merr.). Bachelorarbeit Martin-Luther-Universität Halle-Wittenberg. 61 pages.
- Beven, K., Germann, P., 1982. Macropores and Water Flow in Soils. *Water Resources Research* 18, 1311-1325.
- Beylich, A., Oberholzer, H.-R., Schrader, S., Höper, H., Wilke, B.-M., 2010. Evaluation of soil compaction effects on soil biota and soil biological processes in soils. *Soil & Tillage Research* 109, 133-143.
- Birkás, M., Jolánkai, M., Gyuricza, C., Percze, A., 2004. Tillage effects on compaction, earthworms and other soil quality indicators in Hungary. *Soil & Tillage Research* 78, 185-196.
- Blanco-Canqui, H., Lal, R., 2009. Crop residue removal impacts on soil productivity and environmental quality. *Critical Reviews in Plant Sciences* 28, 139-163.
- BMEL, 2018. Humus in landwirtschaftlich genutzten Böden Deutschlands - Ausgewählte Ergebnisse der Bodenzustandserhebung. Bundesministerium für Ernährung und Landwirtschaft (BMEL), Bonn, 48 pages.
- Böhm, W., 1979. *Methods of studying root systems*. Berlin: Springer.
- Bohne, H., Hartge, K.-H., 1990. Die Bedeutung vertikaler Grobporen für die Ausnutzung von Wasser und Ca sowie K in horizontaler Richtung. *Zeitschrift Pflanzenernährung Bodenkunde* 153, 11-14.
- Boizard, H., Capowiez, Y., Leonard, J., Cadoux, S., Lheureux, S., Cousin, I., Roger-Estrade, J., Richard, G., 2009. Soil structure regeneration after compaction in a loamy soil in Northern France: The influence of climate and earthworms. *ISTRO 18th Triennial Conference Proceedings*, 15-19 June 2009, Izmir-Turkey, T1 49, 1-6.
- Boizard, H., Richard, G., Roger-Estrade, J., Dürr, C., Boiffin, J., 2002. Cumulative effects of cropping systems on the structure of the tilled layer in northern France. *Soil & Tillage Research* 64, 149-164.
- Bojorquez-Tapia, L.A., Cruz-Bello, G.M., Luna-Gonzalez, L., 2013. Connotative land degradation mapping: A knowledge-based approach to land degradation assessment. *Environmental Modelling & Software* 40, 51-64.
- Borin, M., Menini, C., Sartori, L., 1997. Effects of tillage systems on energy and carbon balance in north-eastern Italy. *Soil & Tillage Research* 40, 209-226.
- BoSchätzG, 1970. Bundesgesetz vom 9. Juli 1970 über die Schätzung des landwirtschaftlichen Kulturbodens (Bodenschätzungsgesetz 1970 - BoSchätzG 1970). *BGBI. Nr. 233/1970*.
- Böttcher, F., Schmidt, M., Möbius, A., Haferkorn, U., 2014. Wasserhaushaltsuntersuchungen im landwirtschaftlichen Zwischenfruchtanbau. In: Goldberg, V., Bernhofer, C. (Eds.): *Tharandter Klimaprotokolle*, Band 20, 42-43.
- Bradford, J.M., Gupta, S.C., 1986. Compressibility. In: Klute, A. (Ed.): *Methods of soil analysis. Part 1: Physical and mineralogical methods. Second Edition*. 479-492.
- Brakensiek, D.L., Rawls, W.J., 1994. Soil containing rock fragments: effects on infiltration. *Catena* 23, 99-110.
- Brauer-Siebrecht, W., Jacobs, A., Christen, O., Götze, P., Koch, H.-J., Rücknagel, J., Märländer, B., 2016. Silage maize and sugar beet for biogas production in rotations and continuous cultivation: Dry matter and estimated methane yield. *Agronomy* 6, DOI: 10.3390/agronomy6010002.
- Breland, T.A., 1995. Green manuring with clover and ryegrass catch crops undersown in spring wheat: effects on soil structure. *Soil Use and Management* 11, 163-167.
- Brennan, J., Hackett, R., McCabe, T., Grant, J., Fortune, R.A., Forristal, P.D., 2014. The effect of tillage system and residue management on grain yield and nitrogen use efficiency in winter wheat in a cool Atlantic climate. *European Journal of Agronomy* 54, 61-69.
- Bronick, C.J., Lal, R., 2005. Soil structure and management: a review. *Geoderma* 124, 3-22.
- Brunotte, J., Brandhuber, R., Vorderbrügge, T., 2013. Vorsorge gegen Bodenverdichtungen. *AID 3614/2013. Gute fachliche Praxis Bodenbewirtschaftung und Bodenschutz*. 21-69.
- Brunotte, J., Lorenz, M., Sommer, C., Harrach, T., Schäfer, W., 2008. Verbreitung von Bodenschadverdichtungen in Südniedersachsen. *Berichte über Landwirtschaft* 86, 262-284.
- Brunotte, J., Sommer, C., 2000. Gute fachliche Praxis beim Einsatz leistungsfähiger Erntetechnik. *Landtechnik* 1/2000, 14-16.

- Buhre, C., Apfelbeck, R., Hesse, F., van Look, M., Mielke, C., Ladewig, E., 2014. Survey on production technology - regional differences in sugar beet production. *Sugar Industry* 139, 40-47.
- BUND, 2019. Über die Hälfte der Böden im Norden sind stark verdichtet! Pressemitteilung BUND 09.04.2019. <https://www.bund-mecklenburg-vorpommern.de/service/presse/detail/news/ueber-die-haelfte-der-boeden-im-norden-sind-stark-verdichtet/>
- Cambi, M., Certini, G., Neri, F., Marchi, E., 2015. The impact of heavy traffic on forest soils: A review. *Forest Ecology and Management* 338, 124-138.
- Canarache, A., Horn, R., Colibas, I., 2000. Compressibility of soils in a long term field experiment with intensive deep ripping in Romania. *Soil & Tillage Research* 56, 185-196.
- Capowiez, Y., Cadoux, S., Bouchant, P., Ruy, S., Roger-Estrade, J., Richard, G., Boizard, H., 2009. The effect of tillage type and cropping system on earthworm communities, macroporosity and water infiltration. *Soil & Tillage Research* 105, 209-216.
- Carman, K., 2002. Compaction characteristics of towed wheels on clay loam in a soil bin. *Soil & Tillage Research* 65, 37-43.
- Carof, M., de Tourdonnet, S., Coquet, Y., Hallaire, V., Roger-Estrade, J., 2007. Hydraulic conductivity and porosity under conventional and no-tillage and the effect of three species of cover crop in northern France. *Soil Use and Management* 23, 230-237.
- Casagrande, A., 1936. The determination of pre-consolidation load and its practical significance. In: *Int. Conf. on Soil Mech. and Found. Eng. Proc. of ICSMFE*. Cambridge, MA, 22-26 June 1936. vol. 3. Cambridge, MA, 93-108.
- Castoldi, N., Bechini, L., 2010. Integrated sustainability assessment of cropping systems with agro-ecological and economic indicators in northern Italy. *European Journal of Agronomy* 32, 59-72.
- Cavaliere, K.M.V., Arvidsson, J., Da Silva, A.P., Keller, T., 2008. Determination of precompression stress from uniaxial compression tests. *Soil & Tillage Research* 98, 17-26.
- Chamen, W.C.T., Moxey, A.P., Towers, W., Balana, B., Hallett, P.D., 2015. Mitigating arable soil compaction: A review and analysis of available cost and benefit data. *Soil & Tillage Research* 146, 10-25.
- Chamen, W.C.T., Vermeulen, G.D., Campbell, D.J., Sommer, C., 1992. Reduction of traffic-induced soil compaction: a synthesis. *Soil & Tillage Research* 24, 303-318.
- Chan, K.Y., Heenan, D.P., 1996. The influence of crop rotation on soil structure and soil physical properties under conventional tillage. *Soil & Tillage Research* 37, 113-125.
- Chaplain, V., Defosse, P., Delarue, G., Roger-Estrade, J., Dexter, A.R., Richard, G., Tessier, D., 2011. Impact of lime and mineral fertilizers on mechanical strength for various soil pHs. *Geoderma* 167-168, 360-368.
- Chichester, F.W., Richardson, C.W., 1992. Sediment and nutrient loss from clay soils as affected by tillage. *Journal of Environmental Quality* 21, 587-590.
- Chinkulkijniwat, A., Man-Koksung, E., Uchaipichat, A., Horpibulsuk, S., 2010. Compaction characteristics of non-gravel and gravelly soils using a small compaction apparatus. *Journal of ASTM International*, Vol. 7, No 7, Paper ID JAI102945.
- Curry, J.P., Schmidt, O., 2007. The feeding ecology of earthworms - a review. *Pedobiologia* 50, 463-477.
- da Veiga, M., Horn, R., Reinert, D.J., Reichert, J.M., 2007. Soil compressibility and penetrability of an Oxisol from southern Brazil, as affected by long-term tillage systems. *Soil & Tillage Research* 92, 104-113.
- Dalhäuser, H., 1998. *Der forstliche Standort*. In: *Waldwirtschaft*. 5. Auflage, BLV Verlagsgesellschaft mbH, München.
- Damm, S., Hofmann, B., Gransee, A., Christen O., 2013. Zur Wirkung von Kalium auf ausgewählte bodenphysikalische Eigenschaften und den Wurzeltiefgang landwirtschaftlicher Kulturpflanzen. *Archives of Agronomy and Soil Science* 59, 1-19.
- Dawidowski, J.B., Koolen, A.J., 1994. Computerized determination of the pre-consolidation stress in compaction testing of field core samples. *Soil & Tillage Research* 31, 277-282.
- Dawidowski, J.B., Morrison, J.E., Snieg, M., 2000. Determination of soil precompaction stress from in situ tests. *Advances in GeoEcology* 32, 411-418.
- DBV, 2018. *Situationsbericht 2018/19, Trends und Fakten zur Landwirtschaft*. Berlin, Deutscher Bauernverband e.V.
- Défosse, P., Richard, G., 2002. Models of soil compaction due to traffic and their evaluation. *Soil & Tillage Research* 67, 41-64.

- Défosse, P., Richard, G., Boizard, H., O'Sullivan, M.F., 2003. Modeling change in soil compaction due to agricultural traffic as function of soil water content. *Geoderma* 116, 89-105.
- Deubel, A., Hofmann, B., Orzessek, D., 2011. Long-term effects of tillage on stratification and plant availability of phosphate and potassium in a loess Chernozem. *Soil & Tillage Research* 117, 85-92.
- Deumelandt, P., Hofmann, B., Christen, O., 2010. Effect of various rotations and fallow periods on soil quality parameters and yield in the sugar beet rotation experiment Etzdorf. *Archives of Agronomy and Soil Science* 56, 393-404.
- Dexter, A.R., 1988. Advances in characterization of soil structure. *Soil & Tillage Research* 11, 199-238.
- Dias Junior, M.S., Pierce, F.J., 1995. A simple procedure for estimating preconsolidation pressure from soil compression curves. *Soil Technology* 8, 139-151.
- DIN 18135, 2012. Baugrund - Untersuchung von Bodenproben - Eindimensionaler Kompressionsversuch. Beuth Verlag.
- DIN 19682-10 2007. Methods of soil investigations for agricultural water engineering - Field tests - Part 10: Description and evaluation of soil structure. Berlin, Beuth publishing house.
- DIN ISO 11274, 1998. Soil quality - Determination of the water retention characteristics - Laboratory methods.
- Ding, G., Liu, X., Herbert, S., Novak, J., Amarasiriwardena, D., Xing, B., 2006. Effect of cover crop management on soil organic matter. *Geoderma* 130, 229-239.
- Diserens, E., 2010. TASC V2.0. Excel-Anwendung. Agroscope ART 2010.
- Diserens, E., Spiess, E., 2004. Wechselwirkung zwischen Fahrwerk und Ackerboden. TASC: Eine PC - Anwendung zum Beurteilen und Optimieren der Bodenbeanspruchung. TÄNIKON: FAT Berichte Nr. 613.
- Diserens, E., Steinmann, G., 2002. Calculation of pressure distribution in moist arable soils in eastern Switzerland: A simple model approach for the practice. *Environmental Geomechanics - Monte Verita*. 413-421.
- DLG, 2019. DLG-Zertifikat Nachhaltige Landwirtschaft, Infobroschüre. Fachzentrum Land- und Ernährungswirtschaft. 18 pages.
- Donaghe, R.T., Torrey, V.H., 1994. A compaction test method for soil-rock mixtures in which equipment size effects are minimized. *Geotechnical testing journal, GTJODJ*, Vol. 17, No. 3, 363-370.
- D'Or, D., Destain, M.-F., 2014. Toward a tool aimed to quantify soil compaction risks at a regional scale: Application to Wallonia (Belgium). *Soil & Tillage Research* 144, 53-71.
- Dumbeck, G., 2000. Landwirtschaftliche Rekultivierung im rheinischen Braunkohlenrevier unter besonderer Berücksichtigung bodenkundlicher Aspekte. *Rundgespräche der Kommission für Ökologie*, Bd. 20 Bergbau-Folgeschäden und Ökosysteme, 75-90.
- Duttman, R., Schwanebeck, M., Nolde, M., Horn, R., 2014. Predicting soil compaction risks related to field traffic during silage maize harvest. *Soil Sci. Soc. Am. J.* 78, 408.
- DVWK, 1995. Gefügestabilität ackerbaulich genutzter Mineralböden, Merkblatt 234, Teil 1: Mechanische Belastbarkeit. Bonn: Kommissionsvertrieb Wirtschafts- und Verlagsgesellschaft Gas und Wasser mbH.
- DWA, 2019. Berufenes Mitglied in DWA-Arbeitsgruppe GB-7.5: Verdichtungsgefährdung und Befahrbarkeit von Böden.
- DWD, 2014. Deutscher Wetterdienst. ftp://ftp-cdc.dwd.de/pub/CDC/observations_germany/climate/multi_annual/mean_81-10/.
- Eckert, H., Paul, R., Fettisov, A., 2006. Einschätzung des Beratungsbedarfs für den Schutz der ackerbaulich genutzten Böden Thüringens vor Schadverdichtung. www.tll.de/ainfo/pdf/bods0207.pdf
- Etana, A., Larsbo, M., Keller, T., Arvidsson, J., Schjonning, P., Forkmann, J., Jarvis, N., 2013. Persistent subsoil compaction and its effect on preferential flow patterns in a loamy till soil. *Geoderma* 192, 430-436.
- FAO, 1993. Soil tillage in Africa: needs and changes. *FAO soils bulletin* 69.
- FAO, 1998. World reference base for soil resources. *World soil resources report* 84, Rome.
- FAO, 2014. World reference base for soil resources, 2014. International soil classification system for naming soils and creating legends for soil maps. Rome: Food and Agriculture Organization of the United Nations (World soil resources reports, 106).
- Fazekas, O., Horn, R., 2005. Zusammenhang zwischen hydraulischer und mechanischer Bodenstabilität in Abhängigkeit von der Belastungsdauer. *J. Plant Nutr. Soil Sci.* 168, 60-67.
- Febo, P., Lucarelli, F., Pessina, D., 2000. Soil-tyre interaction parameters influencing soil compaction: A study of contact area prediction models. *Advances in GeoEcology* 32, 191-201.

- Feng, T.-W., Lee, J.-Y., Lee, Y.-J., 2001. Consolidation behaviour of a soft mud treated with small cement content. *Engineering Geology* 59, pp. 327-335.
- Fleige, H., Horn, R., 2000. Field experiments on the effect of soil compaction on soil properties, runoff, inter-flow and erosion. *Advances in GeoEcology* 32, 258-268.
- Fleige, H., Horn, R., Stange, F. 2002. Soil mechanical parameters derived from the CA-database on subsoil compaction. *Advances in GeoEcology* 35. 359-366.
- Folorunso, O.A., Rolston, D.E., Prichard, T., Louie, D.T., 1992. Soil surface strength and infiltration rate as affected by winter cover crops. *Soil Technology* 5, 189-197.
- Franko, U., Kuka, K., Romanenko, I.A., Romanenkov, V.A., 2007. Validation of the CANDY model with Russian long-term experiments. *Reg. Environ. Change* 7, 79-91.
- Frede, H.-G., 1991. Gefügebildende Wirkungen natürlicher Kräfte auf schluffreichen Böden. *Bodennutzung und Bodenfruchtbarkeit. Band 2: Bodengefüge*. Verlag Paul Parey Hamburg und Berlin. 55-68.
- Fulajtár, E., 2000. Assessment and determination of the compacted soils in Slovakia. *Advances in GeoEcology*, 32, 384-387.
- Gaudino, S., Goia, I., Borreani, G., Tabacco, E., Sacco, D., 2014. Cropping system intensification grading using an agro-environmental indicator set in northern Italy. *Ecological Indicators* 40, 76–89.
- Gee, G.W., Bauder, J.W., 1986. Particle-size analysis. In: Klute, A. (Ed.): *Methods of soil analysis. Part 1: Physical and mineralogical methods*. Second Edition. 383-412.
- Ghuman, B.S., Sur, H.S., 2001. Tillage and residue management effects on soil properties and yields of rainfed maize and wheat in a subhumid subtropical climate. *Soil & Tillage Research* 58, 1-10.
- Gieska, M., van der Ploeg, R., Schweigert, P., Pinter, N., 2003. Physikalische Bodendegradierung in der Hildesheimer Börde und das Bundesbodenschutzgesetz. *Berichte über Landwirtschaft* 4, 485-511.
- Glab, T., Kulig, B., 2008. Effect of mulch and tillage system on soil porosity under wheat (*Triticum aestivum*). *Soil & Tillage Research* 99, 169-178.
- Głąb, T., Ścigalska, B., Łabuz, B., 2013. Effect of crop rotations with triticale (*× Triticosecale Wittm.*) on soil pore characteristics. *Geoderma* 202-203, 1-7.
- Götze, P., Rücknagel, J., Christen, O., 2013. Bodenstrukturzustand der unteren Ackerkrume auf langjährig konservierend und tiefenreduziert bearbeiteten mitteldeutschen Ackerflächen. *Bodenschutz* 3-13, 88-93.
- Gysi, M., 2001. Compaction of a Eutric Cambisol under heavy wheel traffic in Switzerland: Field Data and a critical state soil mechanics model approach. *Soil & Tillage Research* 61, 133-142.
- Gysi, M., Ott, A., Flühler, H., 1999. Influence of a single passes with high wheel load on a structured, unploughed sandy loam soil. *Soil & Tillage Research* 52, 141-151.
- Hamidi, A., Salimi, N., Yazdanjou, V., 2011. Shape and size effects of gravel particles on shear strength characteristics of sandy soils. *Geosciences Scientific Quarterly Journal* 20, 189-196.
- Hammel, K., 1994. Soil stress distribution under lugged tires. *Soil & Tillage Research* 32, 163-181.
- Hamza, M.A., Anderson, W.K., 2005. Soil compaction in cropping systems. A review of nature, causes and possible solutions. *Soil & Tillage Research* 82, 121-145.
- Hargreaves, P.R., Baker, K.L., Graceson, A., Bonnett, S., Ball, B.C., Cloy, J.M., 2019. Soil compaction effects on grassland silage yields and soil structure under different levels of compaction over three years. *European Journal of Agronomy* 109, 125916.
- Hartge, K.H., 1994. Soil Structure, its Development and its Implications for Properties and Processes in Soils - a synopsis based on recent research in Germany. *Zeitschrift Pflanzenernährung Bodenkunde* 157, 159-164.
- Hartge, K.H., Bohne, H., 1983. Der Einfluss der Gefüegeometrie auf die Verdichtbarkeit des Bodens und auf Keimung von Roggen. *Zeitschrift für Kulturtechnik und Flurbereinigung* 24, 5-10.
- Hartge, K.-H., Sommer, C., 1982. Einfluss der Bodenentwicklung auf den Zusammenhang zwischen Lagerungszustand und vertikaler Spannung im Boden. *Zeitschrift Pflanzenernährung Bodenkunde* 145, 25-35.
- Hartmann, P., Zink, A., Fleige, H., Horn, R., 2012. Effect of compaction, tillage and climate change on soil water balance of Arable Luvisols in Northwest Germany. *Soil & Tillage Research* 124, 211-218.
- Herbst, F., Hofmann, B., 2005. Ursachen und Auswirkungen von Wachstumsstörungen bei Sommerweizen in einem Feldbestand. *Mitt. Ges. Pflanzenbauwiss.* 17, 38-41.
- Higashi, T., Yunghui, M., Komatsuzaki, M., Miura, S., Hirate, T., Araki, H., Kaneko, N., Ohta, H., 2014. Tillage and cover crop species affect soil organic carbon in Andosol, Kanto, Japan. *Soil & Tillage Research* 138, 64-72.

- Höhne, E., Rücknagel, J., Christen, O., 2011. Relation between soil structural field parameters and soil physical laboratory measurements. Proceedings of the Third Scientific Conference of ISOFAR, Namyangju / Republic of Korea, pp. 25-27.
- Höhne, E., Rücknagel, J., Christen, O., 2013. Bewertung der Bodenstruktur mit Indikatoren der visuellen Gefügeansprache. Thünen Report 8, 33-80.
- Hooker, K.V., Coxon, C.E., Hackett, R., Kirwan, L.E., O'Keeffe, E., Richards, K.G., 2008. Evaluation of cover crop and reduced cultivation for reducing nitrate leaching in Ireland. *Journal of Environmental Quality* 37, 138-145.
- Horn, R., 1986. Auswirkung unterschiedlicher Bodenbearbeitung auf die mechanische Belastbarkeit von Ackerböden. *Zeitschrift Pflanzenernährung Bodenkunde* 149, 9-18.
- Horn, R., 2001. Die Verformung von Böden - Ursachen und Folgen für eine nachhaltige Landnutzung. Rheinische Friedrich-Wilhelms-Universität Bonn: Tagungsband 14. Wissenschaftliche Fachtagung Schadverdichtungen in Ackerböden - Entstehung, Folgen, Gegenmaßnahmen. 75-85.
- Horn, R., Domzal, H., Slowinska-Jurkiewicz, A., Ouwerkerk van, C., 1995. Soil compaction processes and their effects on the structure of arable soils and environment. *Soil & Tillage Research* 35, 23-36.
- Horn, R., Fleige, H., 2003. A method for assessing the impact of load on mechanical stability and on physical properties of soils. *Soil & Tillage Research* 73, 89-99.
- Horn, R., Fleige, H., 2009. Risk assessment of subsoil compaction for arable soils in Northwest Germany at farm scale. *Soil & Tillage Research* 102, 201-208.
- Horn, R., Johnson, C., Semmel, H., Schafer, R., Lebert, M., 1992. Räumliche Spannungsmessungen mit dem Stress State Transducer (SST) in ungesättigten aggregierten Böden - theoretische Betrachtungen und erste Ergebnisse. *Zeitschrift Pflanzenernährung Bodenkunde* 155, 269-274.
- Horn, R., Kutilek, M., 2009. The intensity-capacity concept - How far is it possible to predict intensity values with capacity parameters. *Soil & Tillage Research* 103, 1-3.
- Horn, R., Rostek, J., 2000. Subsoil compaction processes - state of knowledge. *Advances in GeoEcology* 32, 44-54.
- Horn, R., Simota, C., Fleige, H., Dexter, A., Rajkai, K., de la Rosa, D., 2002. Prediction of soil strength of arable soils and stress dependent changes in ecological properties based on soil maps. *J. Plant Nutr. Soil Sci.* 165, 235-239.
- Horn, R., Way, T., Rostek, J., 2003. Effect of repeated tractor wheeling on stress/strain properties and consequences on physical properties in structured arable soils. *Soil & Tillage Research* 73, 101-106.
- Houšková, B., 2002. Assessment of state of soil compaction in Slovakia. *Advances in GeoEcology* 35, 379-385.
- Hülsbergen, K.-J., 2003. Entwicklung und Anwendung eines Bilanzierungsmodells zur Bewertung der Nachhaltigkeit landwirtschaftlicher Systeme. *Berichte aus der Agrarwirtschaft*. Aachen: Shaker Verlag.
- Hülsbergen, K.-J., Feil, B., Biermann, S., Rathke, G.-W., Kalk, W.-D., Diepenbrock, W., 2001. A method of energy balancing in crop production and its application in a long-term fertilizer trial. *Agriculture, Ecosystems and Environment* 86, 303-321.
- ICS 13.080; 65.060.35: Methods of soil investigations for agricultural engineering - Physical laboratory tests - Part 9: Determination of the saturated hydraulic water conductivity in the cylindrical core-cutter.
- Imhoff, S., da Silva, A.P., Fallow, D., 2004. Susceptibility to compaction, load support capacity, and soil compressibility of Hapludox. *Soil Sci. Soc. Am. J.* 68, 17-24.
- Ingelmo, F., Cuadrado, S., Ibanez, A., Hernandez, J., 1994. Hydric properties of some Spanish soils in relation to their rock fragment content: implications for runoff and vegetation. *Catena* 23, 73-85.
- INL, 2019. Personal communication not published.
- ISO 11274:1998: Soil quality - Determination of the water retention characteristics - Laboratory methods.
- Jacobs, A., Auburger, S., Bahrs, E., Brauer-Siebrecht, W., Buchholz, M., Christen, O., Götze, P., Koch, H.-J., Mußhoff, O., Pelka, N., Rücknagel, J., Märländer, B., 2013. The sugar beet as an energy crop in crop rotations on highly productive sites – an agronomic/economic system analysis. *Sugar Industry* 138, 49-59.
- Jacobs, A., Auburger, S., Bahrs, E., Brauer-Siebrecht, W., Buchholz, M., Christen, O., Götze, P., Koch, H.J., Mußhoff, O., Pelka, N., Rücknagel, J., Märländer, B., 2014. The sugar beet as an energy crop in crop rotations on highly productive sites - an agronomic/economic system analysis. *Sugar Industry* 139, 117-127.
- Jegou, D., Brunotte, J., Rogasik, H., Capowiez, Y., Diestel, H., Schrader, S., Cluzeau, D., Impact of soil compaction on earthworm burrow systems using X-ray computed tomography: preliminary study. *European Journal of Soil Biology* 38, 329-336.

- Kaufmann, M., Tobias, S., Schulin, R., 2009. Development of the mechanical stability of a restored soil during the first 3 year of re-cultivation. *Soil & Tillage Research* 103, 127-136.
- Kaufmann, M., Tobias, S., Schulin, R., 2010. Comparison of critical limits for crop plant growth based on different indicators for the state of soil compaction. *J. Plant Nutr. Soil Sci.* 173, 573-583.
- Kautz, T., Stumm, C., Kösters, R., Köpke, U., 2010. Effects of perennial fodder crops on soil structure in agricultural headlands. *J. Plant Nutr. Soil Sci.* 173, 490-501.
- Keller, T., Arvidsson, J., Dawidowski, J.B., Koolen, A.J., 2004. Soil precompression stress II. A comparison of different compaction tests and stress - displacement behaviour of the soil during wheeling. *Soil & Tillage Research* 77, 97-108.
- Keller, T., Arvidsson, J., Schjonning, P., Lamande, M., Stettler, M., Weisskopf, P., 2012. In situ subsoil stress-strain behavior in relation to soil precompression stress. *Soil Science* 177, Number 8, 1-8.
- Keller, T., Defosse, P., Weisskopf, P., Arvidsson, J., Richard, G., 2007. SoilFlex: A model for prediction of soil stresses and soil compaction due to agricultural field traffic including a synthesis of analytical approaches. *Soil & Tillage Research* 93, 391-411.
- Keller, T., Lamande, M., 2010. Challenges in the development of analytical soil compaction models. *Soil & Tillage Research* 111, 54-64.
- Keller, T., Lamande, M., Schjonning, P., Dexter, A., 2011. Analysis of soil compression curves from uniaxial confined compression tests. *Geoderma* 163, 13-23.
- Kenward, M.G., Roger, J.H., 1997. Small sample inference for fixed effects from restricted maximum likelihood. *Biometrics* 3, 983-997.
- Klimanek, E.-M., 1997. Importance of crop and root residues of agricultural crops for soil organic matter. *Arch. Acker- Pfl. Boden.* 41, 485-511.
- Klute, A., Dirksen, C., 1986. Hydraulic conductivity and diffusivity: laboratory methods. In: Klute, A. (Ed.): *Methods of soil analysis. Part 1: Physical and mineralogical methods. Second Edition.* 687-734.
- Koch, H.J., Heuer, H., Tomanova, O., Märlander, B., 2008. Cumulative effect of annually repeated passes of heavy agricultural machinery on soil structural properties and sugar beet yield under two tillage systems. *Soil & Tillage Research* 101, 69-77.
- Koolen, A.J., Lerink, P., Kurstjens, D.A.G., van den Akker, J.J.H., Arts, W.B.M., 1992. Prediction of aspects of soil-wheel systems. *Soil & Tillage Research* 24, 381-396.
- Kroulik, M., Kviz, Z., Masek, J., Misiewicz, P.A., 2012. Benefits of GPS agricultural guidance for sustainable agriculture. *Agrociencia Uruguay Special Issue*, 107-116.
- Krümmlbein, J., Horn, R., Raab, T., Bens, O., Hüttl, R.F., 2010. Soil physical parameters on a recently established agricultural recultivation site after brown coal mining in eastern Germany. *Soil & Tillage Research* 111, 19-25.
- Kuhwald, M., Dörnhöfer, K., Oppelt, N., Duttmann, R., 2018. Spatially explicit soil compaction risk assessment of arable soils at regional scale: The SaSCiA-Model. *Sustainability* 10, 1618.
- Küstermann B., Kainz M., Hülsbergen K.-J., 2008. Modeling carbon cycles and estimation of greenhouse gas emissions from organic and conventional farming systems. *Renewable Agriculture and Food Systems* 23, 38-52.
- Küstermann, B., Christen, O., Hülsbergen, K.-J., 2010. Modelling nitrogen cycles of farming systems as basis of site- and farm-specific nitrogen management. *Agriculture, Ecosystems and Environment* 135, 70-80.
- Lafond, J., Angers, D.A., Laverdiere, M.R., 1992. Compression characteristics of a clay soil as influenced by crops and sampling dates. *Soil & Tillage Research* 22, 233-241.
- Lamande, M., Schjonning, P., 2011a. Transmission of vertical stress in a real soil profile. Part I: Site description, evaluation of the Söhne model, and the effect of topsoil tillage. *Soil & Tillage Research* 114, 57-70.
- Lamande, M., Schjonning, P., 2011b. Transmission of vertical stress in a real soil profile. Part III: Effect of soil water content. *Soil & Tillage Research* 114, 78-85.
- Lamande, M., Schjonning, P., Labouriau, R., 2017. A novel method for estimating soil precompression stress from uniaxial confined compression tests. *Soil Sci. Soc. Am. J.* 81, 1005-1013.
- Larson, W.E., Gupta, S.C., Useche, R.A., 1980. Compression of agricultural soils from eight soil orders. *Soil Sci. Soc. Am. J.* 44, 450-457.
- Lebert, 2010. Entwicklung eines Prüfkonzepthes zur Erfassung der tatsächlichen Verdichtungsgefährdung landwirtschaftlicher Böden. *Umweltbundesamt Texte* 51/2010. 96 pages.

- Lebert, M., 1989. Beurteilung und Vorhersage der mechanischen Belastbarkeit von Ackerböden. Bayreuth: Bayreuther Bodenkundliche Berichte, Band 12.
- Lebert, M., Brunotte, J., Sommer, C., 2004. Ableitung von Kriterien zur Charakterisierung einer schädlichen Bodenveränderung, entstanden durch nutzungsbedingte Verdichtung von Böden / Regelungen zur Gefahrenabwehr. UBA Texte 46-04.
- Lebert, M., Brunotte, J., Sommer, C., 2004. Ableitung von Kriterien zur Charakterisierung einer schädlichen Bodenveränderung, entstanden durch nutzungsbedingte Verdichtung von Böden / Regelungen zur Gefahrenabwehr. Texte Umweltbundesamt 46-04.
- Lebert, M., Burger, N., Horn, R., 1987. Welche Bedeutung kommt der Aggregatstabilität während des Schervorganges zu? Mitt. Dtsch. Bodenk. Ges. 53, 427-432.
- Lebert, M., Horn, R., 1992. Ein Verfahren zur flächendeckenden Erfassung der Bodenstabilität im Hinblick auf die Beurteilung der mechanischen Belastbarkeit von Ackerböden. Z. f. Kulturtechnik u. Landentwicklung 33, 85-99.
- Ledermüller, S., Lorenz, M., Brunotte, J., Fröba, N., 2018. A Multi-Data approach for spatial risk assessment of topsoil compaction on arable sites. Sustainability 10, 2915.
- Lipiec, J., Horn, R., Pietrusiewicz, J., Siczek, A., 2012. Effects of soil compaction on root elongation and anatomy of different cereal plant species. Soil & Tillage Research 121, 74-81.
- Lorenz, M., Brunotte, J., Vorderbrügge, T., Brandhuber, R., Koch, H.-J., Senger, M., Fröba, N., Löpmeier, F.-J., 2016. Anpassung der Lasteinträge landwirtschaftlicher Maschinen an die Verdichtungsempfindlichkeit des Bodens - Grundlagen für ein bodenschonendes Befahren von Ackerland. Sonderdruck der Landbauforschung. 43 pages.
- Lozano, N., Rolim, M.M., Oliveira, V.S., Tavares, U.E., Pedrosa, E.M.R., 2013. Evaluation of soil compaction by modeling field vehicle traffic with SoilFlex during sugarcane harvest. Soil & Tillage Research 129, 61-68.
- Lubetzki, C., 2013. Zusammenhang von Bodengefügeeigenschaften der Ackerkrume, unterschiedlich befahrenen Schlagbereichen und den Ertragsstrukturparametern von Winterweizen auf einem Ackerschlag in der Leipziger Tieflandsbucht. Bachelorarbeit Martin-Luther-Universität Halle-Wittenberg. 39 pages.
- Lütke Entrup, N., 2000. Feldfutterbau und Ackerbegrünung. In: Lütke Entrup, N., Oehmichen, J. (Eds.): Lehrbuch des Pflanzenbaues. Part 2: Kulturpflanzen. Verlag Th. Mann, Gelsenkirchen. 572-669.
- Malhi, S.S., Moulin, A.P., Johnston, A.M., Kutcher, H.R., 2008. Short-term and long-term effects of tillage and crop rotation on soil physical properties, organic C and N in a Black Chernozem in northeastern Saskatchewan. Can. J. Soil. Sci. 88, 273-282.
- Marschall, K., Götze, H., Stahl, H., 2019. Entscheidungshilfe Bodendruck. Sächsisches Landesamt für Umwelt, Landwirtschaft und Geologie. www.boden.sachsen.de/entscheidungshilfe-bodendruck-18974.html
- Mauer, A., 2015. Vermeidung von Bodenschadverdichtungen - eine empirische Analyse in Mitteldeutschland. Masterarbeit Martin-Luther-Universität Halle-Wittenberg. 75 pages.
- McCallum, M.H., Kirkegaard, J.A., Green, T.W., Cresswell, H.P., Davies, S.L., Angus, J.F., Peoples, M.B., 2004. Improved subsoil macroporosity following perennial pastures. Aust. J. Exp. Agric. 44, 299-307.
- Meek, B.D., Rechel, E.A., Carter, L.M., de Tar, W.R., 1989. Changes in infiltration under alfalfa as influenced by time and wheel traffic. Soil Sci. Soc. Am. J. 53, 238-241.
- Mitchell, J.K., Soga, K., 2005. Fundamentals of soil behaviour. 3rd edition. John Wiley & Sons, Inc., USA.
- Mosaddeghi, M.R., Hemmat, A., Hajabbasi, M.A., Alexandrou, A., 2003. Pre-compression stress and its relation with the physical and mechanical properties of a structurally unstable soil in central Iran. Soil & Tillage Research 70, 53-64.
- Mosaddeghi, M.R., Koolen, A.J., Hemmat, A., Hajabbasi, M.A., Lerink, P., 2007. Comparisons of different procedures of pre-compaction stress determination on weakly structured soils. Journal of Terramechanics 44, 53-63.
- Mueller, L., Kay, B.D., Hu, C., Li, Y., Schindler, U., Behrendt, A., Shepherd, T.G., Ball, B.C., 2009. Visual assessment of soil structure: Evaluation of methodologies on sites in Canada, China and Germany, Part I: Comparing visual methods and linking them with soil physical data and grain yield of cereals. Soil & Tillage Research 103, 178-187.
- Mueller, L., Schindler, U., Mirschel, W., Shepherd, T.G., Ball, B.C., Helming, K., Rogasik, J., Eulenstein, F., Wiggering, H., 2010. Assessing the productivity function of soils. A review. Agron. Sustain. Dev. 30, 601-614.

- Nawaz, M.F., Bourrié, G., Trolard, F., 2013. Soil compaction impact and modelling. A review. *Agron. Sustain. Dev.* 33, 291-309.
- Ndaeyo, N.U., 2010. Yields, cost of production and economic return to management of maize/cassava intercrop as influenced by different tillage practices. *Researcher* 2(10), 68-74.
- Nissen, B., 1998. Vorhersage der mechanischen Belastbarkeit von repräsentativen Ackerböden der Bundesrepublik Deutschland - bodenphysikalischer Ansatz. Universität Kiel: Schriftenreihe Institut für Pflanzenernährung und Bodenkunde.
- Nolting, K., Brunotte, J., Lorenz, M., Sommer, C., 2006. Soil compaction: Are things changing? In situ measurements of subsoil settlement under heavy wheel loads. *Landtechnik* 61, 190-191.
- O'Sullivan, M.F., Henshall, J.K., Dickson, J.W., 1999. A simplified method for estimating soil compaction. *Soil & Tillage Research* 49, 325-335.
- Opitz von Boberfeld, W., 1994. Grünlandlehre. Verlag Eugen Ulmer Stuttgart.
- Oquist, K.A., Strock, J.S., Mulla, D.J., 2006. Influence of alternative and conventional management practices on soil physical and hydraulic properties. *Vadose Zone Journal* 5, 356.
- Paracchini, M.L., Bulgheroni, C., Borreani, G., Tabacco, E., Banterle, A., Bertoni, D., Rossi, G., Parolo, G., Oraggi, R., de Paola, C., 2015. A diagnostic system to assess sustainability at a farm level: The SOSTARE model. *Agricultural Systems* 133, 35-53.
- Paul, R., 2004. Verfahren zur Ermittlung der Schadverdichtungsrisiken auf ackerbaulich genutzten Böden. Jena: Thüringer Landesanstalt für Landwirtschaft. Zwischenbericht 46.02.
- Paul, R., 2010. Personal communication not published.
- Paz, A., Guerif, J., 2000. Influence of initial packing density, water content and load applied during compaction on tensile strength of dry soil structural units. *Advances in GeoEcology* 32, 55-63.
- Peng, X.H., Horn, R., 2008. Time-dependent, anisotropic pore structure and soil strength in a 10-year period after intensive tractor wheeling under conservation and conventional tillage. *J. Plant Nutr. Soil Sci.* 171, 936-944.
- Peng, X.H., Horn, R., Zhang, B., Zhao, Q.G., 2004. Mechanisms of soil vulnerability to compaction of homogenised and recompacted Ultisols. *Soil & Tillage Research* 76, 125-137.
- Peth, S., Horn, R., 2006. The mechanical behavior of structured and homogenized soil under repeated loading. *J. Plant Nutr. Soil Sci.* 169, 401-410.
- Peth, S., Horn, R., Fazekas, O., Richards, B.G., 2006. Heavy soil loading and its consequence for soil structure, strength, and deformation of arable soils. *J. Plant Nutr. Soil Sci.* 169, 775-783.
- Peth, S., Rostek, J., Zink, A., Mordhorst, A., Horn, R., 2010. Soil testing of dynamic deformation processes of arable soils. *Soil & Tillage Research* 106, 317-328.
- Poesen, J., Lavee, H., 1994. Rock fragments in top soils: significance and processes. *Catena* 23, 1-28.
- Pöhlitz, J., 2019. Studies on soil compaction combining classic soil mechanical methods and X-ray computed tomography. Dissertation Martin-Luther-Universität Halle-Wittenberg. 114 pages.
- Pöhlitz, J., Rücknagel, J., Koblenz, B., Schlüter, S., Vogel, H.-J., Christen, O., 2018. Computed tomography and soil physical measurements of compaction behaviour under strip tillage, mulch tillage and no tillage. *Soil & Tillage Research* 175, 205-216.
- Pöhlitz, J., Rücknagel, J., Schlüter, S., Vogel, H.-J., Christen, O., 2019. Computed tomography as an extension of classical methods in the analysis of soil compaction, exemplified on samples from two tillage treatments and at two moisture tensions. *Geoderma* 346, 52-62.
- Poodt, M.P., Koolen, A.J., van der Linden, J.P., 2003. FEM analysis of subsoil reaction on heavy wheel loads with emphasis on soil preconsolidation stress and cohesion. *Soil & Tillage Research* 73, 67-76.
- R Core Team, 2017. R: A language and environment for statistical computing.
- Raper, R.L., Reeves, D.W., Burmester, C.H., Schwab, E.B., 2000. Tillage depth, tillage timing, and cover crop effects on cotton yield, soil strength, and tillage energy requirements. *Applied Engineering in Agriculture* 16, 379-385.
- Rasmussen, K.J., 1999. Impact of ploughless tillage on yield and soil quality: A Scandinavian review. *Soil & Tillage Research* 53, 3-14.
- Ravina, I., Magier, J., 1984. Hydraulic conductivity and water retention of clay soils containing coarse fragments. *Soil Sci. Soc. Am. J.*, 48, 736-740.

- Reeleder, R.D., Miller, J.J., Ball Coelho, B.R., Roy, R.C., 2006. Impacts of tillage, cover crop, and nitrogen on populations of earthworms, microarthropods, and soil fungi in a cultivated fragile soil. *Applied Soil Ecology* 33, 243-257.
- Reichert, J.M., Suzuki, L.E.A.S., Reinert, D.J., Horn, R., Hakansson, I., 2009. Reference bulk density and critical degree-of-compactness for no-till crop production in subtropical highly weathered soils. *Soil & Tillage Research* 102, 242-254.
- Reid, J.B., Goss, M.J., 1981. Effect of living roots of different plant species on the aggregate stability of two arable soils. *Journal of Soil Science* 32, 521-541.
- Riggert, R., Fleige, F., Kietz, B., Gaertig, T., Horn, R., 2016. Stress distribution under forest machinery and consequences for soil stability. *Soil Sci. Soc. Am. J.* 80, 38-47.
- Rinnofner, T., Friedel, J.K., de Kruijff, R., Pietsch, G., Freyer, B., 2008. Effect of catch crops on N dynamics and following crops in organic farming. *Agron. Sustain. Dev.* 28, 551-558.
- Rücknagel, J., 2014. *Boden unter Druck: Schadverdichtungen vermeiden - Fruchtbarkeit sichern*. Frankfurt a.M.: DLG-Verlag, 120 pages.
- Rücknagel, J., Brandhuber, R., Hofmann, B., Lebert, M., Marschall, K., Paul, R., Stock, O., Christen, O., 2010. Variance of mechanical precompression stress in graphic estimations using the Casagrande method and derived mathematical models. *Soil & Tillage Research* 106, 165-170.
- Rücknagel, J., Christen, O., 2009. Use of the information system *REPRO* to assess physical aspects of soil fertility. *ISTRO 18th Triennial Conference Proceedings*, June 15-19, 2009 Izmir-Turkey. T1-032, 1-6.
- Rücknagel, J., Christen, O., Hofmann, B., Ulrich, S., 2012a. A simple model to estimate change in precompression stress as a function of water content on the basis of precompression stress at field capacity. *Geoderma* 177-178, 1-7.
- Rücknagel, J., Dumbeck, G., Harrach, T., Höhne, E., Christen, O., 2013a. Visual structure assessment and mechanical soil properties of re-cultivated soils made up of loess. *Soil Use and Management* 29, 271-278.
- Rücknagel, J., Götze, P., Hofmann, B., Christen, O., Marschall, K., 2013b. The influence of soil gravel content on compaction behaviour and precompression stress. *Geoderma* 209-210, 226-232.
- Rücknagel, J., Hofmann, B., Christen, O., 2004. Effect of soil-tillage on soil physical properties, total organic carbon content and winter barley yield in a long-term experiment in Germany. *Proceedings of the 4th International Crop Science Congress Brisbane, Australia*.
- Rücknagel, J., Hofmann, B., Deumelandt, P., Reinicke, F., Bauhardt, J., Hülsbergen, K.-J., Christen, O., 2015. Indicator based assessment of the soil compaction risk at arable sites using the model *REPRO*. *Ecological Indicators* 52, 341-352.
- Rücknagel, J., Hofmann, B., Paul, R., Christen, O., Hülsbergen, K.-J., 2007. Estimating precompression stress of structured soils on the basis of aggregate density and dry bulk density. *Soil & Tillage Research* 92, 213-220.
- Rücknagel, J., Rücknagel, S., Christen, O., 2012b. Impact on soil compaction of driving agricultural machinery over ground frozen near the surface. *Cold Regions Science and Technology* 70, 113-116.
- Sächsisches Staatsministerium für Umwelt und Landwirtschaft, 2018. *Kippboden - Boden des Jahres 2019*. Zentraler Broschürenversand der Sächsischen Staatsregierung Dresden. 36 pages.
- Saffih-Hdadi, K., Défossez, P., Richard, G., Cui, Y.-J., Tang, A.-M., Chaplain, V., 2009. A method for predicting soil susceptibility to the compaction of surface layers as a function of water content and bulk density. *Soil & Tillage Research* 105, 96-103.
- Saini, G.R., Grant, W.J., 1980. Long-term effects of intensive cultivation on soil quality in the potato-growing areas of New Brunswick (Canada) and Maine (U.S.A). *Can. J. Soil Sci.* 60, 421-428.
- Salire, E.V., Hammel, J.E., Hardcastle, J.H., 1994. Compression of intact subsoils under short-duration loading. *Soil & Tillage Research* 31, 235-248.
- SAS Institute, Inc., 2008. *SAS. Version 9.2 TS Level 1M0*. Cary, NC, USA.
- Schäfer-Landefeld, L., Brandhuber, R., Fenner, S., Koch, H.-J., Stockfisch, N., 2004. Effects of agricultural machinery with high axle load on soil properties of normally managed fields. *Soil & Tillage Research* 75, 75-86.
- Schanz, T., 2007. *Bodenmechanik I+II Vorlesungsunterlagen*. Bauhausuniversität Weimar, Studienunterlagen Geotechnik, 6. Auflage. 198 pages.
- Schjonning, P., 1989. Long-term reduced cultivation. II. Soil pore characteristics as shown by gas diffusivities and permeabilities and air-filled porosities. *Soil & Tillage Research* 15, 91-103.
- Schjonning, P., Lamande, M., 2018. Models for prediction of soil precompression stress from readily available soil properties. *Geoderma* 320, 115-125.

- Schjonning, P., Lamande, M., Keller, T., Pedersen, J., Stettler, M., 2012. Rules of thumb for minimizing subsoil compaction. *Soil Use and Management* 28, 378-393.
- Schjonning, P., van den Akker, J.J.H., Keller, T., Greve, M.H., Lamande, M., Simojoki, A., Stettler, M., Arvidsson, J., Breuning-Madsen, H., 2015. Driver-Pressure-State-Impact-Response (DPSIR) analysis and risk assessment for soil compaction - a European perspective. *Advances in Agronomy* 133, 183-237.
- Schlüter, S., Großmann, C., Diel, J., Wu, G.M., Tischer, S., Deubel, A., Rücknagel, J., 2018. Long-term effects of conventional and reduced tillage on soil structure, soil ecological and soil hydraulic properties. *Geoderma* 332, 10-19.
- Schmidt, O., Clements, R.O., Donaldson, G., 2003. Why do cereal-legume intercrops support large earthworm populations? *Applied Soil Ecology* 22, 181-190.
- Schröder, D., 1988. Bodenschonende Rekultivierung von Lössböden in Braunkohletagebauen. *Bodenschutz*, Band 2, 7230, Erich Schmidt Verlag, 1-22.
- Schulze, S., 2017. *Rhizoctonia solani* in sugar beet - Relations between soil physical properties and disease severity as well as quantification of the *Rhizoctonia* inoculum potential in soil. Göttingen: Cuvillier Verlag. Heft 51/2017, 149 pages.
- Semmel, H., Horn, R., 1995. Möglichkeiten zur Bestimmung der mechanischen Belastbarkeit und der Druckfortpflanzung im Boden im Hinblick auf die Ableitung von bodentyp- und maschinenspezifischen Grenzwerten. *KTBL* 362, Münster-Hiltrup, 61-92.
- Six, J., Elliott, E.T., Paustian, K., 1999. Aggregate and soil organic matter dynamics under conventional and no-tillage systems. *Soil Sci. Soc. Am. J.* 63, 1350-1358.
- Söhne, W., 1953. Druckverteilung im Boden und Bodenverformung unter Schlepperreifen. *Grundlagen der Landtechnik* 5, 49-63.
- Stahl, H., Marschall, K., Freytag, A., Götze, H., 2009. Bodendruck im Grünland. Freistaat Sachsen, Schriftenreihe des Landesamtes für Umwelt, Landwirtschaft und Geologie. Heft 3/2009. 60 pages.
- Stahl, H., Marschall, K., Götze, H., 2005. Bodendruck und Bodenbelastbarkeit. Schriftenreihe der Sächsischen Landesanstalt für Landwirtschaft. Heft 15, 10. Jahrgang.
- Statistisches Bundesamt, 2018. Land- und Forstwirtschaft. *Statistisches Jahrbuch* 2018.
- Statistisches Bundesamt, 2019. Flächennutzung - Bodenfläche insgesamt nach Nutzungsarten in Deutschland. <https://www.destatis.de/DE/Themen/Branchen-Unternehmen/Landwirtschaft-Forstwirtschaft-Fischerei/Flaechennutzung/Tabellen/bodenflaeche-insgesamt.html>
- StatSoft Inc., 2009. Statistica for Windows, version 9.0. www.statsoft.com.
- StatSoft, Inc., 2014. STATISTICA. Version 12.0.
- Stettler, M., Keller, T., Schjonning, P., Lamande, M., 2019. Internetplattform *TERANIMO*®. <https://www.terranimo.world/CH/Default.aspx>
- Stettler, M., Keller, T., Weisskopf, P., Lamande, M., Lassen, P., Schjonning, P., 2014. *TERANIMO*® - ein web-basiertes Modell zur Abschätzung des Bodenverdichtungsrisikos. *Landtechnik* 69(3), 132-138.
- Stirzaker, R.J., White, I., 1995. Amelioration of compaction by a cover-crop for no-tillage lettuce production. *Australian Journal of Agricultural Research* 46, 553-568.
- Tebrügge, F., Düring, R.-A., 1999. Reducing tillage intensity - a review of results from a long-term study in Germany. *Soil & Tillage Research* 53, 15-28.
- Topp, G.C., Reynolds, W.D., Cook, F.J., Kirby, J.M., Carter, M.R., 1997. Physical attributes of soil quality. In: Gregorich, E.G. and Carter, M.R. (Eds.): *Soil quality for crop production and ecosystem health*. Amsterdam: Elsevier. 21-58.
- Trautner, A., Arvidsson, J., 2003. Subsoil compaction caused by machinery traffic on a Swedish Eutric Cambisol at different soil water contents. *Soil & Tillage Research* 73, 107-118.
- Trükmann, K., 2011. Quantifizierung der Stabilisierungseffekte von Pflanzenwurzeln als Möglichkeit zur Reduzierung der mechanischen Bodendeformation in Grünland. Kiel: Schriftenreihe Institut für Pflanzenernährung und Bodenkunde. 141 pages.
- UBA, 2013. Verdichtung. www.umweltbundesamt.de/themen/boden-landwirtschaft/bodenbelastungen/verdichtung
- Ulen, B., 1997. Nutrient losses by surface run-off from soils with winter cover crops and spring-ploughed soils in the south of Sweden. *Soil & Tillage Research* 44, 165-177.

- Ulrich, S., Tischer, S., Hofmann, B., Christen, O., 2010. Biological soil properties in a long-term tillage trial in Germany. *J. Plant Nutr. Soil Sci.* 173, 483-489.
- Uteau, D., Pagenkemper, S.K., Peth, S., Horn, R., 2013. Root and time dependent soil structure formation and its influence on gas transport in the subsoil. *Soil & Tillage Research* 132, 69-76.
- Van den Akker, J.J.H., 2004. *SOCOMO*: a soil compaction model to calculate soil stresses and the subsoil carrying capacity. *Soil & Tillage Research* 79, 113-127.
- Van den Akker, J.J.H., Canarache, A., 2001. Two European concerted actions on subsoil compaction. *Landnutzung und Landentwicklung* 42, 15-22.
- Van den Akker, J.J.H., Hoogland, T., 2011. Comparison of risk assessment methods to determine the subsoil compaction risk of agricultural soils in The Netherlands. *Soil & Tillage Research* 114, 146-154.
- Van Dijk, A.I.J.M., Bruijnzeel, L.A., 2003. Terrace erosion and sediment transport model: a new tool for soil conservation planning in bench-terraced steepplands. *Environmental Modelling & Software* 18, 839-850.
- Van Genuchten, M.T., 1980. A closed-form equation for predicting the hydraulic conductivity of unsaturated soils. *Soil Sci. Soc. Am. J.* 44, 892-898.
- Volk, L., 2018. Boden und Reifen in Einklang bringen. *LOP* 12/2018, 28-34.
- Voorhees, W.B., 2000. Long-term effect of subsoil compaction on yield of maize. *Advances in GeoEcology* 32, 44-54.
- Vorderbrügge, T., Brunotte, J., 2011a. Mechanische Verdichtungsempfindlichkeit für Ackerflächen (Unterboden) – Validierung von Pedotransferfunktionen zur Ableitung der Verdichtungsempfindlichkeit bzw. zur Ausweisung „sensibler Gebiete“ in Europa und ein praxisorientierter Lösungsansatz zur Guten fachlichen Praxis. Teil I: Validierung von Pedotransferfunktionen. *Landbauforschung* 61, 1-22.
- Vorderbrügge, T., Brunotte, J., 2011b. Mechanische Verdichtungsempfindlichkeit für Ackerflächen (Unterboden) – Validierung von Pedotransferfunktionen zur Ableitung der Verdichtungsempfindlichkeit bzw. zur Ausweisung „sensibler Gebiete“ in Europa und ein praxisorientierter Lösungsansatz zur Guten fachlichen Praxis. Teil II: Bewertung eines Vorschlages zur Ableitung von Vorsorgewerten gemäß der Bundes-Bodenschutzverordnung sowie der Pedotransferfunktionen zur Ableitung der „Potentiellen mechanischen Verdichtungsempfindlichkeit für Ackerflächen (Unterboden)“ nach LEBERT (2008) als Grundlage zur „Identifizierung sensibler Gebiete“ i.S. der Bodenschutzrahmenrichtlinie (BSRRL) der Europäischen Kommissionen. *Landbauforschung* 61, 23-40.
- Vorderbrügge, T., Brunotte, J., 2011c. Mechanische Verdichtungsempfindlichkeit für Ackerflächen (Unterboden) – Validierung von Pedotransferfunktionen zur Ableitung der Verdichtungsempfindlichkeit bzw. zur Ausweisung „sensibler Gebiete“ in Europa und ein praxisorientierter Lösungsansatz zur Guten fachlichen Praxis. Teil III: Ausweisung von „Risiko Gebieten“ auf Basis von Pedotransferfunktionen – die aktuelle Situation in Europa. *Landbauforschung* 61, 41-50.
- Watson, C.A., Atkinson, D., Gosling, P., Jackson, L.R., Rayns, F.W., 2002. Managing soil fertility in organic farming systems. *Soil Use and Management* 18, 239-247.
- Weiland, P., 2010. Biogas production: current state and perspectives. *Applied microbiology and biotechnology* 85, 849-860.
- Weisskopf, P., Reiser, R., Rek, J., Oberholzer, H.-R., 2010. Effect of different compaction impacts and varying subsequent management practices on soil structure, air regime and microbiological parameters. *Soil & Tillage Research* 111, 65-74.
- Weisskopf, P., Zihlmann, U., Wiermann, C., Horn, R., Anken, T., Diserens, E., 2000. Influence of conventional and onland-ploughing on soil structure. *Advances in GeoEcology* 32, 73-81.
- Wendling, U., 1986. Processing of soil moisture measurement series to characterize the trafficability and workability of different soils. *Tag.-Ber., Akad. Landwirtsch.-Wiss. DDR*, 69-72.
- Werner, D., Paul, R., 1999. Kennzeichnung der Verdichtungsgefährdung landwirtschaftlich genutzter Böden. *Wasser und Boden* 51/12, 10-14.
- Werner, D., Reich, J., 1993. Verbesserung schadverdichteter Ackerböden durch Lockerung. Rationalisierungskuratorium für Landwirtschaft. Sonderdruck aus der Kartei für Rationalisierung 4.1.1.1.0., 437-476.
- Whalen, J.K., Parmelee, R.W., Edwards, C.A., 1998. Population dynamics of earthworm communities in corn agroecosystems receiving organic or inorganic fertilizer amendments. *Biol. Fert. Soils* 27, 400-407.
- Wiermann, C., Werner, D., Horn, R., Rostek, J., Werner, B., 2000. Stress/strain processes in a structured unsaturated silty loam Luvisol under different tillage treatments in Germany. *Soil & Tillage Research* 53, 117-128.

-
- Wild, M., Brandhuber, R., Demmel, M., Gronle, A., Böhm, H., Lux, G., Schmidtke, K., Bruns, C., 2012. Auswirkung differenzierter mechanischer Bodenbelastung auf ausgewählte Eigenschaften des Oberbodens und den Ertrag von Erbse in Reinsaat und Gemenge. *Mitt. Ges. Pflanzenbauwiss.* 24, 170-171.
- Willmott, C.J., 1982. Some comments on the evaluation of model performance. *Bull. Am. Meteorol. Soc.* 63, No. 11, 1309-1313.
- Wilson, G.F., Lal, R., Okigbo, B.N., 1982. Effect of cover crops on soil structure and on yield of subsequent arable crops grown under strip tillage on an eroded Alfisol. *Soil & Tillage Research* 2, 233-250.
- Yang, Y., Lai, Y., Dong, Y., Li, S., 2010. The strength criterion and elastoplastic constitutive model of frozen soil under high confining pressure. *Cold Regions Science and Technology* 60, 154-160.
- Ziegler, K., 2010. Europas Roder im Test. *Zuckerrüben Journal* 4/2010, 6-9.
- Zink, A., Fleige, H., Horn, R., 2010. Load risks of subsoil compaction and depths of stress propagation in arable Luvisols. *Soil Sci. Soc. Am. J.* 74, 1733-1742.

Danksagung

Ich möchte mich bei allen Personen bedanken, die zum Gelingen dieser Arbeit beigetragen haben, auch wenn sie hier nicht im Einzelnen genannt werden können.

Allen voran danke ich aber Herrn Prof. Dr. Olaf Christen für die Gelegenheit zur Anfertigung der Habilitationsschrift und die Ratschläge zu deren Erstellung sowie die von ihm stetig ausgehende Motivation das Habilitationsverfahren zu betreiben. Darüber hinaus möchte ich mich bei ihm sehr für das freundschaftliche Verhältnis mit vielen fachlichen und persönlichen Gesprächen sowie die vielen positiv geprägten gemeinsamen Erlebnisse bedanken.

Auch Herrn Dr. Bodo Hofmann danke ich besonders für die fachliche Unterstützung, seinen Vorbildcharakter und sein Engagement für das bodenphysikalische Labor der Professur für Allgemeinen Pflanzenbau/Ökologischen Landbau in den vielen Jahren. Ohne dieses und das sehr freundschaftliche und menschliche Verhältnis wären die Untersuchungen in vorliegender Arbeit nur bedingt möglich gewesen.

Grundsätzlich danke ich allen Kolleginnen und Kollegen, die an den einzelnen Artikeln mitgewirkt haben für ihr außerordentlich großes Engagement sowie das fachliche und persönliche Interesse.

Für zahlreiche fachliche Diskussionen möchte ich mich unter anderem auch bei Prof. Dr. Tom Schanz†, Prof. Dr. Joachim Spilke, Dr. Heinz-Josef Koch, Dr. Thomas Keller, Karin Marschall, Marc Büchner und vielen mehr bedanken. Speziell bei Herrn Dr. Philipp Götze möchte ich mich für die gründliche Durchsicht von großen Teilen des Manuskripts und die vielen fachlichen Dialoge bedanken. Herrn Martin Schmidt vom Deutschen Wetterdienst (DWD) danke ich für die Bereitstellung von meteorologischen Daten.

Bedanken möchte ich mich überdies bei allen Landwirtschaftsbetrieben (Agrarproduktion Elsteraue GmbH & Co. KG Zwenkau, Geratal Agrar GmbH & Co. KG Andisleben, u.v.m.), Unternehmen (RWE Power AG, Erfstadt; Südzucker AG Mannheim/Ochsenfurt; u.a.) und Versuchsstationen (Thüringer Lehr-, Prüf- und Versuchsgut GmbH Buttstedt, Versuchsstation der Landesanstalt für Landwirtschaft und Gartenbau Sachsen-Anhalt, u.a.) auf deren Flächen ich Untersuchungen, Feldversuche und Bodenprobenahmen durchführen durfte.

Für die professionelle und engagierte Umsetzung des Modellkonzeptes in *REPRO* sei dem Institut für Nachhaltige Landbewirtschaftung (INL) und dabei besonders Frau Gabriele Hensel sehr herzlich gedankt.

Der Deutschen Bundesstiftung Umwelt (DBU) danke ich für die finanzielle Unterstützung des Projektes „Prüfung, Anpassung und Weiterentwicklung des Moduls zur Bewertung der Schadverdichtungsgefährdung im Betriebsbilanzierungsmodell *REPRO*“ (AZ 24275-34/0) durch welches Teile dieser Habilitationsschrift entstehen konnten.

Meiner Familie danke ich für die Freiräume ohne welche die Anfertigung der Habilitationsschrift nicht möglich gewesen wäre. Besonders meiner Frau Sandra danke ich für ihr Vertrauen, ihre Geduld und für die Unterstützung der zahlreichen Versuche auf unserem Landwirtschaftsbetrieb.

Meinen lieben derzeitigen und ehemaligen Kolleginnen und Kollegen aus der Professur für Allgemeinen Pflanzenbau/Ökologischen Landbau sowie unseren zahlreichen Studierenden danke ich sehr für die Unterstützung aller fachlichen Aktivitäten sowie das ausgesprochen angenehme Arbeitsverhältnis und die schönen Stunden außerhalb der wissenschaftlichen Arbeit.

Lebenslauf und wissenschaftlicher Werdegang

geboren am 15.02.1977 in Weimar
verheiratet, drei Kinder

Berufstätigkeit

seit 2010 Wissenschaftlicher Mitarbeiter und Verantwortlicher für das bodenphysikalische Labor an der Professur für Allgemeinen Pflanzenbau/Ökologischen Landbau der Martin-Luther-Universität Halle-Wittenberg

2007 – 2010 Wissenschaftlicher Mitarbeiter (Post-Doc) an der Professur für Allgemeinen Pflanzenbau/Ökologischen Landbau der Martin-Luther-Universität Halle-Wittenberg;
Forschungsthema: „Prüfung, Anpassung und Weiterentwicklung des Moduls zur Bewertung der Schadverdichtungsgefährdung im Betriebsbilanzierungsmodell *REPRO*“

2006 – 2007 Wissenschaftlicher Mitarbeiter an der Professur für Speziellen Pflanzenbau der Martin-Luther-Universität Halle-Wittenberg

2002 – 2005 Angestellter am Dienstleistungszentrum Rheinhessen-Nahe-Hunsrück mit Sitz in Mainz und Bad Kreuznach

2002 Wissenschaftlicher Mitarbeiter im Verein zur Förderung einer nachhaltigen Landwirtschaft e.V. mit Sitz in Halle (Saale)

Studium und Schule

2002 – 2006 Doktorand an der Martin-Luther-Universität Halle-Wittenberg;
Dissertation zum Thema: „Entwicklung eines Modells zur Analyse und Bewertung der Schadverdichtungsgefährdung von Ackerstandorten“, Abschluss: doctor agriculturarum (Dr. agr.), Gesamtnote: magna cum laude (sehr gut)

1997 – 2002 Studium der Agrarwissenschaften an der Martin-Luther-Universität Halle-Wittenberg mit Schwerpunkt Pflanzenwissenschaften;
Diplomarbeit zum Thema: „Einfluss langjährig nichtwendender Bodenbearbeitung auf Bodeneigenschaften, Wurzelwachstum und Ertrag bei Wintergerste“, Abschluss: Diplom-Agraringenieur (Dipl.-Ing. agr.), Gesamtnote: sehr gut

1991 – 1995 Staatliches Gymnasium „Prof. Fritz Hofmann“ in Köllda, Abschluss: Abitur

Theses for

“Methodological aspects and algorithms for estimating soil strength and their applications with the model *REPRO*”

submitted by Dr. Jan Rücknagel

- i. Soil compaction impairs all essential soil functions. In order to secure the various soil functions, soil compaction must be avoided. Mathematical empirical models, especially pseudo-analytical models, are a way to develop situational analyses and specific recommendations for action. These models can be used to limit complex measurements, simulate soil behaviour and derive effective measures from the identified risks. However, existing pseudo-analytical models show a number of shortcomings and potential for development, both in terms of numerous details and algorithms, but also with regard to fundamental questions of evaluation and their potential for application in complex crop cultivation issues. With this in mind, the aim is to develop a model which assesses the risk of soil compaction on arable land based on site-specific data – including information on soil, weather and husbandry in the individual case. The model must estimate the soil strength in response to soil stress for a topsoil and a subsoil layer, also taking into account changes in soil moisture throughout the year. Based on soil strength compared with soil stress, it should be possible to derive an indicator, the Soil Compaction Index (SCI), for each time the machinery passes over the soil. The results from the separate passes should then be integrated for a comprehensive assessment of the risk of soil compaction at farm level. The farm balance model *REPRO* is particularly well suited as a basis for such a model due to its modular structure and complex link with management data. The model will require validation in numerous trials, ensuring a good reflection of actual changes in soil structure.
- ii. Mechanical precompression stress is the yardstick for the strength and compressibility of soils. Precompression stress is certainly related to other important soil properties and

functions, such as packing density (PD), which in principle makes it suitable as a guideline for maximum structural stability in comparison with other structural parameters. Validation of the module in *REPRO* also shows that precompression stress is suitable as a parameter for maximum structural stability and that it is related to changes in other important soil properties and functions. The precompression stress values of different soils exhibit a very large range at comparable matric potential, depending on the intensity of soil tillage, the sampling depth, and general soil structure properties, such as for example the aggregate shape or aggregate arrangement. The effect of these parameters is significantly more important than the soil texture, which is why relying on texture as the sole criterion for the classification of precompression stress must be viewed critically.

- iii. The default method for the estimation of precompression stress is the graphical method according to Casagrande (1936). It involves the subjective perception of the engineer, who not only determines the point of the highest curvature visually, but also decides which points to use for generating the virgin compression line. These estimations will therefore vary from engineer to engineer. Involving several independent engineers should further improve the variance values and thus also reproducibility and comparability of the obtained results. Mathematical models with objective algorithms for the determination of precompression stress exist, derived from the Casagrande method. Subjecting graphically obtained values to mathematical models can reveal considerable deviations between them. An additional thesis is that different parameters on the ordinate of the diagram and the value of the first load step influence the precompression stress in the graphical method according to Casagrande (1936) and mathematical models. The methodological procedure for determining precompression stress by means of soil compression tests is basically suitable for determining the structural stability of agricultural soils.
- iv. Soil water content is a key factor in formation of soil compaction. In order to assess the risk of compaction in arable soils, it is necessary to know the precompression stress for a wide range of soil water content levels. The site-specific determination of relationships between precompression stress and matric potential or water content is, however, highly labour-intensive. Furthermore, existing regression models can only deduce changes in

precompression stress depending on water content to a limited extent, and not for all values. Alternatively, these models do not directly include precompression stress at a matric potential of -6 kPa as the basis of calculation. To solve this problem, it is necessary to derive and validate a simple model which can be used to predict any precompression stress for decreasing soil water content levels. The model should require only an initial precompression stress for a matric potential of -6 kPa and the respective soil water content as a percentage of field capacity. The development of a mathematical model should be performed for different soil texture classes, as well as “all texture classes” collectively. A comprehensive validation of the model on differently textured sites is necessary. Calculation according to different soil texture classes is therefore particularly recommended in the case of applications with high accuracy requirements. It is necessary to integrate the regression model in the soil compaction model in *REPRO*.

- v. Many arable soils have significant horizon-specific gravel content levels. At gravel-rich sites, gravel content consequently influences soil compaction behaviour and precompression stress very strongly. However, low gravel content levels of no more than 10 per cent by volume increase precompression stress only very slightly. By contrast, as gravel content exceeds 10 per cent by volume, precompression stress increases linearly or possibly even exponentially. The stress/density functions of the fine earth should show that the overall compaction of fine earth decreases as gravel content increases. To a certain extent, the shape of the gravel (subrounded to rounded vs. angular to subangular) has an influence on compaction behaviour and precompression stress. For this reason, it is essential that gravel content be considered when assessing such sites' risk of compaction. It is necessary to integrate the effect of gravel content on soil strength in the soil compaction module in *REPRO*.

- vi. Conventional tillage and conservation tillage show structural differences in the lower topsoil. In the case of conservation tillage, the soil structure demonstrates higher dry bulk density as well as lower air capacity and saturated hydraulic conductivity. Aggregate density is mostly similar. These differences lead to a difference in this layer's susceptibility to compaction, and also in density change – in the whole soil and also in the individual aggregates – during the compaction process in both tillage variants. Aggregate density increases relatively slowly during compaction, and often not before high

loading steps. This is why higher precompression stress values in the variants under conservation tillage is mostly the result of a dense compaction of aggregates, indicating higher stability against mechanical loads. However, for both variants the virgin compression section of the stress/bulk density functions should display similar compression behaviour; and generally higher settlement for conventional tillage in the compression test does not result in higher dry bulk densities than with conservation tillage. Stability against mechanical loads in the conservation tillage variants should therefore not be overestimated. Aggregate density and dry bulk density derived from tillage trials are a suitable basis for default values in the soil compaction model in *REPRO*.

- vii. Re-cultivated soils are particularly susceptible to compaction, which is why a simple estimate of mechanical strength is necessary for land management. Packing density (PD), with levels ranging between 1 (very loose soil) and 5 (very highly compacted), is particularly useful as an integrated parameter that combines various properties and is assessed visually in the field. There is a strongly negative relationship between packing density and both the aggregate density/dry bulk density ratio and air capacity. Conversely, mechanical precompression stress increases with packing density. Ranges of the individual parameters can be assigned to each of the packing density levels. Packing density level 3 represents an optimisation with regard to mechanical soil stability whilst maintaining minimum air capacity requirements. The relationship between packing density and precompression stress is a suitable basis for estimating precompression stress in the soil compaction module in *REPRO*.
- viii. In Central Europe, various plant species are grown as catch crops. Catch crop cultivation with large-grain legumes in particular influences soil structure in the topsoil. Mechanical soil stresses caused by driving over the ground and additional working steps used in cultivating catch crops often lead to lower air capacity in these treatments. This higher soil compaction risk with catch cropping can be calculated using the *REPRO* model to a good degree of accuracy. It is important that cultivating catch crops does not result in any new soil compaction as a result of additional working steps. Catch crop cultivation with large-grain legumes cannot contribute in the short term to loosening already compacted topsoils. Moreover, different ploughless tillage conditions during catch crop seeding influence soil structure in the topsoil. Deep ploughless tillage has a positive

effect on air capacity and saturated hydraulic conductivity. This becomes more clearly evident regardless of catch crop cultivation. Deep tillage is more effective at loosening compacted topsoil than growing catch crops.

- ix. The risk of soil compaction is particularly high in early spring or late autumn when soils are wet. Driving over the unfrozen soil leads to a significant compaction of the whole of the topsoil. In temperate climate zones, driving over soils frozen near the surface is one way to partially prevent soil compaction. A depth of frost penetration of as little as 2–3 cm is sufficient to reduce the risk of compaction with a wheel load of approximately 4000 kg and appropriately adjusted inflation pressure. Deeper frost penetration does not buffer soil compaction more significantly.

- x. Avoiding soil compaction caused by agricultural management is a key aim of sustainable land management. The soil compaction risk should be considered when assessing the complete environmental impacts of land use systems. Different crop rotations have a particular influence on soil structure and the risk of soil compaction. The soil compaction model in *REPRO* is a suitable tool to investigate the soil compaction risk of different crop rotations. The modelled soil compaction risks for the crop rotations including sugar beets are higher than for those without sugar beets. This increased soil compaction risk is largely influenced by the sugar beet harvest in years where soil water content is high. Halving the hopper load and adjusting the tyre inflation pressure reduce the soil compaction risk for the crop rotation as a whole. Under these conditions, there are no to low soil compaction risks in the subsoil. Soil physical parameters reflect these calculations. It is recommended to apply the soil compaction model in *REPRO* on arable farms in Germany. For these farms, calculating the soil compaction risk for the subsoils results in low to medium values.

Erklärungen

Hiermit erkläre ich, dass ich bisher keine Habilitationsverfahren an der Martin-Luther-Universität Halle-Wittenberg oder anderen Universitäten beantragt habe und es wurden daher auch keine Habilitationsgesuche an anderen Hochschulen abgelehnt.

Es liegen keine straf- und disziplinargerichtlichen Verurteilungen und anhängige Straf- und Disziplinarverfahren gegen mich vor.

Die vorliegende Habilitationsschrift wurde selbständig und nur unter Verwendung der angegebenen Literatur und Hilfsmittel angefertigt.

Halle/Saale, den 18.01.2021